Electrical Machines I

Basics, Design, Function, Operation

based on a lecture of

Univ.-Prof. Dr.-Ing. Dr. h.c. Gerhard Henneberger

at

Aachen University

Preface

This script corresponds to the lecture “Electrical Machines I” in winter term 2002/2003 at Aachen University.

The lecture describes the status quo of used technologies as well as tendencies in future development of electrical machines.
Basic types of electrical machines, such as transformer, DC machine, induction machine, synchronous machine and low-power motors operated at single phase AC systems are likewise discussed as innovative machine concepts, e.g. switched reluctance machine (SRM), transverse flux machine and linear drive.

Basic principles taking effect in all types of electrical machines to be explained, are combined in the rotating field theory. Apart from theoretical reflections, examples for applications in the field of electrical drives and power generation are presented in this script.

Continuative topics concerning dynamics, power converter supply and control will be discussed in the subsequent lecture “Electrical Machines II”.

It is intended to put focus on an all-embracing understanding of physical dependencies.
This script features a simple illustration without disregarding accuracy. It provides a solid basic knowledge of electrical machines, useful for further studies and practice. Previous knowledge of principles of electrical engineering are required for the understanding.

Please note: this script represents a translation of the lecture notes composed in German. Most subscriptions to appear in equations are not subject to translation for conformity purposes.

Aachen, in November 2002 Gerhard Henneberger

Revision: Busch, Schulte, March 2003

Content

1 Survey

The electrical machine is the essential element in the field of power generation and electrical drives. Duty of the electrical machine is a save, economical and ecological generation of electrical energy as well as its low-loss transformation for distribution purposes and its accordant utilization in electrical drive applications.

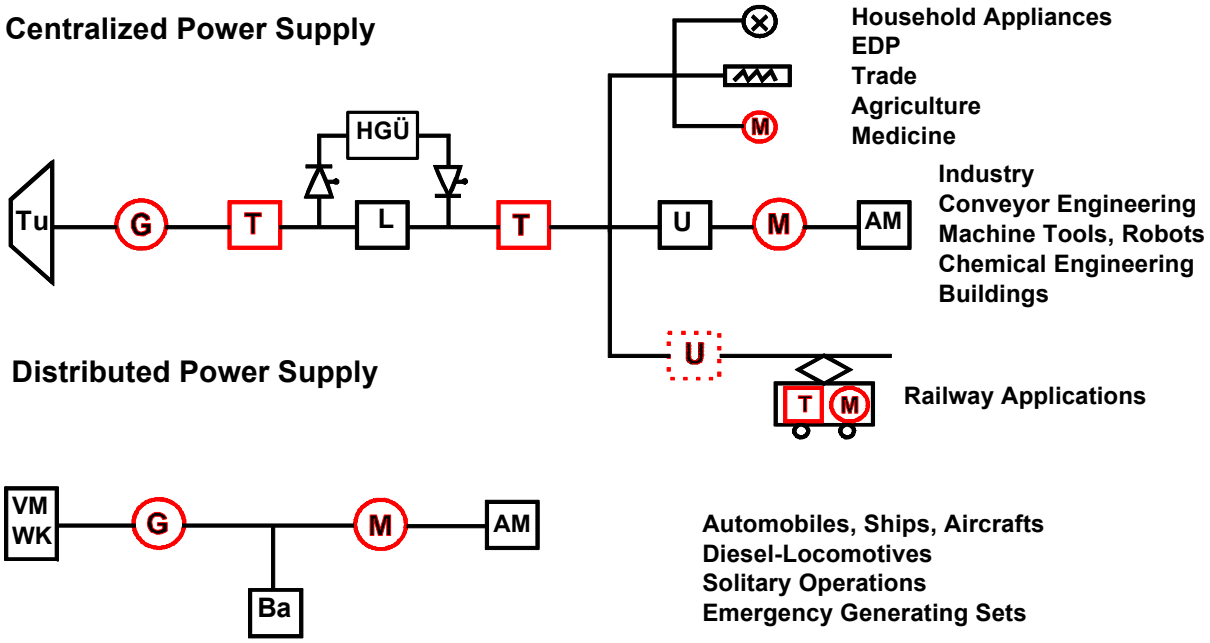

Fig. 1: The electrical machine in the field of power engineering

The electrical machine is utilized in centralized as well as in distributed energy transducer systems. Electrical machines appear as alternators in power plants and in solitary operation, also as transformers and transducers in electrical installations. They are also used as drive motors in industrial, trade, agricultural and medical applications as well as in EDP-systems, machine tools, buildings and household appliances. Railway, automotive, naval, aviation and aeronautic systems are equipped with electrical machines as well. Special machine models are used in magnetic-levitation technology and induction heating. The power range leads from µW to GW. Requirements of the entire system determine the design conditions of the electrical machine. Essential factors like functionality, costs, availability and influence on the environment need to be taken into account.

Focus on research at the IEM is put on electrical machines. Besides calculation, design, dimensioning and construction of electrical machines, the investigation of their static and transient performance characteristics and their interaction with converters and controllers pertain to the scope of our duties. The coverage of new application areas for electrical machines in the field of power generation and drive systems is aimed.

The electrical machine is the particular part of a drive, converting electrical energy into mechanical energy. The according operational status is called motor operation. Every kind of electrical machine is also able to work in generator operation. In this case mechanical energy is transferred into electrical energy.

Electromechanical energy transduction is reversible. This transduction is mainly based on the effect of electromagnetic fields, because its energy density is about decimal powers higher than the energy density of the electric field. This is shown in the following example:

$$w_m = \frac{B^2}{2\mu_0} = \frac{\left(10\frac{Vs}{cm^2}\right)}{1.256\cdot 10^{-8}\frac{Vs}{Acm}} = 0.4\frac{Ws}{cm^3} \tag{1.1}$$

$$w_e = \frac{\varepsilon \cdot E^2}{2} = \frac{0.886\cdot 10^{-13}\left(\frac{10kV}{cm}\right)^2}{2} = 4.4\cdot 10^{-4}\frac{Ws}{cm^3} \tag{1.2}$$

Electrical machines appear as different types of construction. Most common types are DC machines as well as rotating field machines such as induction or synchronous machines.
Due to its name, the DC machine is fed by DC current. Rotating field machines are to be supplied by a three-phase alternating current, called three-phase AC. In case of a single-phase AC current availability, universal motors (AC-DC motors) and single phase induction machines are applied.

Basically three kinds of electrical energy supply are to be distinguished: DC, single-phase AC and three-phase AC. Sometimes the present form of energy does not match the requirement. In order to turn the present energy into the appropriate form, power converters are utilized in drive systems, being capable to change frequency and voltage level in a certain range. Also motor-generator-sets (rotary converters) in railway applications as well as transformers in the field of energy distribution are used for converting purposes.

Power Electronics and their control are means to establish so far surpassed and improved operating characteristics. Innovative concepts such as an electronically commutating DC machine (also known as brushless DC machine, BLDC), converter synchronous machine, power converter supplied induction machine, switched reluctance machine (SRM) and stepping motor are to be mentioned as typical examples.

2 Basics

First of all some fundamental aspects which are required for the understanding of the lectures „Electrical Machines I&II“ and the respective scripts, need to be discussed.
For explicit information please see pertinent literature, please see references for this.

2.1 Fundamental equations

Despite the number of machine type varieties, the method of operation of any type of electrical machines can be described by just three physical basic equations. These are as follows the First Maxwell-Equation (also known as Ampere's Law), Faraday's Law and Lorentz Force Law.

2.1.1 First Maxwell Equation (Ampere's Law,)

First Maxwell Equation is defined in its integral and differential form as follows:

$$\oint_c \vec{H} \cdot d\vec{s} = \iint_F \vec{G} \cdot d\vec{F} = q \qquad \left(rot\vec{H} = \vec{G} \right) \tag{2.1}$$

The line integral of the magnetic force along a closed loop is equal to the enveloped current linkage.
All *w* turns per winding carry single currents *I*, being of the same value each. In electrical machines, the magnetic circuit is subdivided into quasi-homogeneous parts (stator-yoke + stator teeth, rotor-yoke + rotor teeth, air gap).

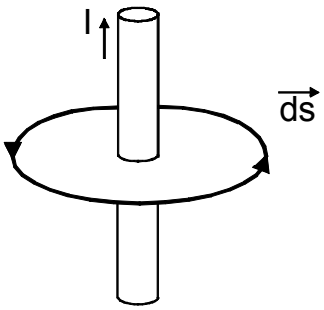

Fig. 2: circulation sense

$$\sum_i H_i \cdot s_i = w \cdot I \tag{2.2}$$

Direction convention:
Current linkage and direction of the line integral are arranged to each other, as shown on the left.
Hint: right hand directions: thump = current(-linkage), bent fingers = direction of the line integral (Fleming's Right-Hand-Rule).

A relation between magnetic force *H* and magnetic flux density *B* is given by the permeability m , a magnetic material attribute:

$$B = m \cdot H \qquad m = m_r \cdot m_0 \tag{2.3}$$

Magnetic constant (permeability of the vacuum):

$$m_0 = 4 \cdot p \cdot 10^{-7} \frac{\mathrm{V \cdot s}}{\mathrm{A \cdot m}} \tag{2.4}$$

Relative permeability:

$$m_r = 1 \qquad \text{in vacuum} \tag{2.5}$$

$$m_r = 1 \cdots 10000 \qquad \text{in iron (ferromagnetic material)} \tag{2.6}$$

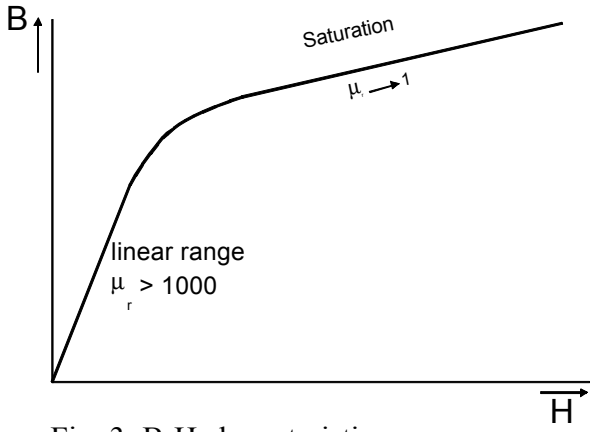

Fig. 3: B-H characteristic

magnetization characteristic

$$B = f(H) \tag{2.7}$$

non-linear coherence

$$m_r = f(H) \tag{2.8}$$

The magnetic field is zero-divergenced (no sinks or sources).

$$div\vec{B} = 0 \tag{2.9}$$

Its effect is described as the area integral of the flux density:

$$f = \iint_A \vec{B} \cdot d\vec{A} \tag{2.10}$$

The magnetic flux f represents the effect of the total field. In case of a homogeneous field distribution and an orientation as per $\vec{A} \parallel \vec{B}$, equation 2.10 simplifies to:

$$f = A \cdot B \tag{2.11}$$

2.1.2 Second Maxwell-Equation (Faraday's Law)

Second Maxwell Equation is given in its integral and differential form as follows:

$$\oint_c \vec{E} \cdot d\vec{s} = -\frac{df}{dt} \qquad \left(rot\vec{E} = -\frac{d\vec{B}}{dt} \right) \tag{2.12}$$

The line integral of the electric force $\vec{E}$ along a closed loop (which matches voltage) is equal to the variation of the magnetic flux linkage with time.

In electrical machines *w* turns per winding are passed through by the magnetic flux f.

$$y = w \cdot f = L \cdot i, \qquad u_i = -w \cdot \frac{df}{dt} \tag{2.13}$$

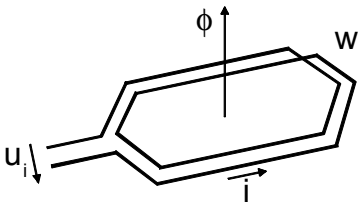

Fig. 4: flux linkage, voltage

Direction conventions:

- Magnetic flux and current are arranged to each other according to Fleming's Right-Hand-Rule (see also 2.1.1).
- An induced current flows in a direction to create a magnetic field which will counteract the change in magnetic flux (Lenz's Law).

The flux linkage of a coil is a function of *x* and *i*: *y (x,i)*. Depending on the way the change of the flux linkage being required for the induction process is caused, the according voltage is called transformer voltage or rotational voltage (transformer e.m.f. or rotational e.m.f.).

$$u_i = -\frac{d}{dt}y\left(x,i\right) = -\underbrace{\frac{\partial y}{\partial i}}_{L}\cdot\frac{di}{dt} - \frac{\partial y}{\partial x}\cdot\underbrace{\frac{dx}{dt}}_{v} = -L\cdot\frac{di}{dt} - B\cdot l\cdot v \tag{2.14}$$

Convention of the rotational voltage:

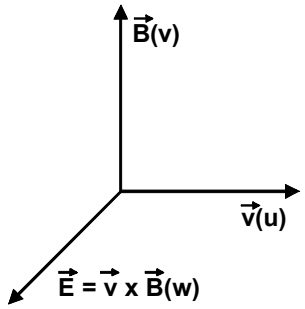

Fig. 5: directions of 2.15

$$u_i = \left(\vec{v}\times\vec{B}\right)\cdot\vec{l} = \vec{E}\cdot\vec{l} \tag{2.15}$$

assumed for the case with direction of the field-vector (v) being arranged orthographic towards the direction of the speed-vector (u) of the conductor (uvw direction convention).

2.1.3 Lorentz Force Law

2.1.3.1 Lorentz Force

A force on a current-carrying conductor in presence of a magnet field is given by:

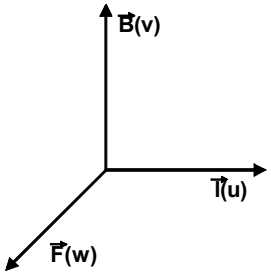

Fig. 6: directions of 2.16

$$F = I\cdot\left(\vec{\mathrm{l}}\times\vec{\mathrm{B}}\right) \tag{2.16}$$

In case of field-vector and direction of the conductor including a right angle (90°), due to the uvw direction convention, equation 2.16 simplifies to:

$$F = I\cdot l\cdot B \tag{2.17}$$

Magnetic Force

A magnetic force appears at the surface between iron and air.

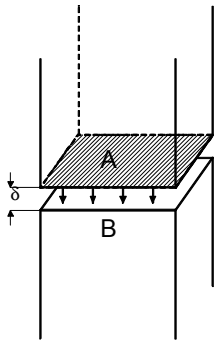

Fig. 7: magnetic force

Tractive force of an electromagnet:

$$F = \frac{B^2}{2m_0} A \tag{2.18}$$

2.1.3.2 Force caused by variation of magnetic energy

For the determination of forces and torques exerted on machine parts, a calculation embracing the variation of the magnetic energy is practical, linear systems assumed.

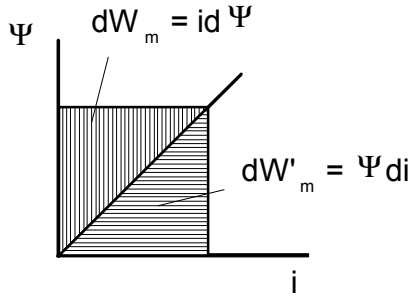

$$F = \left.\frac{\partial W_m}{\partial x}\right|_{i=const} \tag{2.19}$$

with $x = a \cdot r$

$$M = F \cdot r = \frac{\partial W_m}{\partial a} \tag{2.20}$$

Fig. 8: magnetic energy in linear systems

The calculation of exerted force in non-linear systems requires the determination comprising the variation of the magnetic co-energy.

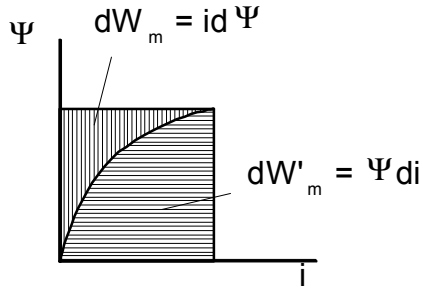

$$F = \frac{\partial W`_m}{\partial x} \tag{2.21}$$

Fig. 9: magnetic energy in non-linear systems

2.2 Reference-Arrow systems

An unambiguous description of conditions in electrical networks requires voltages, currents and powers to be assigned to their accordant positive and negative directions - the choice of the direction is arbitrary, but non-recurring and definite. A negative signed result means a variable, assumed as of opposite reference-arrow direction.

A choice of two possible reference-arrow systems for voltage, current and power are provided:

Load reference-arrow system (VZS)

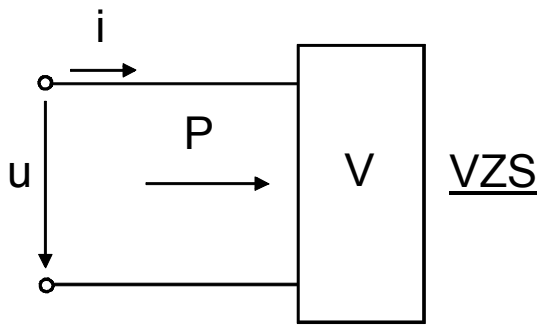

Fig. 10a: VZS

Voltage- and current-arrow of same orientation *at load*, power is absorbed.

Generator reference-arrow system (EZS)

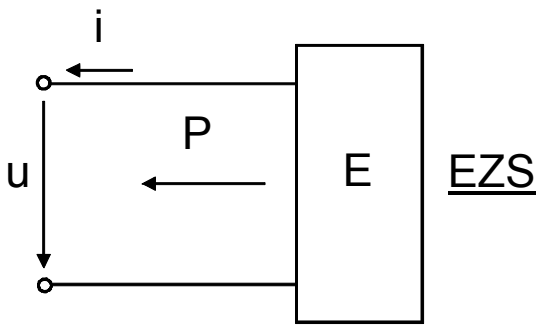

Fig. 10b: EZS

Voltage- and current-arrow of opposite orientation *at source*, power is delivered.

VZS
voltage drop

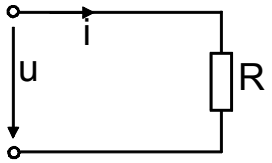

$$u = i \cdot R$$

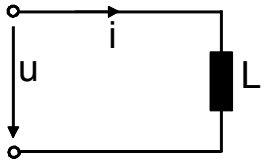

$$u = L \cdot \frac{di}{dt}$$

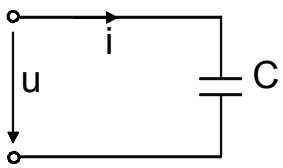

$$u = \frac{1}{C} \int i \cdot dt$$

Fig. 11a-13a: VZS directions at R, L, C components

EZS
voltage generation

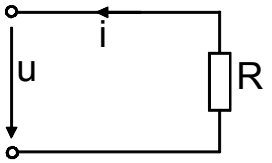

$$u = -i \cdot R$$

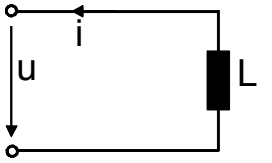

$$u = -L \cdot \frac{di}{dt}$$

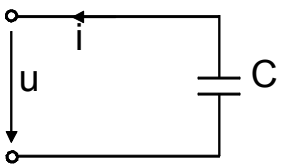

$$u = -\frac{1}{C} \int i \cdot dt$$

Fig. 11b-13b: EZS directions at R, L, C components

The Poynting-Vector defines the power density in electromagnetic fields:

$$\vec{S} = \vec{E} \times \vec{H} \tag{2.22}$$

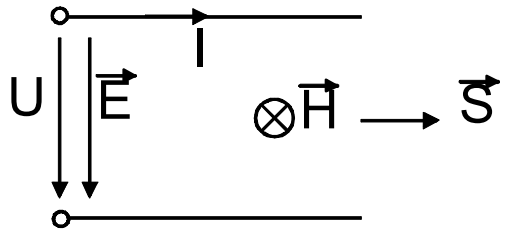

Fig. 14a: power (-density) in VZS

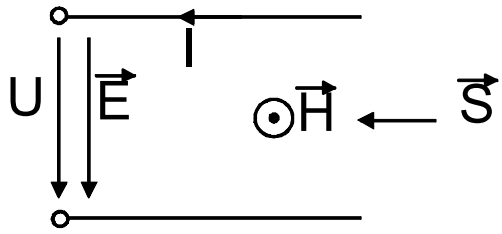

Fig. 14b: power (-density) in EZS

A definition of the positive directions of current and voltage according the energy flow is proved practical.
This is illustrated by the example of a simple DC machine (see below).

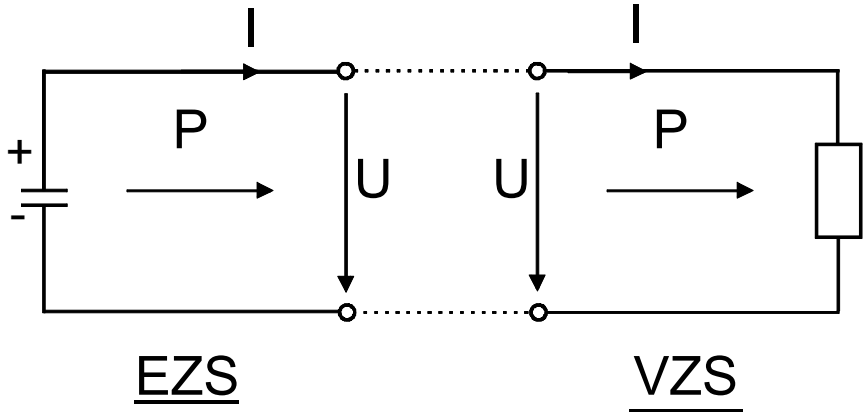

Fig. 15: sample of energy flow (DC machine)

2.3 Average value, rms value, efficiency

On the one hand the knowledge of the instantaneous value is important for the evaluation of according variables. On the other hand a reflection over a longer range of time (e.g. an entire cycle) is of importance, e.g. when determining peak value, average value or rms value (rms=root mean square). Common literature knows different appearances of variables and values. In this script assignments for voltage and current are chosen as follows:

- capital letters for constant variables
- lower case letters for variables variating with time.

Magnetic und mechanic variables, such as e.g. magnetic field and force, are always represented in capital letters. Peak values are usually used for magnetic variables, whereas electric variables appear as rms value.

Further definitions to be used in the following:

- instantaneous value $u = u(t)$ — time-variant variable at instant *t*
- average value: $\overline{U} = \frac{1}{T} \cdot \int_0^T u(t) \cdot dt$ — variable, averaged over a certain period
- rms value: $U = \sqrt{\frac{1}{T} \cdot \int_0^T u^2(t) \cdot dt}$ — square-root of averaged square value
- complex quantity: $\underline{U} = U \cdot e^{j \cdot j}$ — complex representation of sinusoidal variables
- peak value: $\hat{U}$ — maximum value of a periodical function ($= \sqrt{2} \cdot U$ for sinusoidal functions)
- efficiency: $h = \frac{P_{ab}}{P_{auf}}$ — ratio of delivered and absorbed power

2.4 Applied complex calculation on AC currents

In the field of power engineering time variant sinusoidal AC voltages and currents usually appear as complex rms value phasors.

$$u = \sqrt{2} \cdot U \cdot \cos(w \cdot t) = \mathrm{Re}\left\{\sqrt{2} \cdot U \cdot e^{j \cdot w \cdot t}\right\} = \mathrm{Re}\left\{\sqrt{2} \cdot \underline{U} \cdot e^{j \cdot w \cdot t}\right\};\ \underline{U} = U \cdot e^{j \cdot 0} \tag{2.23}$$

$$i = \sqrt{2} \cdot I \cdot \cos(w \cdot t - j) = \mathrm{Re}\left\{\sqrt{2} \cdot I \cdot e^{j \cdot w \cdot t} \cdot e^{-j \cdot j}\right\} = \mathrm{Re}\left\{\sqrt{2} \cdot \underline{I} \cdot e^{j \cdot w \cdot t}\right\};\ \underline{I} = I \cdot e^{-j \cdot j} \tag{2.24}$$

Complex power results from the multiplication of the complex voltage rms value and the conjugate complex rms value of the accordant current:

apparent power: $\underline{S} = \underline{U} \cdot \underline{I}^{*} = P + j \cdot Q \qquad \left(\underline{I}^{*} = I \cdot e^{+j \cdot j}\right)$ (2.25)

active power: $P = U \cdot I \cdot \cos j$ (2.26)

reactive power: $Q = U \cdot I \cdot \sin j$ (2.27)

Complex impedance (phasor, amount, phase angle) are determined by:

$$\underline{Z} = R + j \cdot X = Z \cdot e^{j \cdot j} \quad ; \quad Z = \sqrt{R^2 + X^2} \quad ; \quad \tan j = \frac{X}{R} \tag{2.28}$$

In contrast to the common mathematical definition, the real axis of a complex coordinate system is upward orientated and the imaginary axis points to the right in power engineering presentations. The voltage phasor is defined as to be in parallel to the real axis. Thus the direction of the current phasor follows as shown in Fig. 15:

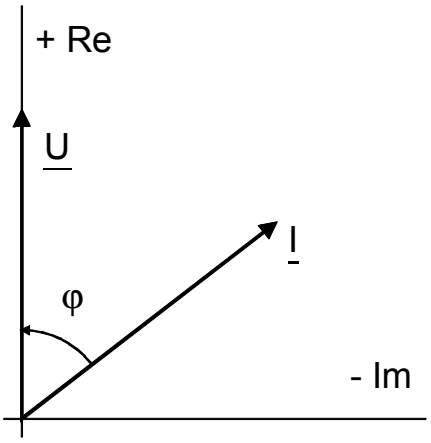

Fig. 15: complexe coordinate system

$$\underline{I} = \frac{\underline{U}}{\underline{Z}} = \frac{U}{Z} \cdot e^{-j \cdot j} \tag{2.29}$$

complex rms value phasor

The phase angle j points <u>from</u> the current phasor <u>to</u> the voltage phasor.

VZS

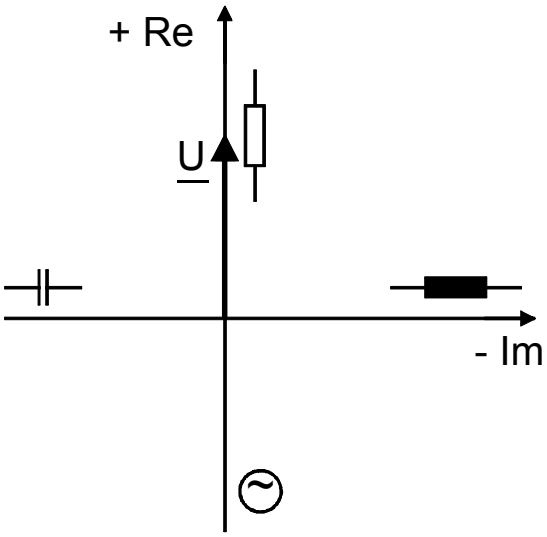

Fig. 16a: components in VZS

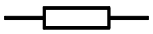

$$\underline{I} = \frac{\underline{U}}{\underline{R}}$$

active power input

$$\underline{I} = \frac{\underline{U}}{j \cdot w \cdot L} = -j \cdot \frac{\underline{U}}{w \cdot L}$$

absorption of lagging reactive power

$$\underline{I} = j \cdot w \cdot C \cdot \underline{U}$$

absorption of leading reactive power

active power output

EZS

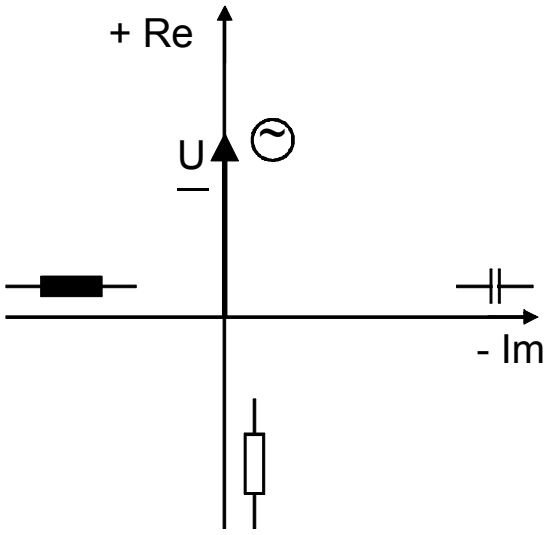

Fig. 16b: components in EZS

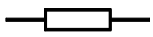

$$\underline{I} = -\frac{\underline{U}}{\underline{R}}$$

active power input

$$\underline{I} = -\frac{\underline{U}}{j \cdot w \cdot L} = j \cdot \frac{\underline{U}}{w \cdot L}$$

absorption of lagging reactive power = delivery of leading reactive power

$$\underline{I} = -j \cdot w \cdot C \cdot \underline{U}$$

absorption of leading reactive power= delivery of lagging reactive power

active power output

2.5 Methods of connection (three-phase systems)

Applications in power engineering often use three-phase systems: *m = 3*
Typical arrangements of balanced three-phase systems without neutral conductor:

star connection (y, Y) (Fig. 17a)

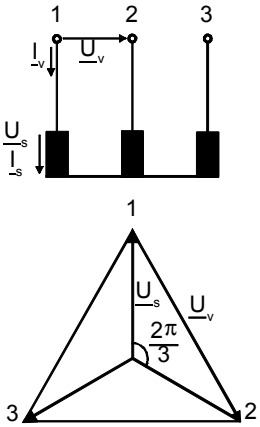

delta connection $(\Delta, \mathrm{d}, \mathrm{D})$ (Fig. 17b)

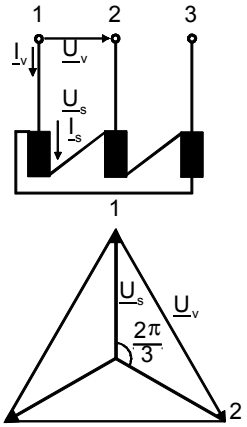

phase quantities (subscript „*s*“)

U_S, I_S	U_S, I_S
$\sum I_S = 0$	$\sum U_S = 0$

linked quantities (subscript „*v*“)

$U_v = \sqrt{3} \cdot U_S$	$I_v = \sqrt{3} \cdot I_S$
$I_v = I_S$	$U_v = U_S$

power is always defined as

$S = 3 \cdot U_S \cdot I_S = 3 \cdot \frac{U_v}{\sqrt{3}} \cdot I_v$	$S = 3 \cdot U_S \cdot I_S = 3 \cdot \frac{I_v}{\sqrt{3}} \cdot U_v$

$$S = \sqrt{3} \cdot U_v \cdot I_v = \sqrt{3} \cdot U \cdot I$$

Since rating plate data is always given as linked quantities, usually the subsript „*y*“ does not appear in the power equation!

Transformation star connection ↔ delta connection:

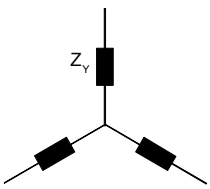

$$Z_Y = \frac{U_S}{I_S} = \frac{U_v / \sqrt{3}}{I_v} \tag{2.30}$$

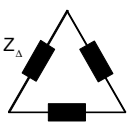

$$Z_\Delta = \frac{U_S}{I_S} = \frac{U_v}{I_v / \sqrt{3}} \tag{2.31}$$

Fig. 18: star/delta connection

Eqt. 2.30 and 2.31 lead to (equal values of *U* and *I* assumed): $Z_\Delta = 3 \cdot Z_Y$ (2.32)

2.6 Symmetrical components

In case of unbalanced load of a balanced three-phase system, caused by e.g.:

- supply with unbalanced voltages
- single-phase load between two phases or between one phase and neutral conductor,

the method of symmetrical components is suitable for a systematic processing.

An occurring unbalanced three-phase system is split up into three symmetrical systems (positive/negative/zero phase sequence system). Based on this subdivision, the network is to be calculated separately for each of these systems. The superposition of the single results is equal to the total result (addition $\Rightarrow$ linearity!).

Therefore the complex phasor $\underline{a}$ is utilized:

$$\underline{a} = e^{j\frac{2p}{3}}; \qquad \underline{a}^2 = e^{j\frac{4p}{3}} = e^{-j\frac{2p}{3}}; \qquad 1 + \underline{a} + \underline{a}^2 = 0;$$

$\underline{a}$ resp. $\underline{a}^2$ are supposed to express a time displacement of $wt = \frac{2p}{3}$ resp. $\frac{4p}{3}$.

Fig. 19 shows an unbalanced three-phase system to be split up into three symmetrical systems:

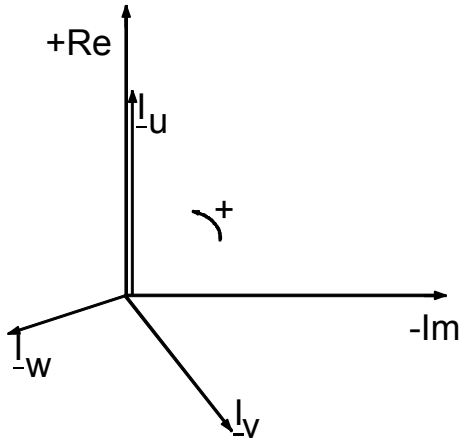

Fig. 19a-d: unbalanced system, split up, symmetrical systems

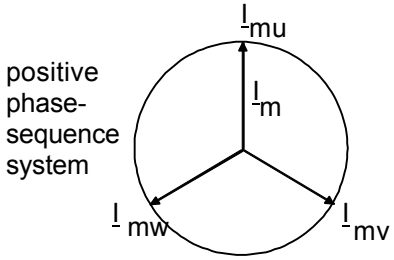

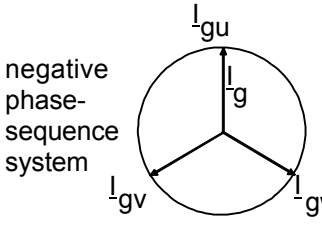

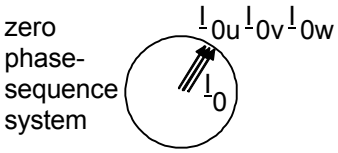

Fig. 19b: positive- (m) Fig. 19c: negative- (g) Fig. 19d: zero-sequence system (0)

$$\underline{I}_{mu} = \underline{I}_m \qquad \underline{I}_{gu} = \underline{I}_g \qquad \underline{I}_{0u} = \underline{I}_{0v} = \underline{I}_{0w} = \underline{I}_0$$

$$\underline{I}_{mv} = \underline{a}^2 \underline{I}_m \qquad \underline{I}_{gv} = \underline{a}\underline{I}_g$$

$$\underline{I}_{mw} = \underline{a}\underline{I}_m \qquad \underline{I}_{gw} = \underline{a}^2 \underline{I}_g$$

Each single current (phases u, v, w) is represented by three components (m, g, 0):

$$\underline{I}_u = \underline{I}_{mu} + \underline{I}_{gu} + \underline{I}_{0u} \tag{2.33}$$

$$\underline{I}_v = \underline{I}_{mv} + \underline{I}_{gv} + \underline{I}_{0v} \tag{2.34}$$

$$\underline{I}_w = \underline{I}_{mw} + \underline{I}_{gw} + \underline{I}_{0w} \tag{2.35}$$

Insertion of the definitions (due to Fig. 19b-d) results in:

$$\begin{pmatrix} \underline{I}_u \\ \underline{I}_v \\ \underline{I}_w \end{pmatrix} = \begin{pmatrix} 1 & 1 & 1 \\ \underline{a}^2 & \underline{a} & 1 \\ \underline{a} & \underline{a}^2 & 1 \end{pmatrix} \begin{pmatrix} \underline{I}_m \\ \underline{I}_g \\ \underline{I}_0 \end{pmatrix} \tag{2.36}$$

Hence follows by solving matrix 2.36:

$$\begin{pmatrix} \underline{I}_m \\ \underline{I}_g \\ \underline{I}_0 \end{pmatrix} = \frac{1}{3} \begin{pmatrix} 1 & \underline{a} & \underline{a}^2 \\ 1 & \underline{a}^2 & \underline{a} \\ 1 & 1 & 1 \end{pmatrix} \begin{pmatrix} \underline{I}_u \\ \underline{I}_v \\ \underline{I}_w \end{pmatrix} \tag{2.37}$$

With set 2.37 voltage equations can be established:

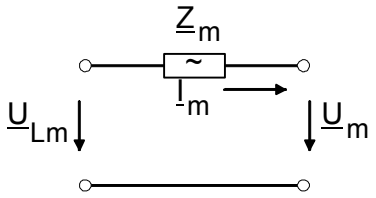

Fig. 20a

$$\underline{U}_m = \underline{U}_{Lm} - \underline{Z}_m \underline{I}_m \tag{2.38}$$

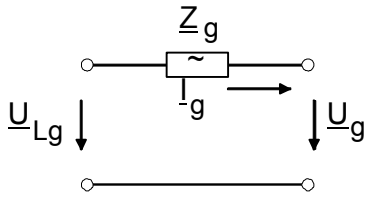

Fig. 20b

$$\underline{U}_g = \underline{U}_{Lg} - \underline{Z}_g \underline{I}_g \tag{2.39}$$

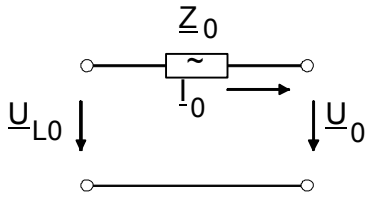

Fig. 20c

$$\underline{U}_0 = \underline{U}_{L0} - \underline{Z}_0 \underline{I}_0 \tag{2.40}$$

Usually the supply is provided by a symmetrical three-phase system. Then follows:

$$\underline{U}_{LM} = \underline{U}_L \tag{2.41}$$

$$\underline{U}_{Lg} = 0 \tag{2.42}$$

$$\underline{U}_{L0} = 0 \tag{2.43}$$

After calculation of the positive, negative and zero sequence voltage components, the wanted phase voltages (u, v, w) can be determined by inverse transformation:

$$\begin{pmatrix} \underline{U}_u \\ \underline{U}_v \\ \underline{U}_w \end{pmatrix} = \begin{pmatrix} 1 & 1 & 1 \\ \underline{a}^2 & \underline{a} & 1 \\ \underline{a} & \underline{a}^2 & 1 \end{pmatrix} \begin{pmatrix} \underline{U}_m \\ \underline{U}_g \\ \underline{U}_0 \end{pmatrix} \tag{2.44}$$

Equivalent to the case of an unbalanced load, the same process is to be applied in case of a given unsymmetrical power supply with demanded phase voltages.

3 Transformer

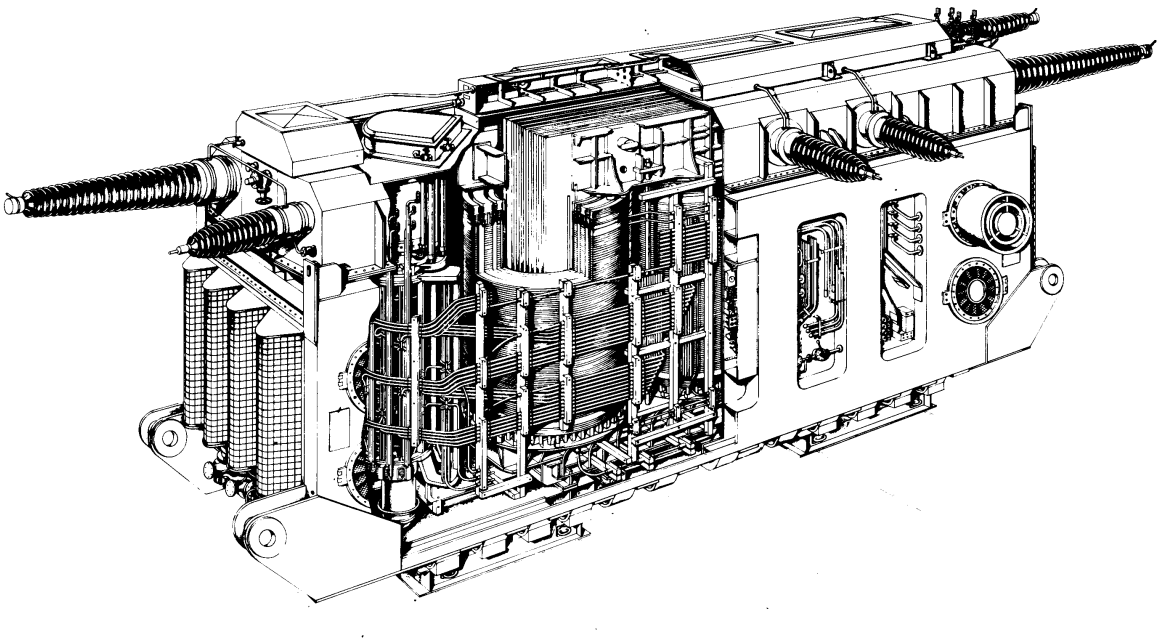

Fig. 21: three-phase transformer 150 MVA (ABB)

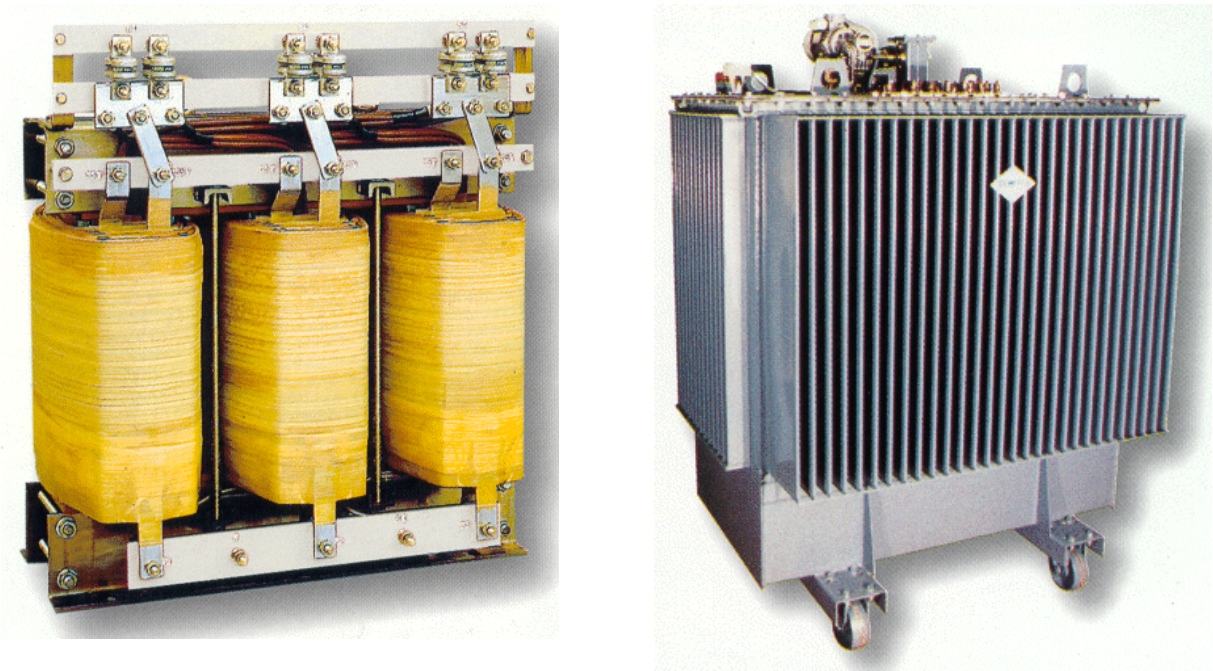

Fig. 22a/b: three-phase transformer 100 kVA (Ortea)

3.1 Equivalent circuit diagram

The general two-winding transformer is a linear system, consisting of two electric circuits.

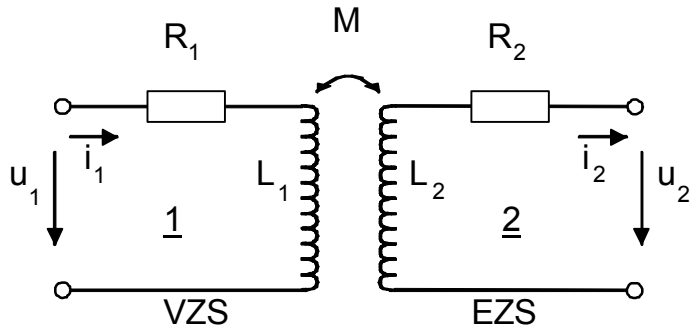

Fig. 23: transformer, general single phase equivalent circuit diagram

The ohmic resistances R_1 and R_2 as well as self-inductances L_1 und L_2 and the mutual inductance M can be measured between the terminals of the transformer. Neither the spatial distribution of the transformer arrangement, nor a definition of the number of turns is taken into account initially. Side 1 is defined to be subject to the load reference-arrow system (VZS), whereas side 2 is assigned to the generator reference-arrow system.

Thereby the voltage equations for both sides (1 and 2) appear as:

$$u_1 = R_1 i_1 + \frac{\mathrm{d}y_1}{\mathrm{d}t} \tag{3.1}$$

$$u_2 = -R_2 i_2 - \frac{\mathrm{d}y_2}{\mathrm{d}t} \tag{3.2}$$

with the accordant flux linkages:

$$y_1 = L_1 i_1 - M i_2 \tag{3.3}$$

$$y_2 = L_2 i_2 - M i_1 \tag{3.4}$$

Currents i_1 und i_2 magnetize in opposite direction, due to the real physical occurrence.

Disregarding ohmic resistances , the transformer voltage equations simplify to:

$$u_1 = L_1 \frac{\mathrm{d}i_1}{\mathrm{d}t} - M \frac{di_2}{dt} \tag{3.5}$$

$$u_2 = -L_2 \frac{\mathrm{d}i_2}{\mathrm{d}t} + M \frac{\mathrm{d}i_1}{\mathrm{d}t} \tag{3.6}$$

If the transformer is supplied from only one side, respective inductances for no-load and short-circuit can be determined:

	supply from side 1	supply from side 2
no-load	$i_2 = 0$ $u_1 = L_1 \frac{\mathrm{d}i_1}{\mathrm{d}t}$ (3.7)	$i_1 = 0$ $u_2 = -L_2 \frac{\mathrm{d}i_2}{\mathrm{d}t}$ (3.8)
short circuit	$u_2 = 0$ $\frac{\mathrm{d}i_2}{\mathrm{d}t} = \frac{M}{L_2}\frac{\mathrm{d}i_1}{\mathrm{d}t}$ (3.9) $u_1 = L_1 \frac{\mathrm{d}i_1}{\mathrm{d}t} - \frac{M^2}{L_2}\frac{\mathrm{d}i_1}{\mathrm{d}t}$ (3.10) $= L_1 \frac{\mathrm{d}i_1}{\mathrm{d}t}\left(1 - \frac{M^2}{L_1 L_2}\right)$ $= sL_1 \frac{\mathrm{d}i_1}{\mathrm{d}t}$	$u_1 = 0$ $\frac{\mathrm{d}i_1}{\mathrm{d}t} = \frac{M}{L_1}\frac{\mathrm{d}i_2}{\mathrm{d}t}$ (3.11) $u_2 = -L_2 \frac{\mathrm{d}i_2}{\mathrm{d}t} + \frac{M^2}{L_1}\frac{\mathrm{d}i_2}{\mathrm{d}t}$ (3.12) $= -L_2 \frac{\mathrm{d}i_2}{\mathrm{d}t}\left(1 - \frac{M^2}{L_1 L_2}\right)$ $= -sL_2 \frac{\mathrm{d}i_2}{\mathrm{d}t}$

Result: The ratio of short circuit and no-load inductance is equal to σ, independent from the choice of supply side. The variable σ is called Heyland factor.

$$s = 1 - \frac{M^2}{L_1 L_2} = \frac{L_k}{L_0} = \frac{I_0}{I_k}\bigg|_{u=\text{const}} \tag{3.13}$$

It turned out to be convenient, to use a general equivalent circuit diagram (ecd), with eliminated galvanic separation and only resistances and inductances to appear.

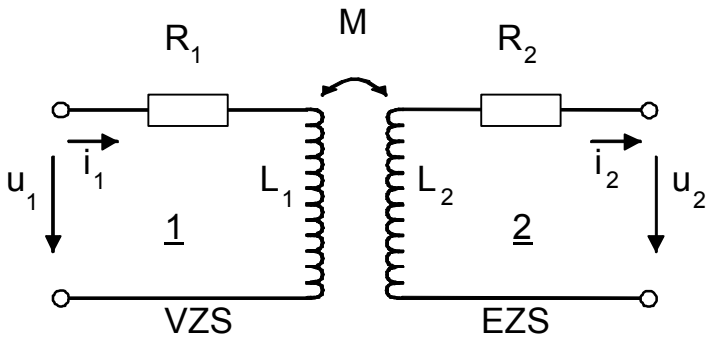

Fig. 24: ecd with galvanic separation

$$u_1 = R_1 i_1 + L_1 \frac{\mathrm{d}i_1}{\mathrm{d}t} - M \frac{\mathrm{d}i_2}{\mathrm{d}t} \tag{3.14}$$

$$u_2 = -R_2 i_2 - L_2 \frac{\mathrm{d}i_2}{\mathrm{d}t} + M \frac{\mathrm{d}i_1}{\mathrm{d}t} \tag{3.15}$$

Therefore an arbitrary variable *ü*, acting as actual transformation ratio is introduced. The derivation of *ü* is discussed later.

$$u_1 = R_1 i_1 + L_1 \frac{\mathrm{d}i_1}{\mathrm{d}t} - \ddot{u}M \frac{\mathrm{d}i_2 / \ddot{u}}{\mathrm{d}t} - \ddot{u}M \frac{\mathrm{d}i_1}{\mathrm{d}t} + \ddot{u}M \frac{\mathrm{d}i_1}{\mathrm{d}t} \tag{3.16}$$

$$\ddot{u}u_2 = -\ddot{u}^2 R_2 \frac{i_2}{\ddot{u}} - \ddot{u}^2 L_2 \frac{\mathrm{d}i_2 / \ddot{u}}{\mathrm{d}t} + \ddot{u}M \frac{\mathrm{d}i_1}{\mathrm{d}t} - \ddot{u}M \frac{\mathrm{d}i_2 / \ddot{u}}{\mathrm{d}t} + \ddot{u}M \frac{\mathrm{d}i_2 / \ddot{u}}{\mathrm{d}t} \tag{3.17}$$

There is a general transformation as follows:

$$u_2^* = \ddot{u}u_2 \quad , \quad i_2^* = \frac{i_2}{\ddot{u}} \quad , \quad R_2^* = \ddot{u}^2 R_2 \quad , \quad L_2^* = \ddot{u}^2 L_2 \tag{3.18}$$

The transformation is power invariant so that:

$$u_2^* i_2^* = u_2 i_2 \tag{3.19}$$

$$R_2^* i_2^{*2} = R_2 {i_2}^2 \tag{3.20}$$

$$\frac{1}{2} L_2^* i_2^{*2} = \frac{1}{2} L_2 {i_2}^2 \tag{3.21}$$

Based on equations 3.16-3.21 the following equation set can be established:

$$u_1 = R_1 i_1 + \left(L_1 - \ddot{u}M\right)\frac{\mathrm{d}i_1}{\mathrm{d}t} + \ddot{u}M\left(\frac{\mathrm{d}i_1}{\mathrm{d}t} - \frac{\mathrm{d}i_2^*}{\mathrm{d}t}\right) \tag{3.22}$$

$$u_2^* = -R_2^* i_2^* - \left(L_2^* - \ddot{u}M\right)\frac{\mathrm{d}i_2^*}{\mathrm{d}t} + \ddot{u}M\left(\frac{\mathrm{d}i_1}{\mathrm{d}t} - \frac{\mathrm{d}i_2^*}{\mathrm{d}t}\right) \tag{3.23}$$

These equations (3.22, 3.23) form the basis of the T-ecd as the general transformer ecd:

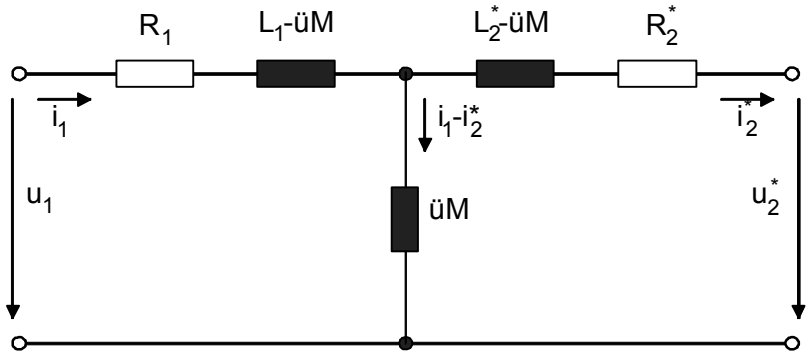

Fig. 24: T-ecd as general transformer ecd

3.2 Definition of the transformation ratio (*ü*)

Two opportunities for the definition of the transformation ratio *ü* need to be discussed.

3.2.1 ü=w1/w2, design data known

It is not possible to determine the ratio of $\frac{w_1}{w_2}$ by either rating plate data or by measuring. The definition of $ü = \frac{w_1}{w_2}$ is quite important for construction and calculation of transformers. It permits a distinction between leakage flux and working flux. This facilitates to take saturation of the used iron in the magnetic circuit into account. Using $ü = \frac{w_1}{w_2}$, a definition of variables arises as follows:

$L_1 - \frac{w_1}{w_2} M = L_{1s}$ leakage inductance on side 1

$\frac{w_1}{w_2} M = L_{1h}$ magnetizing inductance

$\left(\frac{w_1}{w_2}\right)^2 L_2 - \frac{w_1}{w_2} M = L_{2s}'$ leakage inductance on side 2

$\left(\frac{w_1}{w_2}\right)^2 L_2 = L_2'$

$\left(\frac{w_1}{w_2}\right)^2 R_2 = R_2'$

$\frac{w_1}{w_2} u_2 = u_2'$

$\frac{i_2}{\frac{w_1}{w_2}} = i_2'$

} variables converted to side 1 (using *ü*)

These replacements lead to the following voltage equations:

$$u_1 = R_1 i_1 + L_{1s} \frac{\mathrm{d}i_1}{\mathrm{d}t} + L_{1h} \frac{\mathrm{d}i_m}{\mathrm{d}t} \tag{3.24}$$

$$u_2' = -R_2' i_2' - L_{2s}' \frac{\mathrm{d}i_2'}{\mathrm{d}t} + L_{1h} \frac{\mathrm{d}i_m}{\mathrm{d}t} \tag{3.25}$$

with: $i_m = i_1 - i_2'$ (3.26)

and the accordant ecd:

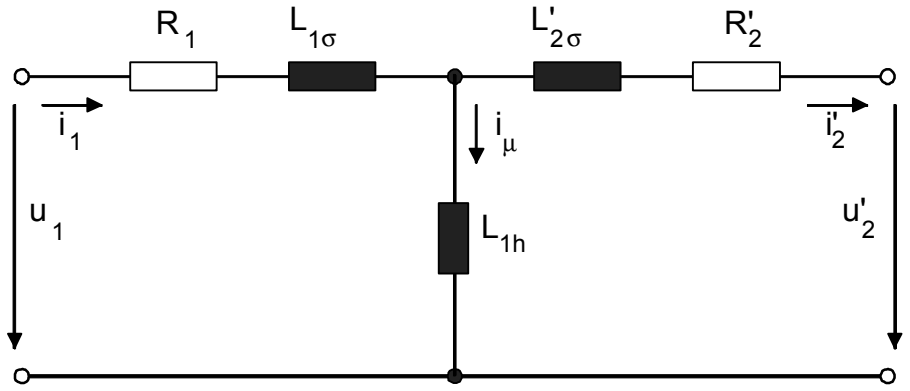

Fig. 25: T-ecd with converted elements

i_m is called the magnetizing current, exciting the working flux f_h, which is linked to both coils (on side 1 and 2):

$$w_1 f_h = L_{1h} i_m \tag{3.27}$$

If magnetic saturation is taken into account, L_{1h} is not of constant value, but dependent on i_m :

$$f_h = f(i_m) \qquad \text{(magnetization characteristic)} \tag{3.28}$$

Leakage flux fractions, linked to only one coil each are represented as leakage inductances L_{1s} und L_{2s}' , as shown on the horizontal branches in Fig. 25.:

$$w_1 f_{1s} = L_{1s} i_1 \tag{3.29}$$

$$w_1 f_{2s}' = L_{2s}' i_2' \qquad \text{(with reference to side 1)} \tag{3.30}$$

Leakage flux fractions always show linear dependencies on their exciting currents.

Definition of the leakage factor:

$$s_1 = \frac{f_{1s}}{f_{1h}} = \frac{L_{1s}}{L_{1h}} \tag{3.31}$$

$$s_2 = \frac{f_{2s}`}{f_{1h}} = \frac{L`_{2s}}{L_{1h}} \tag{3.32}$$

Equations 3.27-3.32 potentiate a description of the total flux in the magnetization circuit by distinguishing between working flux and leakage flux, excitet by currents through magentizing and leakage inductances:

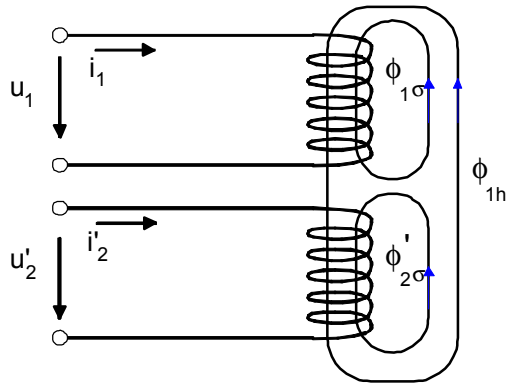

$$f_1 = f_{1h} + f_{1s} = (1+s_1) f_{1h} \tag{3.33}$$

$$f_2' = f_{1h} + f_{2s}` = (1+s_2) f_{1h} \tag{3.34}$$

$$L_1 = L_{1h} + L_{1s} = (1+s_1) L_{1h} \tag{3.35}$$

$$L_2' = L_{1h} + L_{2s}' = (1+s_2) L_{1h} \tag{3.36}$$

Fig. 26: working flux, leakage flux in magnetic circuit

Interrelation of inductances and leakage factor:

$$s = 1 - \frac{M^2}{L_1 L_2} = 1 - \frac{\ddot{u}^2 M^2}{L_1 \ddot{u}^2 L_2} = 1 - \frac{L_{1h}^2}{L_1 L_2'} \tag{3.37}$$

$$= 1 - \frac{1}{\frac{L_1}{L_{1h}} \cdot \frac{L_2'}{L_{1h}}} = 1 - \frac{1}{(1+s_1)(1+s_2)}$$

Complex rms value phasors are utilized for the description of steady state AC conditions. Thus voltage equations 3.24-3.25 can be depicted as:

$$\underline{U}_1 = R_1 \underline{I}_1 + jX_{1s} \underline{I}_1 + jX_{1h} \underline{I}_m \tag{3.38}$$

$$\underline{U}_2' = -R_2' \underline{I}_2' - jX_{2s}' \underline{I}_2' + jX_{1h} \underline{I}_m \tag{3.39}$$

$$\underline{I}_m = \underline{I}_1 - \underline{I}_2' \tag{3.40}$$

This leads to the accordant ecd as follows:

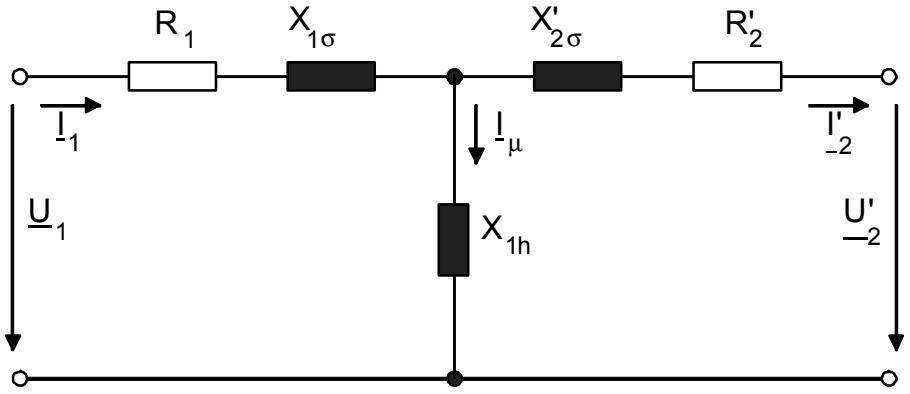

Fig. 27: ecd using complex rms value phasor designations

The ratio between both side 1 and side 2 no-load voltages is to be calculated as follows:

$$\underline{I}`_2 = 0 \qquad \text{d.h.} \qquad \underline{I}`_m = \underline{I}_{10} \tag{3.41}$$

$$\underline{U}_{10} = \underbrace{R_1 \underline{I}_{10}}_{=0} + j\left(X_{1s} + X_{1h}\right)\underline{I}_{10} \tag{3.42}$$

An occurring voltage drop at the resistor R_1 can be neglected (for $R_1 << X_{1h}$):

$$\underline{U}'_{20} = jX_{1h}\underline{I}_{10} \tag{3.43}$$

$$\frac{U_{10}}{U`_{20}} = \frac{U_{10}}{\ddot{u}U_{20}} = \frac{X_{1s} + X_{1h}}{X_{1h}} = 1 + s_1 \tag{3.44}$$

Voltage transformation ratio:

$$\frac{U_{10}}{U_{20}} = \frac{w_1}{w_2}\left(1 + s_1\right) \neq \frac{w_1}{w_2} \quad ! \tag{3.45}$$

$\frac{U_{10}}{U_{20}}$ is measureable due to VDE (see reference). Only if transformation ratio $\frac{w_1}{w_2}$ is known, equation 3.45 can be separated into $\frac{w_1}{w_2}$ and $\left(1 + s_1\right)$.

3.2.2 Complete phasor diagramm

With knowledge of the voltage equations 3.38-3.39 and appearing ecd elements the complete phasor diagram of the loaded transformer can be drawn.

With a given load of R_B and X_B, as well as voltage $\underline{U}_2$, current $\underline{I}_2$ results from:

$$\underline{I}_2 = \frac{\underline{U}_2}{R_B + jX_B} \tag{3.46}$$

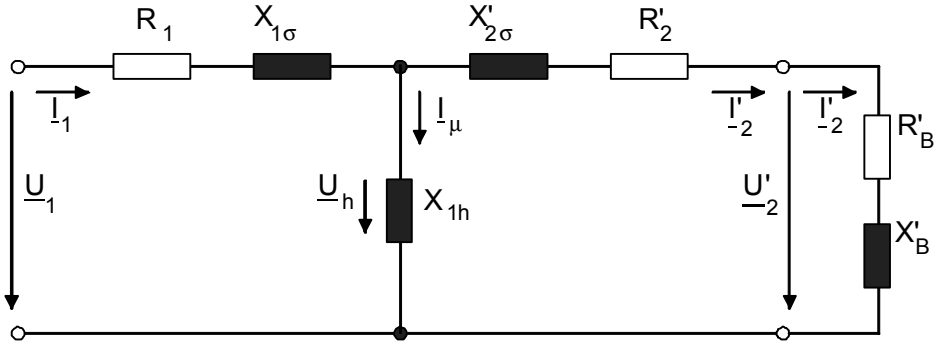

Fig. 28: ecd of loaded transformer

Hence $\underline{U}_2$‘ and $\underline{I}_2$’can be determined:

$$\underline{U}_2^{'} = \ddot{u}\underline{U}_2 \tag{3.47}$$

$$\underline{I}_2^{'} = \frac{\underline{I}_2}{\ddot{u}} \tag{3.48}$$

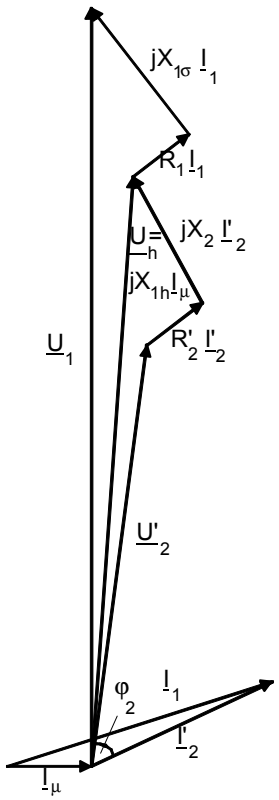

Fig. 29: phasor diagram

Voltage drops on R_2‘ and $X_{2\sigma}$‘ are vectorially added to $\underline{U}_2$‘:

$$\underline{U}`_2 + R_2`\underline{I}`_2 + jX`_{2s}\,\underline{I}`_2 = jX_{1h}\underline{I}_m = \underline{U}_h \tag{3.49}$$

$\underline{I}_\mu$ arises from the voltage drop on X_{1h}:

$$\underline{I}_m = \frac{\underline{U}_h}{jX_{1h}} = -j\frac{\underline{U}_h}{X_{1h}} \tag{3.50}$$

$\underline{I}_1$ is equal to the sum of $\underline{I}_2^{'}$ and $\underline{I}_m$:

$$\underline{I}_1 = \underline{I}_2^{'} + \underline{I}_m \tag{3.51}$$

The addition of voltage $\underline{U}_h$ and the voltage drops on R_1 and $X_{1\sigma}$ results in $\underline{U}_1$:

$$\underline{U}_h + R_1\underline{I}_1 + jX_{1s}\,\underline{I}_1 = \underline{U}_1 \tag{3.52}$$

Voltage drops on resistances and leakage inductances are illustrated oversized for a better understanding. In real transformer arrangements of power engineering application those voltage drops only amount a low percentage of the terminal voltage.

3.2.3 ü=U10/U20, measured value given

a) $\ddot{u}$ is defined as the voltage ratio in no-load condition on side 2 (with R_1=0).

$$\ddot{u} = \frac{U_{10}}{U_{20}} = (1+s_1)\frac{w_1}{w_2} = \frac{L_{1h}+L_{1s}}{L_{1h}\dfrac{w_2}{w_1}} = \frac{L_1}{M} \tag{3.53}$$

With $\ddot{u}$ chosen as in 3.53, the elements of the general transformer ecd:

$$L_1 - \ddot{u}M = 0 \tag{3.54}$$

$$\ddot{u}M = L_1 \tag{3.55}$$

$$L_2^* - \ddot{u}M = \frac{L_1^2}{M^2}L_2 - L_1 = L_1\left(\frac{L_1 L_2}{M^2} - 1\right) = L_1\left(\frac{1}{1-s} - 1\right) = L_1\frac{s}{1-s} \tag{3.56}$$

$$R_2^* = (1+s_1)^2\left(\frac{w_1}{w_2}\right)^2 R_2 = (1+s_1)^2 R_2' \tag{3.57}$$

$$u_2^* = (1+s_1)\frac{w_1}{w_2}u_2 = (1+s_1)u_2' \tag{3.58}$$

$$i_2^* = \frac{i_2}{(1+s_1)\frac{w_1}{w_2}} = \frac{i_2'}{1+s_1} \tag{3.59}$$

form the reduced (simplified) ecd:

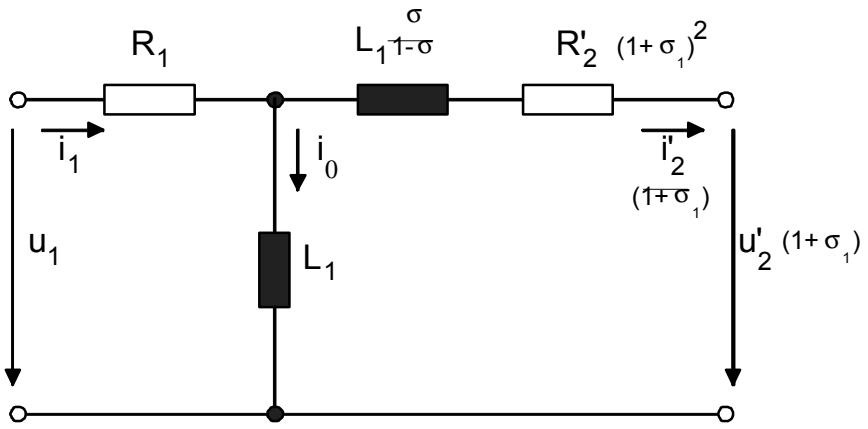

Fig. 30: reduced ecd of a transformer

$$i_1 - i_2^* = i_1 - \frac{i_2'}{(1+s_1)} = i_0 \qquad \text{(no-load current)} \tag{3.60}$$

With neglect of the magnetic saturation this ecd (Fig. 30) based on the definition $\ddot{u} = \frac{U_{10}}{U_{20}}$ is equal to the ecd based on $\ddot{u} = \frac{w_1}{w_2}$ (Fig. 27) concerning operational behaviour.

Since L_{1s} is set to $L_{1s} = 0$, the calculation is simplified. All elements of the ecd can be determined by measures. Therefore the described representation is also often used for rotating electrical machines.

The shunt arm current i_0 complies with the real no-load current if $R_1 = 0$ applies.

b) The definition of $\ddot{u}$ to be the voltage ratio at no-load condition on side 1 with $R_2 = 0$ shows equivalent results:

$$\ddot{u} = \frac{U_{10}}{U_{20}} = \frac{\frac{w_1}{w_2}}{(1+s_2)} = \frac{L_{1h}\frac{w_1}{w_2}}{(L_{1h}+L'_{2s})}$$
$$= \frac{L_{1h}\frac{w_2}{w_1}}{\left(\frac{w_2}{w_1}\right)^2 (L_{1h}+L'_{2s})} = \frac{M}{L_2} \tag{3.61}$$

This choice of $\ddot{u}$ leads to:

$$L_1 - \ddot{u}M = L_1 - \frac{M^2}{L_2} = L_1\left(1 - \frac{M^2}{L_1 L_2}\right) = sL_1 \tag{3.62}$$

$$\ddot{u}M = \frac{M^2}{L_2} = L_1\frac{M^2}{L_1 L_2} = L_1(1-s) \tag{3.63}$$

$$R_2^* = \left(\frac{w_1}{w_2}\right)^2 \frac{R_2}{(1+s_2)^2} = \frac{R'_2}{(1+s_2)^2} \tag{3.64}$$

$$u_2^* = \frac{w_1}{w_2}\frac{u_2}{(1+s_2)} = \frac{u'_2}{1+s_2} \tag{3.65}$$

$$i_2^* = \frac{i_2}{\frac{w_1}{w_2}}(1+s_2) = i'_2(1+s_2) \tag{3.66}$$

an ecd which is also used for rotating electrical machines.

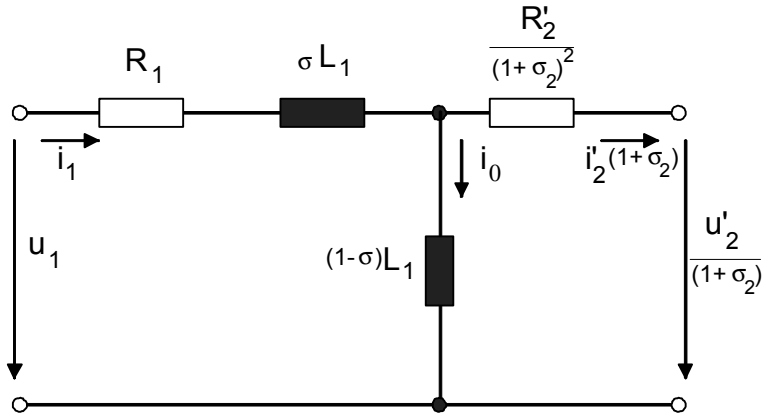

Fig. 31: ecd for alternative definition of $\ddot{u}$ (due to b.))

no-load current

$$i_1 - i_2^* = i_1 - i'_2(1+s_2) = i_0 \tag{3.67}$$

There are other opportunities left, expressing $\ddot{u}$, which are not subject to further discussion.

3.3 Operational behavior

Four essential working points need to be discussed. Those are named as follows:

- no-load condition
- short-circuit condition
- load with nominal stress
- parallel connection

3.3.1 No-load condition

The operational behavior of a transformer in no-load condition is characterized similiarily like an iron-cored reactor with ohmic resistance. Occurring losses are caused by magnetic reversal in iron parts and also in windings by Joulean heat.

Iron losses compose of two different physical effects:

- Eddy-current losses caused by alternating flux.

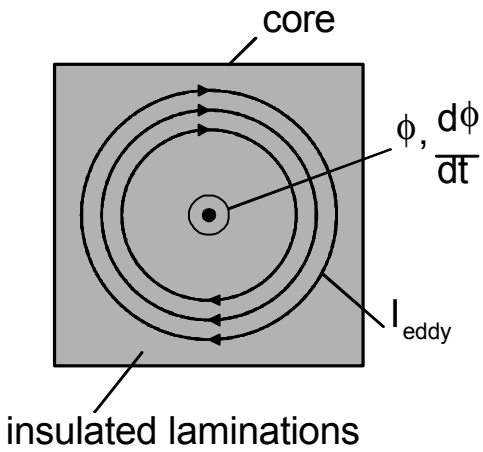

An induced current flows in a direction to create a magnetic field which will counteract the change in magnetic flux (Lenz's Law, see also 2.1.2). Eddy-current losses emerge as:

$$V_W \sim B^2 f^2 \tag{3.68}$$

Those can be reduced by using isolated, laminated iron for the core and by admixture of Silicon to the alloy, increasing the specific resistance.

Fig. 32: eddy current

- Hysteresis losses, caused by magnetic reversal.

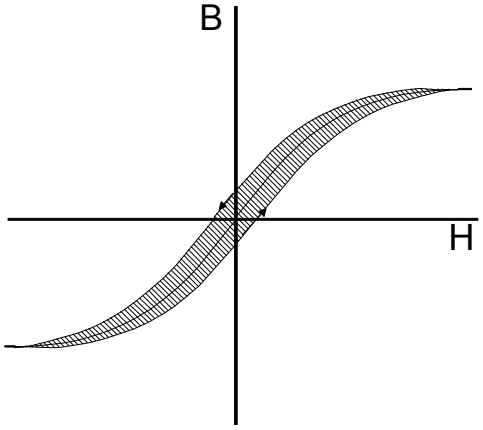

The amount of occurring hysteresis losses is proportional to the enclosed area surrounded in a cycle of the hysteresis loop:

$$V_H \sim B^2 f \tag{3.69}$$

Therefore magnetically soft material with narrow hysteresis loop width is used for transformers.

Fig. 33: hysteresis loop

The specific iron losses of electric sheet steel is specified in W/kg at 1,5 T and 50 Hz.

Iron losses can be taken into account by using resistance R_{Fe}, arranged in parallel to the magnetiziation reactance X_{1h}. Joulean losses at no-load operation are regarded with R_1.

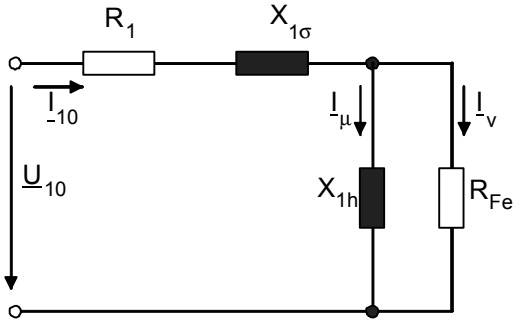

Fig. 34: ecd, regarding losses

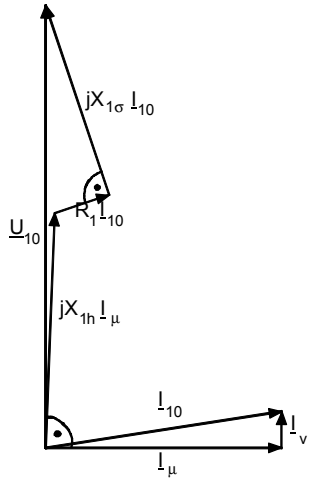

Fig. 35: phasor diagram regarding losses

The no-load current I_{10} is fed into the primary windings. It is composed of the magnetizing current I_μ and the current fraction I_V responsible for iron losses.

3.3.2 Short-circuit

The high-resistive shunt arm, including X_{1h} and R_{Fe} can be neglected in short circuit operation $\left(X_{1h}, R_{Fe} >> R_2^{'}\right)$. With that assumption, the equivalent circuit diagram (ecd) appears as:

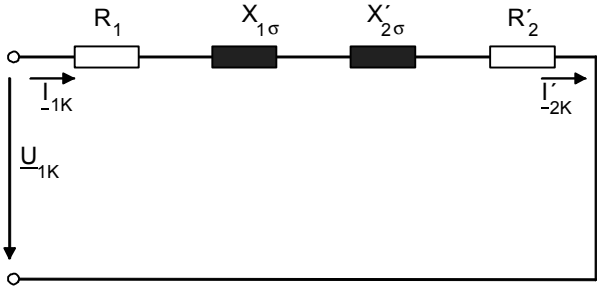

Fig. 36: short-circuit ecd of an transformer

$$\underline{U}_2^{'} = 0 \tag{3.70}$$

$$\underline{I}_{2K}^{'} = \underline{I}_{1K} \tag{3.71}$$

All resistances and leakage reactances are combined to a short-circuit impedance, referred to side 1:

$$R_{1K} = R_1 + R_2^{'} \tag{3.72}$$

$$X_{1K} = X_{1s} + X_{2s}^{'} \tag{3.73}$$

$$Z_{1k} = \sqrt{R_{1K}^2 + X_{1K}^2}, \quad \tan j_K = \frac{X_{1K}}{R_{1K}} \tag{3.74}$$

Also in short-circuit operation the response of a transformer is equal to an iron-cored reactor with ohmic resistance. Mind $Z_{1K} << Z_{10}$ in this case!

Short-circuit measurement with nominal current due to VDE regulations:

Short-circuit voltage U_{1k} is called the voltage to appear at nominal current and nominal frequency on the input side, if the output side is short-circuited (terminals connected without resistance):

$$U_{1K} = Z_{1K} I_{1N} \tag{3.75}$$

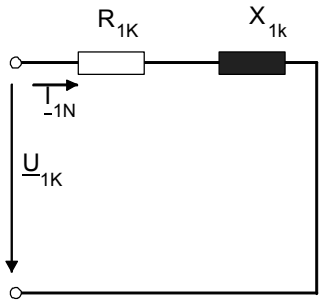

Fig. 37: short-circuit ecd

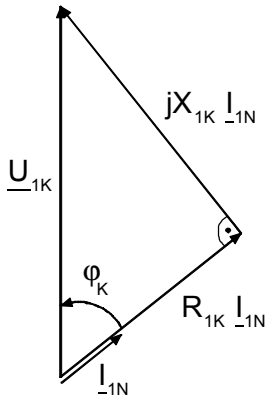

Fig. 38: phasor diagram

For a reasonable comparison of transformers of different sizes and power ratings, a variable called “relative short circuit voltages” is introduced. These are short circuit voltage values normalized to the nominal voltage.

$$u_K = \frac{U_{1K}}{U_{1N}} = \frac{Z_{1K} I_{1N}}{U_{1N}} \qquad \text{(in practice} \approx 0{,}05 - 0{,}1) \tag{3.76}$$

$$u_R = \frac{R_{1K} I_{1N}}{U_{1N}} \qquad (3.77); \qquad u_X = \frac{X_{1K} I_{1N}}{U_{1N}} \tag{3.78}$$

$$u_K = \sqrt{u_R^2 + u_X^2} \qquad (3.79); \qquad \tan j_K = \frac{u_X}{u_R} \tag{3.80}$$

Short-circuit current at nominal voltage is determined by:

$$\frac{I_{1K}}{I_{1N}} = \frac{\frac{U_{1N}}{Z_{1K}}}{I_{1N}} = \frac{1}{u_K} \qquad \text{(real} \approx 10 - 20) \tag{3.81}$$

3.3.3 Load with nominal stress

Due to relations applied in real transformers

$R : X_\sigma : X_h : R_{Fe} \approx 1 : 2 : 1000 : 10000$,

sufficient accuracy is reached with usage of the simplified ecd (shown in Fig. 39).

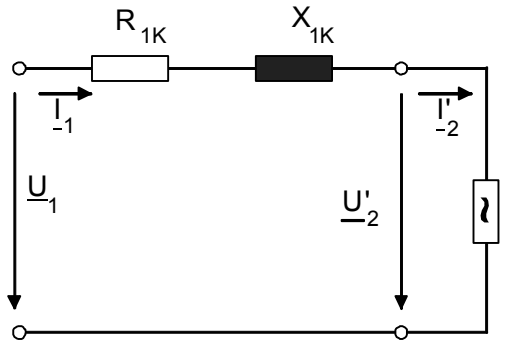

Fig. 39: simplified ecd (nominal stress)

This leads to a simplified phasor diagram (Fig. 40).
The input voltage U_1 and the terminal voltage U_2‘ (being referred to the input side) differ from an incremental vector, being hypotenuse of the Kapp’s triangle (see Fig. 40).
At constant frequency and constant current stress $\underline{I}_1$ the lengths of the triangle legs remain constant. Kapp’s triangle turns around the phasor tip of a given input voltage $\underline{U}_1$, dependent on the phase angle of the input current $\underline{I}_1$.
The voltage ratio depends on the type of load as follows

- ohmic – inductive load: $U_2‘ < U_1$ voltage reduction
- ohmic – capacitive load: $U_2‘ > U_1$ voltage increase

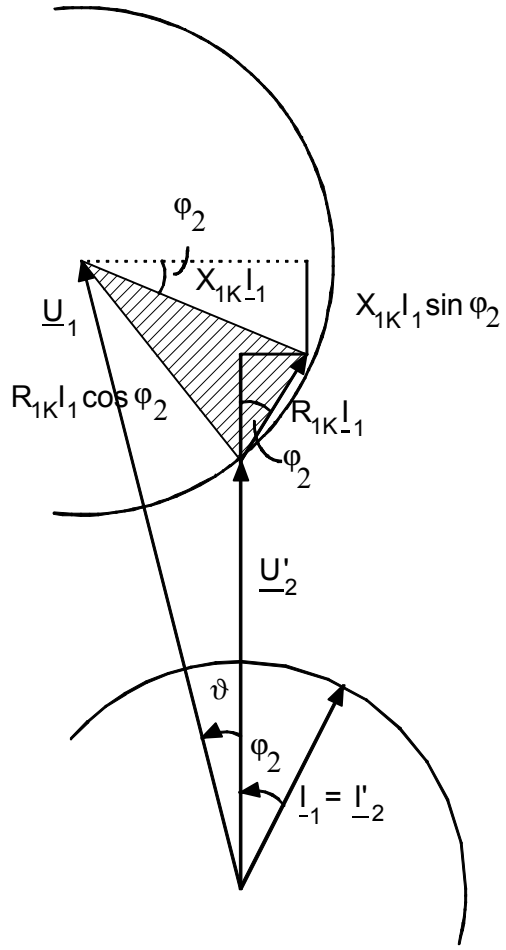

Fig. 40: simplified phasor diagramm, Kapp’s triangle

Determination of the relative voltage drop:

$$U_1 \cos J = U_2^{'} + R_{1K} I_1 \cos j_2 + X_{1K} I_1 \sin j_2 \tag{3.82}$$

with $\cos J \approx 1$ and $U_1 = U_{1N}$ follows:

$$\frac{U_{1N} - U`_2}{U_{1N}} = \frac{I_1}{I_{1N}} \left(\frac{R_{1K} I_{1N}}{U_{1N}} \cos j_2 + \frac{X_{1K} I_{1N}}{U_{1N}} \sin j_2 \right) \tag{3.83}$$

$$u_j = \frac{I_1}{I_{1N}} \left(u_R \cos j_2 + u_X \sin j_2 \right) \tag{3.84}$$

3.3.4 Parallel connection

Two variations of parallel connections need to be distinguished:

- network parallel connection: compensating networks are arranged between transformers connected in parallel – non-critical
- bus bar parallel connection: transformers are directly connected in parallel on the secondary side (output side).

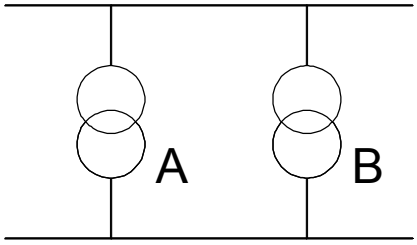

Fig. 41: transformers in parallel

In order to achieve a load balance according to the respective nominal powers it is of importance not to cause compensating currents.

Usage of the simplified equivalent circuit diagram, converted to output side values:

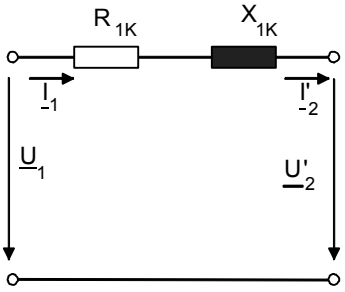

Fig. 42: conversion to side 2

$$\underline{I}_2 = \underline{I}_1 \ddot{u} \quad , \quad \underline{U}_{20} = \frac{\underline{U}_1}{\ddot{u}}$$

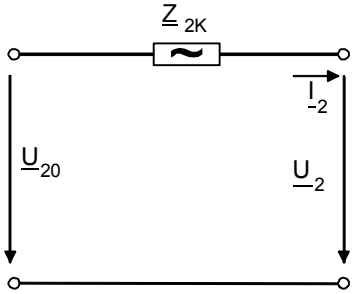

Fig. 43: impedance

$$\underline{Z}_{2K} = R_{2K} + jX_{2K} = \frac{R_1}{\ddot{u}^2} + R_2 + j\frac{X_{1s}}{\ddot{u}^2} + jX_{2s}$$

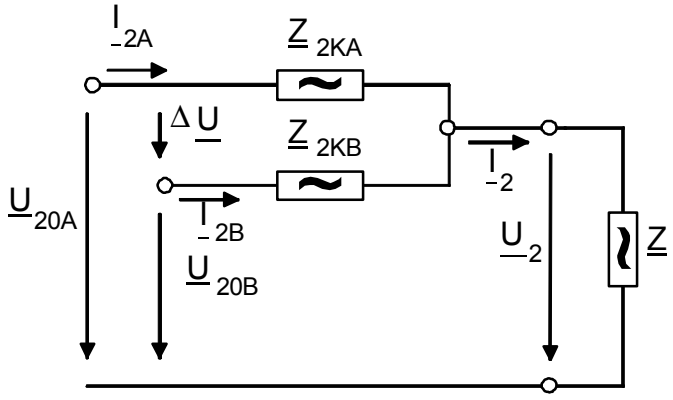

Fig. 44: parallel connection on output side

If $\Delta\underline{U} = \underline{U}_{20A} - \underline{U}_{20B} \neq 0$, compensating currents flow (already in no-load operation):

$$\underline{I}_{2A} = -\underline{I}_{2B} = \frac{\Delta\underline{U}}{\underline{Z}_{2KA} + \underline{Z}_{2KB}} \tag{3.85}$$

The no-load voltages of both transformers must be of the same value concerning amount and phase angle, in order to avoid compensating currents. That requires:

- same transformation ratio (*ü*)
- same connection of primary and secondary side, same vector group (three-phase transformers)

Condition $\Delta U = 0$ is taken as granted. The partition of the load currents is directly opposed to the short-circuit impedances. Load current ratio and short-circuit impedance ratio are reciprocal. The voltage drop at both short-circuit impedances must be the same for $\Delta U = 0$.

$$\frac{\underline{I}_{2A}}{\underline{I}_{2B}} = \frac{\underline{Z}_{2KB}}{\underline{Z}_{2KA}} = \frac{Z_{2KB}}{Z_{2KA}} e^{j(j_{KB} - j_{KA})} \tag{3.86}$$

In case of different short circuit phase angles, both load currents are phase displaced against each other.

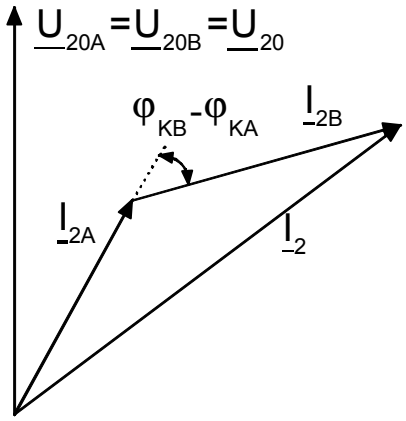

Fig. 45: phase shift of load currents

This results in a lower geometrical sum of the load currents compared to the arithmetical sum.

$$\frac{I_{2A} / I_{2AN}}{I_{2B} / I_{2BN}} = \frac{Z_{2KB}}{Z_{2KA}} \frac{I_{2BN} / U_{2N}}{I_{2AN} / U_{2N}} = \frac{u_{KB}}{u_{KA}} \tag{3.87}$$

The percental load shares react contrariwise to the relative short-circuit voltages. That means higher percental load for the transformer with lower u_k.

3.4 Mechanical construction

3.4.1 Design

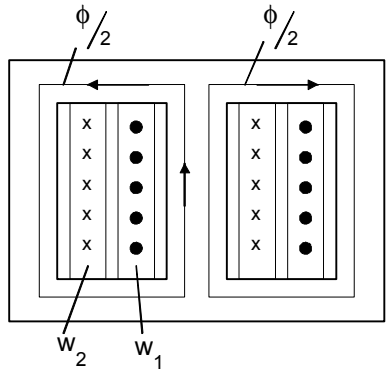

Fig. 46: shell-type transformer

low overall height

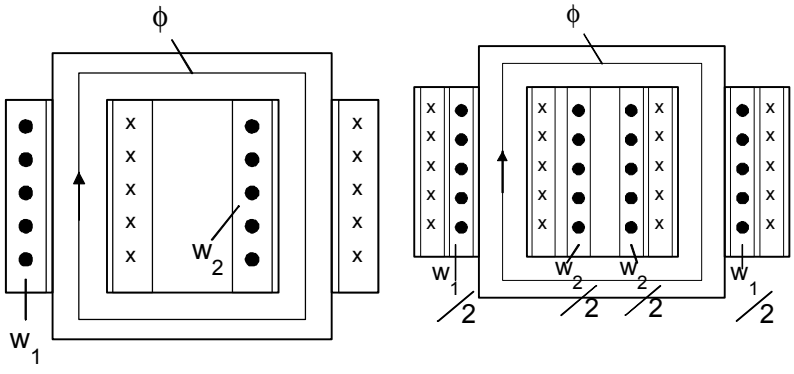

Fig. 47a,b: core-type transformers

high magnetic leakage → useless!

low magnetic leakage

windings: low-leakage models

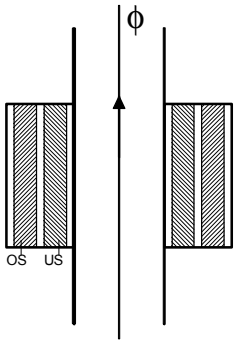

Fig. 48a: cylindrical winding

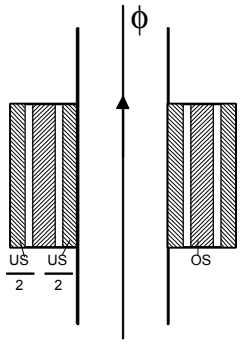

Fig. 48b: double cylindrical winding

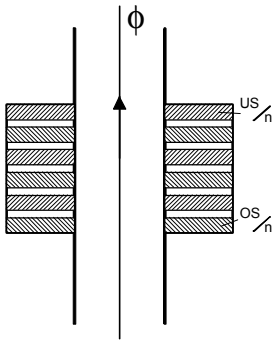

Fig. 48c: disc winding/ sandwich winding

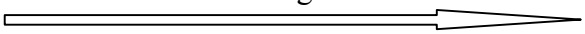

improved magnetic coupling, lower leakage

core cross sections: adaption to circle

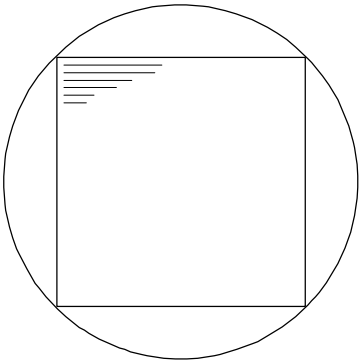

Fig. 49a: VA

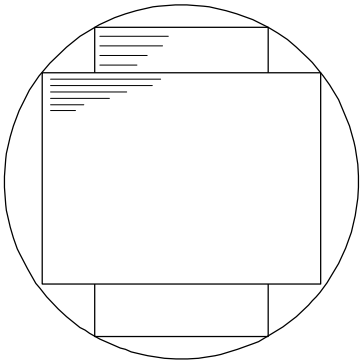

Fig. 49b: kVA

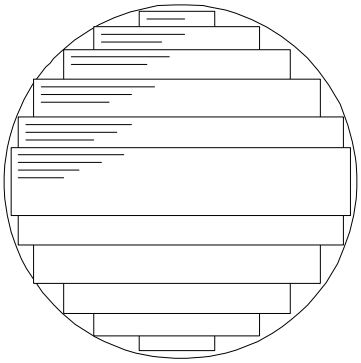

Fig. 49c: MVA

joints: air gaps are to be avoided

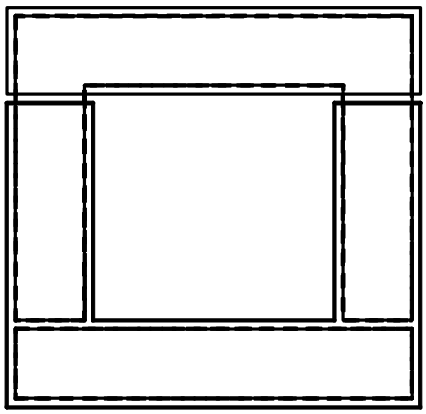

Fig. 50: joints, air gaps of a core

3.4.2 Calculation of the magnetizing inductance

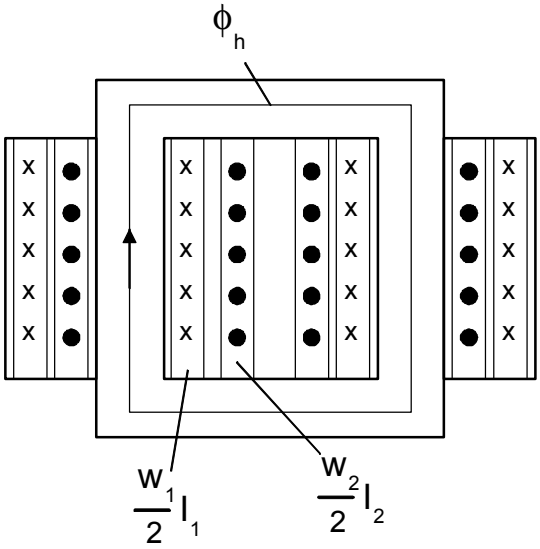

Fig. 51: core, windings

Appliance of Ampere's Law:

$$q = \oint \vec{H} \mathrm{d}\vec{s} \tag{3.88}$$

(magnetical quantity: peak values,
elektrical quantities: rms values)

$$\begin{aligned} w_1 I_1 \sqrt{2} - w_2 I_2 \sqrt{2} &= w_1 \sqrt{2} \left(I_1 - \frac{I_2}{w_1 / w_2} \right) \\ &= w_1 \sqrt{2} I_m \\ &= H_{\mathrm{Fe}} l_{\mathrm{Fe}} \\ &= \frac{B_{\mathrm{Fe}}}{m_0 m_r} l_{\mathrm{Fe}} \end{aligned} \tag{3.89}$$

m_r high, so that $I_m \to 0$!

$$B_{\mathrm{Fe}} = \frac{m_0 m_r}{l_{\mathrm{Fe}}} w_1 \sqrt{2} I_m \tag{3.90}$$

The calculation of inductances using the magnetic energy is most reliable:

$$W_m = \frac{1}{2} \int_V HB \, \mathrm{d}V = \frac{1}{2} L i^2 \tag{3.91}$$

$$W_m = \frac{1}{2} \frac{B_{Fe}^{\ 2}}{m_0 m_r} V = \frac{1}{2 m_0 m_r} \left(\frac{m_0 m_r}{l_{Fe}} w_1 \sqrt{2} I_m \right)^2 l_{Fe} A_{Fe} = \frac{1}{2} L_{1h} \left(\sqrt{2} I_m \right)^2 \tag{3.92}$$

$$\Rightarrow \quad \boxed{L_{1h} = w_1^2 \frac{m_0 m_r A_{\mathrm{Fe}}}{l_{\mathrm{Fe}}}} \tag{3.93}$$

For $L_{1h} \to \infty$ high permeable steel is assumed – e.g. cold-rolled, grain-orientated sheets.

3.4.3 Proportioning of R_1 and R'_2

For $X_{1h} \to \infty$, leading to $I_m \to 0$ follows:

$$w_1 I_1 = w_2 I_2 \qquad \text{(equivalent to } I_1 = I_2^{'}\text{)} \tag{3.94}$$

$$w_1 q_{L1} S_1 = w_2 q_{L2} S_2 \tag{3.95}$$

$$A_{cu1} S_1 = A_{cu2} S_2 \tag{3.96}$$

with equal current densities: $S_1 = S_2$ (3.97)

then follows: $A_{cu1} = A_{cu2}$ (3.98)

and therefore: $l_{m1} = l_{m2}$ (3.99)

This means equal dimensions of primary and secondary windings.

Copper losses (ohmic losses) result in:

$$\begin{aligned} V_{cu1} &= R_1 I_1^{\,2} = r\,\frac{w_1 l_{m1}}{q_{L1}}\frac{q_{L1}}{q_{L1}} I_1^{\,2} = r S_1^{\,2} A_{cu1} l_{m1} \\ &= r S_2^{\,2} A_{cu2} l_{m2} = R_2 I_2^{\,2} = R_2^{'} I_2^{'\,2} = R_2^{'} I_1^{\,2} = V_{cu2} \end{aligned} \tag{3.100}$$

This leads to: $R_1 = R_2^{'}$ and $V_{cu1} = V_{cu2}$.

<u>Time constant of an iron-cored reactor:</u> transformer in no-load:

$$T_1 = \frac{L_{1h}}{R_1} = \frac{w_1^{\,2}\left(\frac{m_0 m_r}{l_{\mathrm{Fe}}}\right) A_{\mathrm{Fe}}}{r\,\frac{w_1 l_{m1}}{q_{L1}}\frac{w_1}{w_1}} = \frac{\frac{m_0 m_r}{l_{\mathrm{Fe}}} A_{\mathrm{Fe}}}{r\,\frac{l_{m1}}{A_{cu1}}} = m_0 m_r \frac{A_{\mathrm{Fe}}}{l_{Fe}}\frac{1}{r}\frac{A_{cu1}}{l_{m1}} \tag{3.101}$$

The time constant is independent from the number of turns. Effective influence is only given by:

- core permeance: $\Lambda_m = m_0 m_r \frac{A_{\mathrm{Fe}}}{l_{\mathrm{Fe}}}$ (3.102)
- conductivity of the winding: $\Lambda_{el} = \frac{1}{r}\frac{A_{cu1}}{l_{m1}}$ (3.103)

which leads to:

$$\boxed{T_1 = \Lambda_m \Lambda_{el}} \tag{3.104}$$

3.4.4 Calculation of the leakage inductances

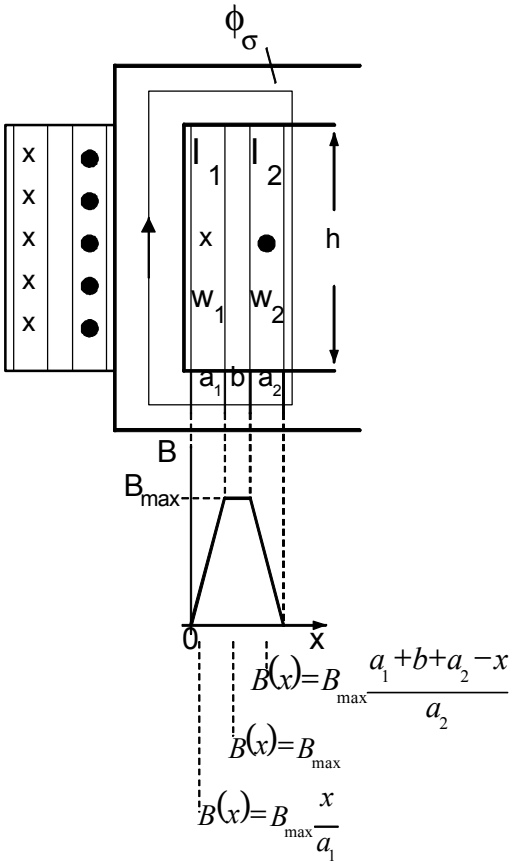

Fig. 52: leakage flux of core

Assumption: transformer to be short-circuited

$$I_m = 0\,, \qquad \text{d. h.} \qquad I_1 = I_2'$$

Ampere's Law:

$$q(x) = \oint \vec{H}\,\mathrm{d}\vec{s} = H(x)h = \frac{B(x)}{m_0}h \tag{3.105}$$

$$B(x) = \frac{m_0}{h}q(x) \tag{3.106}$$

$$B_{\max} = \frac{m_0}{h}w_1 I_1\sqrt{2} = \frac{m_0}{h}w_2 I_2\sqrt{2} \tag{3.107}$$

A mean length of turns l_m is introduced for simplification purposes of calculations.

Calculation of the short-circuit inductance based on the magnetic energy:

$$\begin{aligned} W_m &= \frac{1}{2}\int_V HB\,\mathrm{d}V = \frac{hl_m}{2m_0}\int_0^{a_1+b+a_2} B^2(x) \\ &= \frac{hl_m}{2m_0}B_{\max}^2\left\{\int_0^{a_1}\left(\frac{x}{a_1}\right)^2\mathrm{d}x + \int_{a_1}^{a_1+b}\mathrm{d}x + \int_{a_1+b}^{a_1+b+a_2}\left(\frac{a_1+b+a_2-x}{a_2}\right)^2\mathrm{d}x\right\} \\ &= \frac{hl_m}{2m_0}\left(\frac{m_0}{h}w_1 I_1\sqrt{2}\right)^2\left(\frac{a_1}{3}+b+\frac{a_2}{3}\right) = \frac{1}{2}L_K\left(\sqrt{2}I_1\right)^2 \end{aligned} \tag{3.108}$$

$$\rightarrow L_K = L_{1s} + L_{2s}' = w_1^2\,\frac{m_0 l_m}{h}\left(\frac{a_1}{3}+b+\frac{a_2}{3}\right) \tag{3.109}$$

L_K is just arbitrarily separable into L_{1s} and L_{2s}'. In order to keep leakage inductances low, the distance *b* between windings needs to be reduced, without neglecting winding insulation. The winding dimensions a_1 and a_2 are limited by specified current densities.

Alternatives: Double cylindric winding or disc winding (sandwich winding)

3.5 Efficiency

efficiency: $$\eta = \frac{P_2}{P_1} = \frac{P_2}{P_2 + V_{\mathrm{Cu}} + V_{\mathrm{Fe}}} \tag{3.110}$$

iron losses: $$V_{\mathrm{Fe}} = V_{\mathrm{Fe0}} \left(\frac{U}{U_N} \right)^2 \tag{3.111}$$

copper losses (ohmic losses): $$V_{\mathrm{Cu}} = V_{\mathrm{Cu}N} \left(\frac{I}{I_N} \right)^2 \tag{3.112}$$

delivered power: $$P_2 = P_N \frac{I}{I_N} \frac{U}{U_N} \tag{3.113}$$

For operation in networks of constant voltage, efficiency is defined as:

$$\eta = \frac{P_N \frac{I}{I_N}}{P_N \frac{I}{I_N} + V_{\mathrm{Cu}N} \left(\frac{I}{I_N} \right)^2 + V_{\mathrm{Fe0}}} \tag{3.114}$$

Maximum efficiency appears if:

$$\begin{aligned} \frac{\mathrm{d}\eta}{\mathrm{d}\left(\frac{I}{I_N} \right)} &= 0 \\ &= \frac{\left(P_N \frac{I}{I_N} + V_{\mathrm{Cu}N} \left(\frac{I}{I_N} \right)^2 + V_{\mathrm{Fe0}} \right) P_N - P_N \frac{I}{I_N} \left(P_N + 2 V_{\mathrm{Cu}N} \frac{I}{I_N} \right)}{N^2} \end{aligned} \tag{3.115}$$

This operational point is characterized by equal iron- and copper losses:

$$V_{\mathrm{Fe0}} = \left(\frac{I}{I_N} \right)^2 V_{\mathrm{Cu}N} \tag{3.116}$$

Is the transformer intended to be stressed with partial load, it is useful to choose the efficiency maximum peak as per $0 < \frac{I}{I_N} < \frac{1}{2}$. In case of a durable full load, a choice as per $\frac{1}{2} < \frac{I}{I_N} < 1$ is proven reasonable.

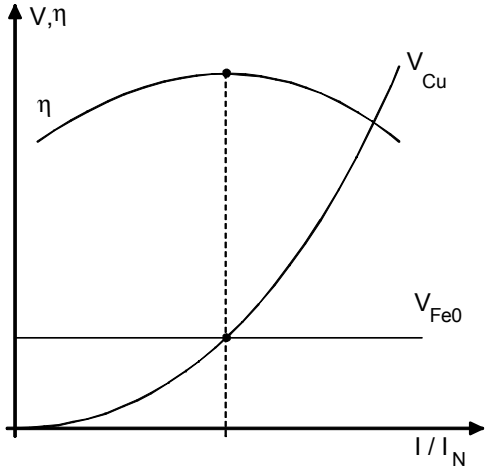

Fig. 53: losses, efficiency characteristic

3.6 Growth conditions

Interdependencies between electrical quantities and size can be shown for transformers and also for rotating machines.

If the nominal voltage is approximately set as:

$$U_{1N} = \frac{w_N}{\sqrt{2}} w_1 f_h = \frac{w_N}{\sqrt{2}} w_1 B_{\mathrm{Fe}} A_{\mathrm{Fe}} \tag{3.117}$$

and the nominal current amounts:

$$I_{1N} = \frac{S_1 A_{cu1}}{w_1} \tag{3.118}$$

the nominal apparent power follows as:

$$S_N = U_{1N} I_{1N} = \frac{w_N}{\sqrt{2}} S_1 B_{\mathrm{Fe}} A_{cu1} A_{\mathrm{Fe}} \tag{3.119}$$

With constant flux density and current density, the nominal apparent power is proportional to the 4th power of linear dimensions:

$$S_N \sim L^4 \tag{3.120}$$

Nominal apparent power, referred to unit volume, increases with incremental size:

$$\frac{S_N}{L^3} \sim L \tag{3.121}$$

Equations for Joulean heat and core losses show size dependencies as follows:

$$V_{\mathrm{Cu}} = \rho S^2 l_m A_{\mathrm{cu}} \sim L^3 \tag{3.122}$$

$$V_{\mathrm{Fe}} = v_{Fe} l_{\mathrm{Fe}} A_{\mathrm{Fe}} \sim L^3 \tag{3.123}$$

Cooling becomes more complicated with increasing size, because losses per surface unit increase with size:

$$\frac{V_{\mathrm{Cu}} + V_{\mathrm{Fe}}}{O} \sim L \tag{3.124}$$

Efficiency improves with increasing size:

$$\eta = 1 - \frac{V_{Cu} + V_{Fe}}{S_N} \sim 1 - \frac{1}{L} \tag{3.125}$$

Relative short circuit voltages show the dependencies:

$$u_R = \frac{R_{1K} I_{1N}}{U_{1N}} \frac{I_{1N}}{I_{1N}} = \frac{V_{Cu1}}{S_N} \sim \frac{1}{L} \tag{3.126}$$

$$u_X = \frac{X_{1K} I_{1N}}{U_{1N}} = \frac{w_N m_0 w_1^2 \frac{l_m}{h} \left(\frac{a_1}{3} + b + \frac{a_2}{3} \right) \frac{S_1 A_{Cu}}{w_1}}{\frac{w_N}{\sqrt{2}} w_1 B_{Fe} A_{Fe}} \sim L \tag{3.127}$$

means: increasing size leads to decreasing u_R and increasing u_X.

3.7 Three-phase transformer

3.7.1 Design, Vector group

A three-phase transformer consists of the interconnection of three single-phase transformers in Y– or Δ – connection. This transformer connects two three-phase systems of different voltages (according to the voltage ratio).

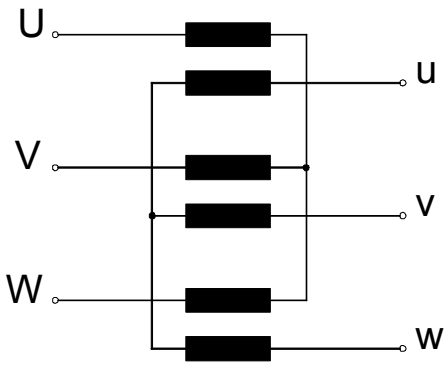

This arrangement is mainly used in the USA – in Europe only for high power applications (>200 MVA) because of transportation problems. The combination in one single three-phase unit instead of three single-phase units is usual elsewhere.

Fig. 54: three-phase assembly

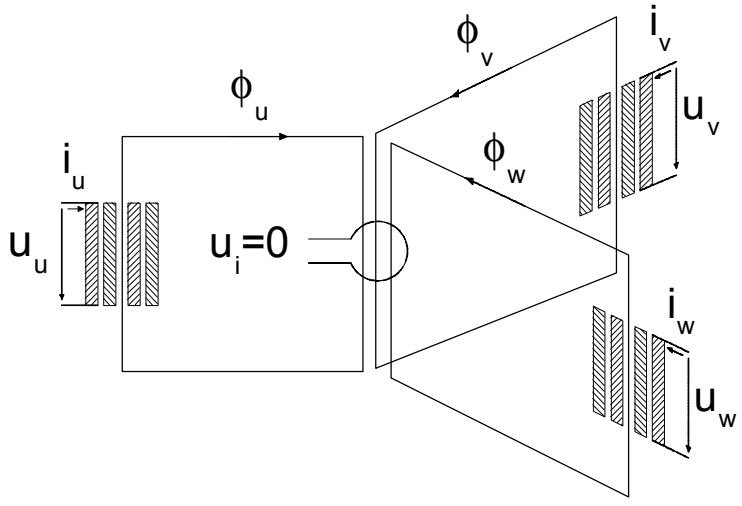

The technical implementation is very simple. Three single-phase transformers, connected to three-phase systems on primary and secondary side, are to be spatially arranged. A complete cycle of the measuring loop around the three iron cores results in $u_i = 0$ and:

$$f_u(t) + f_v(t) + f_w(t) = 0 \tag{3.128}$$

Fig. 55: spatial arrangement

- three-leg transformer

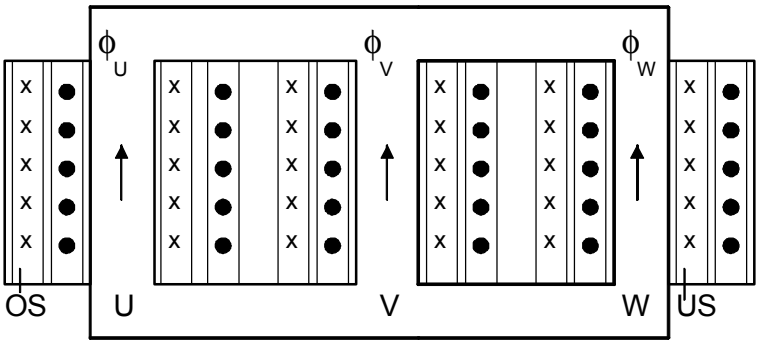

The magnetic return paths of the three cores can be dropped, which results in the usual type of three-phase transformers.
One primary and one secondary winding of a phase is arranged on any leg.

Fig. 56: three-leg transformer

- five-leg transformer

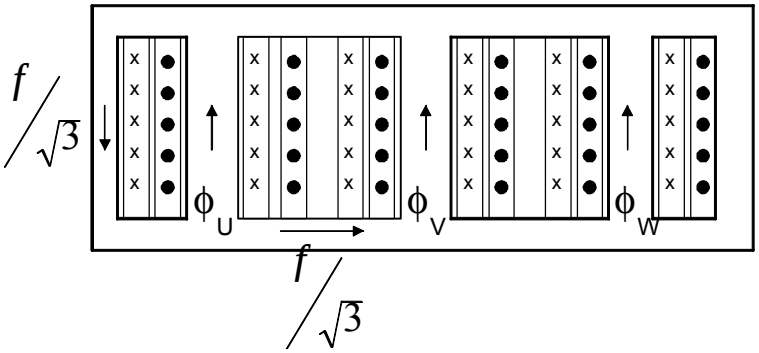

Five-leg transformers are used for high power applications (low overall height).

Fig. 57: five-leg transformer

Primary and secondary winding can be connected in Y– or Δ – connection, according to requirements. The additional opportunity of a so called zigzag connection can be used on the secondary side. The separation of the windings into two parts and their application on two different cores characterize this type of connection. This wiring is particularly suitable for single-phase loads. Significant disadvantage is the additional copper expense on the secondary side increased about a factor $\frac{2}{\sqrt{3}}$ compared to Y– or Δ – connection.

A conversion from line-to-line quantities to phase quantities and the usage of single-phase ecd and phasor diagram is reasonable for the calculation of the operational behaviour of balanced loaded three-phase transformers.

The method of symmetrical components (see 2.6) is suited for calculations in case of unbalanced load conditions.

In a parallel connection of two three-phase transformers the transformation ratio as well as the phase angle multiplier of the according vector group need to be adapted.

Examples for vector groups (based on VDE regulations):

phase angle multiplier	vector group	phasor diagram		ecd		ratio
		primary side	secondary side	primary side	secondary side	
0	Yy0	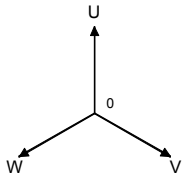	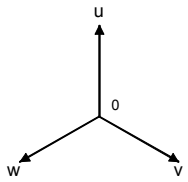	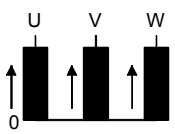	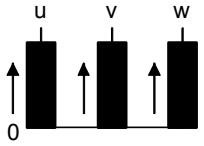	$\frac{w_1}{w_2}$
6	Yy6	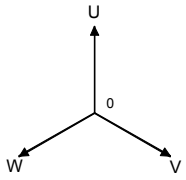	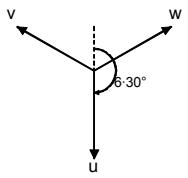	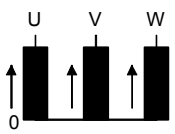	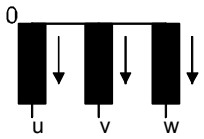	$\frac{w_1}{w_2}$
5	Yd5	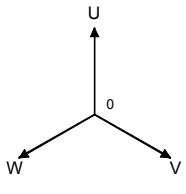	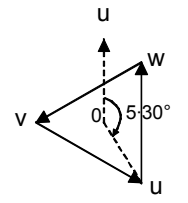	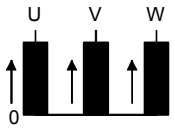	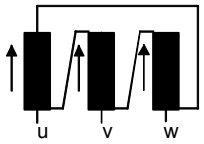	$\frac{\sqrt{3}w_1}{w_2}$
	Yz5	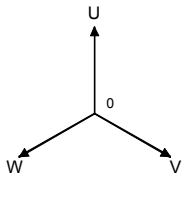	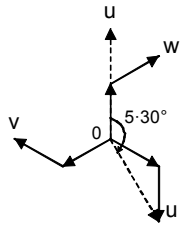	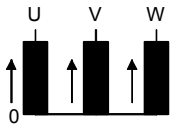	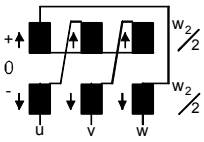	$\frac{2w_1}{\sqrt{3}w_2}$

Fig. 58: table showing phasor diagrams and ecd according to vector group and multiplier

with:

- upper case letter → vector group on primary side
- lower case letter → vector group on secondary side
- Y, y → star connection
- D, d → delta connection (?)
- z → zigzag connection

The multiplier gives the number of multiples of 30°, defining the total phase shift, of which the low voltage (secondary side) lags behind the higher voltage (same orientation of reference arrow assumed).

Mnemonic: clock

- higher voltage: 12 o'clock
- lower voltage: number of multiplier (on the clock)

3.7.2 Unbalanced load

A three-phase transformer of any vector group may be single-phase loaded on the neutral conductor:

$$\underline{I}_u = \underline{I}_B, \qquad \underline{I}_v = \underline{I}_w = 0$$

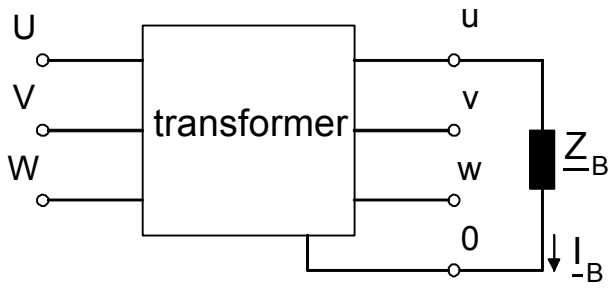

Fig. 59 unbalanced load of three-phase transformer

Appliance of the method of symmetrical components:

1. segmentation of the currents into positive-, negative- and zero sequence system:

$$\begin{pmatrix} \underline{I}_m \\ \underline{I}_g \\ \underline{I}_0 \end{pmatrix} = \frac{1}{3}\begin{pmatrix} 1 & \underline{a} & \underline{a}^2 \\ 1 & \underline{a}^2 & \underline{a} \\ 1 & 1 & 1 \end{pmatrix}\begin{pmatrix} \underline{I}_u \\ \underline{I}_v \\ \underline{I}_w \end{pmatrix} = \frac{1}{3}\begin{pmatrix} \underline{I}_B \\ \underline{I}_B \\ \underline{I}_B \end{pmatrix} \tag{3.129}$$

2. set up of the voltage equations:

   - note: $\underline{Z}_m = \underline{Z}_g = \underline{Z}_K \rightarrow$ generally valid for transformers
     and: $\underline{Z}_0 \rightarrow$ dependent on the vector group.
   - regard: no-load voltages are balanced $\underline{U}_{Lm} = \underline{U}_L, \quad \underline{U}_{Lg} = \underline{U}_{L0} = 0$

$$\underline{U}_m = \underline{U}_{Lm} - \underline{Z}_m \underline{I}_m = \underline{U}_L - \underline{Z}_K \frac{\underline{I}_B}{3} \tag{3.130}$$

$$\underline{U}_g = \underline{U}_{Lg} - \underline{Z}_g \underline{I}_g = -\underline{Z}_K \frac{\underline{I}_B}{3} \tag{3.131}$$

$$\underline{U}_0 = \underline{U}_{L0} - \underline{Z}_0 \underline{I}_0 = -\underline{Z}_0 \frac{\underline{I}_B}{3} \tag{3.132}$$

3. inverse transformation

$$\underline{U}_u = \underline{U}_m + \underline{U}_g + \underline{U}_0 = \underline{U}_L - \frac{\underline{I}_B}{3}\left(2\underline{Z}_K + \underline{Z}_0\right) \tag{3.133}$$

$$\underline{U}_v = \underline{a}^2\underline{U}_m + \underline{a}\underline{U}_g + \underline{U}_0 = \underline{a}^2\underline{U}_L - \frac{\underline{I}_B}{3}\left(\underbrace{\left(\underline{a}^2 + \underline{a}\right)}_{=-1}\underline{Z}_K + \underline{Z}_0\right) \tag{3.134}$$

$$\underline{U}_w = \underline{a}\underline{U}_m + \underline{a}^2\underline{U}_g + \underline{U}_0 = \underline{a}\underline{U}_L - \frac{\underline{I}_B}{3}\left(\underbrace{\left(\underline{a} + \underline{a}^2\right)}_{=-1}\underline{Z}_K + \underline{Z}_0\right) \tag{3.135}$$

With neglecting the voltage drop along Z_K and assumption of a pure inductive load, the phase voltages are determined by:

$$\underline{U}_u = \underline{U}_L - jX_0 \frac{\underline{I}_B}{3} \tag{3.136}$$

$$\underline{U}_v = \underline{a}^2 \underline{U}_L - jX_0 \frac{\underline{I}_B}{3} \tag{3.137}$$

$$\underline{U}_w = \underline{a}\underline{U}_L - jX_0 \frac{\underline{I}_B}{3} \tag{3.138}$$

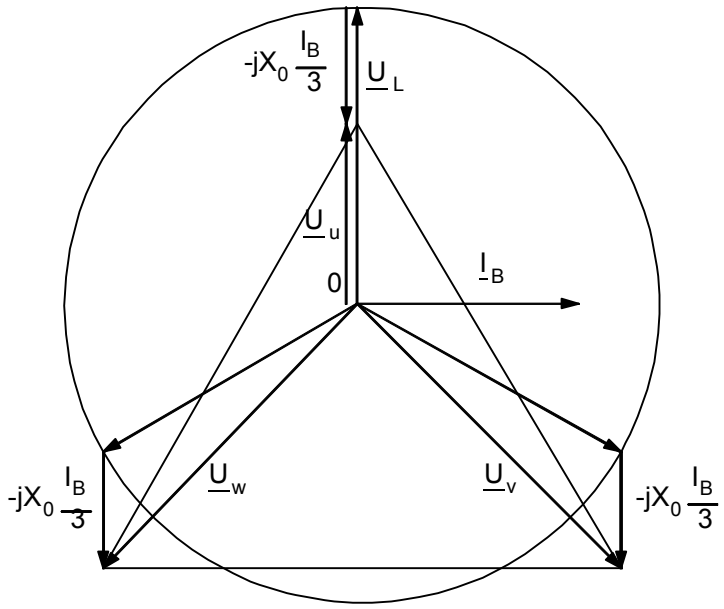

Fig. 60: phasor diagram

Since the voltage drop along X_0 is equal and in-phase, the three-phase phasor diagram (Fig. 60) is distorted, caused by a star point displacement.

This voltage drop needs to be limited, otherwise phase voltage U_u collapses in a worst case condition – leading to increased phase voltages U_v und U_w by factor $\sqrt{3}$.

A correspondence of $\underline{Z}_0 = \underline{Z}_K$ is aimed for a trouble-free single phase load.

It is to be discussed, which of the vector groups match the requirements and how the zero sequence impedance can be determined.

Measurement of the zero sequence impedance:

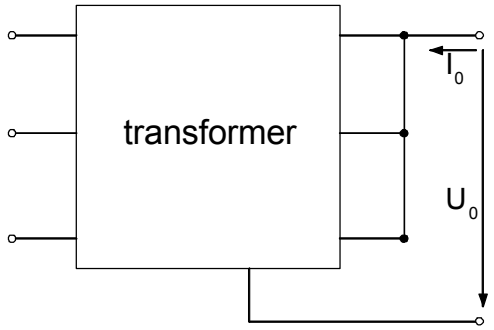

$$\underline{Z}_0 = \frac{3\underline{U}_0}{\underline{I}_0} \tag{3.139}$$

Fig. 61: transformer, zero sequence impedance

a) Yy...

I_0 excites in-phase fluxes in all of the three limbs. The flux distributions establish a closed loop via leakage path, ambient air or frame. This effect leads to improper temperature rise. High resistance of the leakage paths leads to:

$$Z_K < Z_0 < Z_h$$

→ star loading capacity: 10% I_N (maximum)

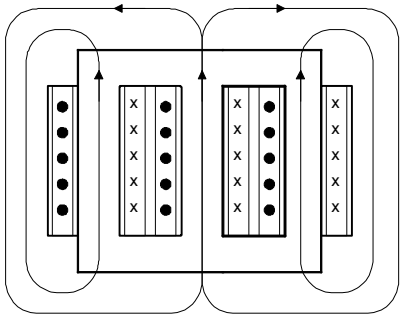

Fig. 62 a

b) Dy...

The ? -connected higher voltage-winding (primary side) is equal to a short circuit of the in-phase fluxes:

$$Z_0 \approx Z_K$$

→ load with zero sequence system possible

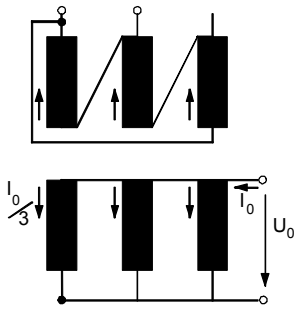

Fig. 62b

c) Yz...

Currents in a winding of any limb equalize each other, without exciting working flux:

$$Z_0 \approx Z_K$$

→ load with zero sequence system possible

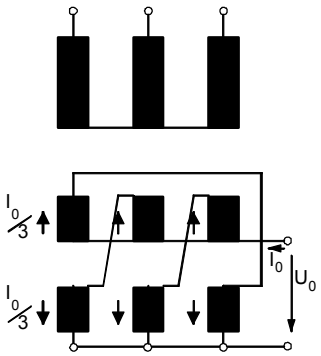

Fig. 62c

Fig. 62 a-c: selection of vector group combinations matching requirements (due to 3.7.2)

3.8 Autotransformer

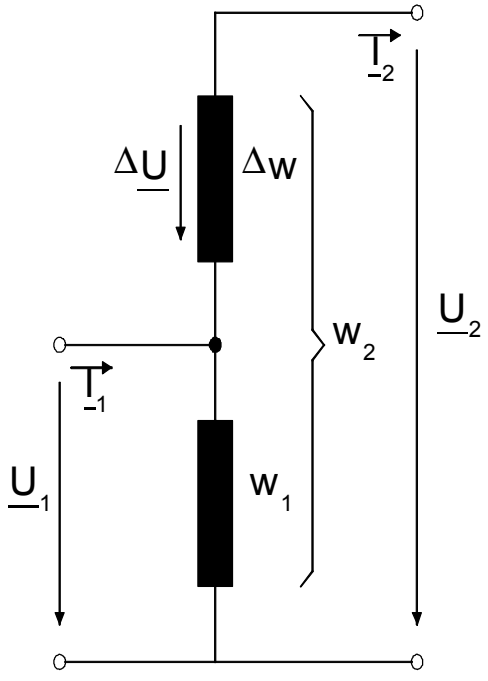

Fig. 63: autotransformer

A special type of power transformer, consisting of a single, continuous winding that is tapped on one side to provide either a step-up or step-down function (inductive voltage divider).

Advantage: significant material savings

Disadvantage: primary and secondary side feature galvanic coupling

voltage ratio: ($I_m > 0, L_{1s} > 0$)

$$\ddot{u} = \frac{U_1}{U_2} = \frac{w_1}{w_2} = \frac{w_1}{w_1 + \Delta w} \tag{3.140}$$

throughput rating = transmittable power:
($R_1 = 0, R_2 = 0$)

$$P_D = U_1 I_1 = U_2 I_2 \tag{3.141}$$

unit rating = design rating:

$$\begin{aligned} P_T &= \Delta U I_2 = (U_2 - U_1) I_2 \\ &= U_2 I_2 \left(1 - \frac{U_1}{U_2}\right) \\ &= P_D (1 - \ddot{u}) \end{aligned} \tag{3.142}$$

In contrast to separate winding transformers, the throughput rating P_D of autotransformers is only partially transmitted by induction (unit rating P_T), the residuary fraction is transmitted by DC coupling (galvanic). In border case condition characterized by $\ddot{u}$ close to 1, the unit rating P_T becomes very low.

Applications: power supply of traction motors, system interconnection 220 / 380 kV

Another disadvantage of the economizing circuit of autotransformers is given by the increased short-circuit current (compared to separate winding transformers) in fault scenarios.

Example: short-circuit on secondary side

$$\begin{aligned} Z_{1KST} &= \frac{Z_{1K} \Delta Z_K}{Z_{1K} + \Delta Z_K} = Z_{1K} \frac{\Delta Z_K}{Z_{2K}} = Z_{1K} \frac{(w_2 - w_1)^2}{w_2^2} \\ &= Z_{1K} (1 - \ddot{u})^2 \end{aligned} \tag{3.143}$$

For $\ddot{u}$ close to 1, the short-circuit current rises high!

4 Fundamentals of rotating electrical machines

Rotating electrical machines are electromechanical energy converters:

motor – generator

The described energy conversion, expressed as forces on the mechanical side, whereas it appears as induced voltages on the electrical side. Basically electrical machines can be operated in both motor- and generator mode.

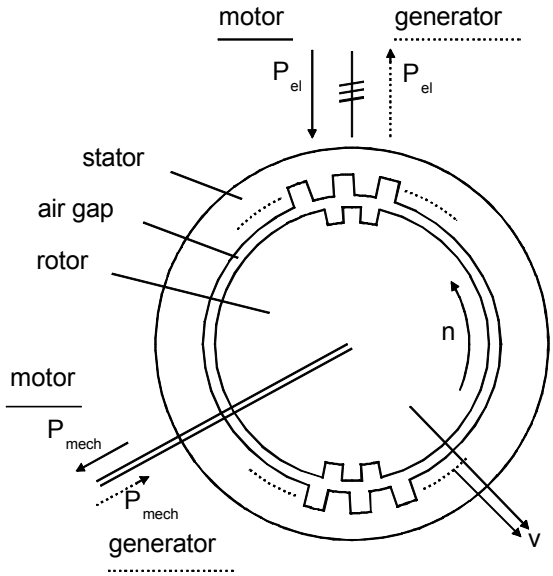

Fig. 64: scheme of energy conversion

The general design of rotating electrical machines in shown in Fig. 64. Electrical power is either supplied to – or dissipated from the stator, whereas mechanical power is either dissipated from – or supplied to the rotor. The electrical energy conversion occurs in the air gap. Losses appear in stator and rotor.

Stator and rotor are usually fitted with windings, with voltages to be induced, caused by spatiotemporal flux alteration.
Forces either appear as Lorentz force in conductors or as interfacial forces on (iron) core surfaces.

Technical demands on energy converters:

1. time independent constant torque (motor) and according constant power output (generator) in steady state operation

2. quick adjustment of torque and speed (motor) and according voltage and current (generator) in transient operation

Electrical machines are usually supplied by either DC or AC systems. The latter differ from balanced three-phase rotating field systems or single-phase alternating systems. Time independent and constant power is to be found in DC and three-phase systems. Transmitted power of single-phase systems pulsates at *doubled* system frequency.

Basically three types of electrical machines need to be distinguished:

- DC machines: air gap field with steady orientation towards stator; rotating armature

- Rotating field machines:
  - induction machines (asynchronous behaviour)
  - synchronous machines
    synchronuous speed of air gap field, rotor follows synchronous or asynchronous

4.1 Operating limits

Operating limits as borders cases in a specific M/n operation diagram (torque/speed diagram) exist for any electrical machine. The complete range of achievable load cases is contained in this diagram (Fig. 65).

Nominal quantities and maximum quantities need to be differentiated. Working points with nominal quantities such as nominal torque M_N and nominal power P_N can be operated enduring, whereas maximum quantities such as maximum torque M_{max} and maximum power P_{max} can only be driven momentarily. Limiting parameters are temperature, mechanical strength and life cycle. In the event of a load condition exceeding the specified range, the machine becomes subject to a thermal overload, caused by excessive currents. Bearings operated at excessive speed reach their thermal acceptance level, followed by a reduction of the life cycle. Excessive speed may destroy the rotor by centrifuging, provoked by centrifugal force (radial).

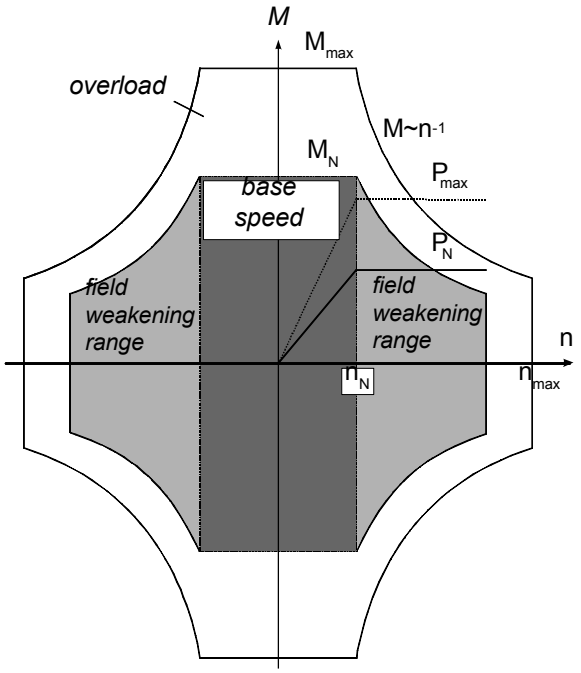

Fig. 65: M/n operation diagram

Two general operating areas appear for electrical machines. There is the *base speed range* at first. This range is characterized by the opportunity that at least the nominal torque can be performed at any speed, even at 0 rpm. At constant torque M_N the mechanical power increases linear with increasing speed, until nominal power P_N is optained. Nominal speed n_N is reached in this working point:

$$n_N = \frac{P_N}{2p \cdot M_N} \tag{4.1}$$

Nominal power P_N must not be exceeded in enduring operation. In order to still run higher speeds, driving torque must be decreased at increasing speed.

$$M = \frac{P_N}{2p \cdot n} \tag{4.2}$$

This area – being the second out of the two described - is called *range of constant power* (according to equation 4.2). The described condition of decreased driving torque is achieved by weakening of the magnetic field, therefore the operation range is also called *field weakening range*.

4.2 Equation of motion

Electrical drives are utilized for conversion of electrical energy in mechanical motion processes and also the other way around. The torque balance of a drive system describes the fundamental relation for the determination of a motion sequence. It necessarily needs to be fulfilled at any time.

$$M_A - M_W - M_B = 0 \tag{4.3}$$

M_A driving torque of a motor

M_W load torque or resistance torque of the load engine with friction torque and loss torque contained

$M_B = J \cdot \frac{d\Omega}{dt}$ acceleration torque of all rotating masses (4.4)

$J = \int r^2 \cdot dm$ mass moment of inertia (4.5)

$\Omega = 2 \cdot p \cdot n$ mechanical angular speed (4.6)

In stationary operation, characterized by $n=const$, the acceleration torque is $M_B=0$.

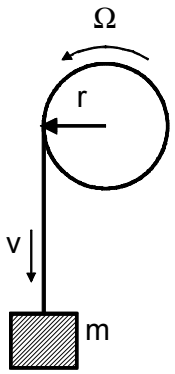

Fig. 66: rot./trans. conversion

The conversion from rotary motion into translatory motion (and the other way around as well) is performed with regard to the conservation of kinectic energy:

$$\frac{1}{2} \cdot m \cdot v^2 = \frac{1}{2} \cdot J \cdot \Omega^2 \tag{4.7}$$

$$J = m \cdot \left(\frac{v}{\Omega} \right)^2 = m \cdot \left(\frac{\Omega \cdot r}{\Omega} \right)^2 = m \cdot r^2 \tag{4.8}$$

The following table shows rotary and translatory physical quantities:

translation			rotation		
name and symbol	equations	unit	name and symbol	equations	Unit
distance s	$s = r \cdot j$	m	angle j	$j = \frac{s}{r}$	rad
speed v	$v = \frac{ds}{dt}$ $v = r \cdot \Omega_m$	m/s	angular speed W_m	$\Omega_m = \frac{dj}{dt}$ $\Omega_m = \frac{v}{r}$	1/s
acceleration a	$a = \frac{dv}{dt}$	m/s^2	angular acceleration a	$a = \frac{d\Omega_m}{dt}$	1/s^2
			tangential acceleration a_t	$a_t = r \cdot a$	m/s^2
mass m		kg	mass moment of inertia J	$J = \int r^2 dm$	kg m^2
force F	$F = m \cdot \frac{dv}{dt}$	N	torque M	$M = J \cdot \frac{d\Omega_m}{dt}$	Nm
power P	$P = F \cdot v$	W	power P	$P = M \cdot \Omega_m$	W
energy W	$W = \frac{1}{2} m \cdot v^2$	J	energy W	$W = \frac{1}{2} \cdot J \cdot \Omega_m^2$	J

Fig. 67: rotary and translatory quantities, according symbols, equations and units

4.3 Mechanical power of electrical machines

An electrical machine can either be used as motor or as generator. In motor mode electrical energy is converted into mechanical energy, in generator mode mechanical energy is transformed into electrical energy. The power rating plate data is always given as the output power. Mechanical power working on the shaft is meant for the motor operation, electrical power being effective at the terminals is meant for the generator.

Mechanical power P is determined by

$$P = \Omega \cdot M = 2 \cdot p \cdot n \cdot M \tag{4.9}$$

Mechanical speed *n* and torque *M* are signed quantities (+/-) – per definition is:

- output power signed positive

That means positive algebraic sign (+) for mechanical power in motor operation.

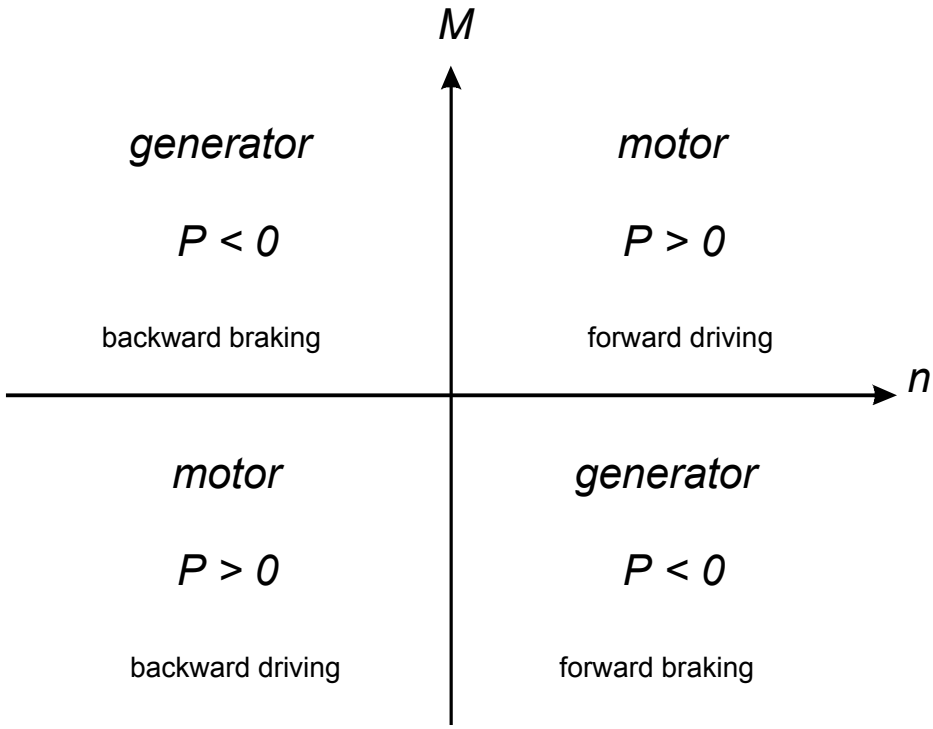

Fig. 68: operation modes, directions of electrical machines

An electrical drive can be driven in all of the four quadrants of the M/n diagram (see Fig. 65 and 68). An automotive vehicle is supposed to be taken as an example: if speed *n* and torque *M* are signed identically, the according machine is in motor operation. We get forward driving with positive signed speed (1st quadrant) and backward driving with negative signed speed (3rd quadrant). In case of different algebraic signs for speed and torque, the machine works in generator mode, battery and supply systems are fed with electrical energy. This takes effect in braked forward driving (4th quadrant) as well as in braked backward driving (2nd quadrant).

4.4 Load- and motor characteristics, stability

Motor operation and generator mode of operation need to be discussed separately.

4.4.1 Motor and generator characteristics

motor characteristics: $M_A = f(n)$

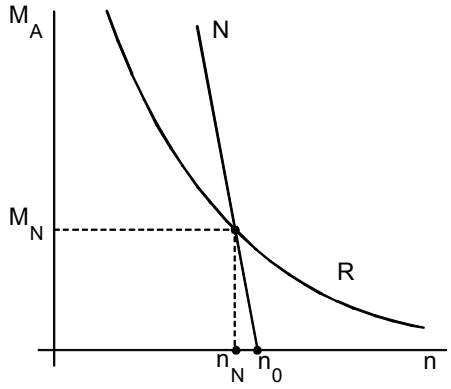

Fig. 69a: shunt characteristic

$n \approx \text{const}_{|M}, n_0$

series characteristic

$M \sim \frac{1}{n}$

generator characteristics: $U_G = f(I)$

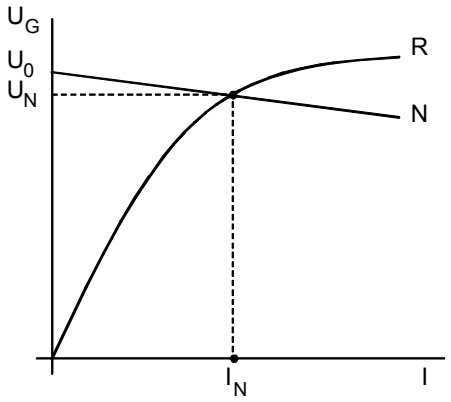

Fig. 69b: shunt characteristic

$U \approx \text{const}_{|I}, U_0$

series characteristic

$U \sim f(I)$

4.4.2 Load characteristics

$M_w = f(n)$

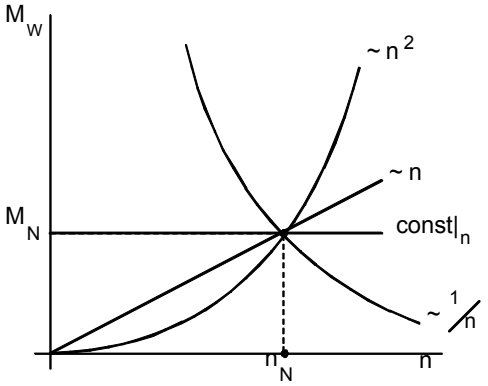

Fig. 70a: motor load characteristic

$M_w = \text{const}$	:	friction, gravitation
$M_w \sim n$	:	elektric brake
$M_w \sim n^2$	:	fans, pumps
$M_w \sim \frac{1}{n}$	:	winches

$U_B = f(I)$

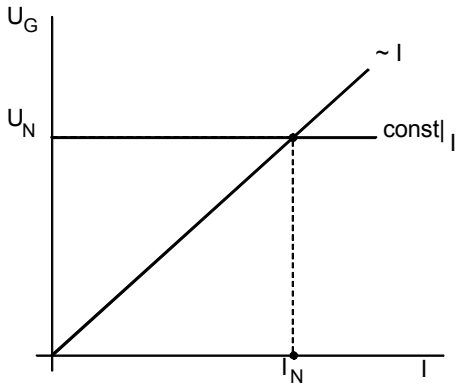

Fig. 70b: generator load characteristic

$U_B = U_N = \text{const}$	:	stiff system
$U_B = RI$	:	load resistance

4.4.3 Stationary stability

stable motor operation

$$\frac{\partial M_w}{\partial n} > \frac{\partial M_A}{\partial n} \qquad (4.10)$$

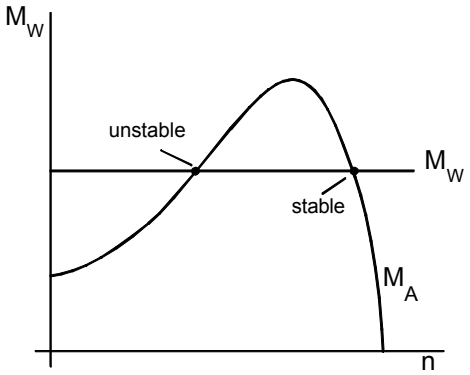

Fig. 71a: motor stability characteristic

The *load torque* needs to increase stronger with increasing speed than the *motor torque*.

stable generator operation

$$\frac{\partial U_B}{\partial I} > \frac{\partial U_G}{\partial I} \qquad (4.11)$$

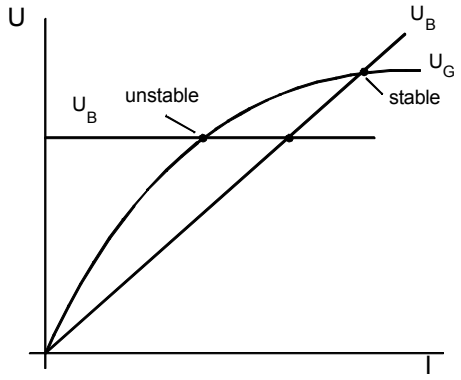

Fig. 71b: generator stability characteristic

The *voltage at the load* needs to increase stronger with increasing current than the *generator voltage*.

5 DC Machine

5.1 Design and mode of action

The stator of a DC machine usually consists of a massive steel yoke, fitted with poles. Those stator poles carry DC exciter windings. The magnetic field excited by the excitation current permeates the rotor (also called armature for DC machines), the magnetic circuit is closed via the stator iron core. The armature core is composed of slotted iron laminations that are stacked to form a cylindrical core. The armature winding is placed in the armature slots.

The method of DC machine armature current supply to create uniform torque in motor operation is subject to the following consideration.

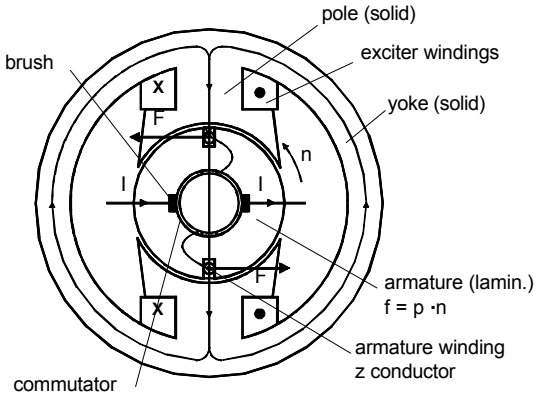

Fig. 72: DC machine, general design

Is the conductor (Fig. 72) fed with DC current of constant value, a force F is exerted on the conductor as long as it remains underneath the stator pole. Effective field and according force are equal to zero beneath the poles. Does the armature pass these regions caused by its mass moment of inertia, a magnetic field of opposite direction is reached next. With unreversed current direction a braking force is exerted on the rotor.

This consideration leads to the result, the armature current needs to be reversed until the armature conductor reaches the field of opposite poles. This current reversal is performed by the so called commutator of collector. The commutator is composed of a slip ring that is cut in segments, with each segment insulated from the other as well as from the shaft. The commutator revolves with the armature; the armature current is supplied or picked up by stationary brushes. The current reversal, performed by the commutator, is done in the way to create a spatiotemporal magnetomotive force (mmf), perpendicular orientated to the exciter field.
The armature needs to be laminated, because armature bars carry currents of frequency $f = p \cdot n$. Since number of pole pairs and speed is not related for DC machines, frequencies higher than 50 Hz may appear.

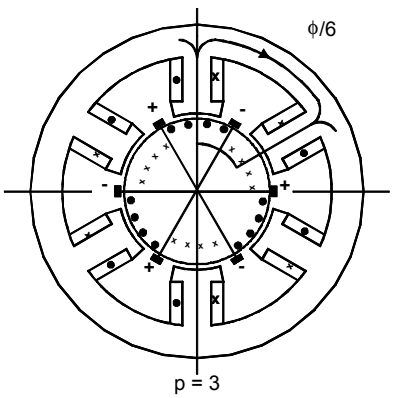

Fig. 73: DC machine, poles

Large DC machine models are designed with more than 2 poles. Machines with p poles show p-times repeating electrical structure along the circumference.

Advantages: lower core cross sections, shorter end turns, short magnetic distances

Disadvantages: more leakage, more iron losses, caused by higher armature current frequency, commutation more difficult.

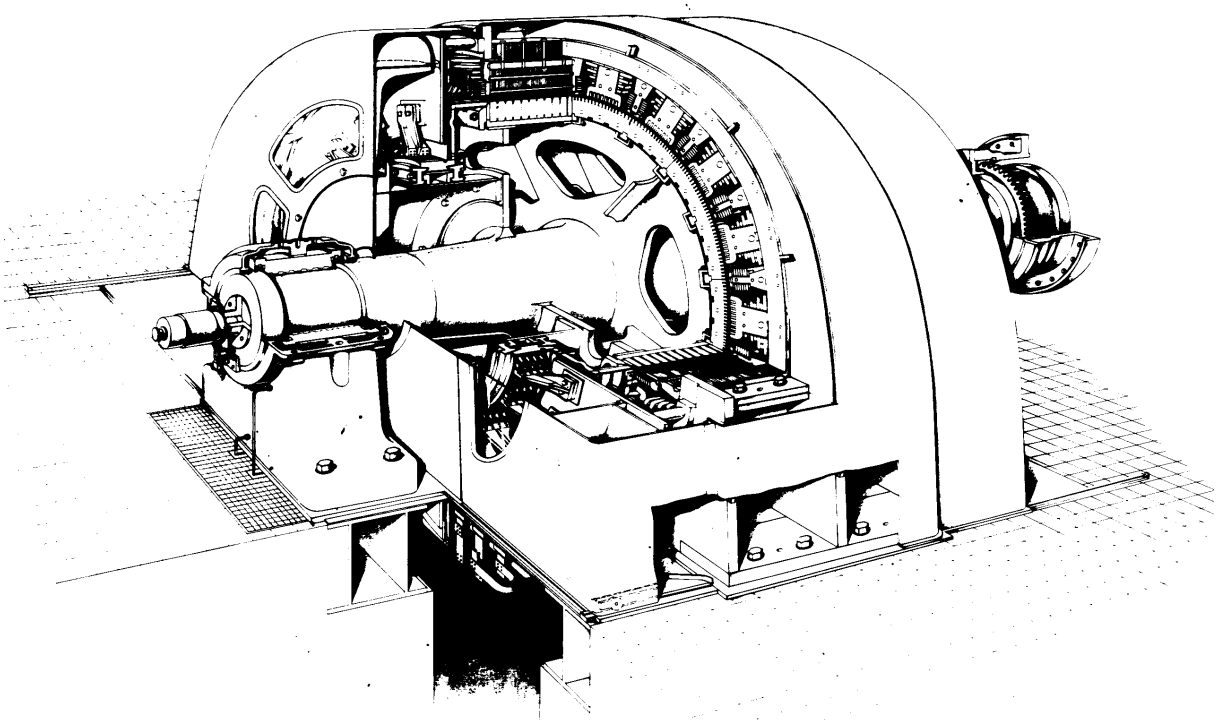

Fig. 74: DC motor 8440 kW (ABB)

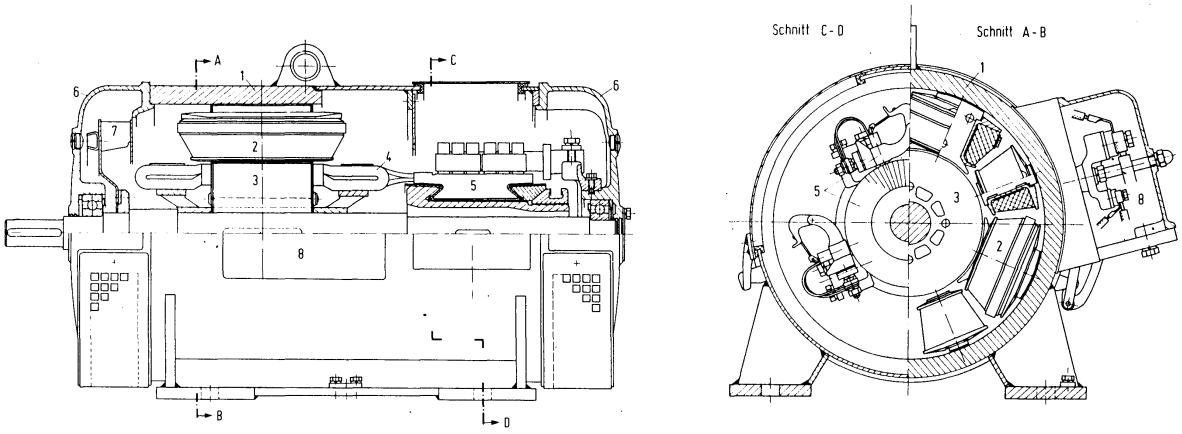

Fig. 75a/b: section through DC motor 30 kW (side/left)

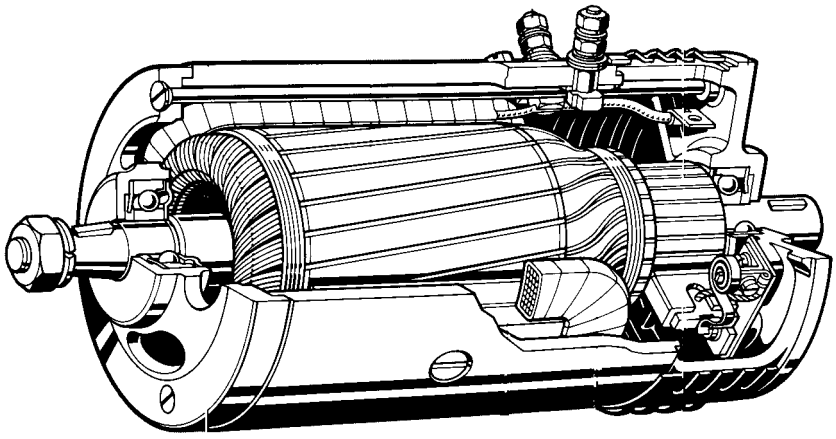

Fig. 76: DC generator 1 kW (Bosch)

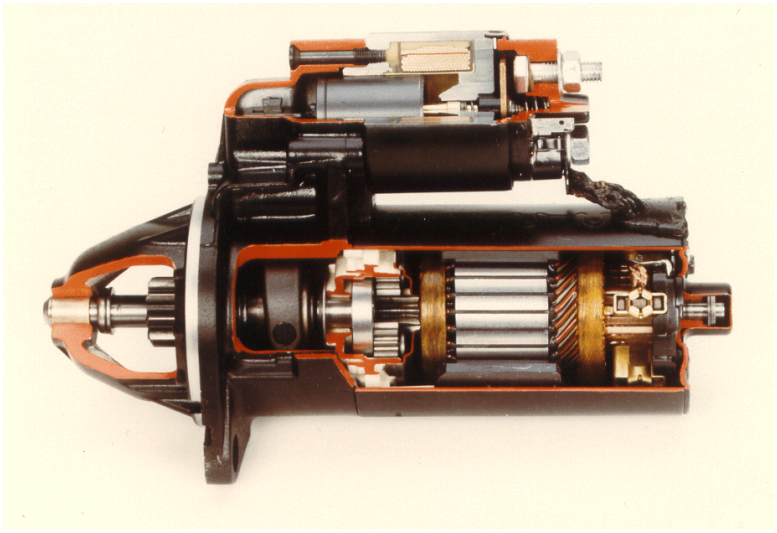

Fig. 77: permanent-field transmission gear 1.5 kW (Bosch)

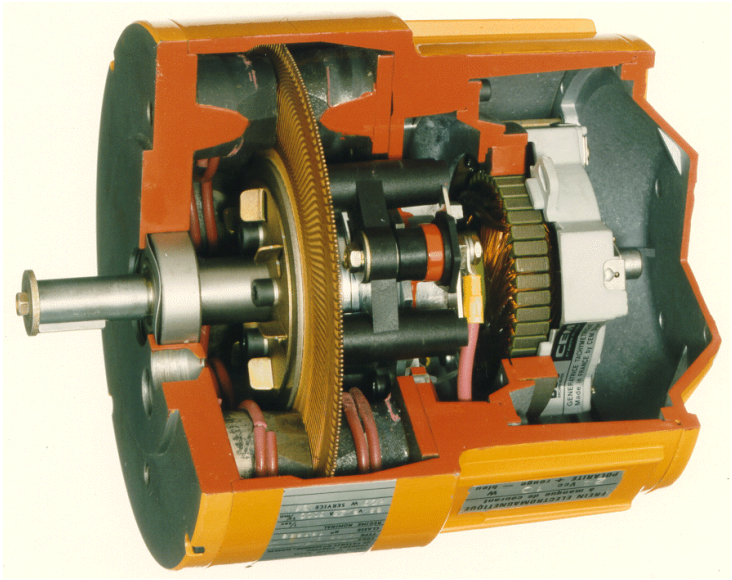

Fig. 78: DC disc-type rotor1 kW (ABB)

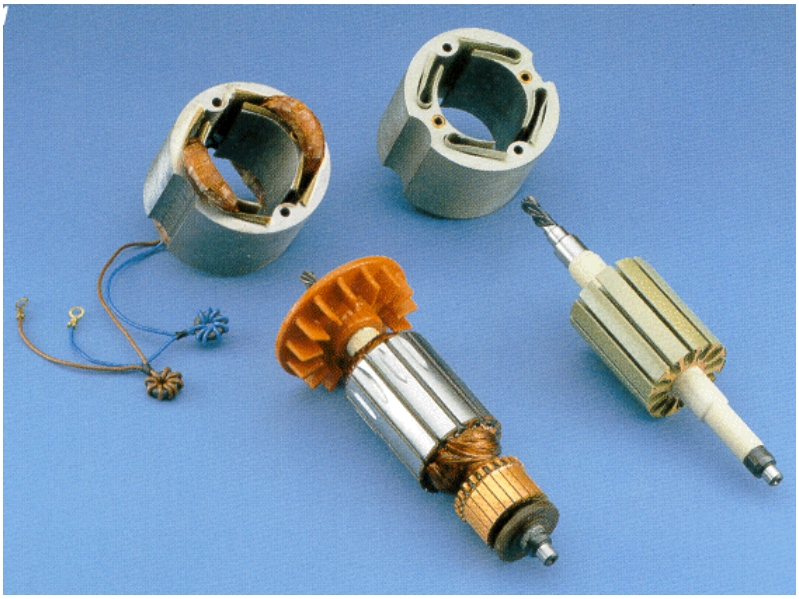

Fig. 79: universal motor (AC-DC) 300W (Miele)

The armature winding of a DC machine is modelled as double layer winding, consisting of line conductor in the top layer and return conductor in the bottom layer.
Around the armature circumference, a number of z bars altogether are uniformly distributed in slots, connected to the according commutator bar. Two different wiring methods are used for separate windings:

- lap winding (in series)
- wave winding (in parallel)

Lap windings are characterized by a connection of a coil end at the commutator directly with the beginning of the next coil of the same pole pair. Only one coil is arranged between two commutator bars. In cause of the existence of $2p$ brushes, all p pole pairs are connected in parallel. The number of parallel pathes of armature windings amounts $2a = 2p$.

Wave windings consist of coil ends at the commutator, connected with the beginning of the accordant coil of the next pole pair, so that a complete circulation around the armature with p coils leads to the next commutator bar. Using only 2 brushes, all p pole pairs are connected in series. The number of parallel pathes of armature windings amounts $2a = 2$ in this case.

Usual for the design of large DC machines is an arrangement of any coil being composed of more than one turn ($w_s > 1$) and a slot filling with more than one coil each ($u > 1$).

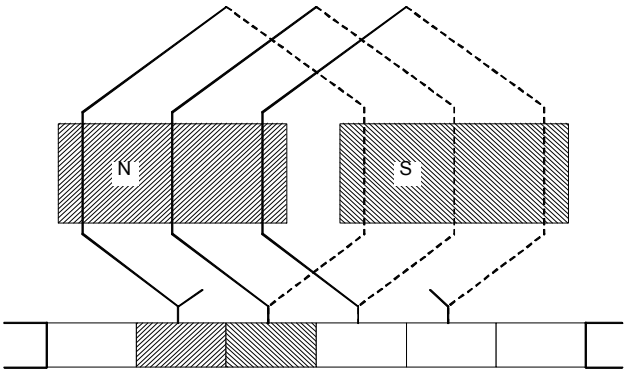

Fig. 80b: lap winding

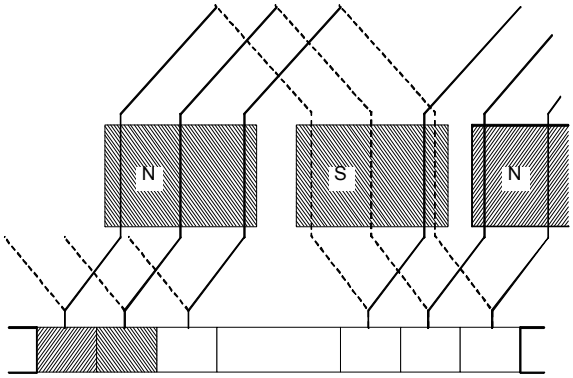

Fig. 80b: wave winding

5.2 Basic equations

As the general design of a DC machine is illustrated in Fig. 81, Fig. 82 shows the air gap field caused by exciter windings versus a complete circumference of the armature.

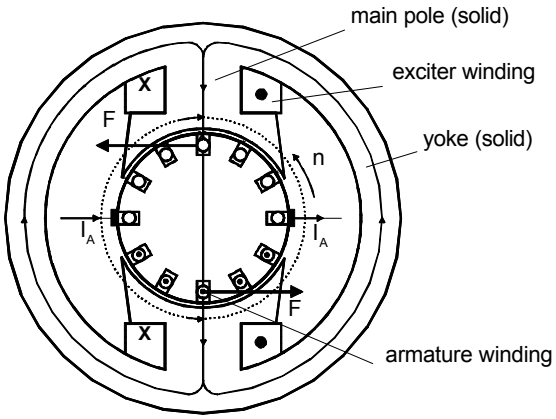

Fig. 81: DC machine, basic design

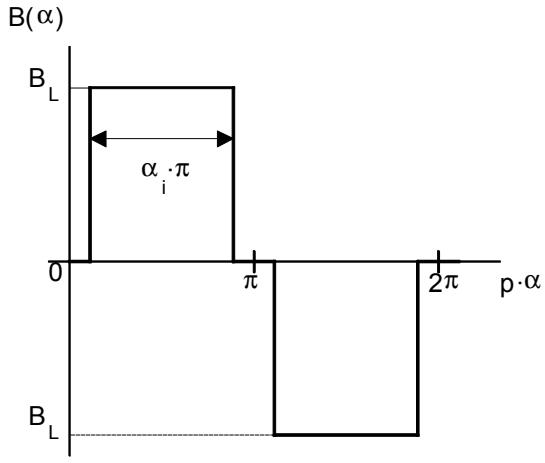

Fig. 82: air gap field vs. circumference angle

Faraday's Law (VZS) is utilized for the calculation of the induced voltage:

$$u_i = \frac{dy}{dt} = w \cdot \frac{df}{dt} = w \cdot \frac{\Delta f}{\Delta t} \tag{5.12}$$

Equivalent to an armature turn of one pole pitch, the flux linkage of the armature winding reverses from $+f$ to $-f$.

$$\Delta f = 2 \cdot f \tag{5.13}$$

the according period of time lasts:

$$\Delta t = \frac{1}{n} \cdot \frac{1}{2 \cdot p} \tag{5.14}$$

The number of armature conductors is z. With $2a$ pairs of parallel paths of armature windings, the effective number of armature windings is determined by:

$$w = \frac{z}{2} \cdot \frac{1}{2 \cdot a} \tag{5.15}$$

e.g.: $2 \cdot a = 2$

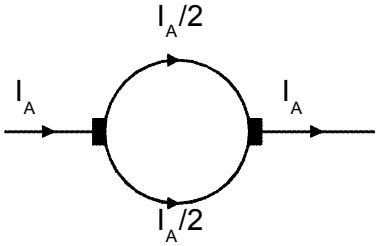

Fig. 83: armature current

This leads to an equation for the induced voltage of DC machines - first basic equation:

$$U_i = w \cdot \frac{\Delta f}{\Delta t} = \frac{z}{2} \cdot \frac{1}{2 \cdot a} \cdot 2 \cdot f \cdot n \cdot 2 \cdot p = z \cdot \frac{p}{a} \cdot n \cdot f \tag{5.16}$$

$$U_i = k \cdot f \cdot n \qquad k = z \cdot \frac{p}{a} \tag{5.17}$$

The armature winding shows an ohmic resistance R_A, to be regarded in a complete mesh loop - second basic equation :

$$U = U_i \pm I_A \cdot R_A \qquad \text{(+) motor, (-) generator} \tag{5.18}$$

Torque can be derived from the magnetic energy with same assumptions (see equations. 5.12-5.16 above) concerning parallel paths of armature windings, pole pitch etc. as for the induced voltage – third basic equation:

$$M = \frac{dW_m}{da} = \frac{I \cdot d\Psi}{da} = \frac{I \cdot w \cdot \Delta f}{\Delta a} = I \cdot \frac{z}{2} \frac{1}{2a} \cdot \frac{2f}{\frac{p}{p}} = \frac{z \cdot p}{a} \frac{1}{2p} \cdot f \cdot I \tag{5.19}$$

$$M = \frac{k}{2p} \cdot f \cdot I \tag{5.20}$$

The power balance equation confirms described dependencies (+ motor, - generator):

$$\underbrace{U \cdot I_A}_{P_{auf}} = \underbrace{U_i \cdot I_A}_{P_{mech}} \pm \underbrace{I_A^2 \cdot R_A}_{V_{Cu}} \tag{5.21}$$

$$P_{mech} = U_i \cdot I_A = k \cdot n \cdot f \cdot I_A = 2 \cdot p \cdot n \cdot M \tag{5.22}$$

$$M = \frac{k}{2 \cdot p} \cdot f \cdot I_A \tag{5.23}$$

The armature resistance of a DC machine can be determined by using Joulean heat losses:

$$V_{Cu} = \left(\frac{I_A}{2a} \right)^2 \cdot r \cdot \frac{z \cdot (l + t_p)}{q_L} = I_A^2 \cdot R_A \tag{5.24}$$

$$R_A = \frac{z \cdot r}{4 \cdot a^2} \cdot \frac{\left(l + t_p \right)}{q_L} \tag{5.25}$$

5.3 Operational behaviour

5.3.1 Main equations, ecd, interconnections

The following general ecd is used for DC machines:

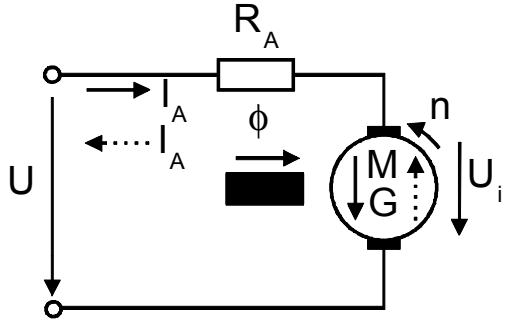

Sense of rotation:

——— motor operation (VZS):
armature current arrow rotates in direction of exciter field

- - - - - - generator operation(EZS):
armature current arrow against the direction of the exciter field

Fig. 84: DC machine, general ecd

The operational behaviour of a DC machine is completely described with appliance of the three basic equations (5.26 – 5.28):

$$U_i = k \cdot f \cdot n \tag{5.26}$$

$$U = U_i \pm I_A \cdot R_A \tag{5.27}$$

$$M = \frac{k \cdot f}{2 \cdot p} \cdot I_A \tag{5.28}$$

Neglect of saturation in the magnetic circuit of the DC machine assumed, a linear dependence between air gap flux and exciter current is supposed:

$$k \cdot f = M \cdot I_F \qquad \text{(M: magnetizing inductance)} \tag{5.29}$$

The dependency $k \cdot f = f(I_F)$ can be measured as no-load characteristic. The DC machine is therefore driven with currentless armature ($I_A = 0$) at constant speed (n = const.), the induced voltage is measured with variating exciter current.

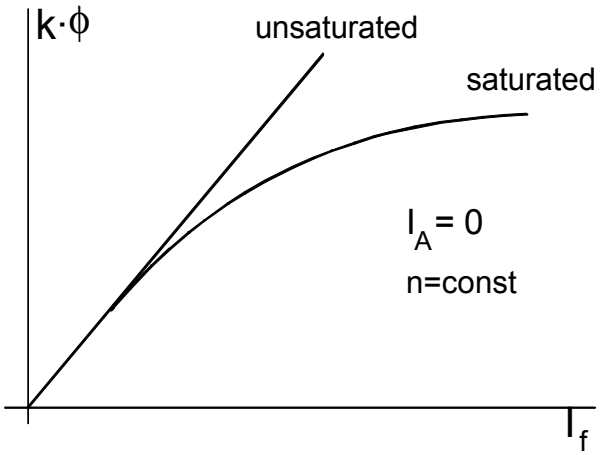

$$k \cdot f = \frac{U_i}{n} \tag{5.30}$$

Fig. 85: no-load characteristic

The characteristical speed/torque-behaviour likewise ensues from the basic equations (equations. 5.26-5.28):

speed:

$$n = \frac{U_i}{k \cdot f} = \frac{U}{k \cdot f} - \frac{I_A \cdot R_A}{k \cdot f} \tag{5.31}$$

torque:

$$M = \frac{k \cdot f}{2 \cdot p} \cdot I_A \tag{5.32}$$

The operational behaviour of DC machines is dependent on the exciter winding interconnection type arrangement versus the armature. The following types of interconnection are discussed in the following:

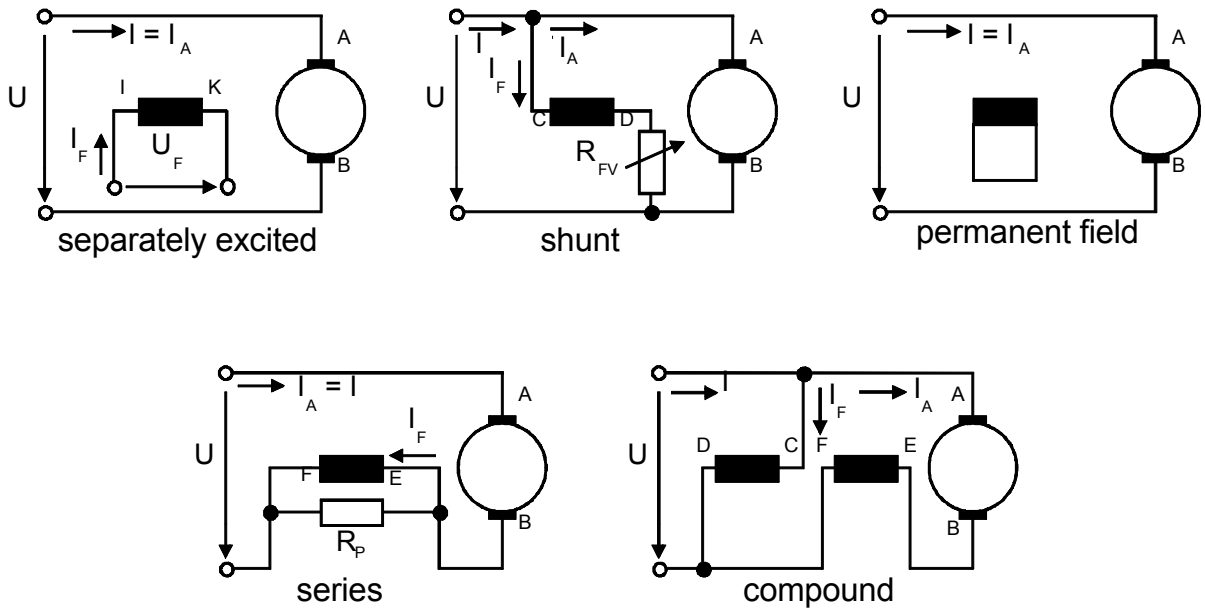

Fig. 86a-e: DC machine interconnection variations

5.3.2 Separately excitation, permanent-field, shunt machine

As long as separately excited, permanent-field and shunt machine are supplied by constant voltage U_N, their operational behaviour does not differ at all. Only the amount of exciter voltage is different for shunt machines. No opportunity for an exciter flux variation is provided for permanent-field machines.

There is:

$$U_f = const \rightarrow I_f = const \rightarrow f_N = const$$

torque:

$$M \sim I_A \tag{5.33}$$

no-load:

$$I = 0\ ,\ M = 0\ \Rightarrow n_0 = \frac{U_N}{k \cdot f_N} \tag{5.34}$$

speed:

$$n = \frac{U_N}{k \cdot f_N} - \frac{I_A \cdot R_A}{k \cdot f_N} = n_0 - n_0 \cdot \frac{I_A \cdot R_A}{U_N} \tag{5.35}$$

} shunt characteristic

The short-circuit current needs to be limited by a series resistor.

$$I_K = \frac{U_N}{R_A} \rangle\rangle I_N \tag{5.36}$$

Speed can be adjusted by either:

- variation of the armature voltage (1):

$$U < U_N : n = \frac{U}{U_N} \cdot n_0 - n_0 \cdot \frac{I_A \cdot R_A}{U_N} \tag{5.37}$$

- field weakening (2):

$$f < f_N : n = n_0 \cdot \frac{f_N}{f} - n_0 \cdot \frac{f_N}{f} \cdot \frac{I_A \cdot R}{U_N} \tag{5.38}$$

- utilization of starting resistor (3):

$$R_A^* = R_{AV} + R_A : n = n_0 - \frac{I_A \left(R_A + R_{AV}\right)}{U_N} \cdot n_0 \tag{5.39}$$

The sense of rotation can be reversed by changing the polarity of either the armature- or the exciter voltage. Speed adjustment using variation of the armature voltage is non-dissipative, whereas the speed adjustment utilizing a starting resistor is lossy. With regard to armature reaction, the field weakening range needs to be limited to f < 3.

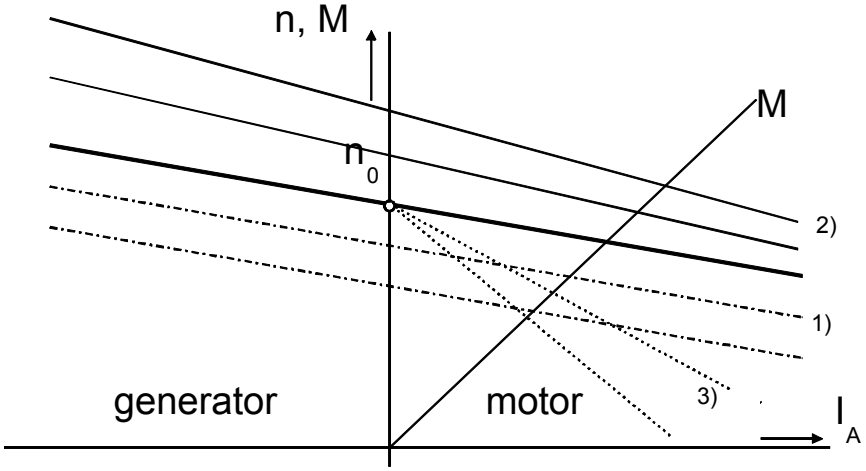

Fig. 87: shunt characteristic

A continuous transition from motor- to generator mode permits utilization as variable speed drive in conveyor motor and manipulator applications.

5.3.3 Series machine

A series machine is characterized by a series connection of armature- and exciter windings. The total resistance to be measured at the terminals is:

$$R = R_A + R_F \tag{5.40}$$

Exciter windings are supplied by the armature current:

$$I = I_F = I_A \tag{5.41}$$

with neglect of saturation follows:

$k \cdot f = M \cdot I_A$ (M = magnetizing inductance)

torque proportionality ensues as:

$M \sim I_A^2$

speed is determined as (by insertion):

$$n = \frac{U_N}{M \cdot I_A} - \frac{R}{M}$$

mind the no-load case with: $I_A = 0$

$n_{(I_A=0)} \rightarrow \infty$ **!!!**

} series characteristic (5.42)

conclusion: a series machine runs away in case of unloading!

Short circuit current

$$I_K = \frac{U_N}{R}$$

A polarity change of the armature voltage does **not** lead to a reversal of the rotation sense of a DC series machine.

Speed can be adjusted by either:

- variation of the armature voltage (1):

$$U < U_N : n = \frac{U}{U_N} \cdot \frac{U_N}{M \cdot I_A} - \frac{R}{M} \tag{5.43}$$

- field weakening (2):

$$I_F < I_A \text{ mit } R_P: \quad f = \frac{I_A}{I_F} = 1 + \frac{R_F}{R_P}$$

$$n = f \cdot \frac{U_N}{M \cdot I_A} - f \cdot \frac{R_A + R_F / f}{M} \tag{5.44}$$

- utilization of starting resistor (3):

$$R^* = R_V + R_A + R_F \tag{5.45}$$

$$n = \frac{U_N}{M \cdot I_A} - \frac{R^*}{M} \tag{5.46}$$

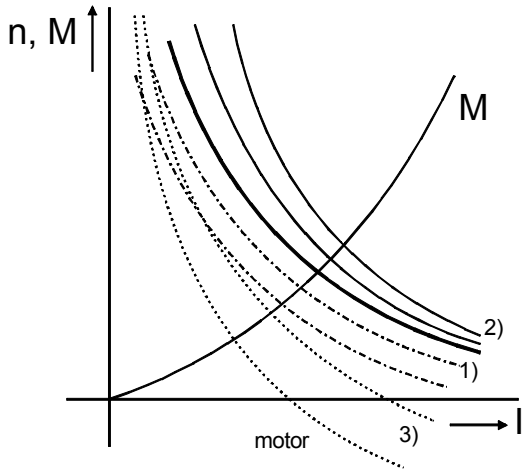

Fig. 88: series machine characteristic

A continuous transition from motor- to generator mode is not possible for a series machine!

Series machines must not be unloaded!

DC series machines are utilized for traction drives in light rail- and electric vehicle applications as well as for starters in automotive applications. Major advantage is a high torque value already at low speeds, sufficing traction efforts particularly at start-up.

5.3.4 Compound machine

By separation of exciter windings in shunt- and series windings, shunt characteristic is achieved in the proximity of no-load operation, series characteristic is achieved under load. Machines which are designed due to this method are called compound machines.
Note their features:

- definite no-load speed
- continuous transition from motor mode to generator mode ppossible
- under load: decreasing speed according to the dimensioning of the series windings.

Fig. 89 and 90 show comparisons of the different characteristics of all discussed DC machine types for both motor- and generator mode.

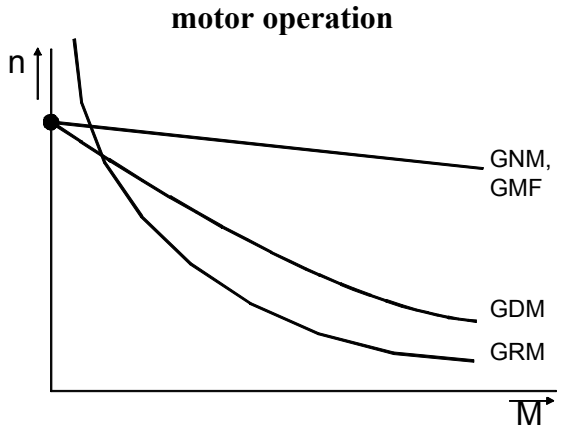

GMF[1]:
separately excited DC machine

GNM:
DC shunt machine

GRM:
DC series machine

GDM:
DC compound machine

Fig. 89: DC machine types, motor operation

DC compound machines are used as motor in flywheel drives as well as generator in solitary operation.

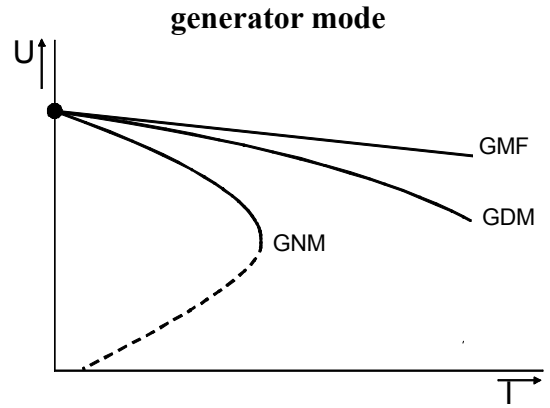

Fig. 90: DC machine types, generator mode

1) abbreviations, based on their German origin are not intuitive in English. They have not been translated for conformity purposes.

5.3.5 Universal machine (AC-DC machine)

Universal machines are DC series machines as a matter of principle, their stator is composed of stacked iron laminations. A universal machine can be supplied either by DC or by AC current – therefore the alternative denomination as AC-DC machine. The described DC machine basic equations 5.26-5.28 are still applicable for AC supply at frequency f, in this case to appear in their time-variant form.

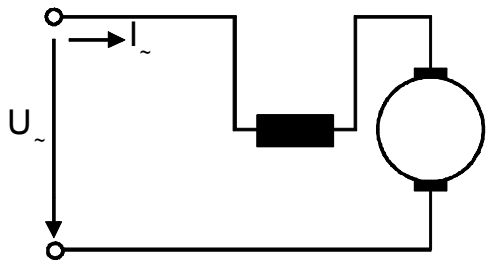

Fig. 91: universal machine, general ecd

Approach for flux determination:

$$j(t) = f \cdot \sin(w \cdot t) \tag{5.47}$$

A phase shift applies for the armature current approach:

$$i(t) = \sqrt{2} \cdot I \cdot \sin(w \cdot t - r) \tag{5.48}$$

The induced voltage results in:

$$u_i(t) = k \cdot j(t) \cdot n \tag{5.49}$$

$$U_i = \frac{k \cdot f \cdot n}{\sqrt{2}} \tag{5.50}$$

the torque equation appears as

$$M(t) = \frac{k}{2 \cdot p} \cdot j(t) \cdot i(t) = \frac{k}{2 \cdot p} \cdot \frac{f \cdot I}{\sqrt{2}} \cdot (\cos r - \cos(2 \cdot w \cdot t - r)) \tag{5.51}$$

$$M_{mittel} = \frac{k}{2 \cdot p} \cdot \frac{f \cdot I}{\sqrt{2}} \cdot \cos r \tag{5.52}$$

The time variant torque pulsates with twice the nominal frequency f between zero and the doubled average value (as shown in Fig. 92).

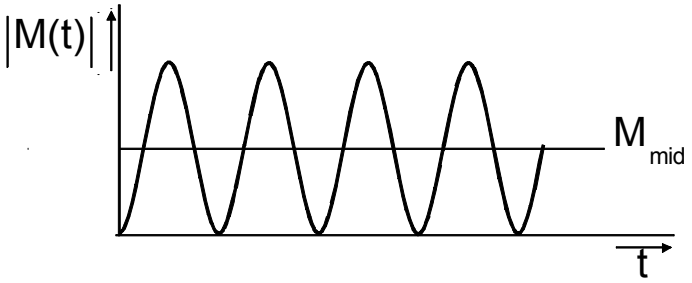

Fig. 92: torque waveform vs. time

highest possible direct component assumes:

$$\cos r \to 1 \qquad \text{and} \quad r \to 0$$

meaning: flux and armature current need to be <u>in-phase</u>!

This condition is fulfilled for the series motor. Occuring pulsating torque is damped by the inert mass of the rotor. The working torque is equal to the direct torque component.

As to be seen on equivalent circuit diagrams (Fig. 93a,b) and phasor diagrams (Fig. 94a,b), a phase shift of almost $\pi/2$ between armature current and flux occurs for the shunt machine, whereas they are in-phase for the series wound machine.

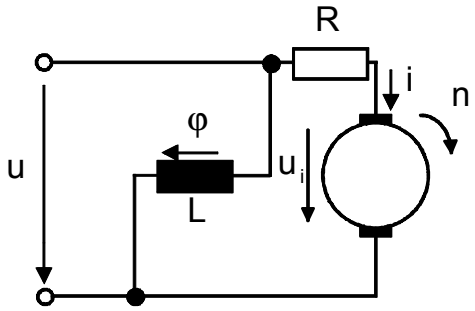

Fig. 93a: shunt machine, ecd

$$(j,i) \approx \frac{p}{2}$$

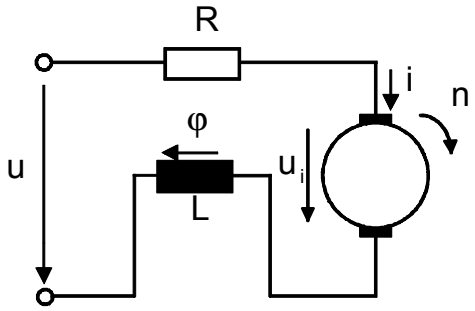

Fig. 93b: series machine, ecd

$$(j,i) \approx 0$$

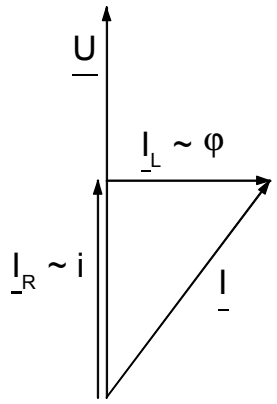

Fig. 94a: shunt machine, phasor diagram

for $n = 0 \Rightarrow U_i = 0$

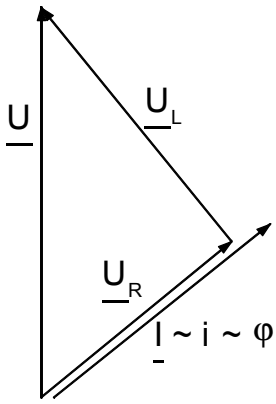

Fig. 94b: series machine, phasor diagram

for $n = 0 \Rightarrow U_i = 0$

Additionally to the ohmic voltage drop at the resistor sum

$$R = R_A + R_F\,, \tag{5.53}$$

the inductive voltage drop at the inductance sum

$$L = L_A + L_F \tag{5.54}$$

must be taken into account for universal machines with AC supply.

Therefore the voltage equation due to a mesh loop is determined by

$$\underline{U} = \underline{U}_i + R \cdot \underline{I} + jX \cdot \underline{I} \tag{5.55}$$

Induced voltage U_i and armature current I are in-phase, because

$$U_i = \frac{k \cdot f}{\sqrt{2}} \cdot n \tag{5.56}$$

U_i is in-phase with f, as well as f is in-phase with I.

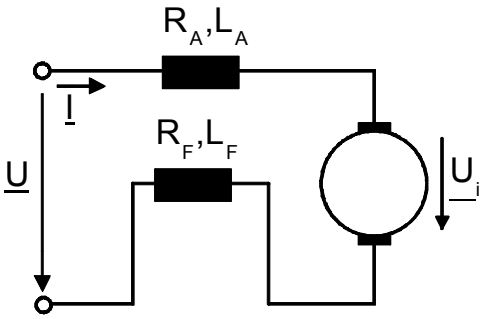

Fig. 95a: universal machine, ecd

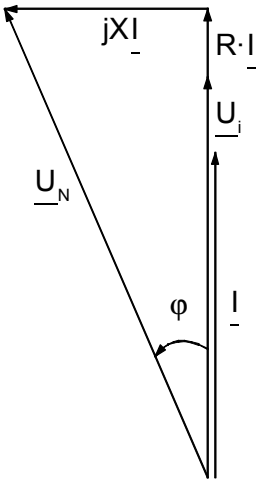

Fig. 95b: phasor diagram

Universal motors absorbes lagging reactive power (inductive):

$$\cos j_N \approx 0.9$$

The motor utilization in AC operation is decreased by $1/\sqrt{2}$ compared to DC operation – same thermal and magnetic stress assumed.

The according speed characteristic is the same as of DC series wound machines

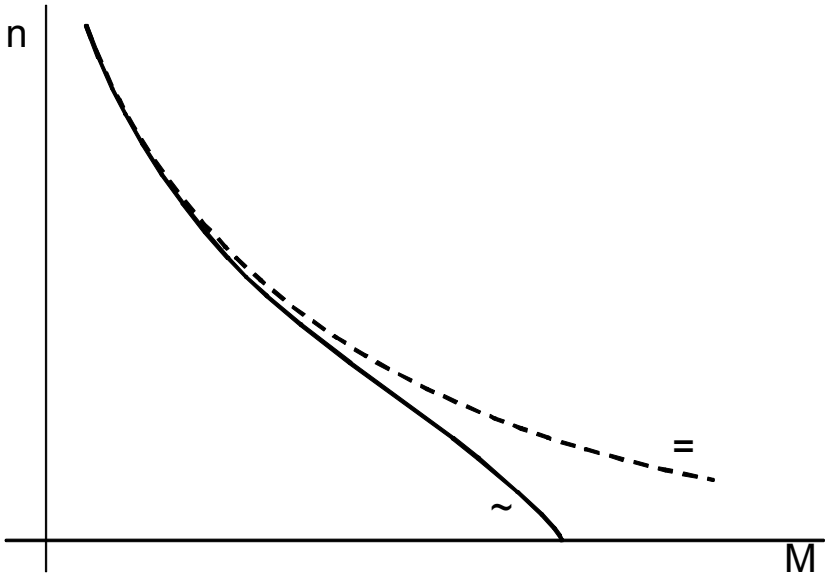

Fig. 96: universal machine, speed characteristic (AC, DC)

Appliance

Single phase series wound motors are used as universal motors in household- and tool applications at 50 Hz supply:

- power < 1 kW
- speed < 40.000 min^{-1}
- speed variation by voltage variation

Types of construction

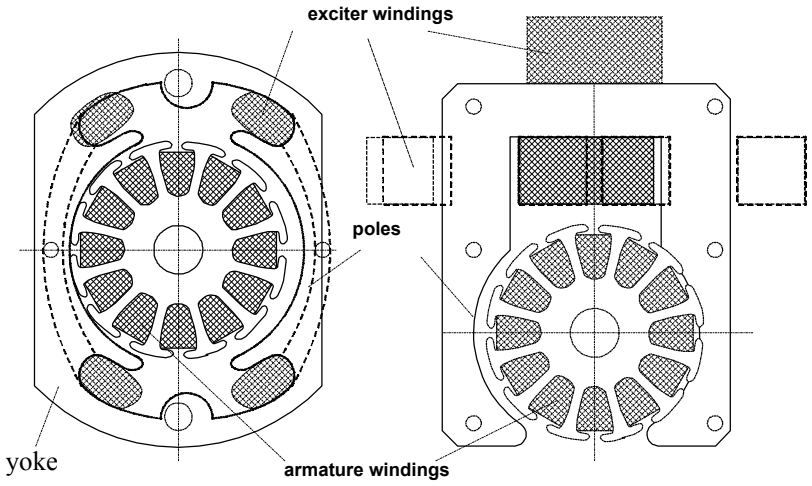

Fig. 97: universal machine, design variations

Large machines are mainly used for traction drives in railway applications.
The line-frequency needs to be reduced down to $16^2/_3$ Hz in cause of the induced voltage $(U_{ind} \sim f)$.

5.3.6 Generator mode

Some specific features of shunt- and series wound machines need to be taken care of in generator mode, which do not appear for separately excited and permanent-field machines with constant energy flux.

5.3.6.1 Shunt generator

Process of self-excitation:

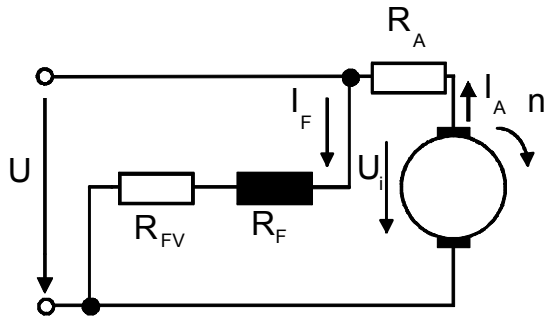

Fig. 98a: shunt generator, ecd

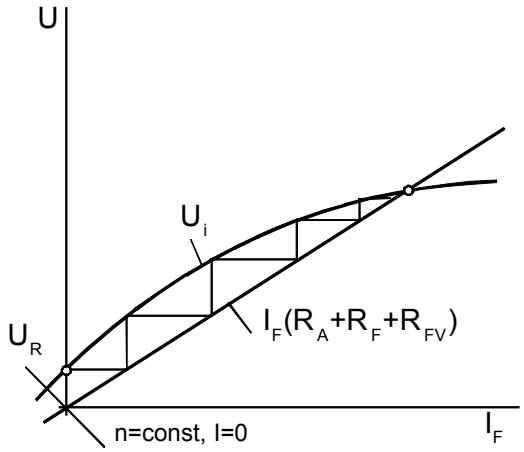

Fig. 98b: shunt generator, no-load char.

Using a series resistor the exciter windings are to be connected in parallel to the armature. The machine is to be operated with constant speed at no-load. A remanent voltage U_R is induced by remanence, which is present in any magnetic circuit. This induced voltage evokes an exciter current I_F then. The engendered exciter current reinforces the residual magnetic field – the induced voltage is increased perpetually. A stable operating point is reached if the induced voltage is as high as the voltage drop to occur at the exciter circuit resistors. („dynamoelectric principle“):

$$U_i = I_F\left(R_A + R_{FV} + R_F\right) \tag{5.57}$$

In case of false polarity, the exciter current I_F acts demagnetizing, a self-excitation process does not occur.

Voltage can be adjusted using series resistor R_{FV}.

Load characteristic:

In comparison to a separately excited machine, the load characteristic $U = f(I)$ of a self-excited generator is non-linear

$$U = U_N - I_A R_A \tag{5.58}$$

and with eqt. 5.58 the terminal voltage is even more load-dependent.

As ensued for the load case:

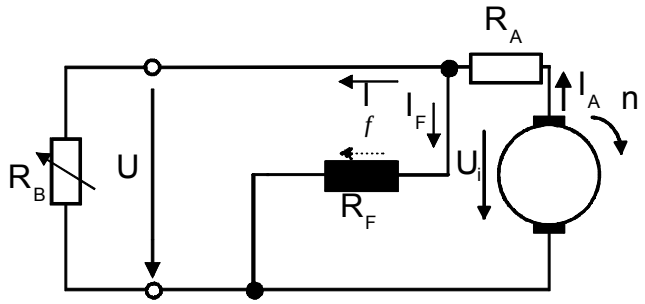

Fig. 99: self excited generator, load case (EZS)

$$U_i = I_A R_A + I_F R_F \tag{5.59}$$

$$I_A = I + I_F \tag{5.60}$$

$$U = I_F R_F \tag{5.61}$$

then follows:

$$U_i = I\,R_A + I_F\left(R_A + R_F\right) \tag{5.62}$$

and

$$I = \frac{1}{R_A}\left(U_i - I_F\left(R_A + R_F\right)\right) \tag{5.63}$$

With cognition of the no-load characteristic and the resistance line, the load characteristic can be created graphically.

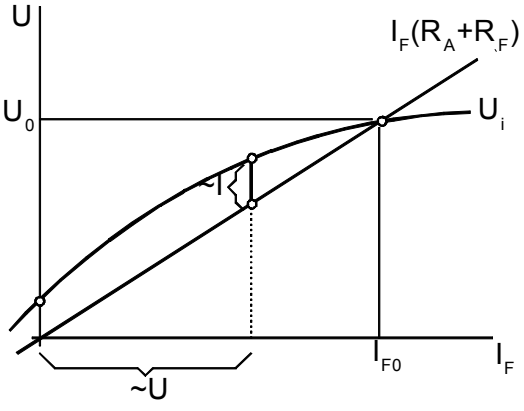

Fig. 100: no-load-/resistor characteristic

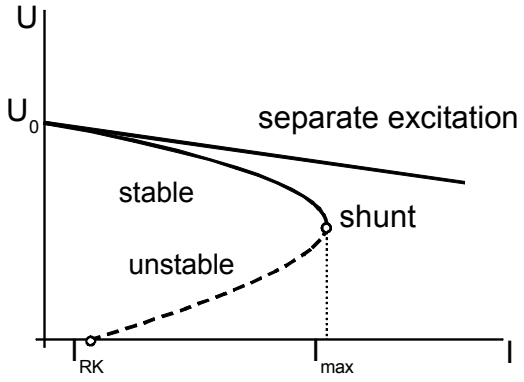

Fig. 101: load characteristic

The generator current is limited to I_{max}. The terminal voltage collapses at higher loads with the consequence of only short-circuit current flowing, to be evoked by the remanent voltage.

5.3.6.2 Series generator

Are DC series machines operated in generator mode, the self-exciting process takes place simultaneously to shunt machines. A distinction is to be made whether the series machine is working on a system of constant voltage or on a load resistor.

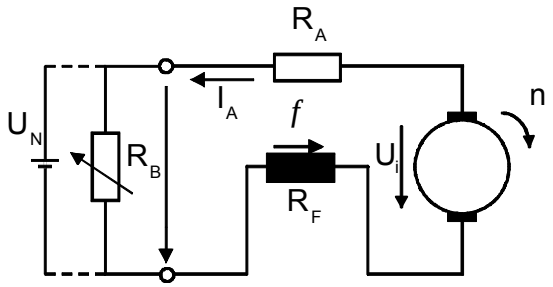

Fig. 102: DC series generator (EZS)

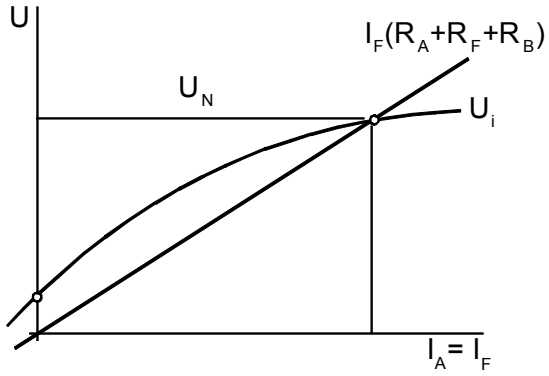

Fig. 103: load characteristic

A stable operation with load resistor R_B is given, because of $\frac{\partial U_B}{\partial I_A} > \frac{\partial U_i}{\partial I_A}$.

Terminal voltage is not adjustable, but dependent on R_B.

Stable operation at constant voltage system is not possible, because of $\frac{\partial U_N}{\partial I_A} < \frac{\partial U_i}{\partial I_A}$.

The series generator as such is unpopular, it is only used as dynamic brake in traction drive applications.

5.3.7 DC machine supply with variable armature voltage for speed adjustment

A *Ward-Leonard-Converter* is a machine-set, consisting of an induction machine (motor) and a DC machine (generator), which feeds another DC machine (to be controlled) with variable armature voltage. A Ward-Leonard-Converter can be operated in any of the four quadrants.

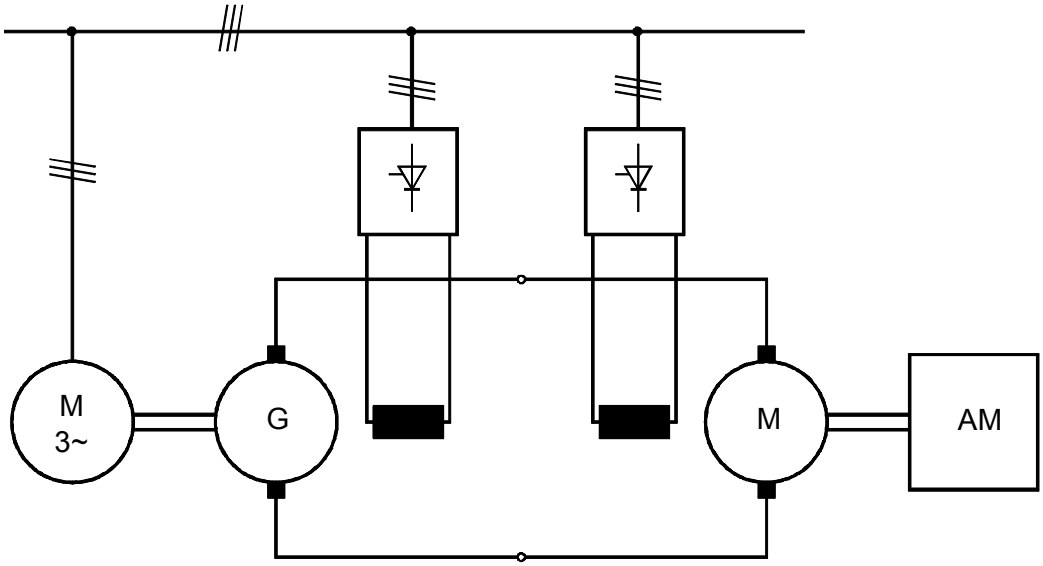

Fig. 104: Ward-Leonard-Set

The long-term used and popular Ward-Leonard-Set is almost completely replaced by *power converter supplied DC drive systems*. The following circuit arrangements are mainly used.

- back-to-back connection of two controlled three-phase bridges with thyristors for high-voltage applications and four-quadrant-operation („reversible converter“). Voltage adjustment is achieved by phase control.

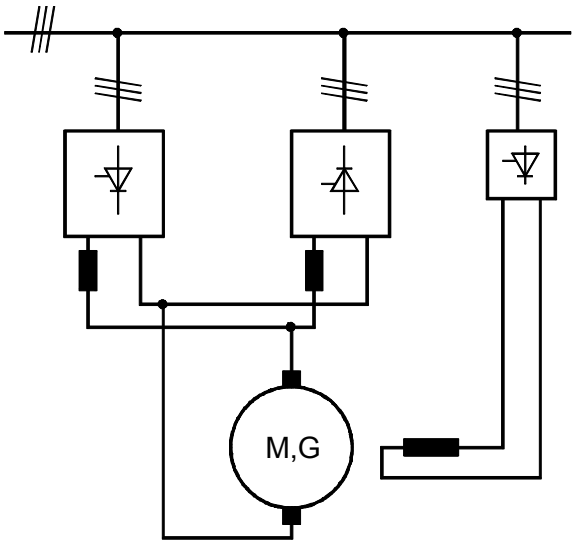

Fig. 105: back-to-back converter arrangement

- uncontrolled converter bridge with voltage DC link as a composition of transistors in H-arrangement for low power applications („servo amplifier “). Therefore usually utilized permanent-field DC motors can be operated in any of the four quadrants, if either a braking resistor or an anti-parallel converter bridge is provided. Voltage adjustment is performed by timing devices.

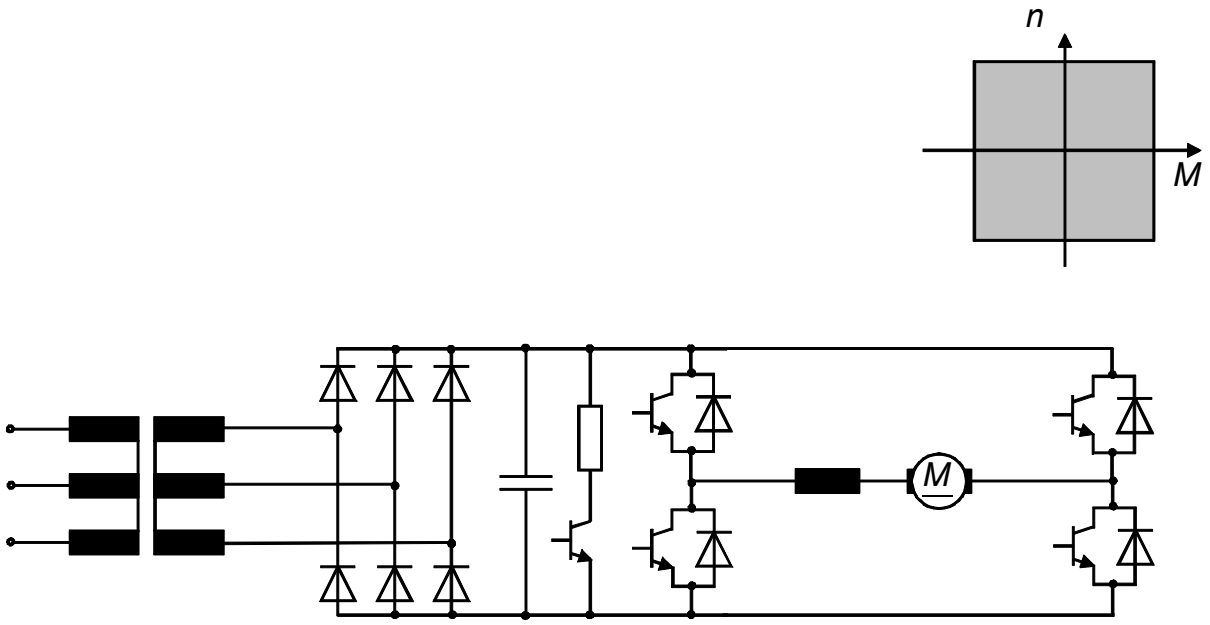

Fig. 106: DC drive (servo), four-quadrant converter

- Simple DC choppers with transistors or thyristors are often used in battery supplied systems. Voltage adjustment is also performed by timing devices. Without reversion, only one-quadrant operation is possible.

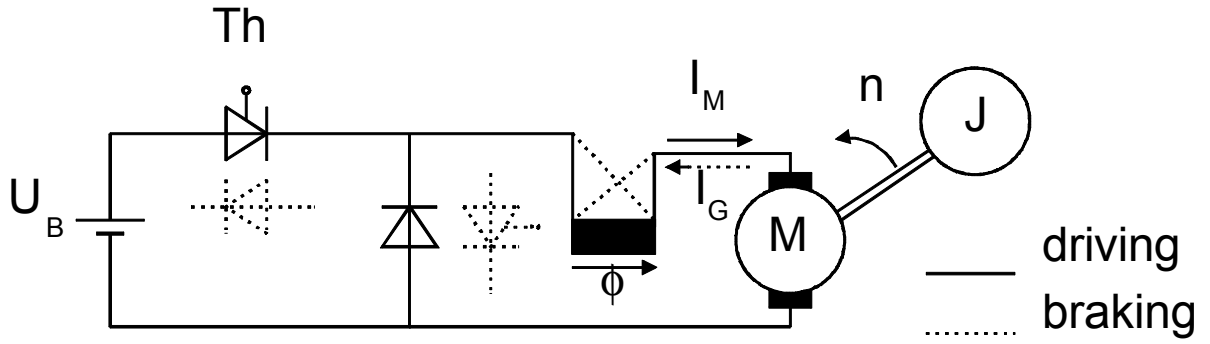

Fig. 107: electric vehicle drive, DC machine with chopper

5.4 Permanent magnets

If permanent magnets are used instead of electrical field excitation, the following advantages appear for DC machines as well as for synchronous machines in principle:

- higher efficiency

$$h = 1 - \frac{\sum V}{P_{auf}} = 1 - \frac{I_A^2 \cdot R_A + \overbrace{I_F^2 \cdot R_F}^{=0} + V_{Fe}}{U_N \cdot I_N} \tag{5.64}$$

- less volume and weight

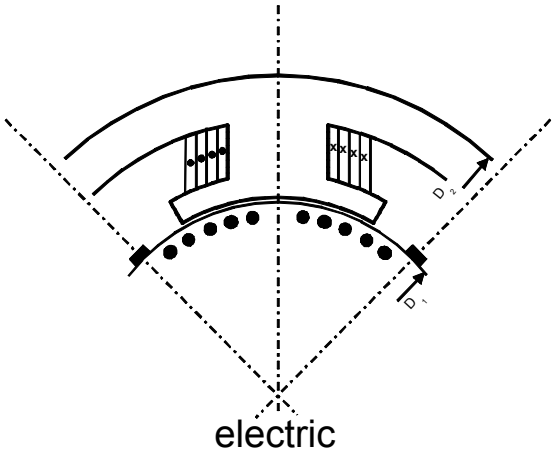

Fig. 108a: electric excitation

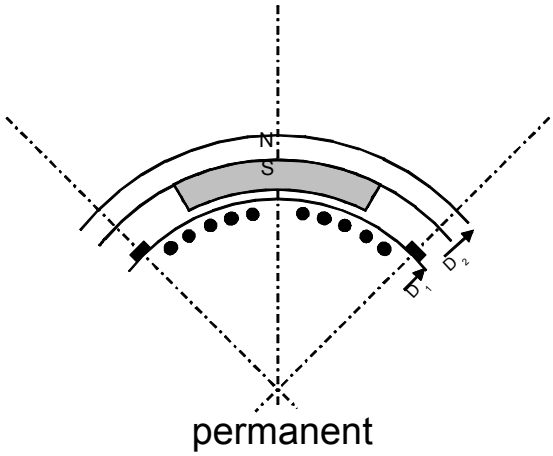

Fig. 108b: permanent field

$$D_{1elektr.} = D_{1perm.}$$
$$D_{2elektr.} > D_{2Perm.}$$

- improved dynamic behaviour

$$T_A = \frac{L_A}{R_A} = \frac{T_{AElektr.}}{1 + \frac{h_M}{d}} << T_{AElektr.} \tag{5.65}$$

- cheaper production

Permanent-magnets are mainly used in DC-, synchronous- and step motors for automotive auxiliary applications, household and consumer goods, office and data systems technology as well as for industrial servo drives.

Besides some exemptions, the power range of permanent-magnet equipped motors leads from a few W to some 10 kW. Power limitations are either given by material parameters or by costs of the permanent-magnets. A widespread implementation of permanent-magnets in electrical machines as well as an expansion up to higher power ranges are to be expected for the future.

Permanent-magnet materials are desribed by their hysteresis loop in the II. quadrant.

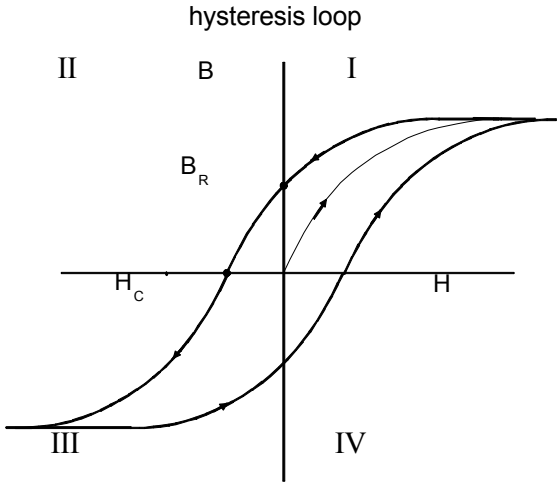

Fig. 109: hysteresis loop

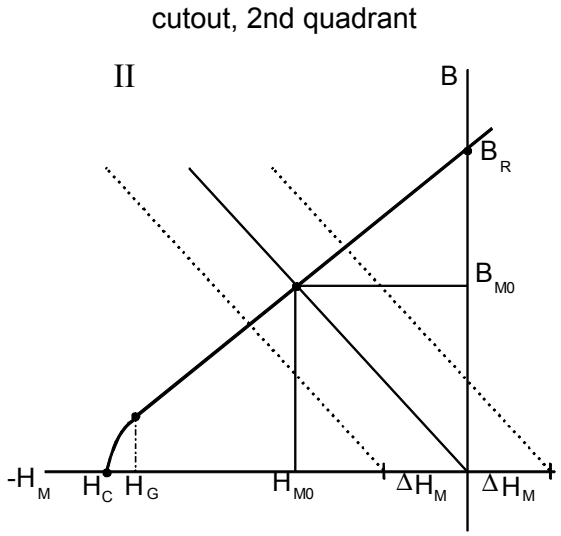

Fig. 110: hysteresis loop, II. quadrant

demagnetization curve: $B_M = B_R + m_0 \cdot m_R \cdot H_M$

remanent flux density: $H = 0 : \mathrm{B} = B_R$

coercive field strength: $B = 0 : H = H_C$

reversible permeability: $m_R \approx 1$

border case field strength: H_G

In order to avoid enduring demagnetization, permanent-magnets are supposed to be operated in between the linear range of the characteristic (Fig. 110). The operating point exceeds the linear range at opposing field strengths higher than H_G (break point), irreversible flux losses appear as a consequence.

A cross section of a four-pole permanent-field DC machine is shown in Fig. 111. Current directions are assumed for motor operation and counter-clockwise rotation. Field strength distribution along the air gap is depicted in Fig. 112 for no-load and load case.

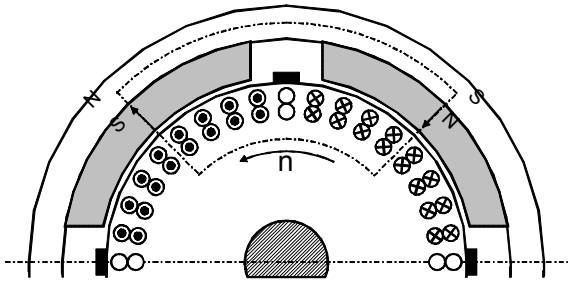

Fig. 111: DC machine, cross section

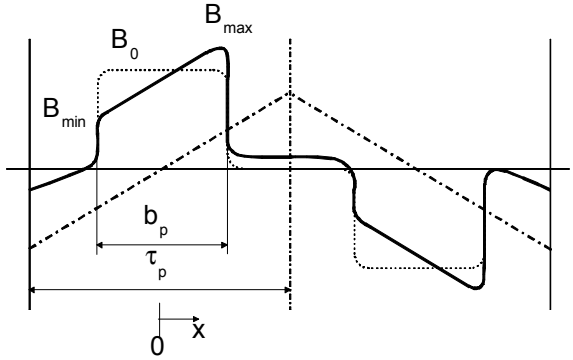

Fig. 112: field strength distribution

The operating point of magnetic circuits can be determined with appliance of:

1) Ampere's Law at pole edges for $\mu_{Fe} \to \infty$ (**D**):

$$\frac{B_L}{m_0} \cdot 2d + H_M \cdot 2h_M = \pm a_i \cdot A \cdot t_p \tag{5.66}$$

2) Demagnetizing curve (**E**):

$$B_M = B_R + m_0 \cdot m_R \cdot H_M \tag{5.67}$$

3) zero-divergence of the magnetic flux for $\sigma_M = 0$ (**Q**):

$$B_L \cdot A_L = B_M \cdot A_M \tag{5.68}$$

with current coverage:

$$A = \frac{z \cdot \frac{I_A}{2a}}{p \cdot D} \tag{5.69}$$

and pole pitch factor:

$$a_i = \frac{b_p}{t_p} \tag{5.70}$$

The air gap line (**L**) results from **D** and **Q**:

$$B_M = \frac{m_0}{2d} \cdot \frac{A_L}{A_M} \cdot \left(- H_M \cdot 2h_M \pm a_i \cdot A \cdot t_p \right) \tag{5.71}$$

The operating point ensues from intersection of **L** and **E** :

$$B_{M0} = \frac{B_R}{1 + m_R \cdot \frac{d}{h_M} \cdot \frac{A_M}{A_L}} \qquad H_{M0} = \frac{\frac{-B_R}{m_0 m_R}}{1 + \frac{h_M}{d \cdot m_R} \cdot \frac{A_L}{A_M}} \tag{5.72, 5.73}$$

$$\Delta H_M = \frac{\pm a_i \cdot A \cdot t_p}{2 \cdot \left(m_R \cdot \frac{A_M}{A_L} \cdot d + h_M \right)} \tag{5.74}$$

Static load or no-load respectively lead to the operating point of the magnet defined by H_{M0} and B_{M0}. This is the intersection of the demagnetizing curve of the magnet and the load line of the magnetic circuit.

The operating point gets moved about *DH* to the right (field strengthening) or to the left (field weakening) caused by armature reaction. Demagnetizing is getting critical at the leaving edge of the magnet. The magnetic circuit needs to be designed in the way, that the operating point does not exceed H_G even under maximum load condition in order to avoid irreversible partial demagnetization. The higher a magnet is designed, the higher is the amount of air gap flux density and the lower the demagnetizing field strength gets.

A selection of magnet materials is given in Fig. 113:

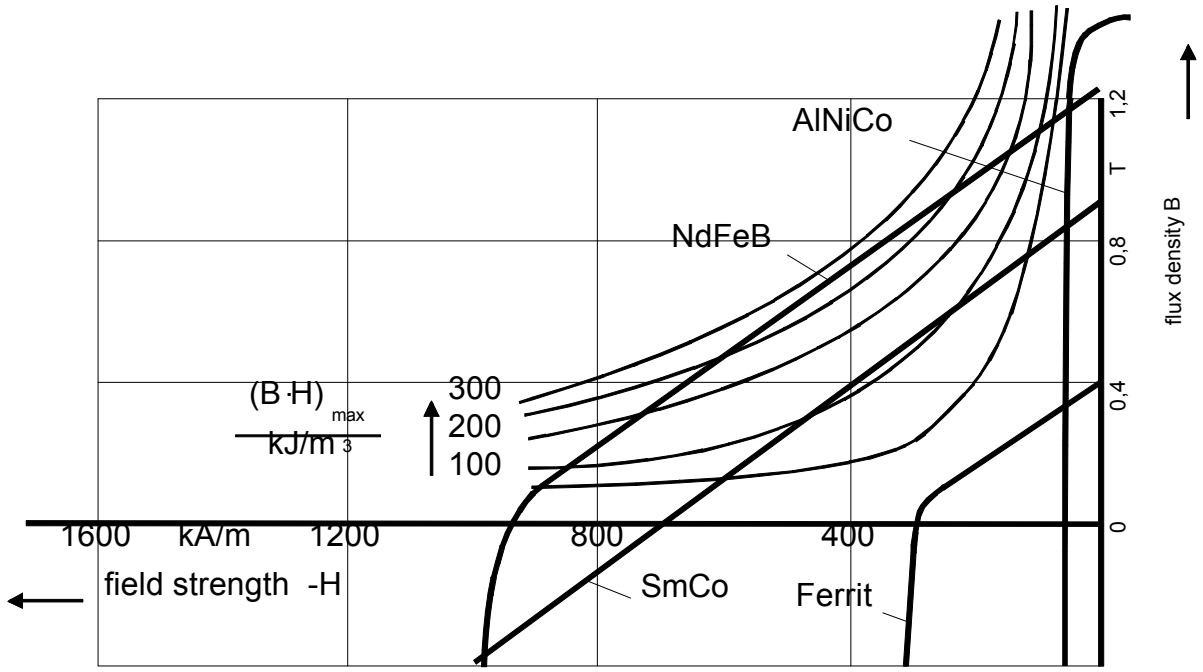

Fig. 113: Selection of magnet materials

Most suitable magnet materials for cost-efficient applications are:

- Ferrites: cheap, low energy density
- AlNiCo: cost-efficient, B_R high, H_C low

and for high-quality small-batch production:

- SmCo: expensive, high energy density, linear characteristic down to III. quadrant
- NdFeB: new, eventually more economic than SmCo, high energy density.

5.5 Commutation

5.5.1 Current path

Commutators permanently reverse the current direction in revolving armature windings using brushes mounted in neutral zones. The direction therefore changes from + to – and the other way around. Armature windings are riddled with AC current of $f_A = pn$. A commutation of the coil currents is necessary in order to achieve time-constant exciter field with perpendicular orientation towards the armature magnetomotive force (mmf).

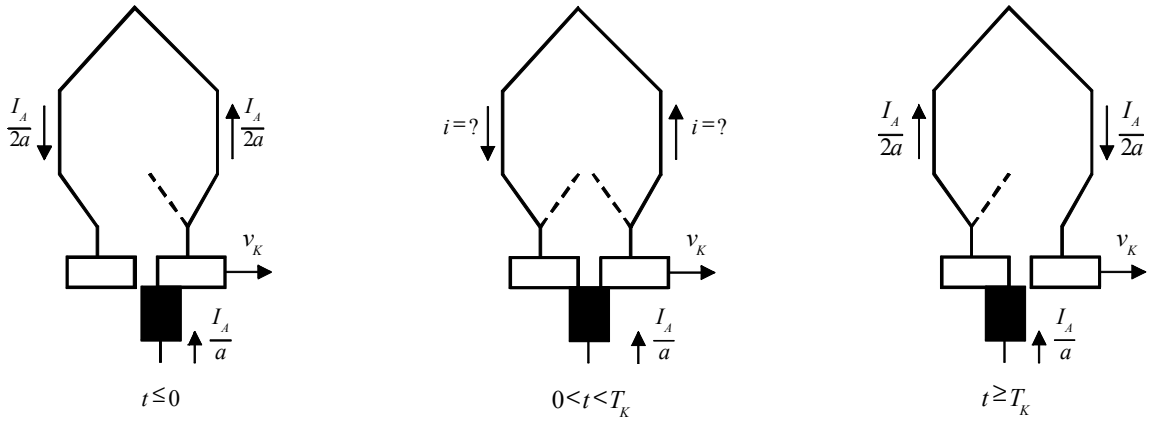

Fig. 114a-c: commutation

coil current: $\frac{I_A}{2a}$ (5.75)

brush width: b_B

commutator circumferential speed: $v_K = pD_K n$ (5.76)

commutating period: $T_K = \frac{b_B}{v_K}$ (5.77)

armature frequency: $f_A = pn$ (5.78)

current coverage: $A = \frac{z\frac{I_A}{2a}}{pD} = \frac{2w_A I_A}{pD}$ (5.79)

An idealized illustration of the current in a single armature coil is given in Fig. 115:

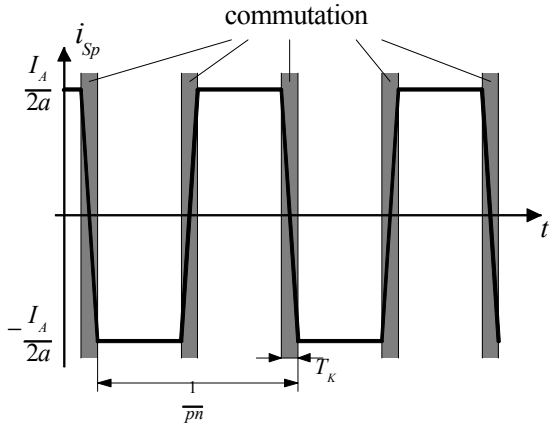

Fig. 115: current in single coil (idealized)

Before the commutation process, an armature coil carries a current $+\frac{I_A}{2a}$, whereas after the process the current amount is $-\frac{I_A}{2a}$. The current form in the short-circuited armature coil is formed according to a function determined by contact resistance (brushes) and coil inductance during the commutating period. With usage of electrographite the influence of the coil resistance is negligible.

At first $L_{Sp} = 0$ is to be assumed (this restriction will be abolished later). With that assumption and $R_B >> R_{Sp}$, simplified illustrations of the arrangement and equations apply as:

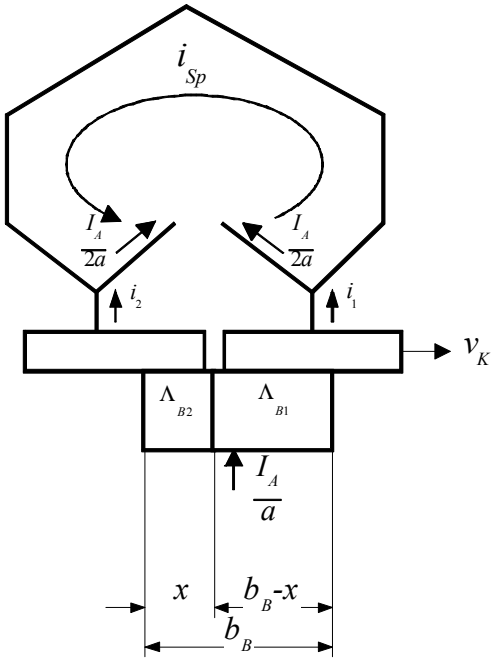

$$\frac{i_2}{i_1} = \frac{\Lambda_{B2}}{\Lambda_{B1}} = \frac{x}{b_B - x} = \frac{t}{T_K - t} \tag{5.80}$$

$$\frac{I_A}{a} = i_1 + i_2 \tag{5.81}$$

$$i_1 = i_{Sp} + \frac{I_A}{2a} \tag{5.82}$$

Fig. 116: commutation, (simplified)

With 5.80-5.82 the current flow in short-circuited coils can be calculated:

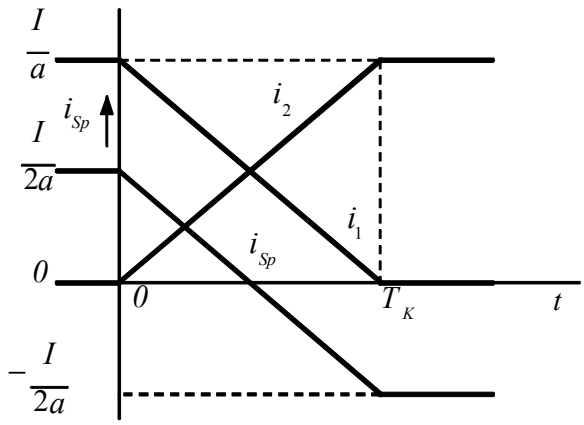

$$i_1 = \frac{I}{a}\left(1 - \frac{t}{T_K}\right) \tag{5.83}$$

$$i_2 = \frac{I}{a}\frac{t}{T_K} \tag{5.84}$$

$$i_{Sp} = \frac{I}{2a}\left(1 - \frac{2t}{T_K}\right) \tag{5.85}$$

Fig. 117: commutation, current flow

A linear current run is to be ascertained („resistance commutation“) and furthermore to be aimed with regard to the reactance voltage of commutation.

5.5.2 Reactance voltage of commutation

Getting back to the assumption of negligible coil inductance, the reality actually shows a commutating coil with finite inductance, caused by slot- and coil-end leakage. This results in self-induced voltage, excited by current change in the short-circuited coil:

$$u_s = -L_{Sp}\frac{\mathrm{d}i_{Sp}}{\mathrm{d}t} = L_{Sp}\frac{\frac{I_A}{a}}{T_K} = L_{Sp}\frac{\frac{I_A}{a}}{b_B}pD_K n \sim I_A n \tag{5.86}$$

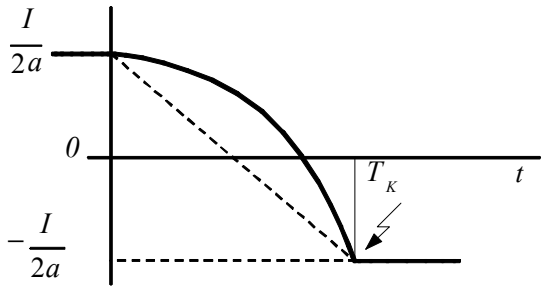

Fig. 118: commutation, reactance voltage

u_s is called "reactance voltage of commutation". A proportionality exists between this voltage and the armature current and rotational speed . Due to Lenz's Law, the reactance voltage of commutation is orientated in the way to counteract its original cause - the change of current, which leads to a lagging commutation. This effect causes sparks at the leaving brush edges, resulting in increased wear of brushes and commutator.

5.5.3 Commutating poles

A compensation of the reactance voltage in commutating coils (evoked by self-induction, caused by current change) by inducing a rotatory voltage is aimed, in order to achieve linear commutation.

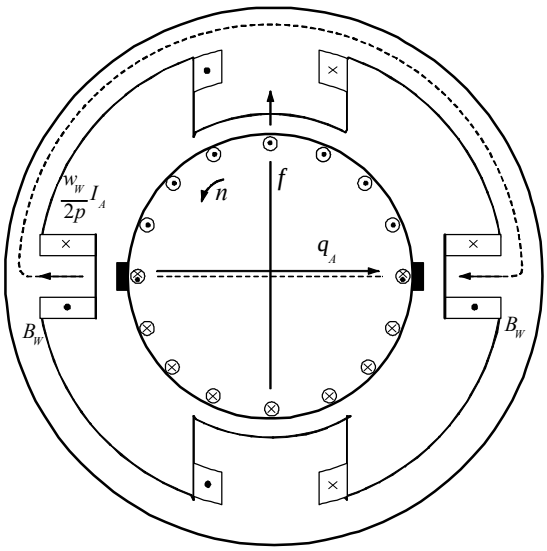

Fig. 119: DC machine, commutating poles

So called commutating poles are arranged in the commutating zone (= pole gap, in which the commutation takes place). Their windings are connected in series with the armature windings.

The commutating pole mmf needs to:

1) eliminate the back-ampere-turns mmf in the pole gap
2) excite a commutating field in order to compensate the reactance voltage of computation.

Fig. 119 shows the reactance voltage trying to maintain the current direction in the commutating coil and the compole voltage counteracting.

Appliance of Ampere's Law on the commutation circuit leads to:
(Exception: commutating windings implemented)

$$q_W - q_A(1-a_i) = \frac{B_W}{m_0} 2d_W \tag{5.87}$$

$$B_W = \frac{m_0}{2d_W}\left(\frac{w_W}{p} I_A - (1-a_i) t_P A\right) \sim I_A \tag{5.88}$$

Commutating field strength and flux density are proportional to the armature current I_A, as long as the commutating pole circuit is unsaturated. The compole voltage calculates from:

$$u_w = B_W 2l w_S v_A \sim n I_A \tag{5.89}$$

Therewith the compensation of u_s by dint of the u_w-condition (equation 5.89) is fulfilled for any rotational speed and any current. In case of proper design, commutating poles act as if $L_{Sp} = 0$.

The installation of commutating poles raises the price of DC machines significantly, so that an implementation makes sense only for large DC machines.

5.6 Armature reaction

5.6.1 Field distortion

Magnetic fields in DC machines are to be considered as being excited only by the exciter windings, arranged on the main poles so far. This does only apply in no-load, where the magnetic flux density underneath the poles is to be seen as almost constant. Considering load cases, armature reaction is to be regarded additionally. Armature currents automatically evolve mmf with perpendicular orientation towards the pole axis – armature quadrature-axis mmf –, which superposes the exciter mmf, adding up to a resulting field. Under load, there is no constant field distribution underneath the poles, so that the orientation of the field axis changes.

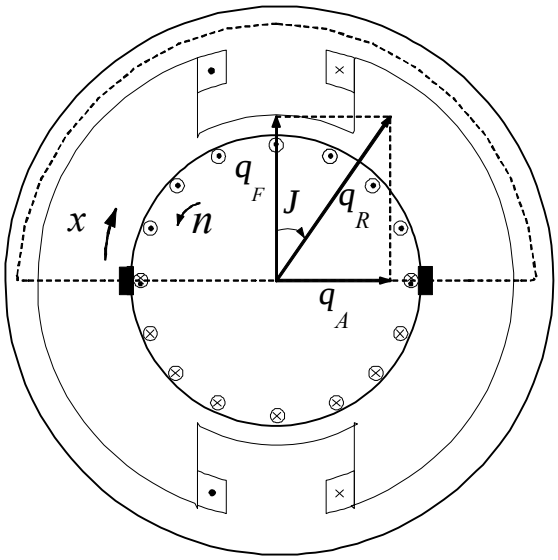

Fig. 120: DC machine, armature reaction

A two-pole DC machine is considered for the determination of the resulting field under load. Ampere's Law applies to:

$$q_F(a)+q_A(a)=\frac{B(a)}{m_0}2d(a) \qquad (5.90)$$

with neglect of saturation effects and the magnetic voltage drop along the iron core ($m_r \to \infty$).

exciter mmf:

$$0<a<\frac{p}{2}(1-a_i),\quad \frac{p}{2}(1+a_i)<a<p \qquad q_F(a)=0 \qquad (5.91)$$

$$\frac{p}{2}(1-a_i)<a<\frac{p}{2}(1+a_i) \qquad q_F(a)=w_F\cdot I_F=q_F \qquad (5.92)$$

armature mmf::

$$0<a<p \qquad q_A=A\cdot t_P\cdot\left(1-\frac{2a}{p}\right) \qquad (5.93)$$

resulting field:

$$B(a)=\frac{m_0}{2d(a)}(q_F(a)+q_A(a)) \qquad (5.94)$$

The axis of the resulting field and therefore the neutral zone moves to oppose the sense of rotation in motor operation with dependence on the armature current.

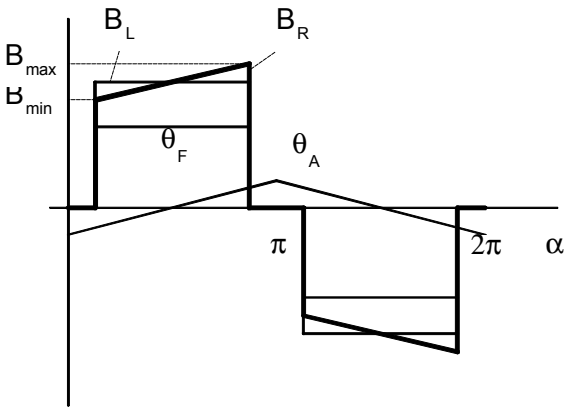

Fig. 121: armature reaction, field distortion

Field distortion comes up: the magnetic field strength increases on the leading edge whereas is decreases at the leaving edge.

Maximum field distortion appears at the pole edges:

$$a_{Pk} = \frac{p}{2}(1 \pm a_i) \tag{5.95}$$

$$B_{Pk} = \frac{m_0}{2d} q_F \pm \frac{m_0}{2d} a_i t_P A = B_L \pm \Delta B \tag{5.96}$$

In order to assure the commutation process within the neutral zone under load, brushes can be moved about an according angle ϑ:

- motor operation: opposing the direction of rotation
- generator operation: in direction of rotation

This method is advantageously for the life cycle of the used brushes.

Besides displacement of the neutral zone, occurring field distortion under load also results in increased segment voltage.

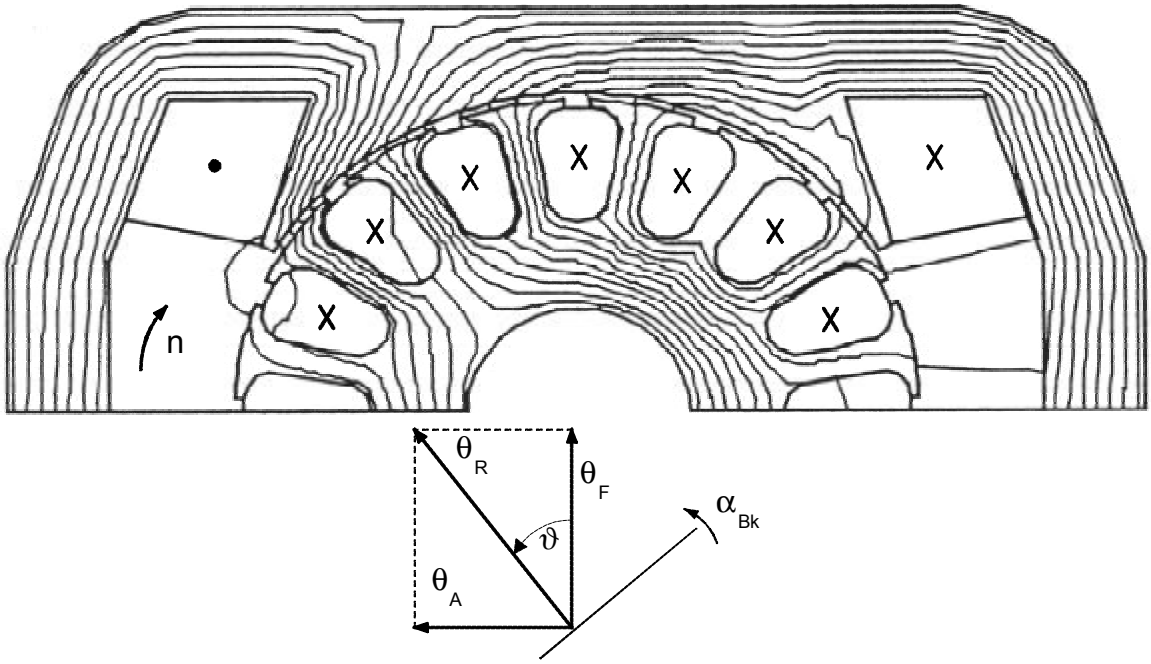

Fig. 122: universal machine, FE-calculated field distribution at nominal load

5.6.2 Segment voltage

Segment voltage is to be mentioned as an important item to be treated in DC machine operation, to occur between two adjoining segments.

The segment voltage average value computes from the armature voltage, divided by the number of segments per pole-pitch:

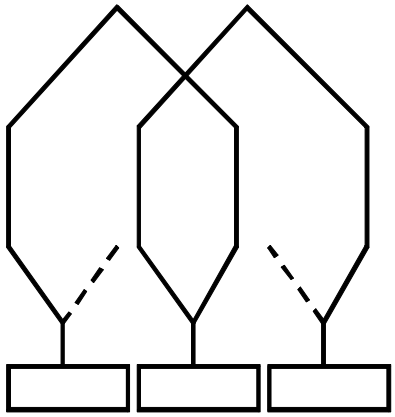

Fig. 123: DC machine, segments

$$U_{L,\text{mittel}} = \frac{armature\ \ voltage}{segments\ \ per\ \ pole-pitch} = \frac{U}{\frac{k}{2p}} \tag{5.97}$$

Caused by field distortion under load, the segment voltage is not evenly spread over corresponding commutator segments, but only $a_i \cdot \frac{k}{2p}$-coils participate at the accumulation of voltage underneath the poles. Therefore the real segment voltage ensues for the no-load case:

$$U_L = \frac{U_{L,\text{mittel}}}{a_i} \tag{5.98}$$

Coils voltage underneath the poles is U_L, whereas coil voltage in the pole gap is 0.

Flux density at pole edges is $B(a) = B_{Pk}$ under load and therefore the segment voltage of these coils:

$$U_{L,\max} = \frac{U_{L,\text{mittel}}}{a_\text{i}} \frac{B_{Pk}}{B_L} = U_L \left(1 + \frac{\Delta B}{B_L}\right) \tag{5.99}$$

that means: segment voltage may increase significantly regionally.

Segment voltage turned out to find a maximum limit at 40V that may not be exceeded. Otherwise spark overs between segments may occur, that may finally lead to a flash over around the entire commutator.

The ratio $U_{L,max}/U_L$ gets awkward in field weakening operation, because the main field gets weaker as the armature reaction remains constant.

$$\frac{U_{L,\max}}{U_L} = 1 + \frac{\Delta B}{B_L}$$

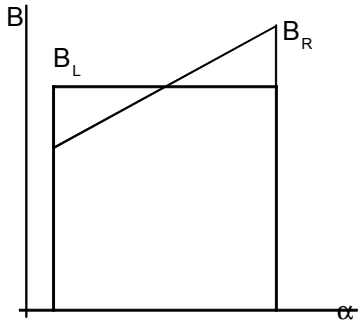

f = 1

Fig. 124a: ratio of:

$$\frac{U_{L,\max}}{U_L} = 1.5$$

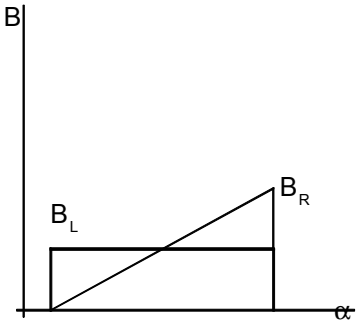

f = 2

Fig. 124b: ratio of:

$$\frac{U_{L,\max}}{U_L} = 2$$

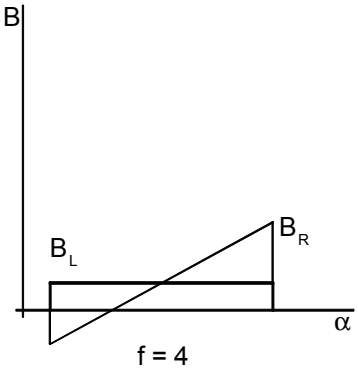

f = 4

Fig. 124c: ratio of

$$\frac{U_{L,\max}}{U_L} = 3$$

The resulting field may turn negative underneath the leaving edge in motor operation!

5.6.3 Compensating winding

DC machines can be fitted with compensation windings in order to compensate armature reaction and its negative consequences. Main poles are slotted. Bars are placed inside the slots, to carry currents of a direction opposing the armature current. The number of conductor bars is design in the way to just equalize the armature mmf underneath the poles.

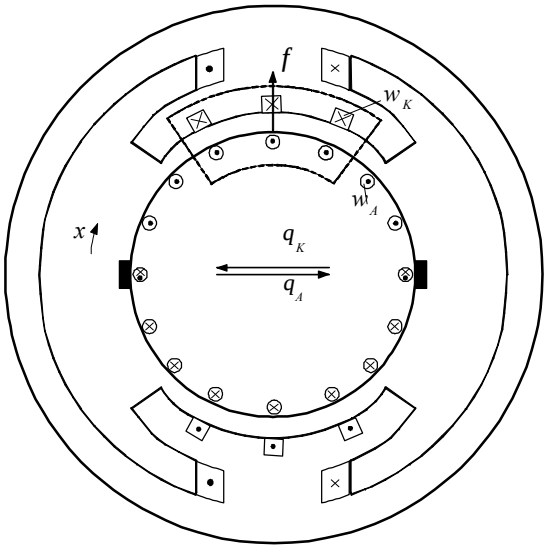

Fig. 125: compensating windings

Armature mmf quadrature fraction is equalized by the effect of the compensating windings in regions around the main poles, whereas commutating windings are supposed to compensate in pole gap regions..

$$q_K = w_K I_A \overset{!}{=} q_A = a_i A t_p \qquad (5.100)$$

Field distribution underneath the poles is equal to that of no-load. Axis directions of resulting field and exciter field are alike. Commutation is performed within the neutral zone, as it is supposed to be.

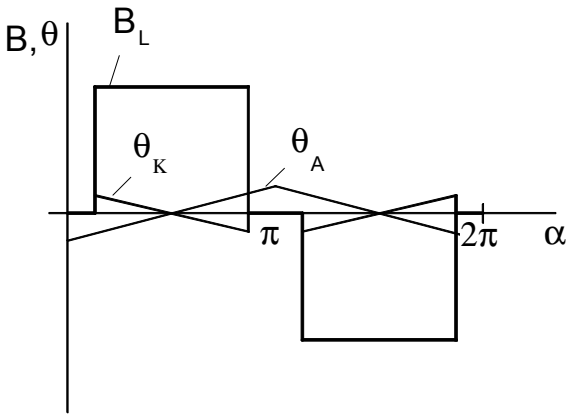

Fig. 126: equalizing mmf fractions

Design of compensating windings:

$$w_K = \frac{a_i A t_p}{I_A} = \frac{a_i \frac{2 w_A I_A}{pD} \frac{pD}{2p}}{I_A} = \frac{a_i w_A}{p} \qquad (5.101)$$

The installation of compensating windings has a significant influence on the price of DC machines, so that an implementation makes sense only for large DC machines. High-quality DC machines feature both commutating and compensating windings.

6 Rotating field theory

6.1 General overview

Basically two different types of rotating electrical machines need to be discussed in case of three-phase rotating system supply.

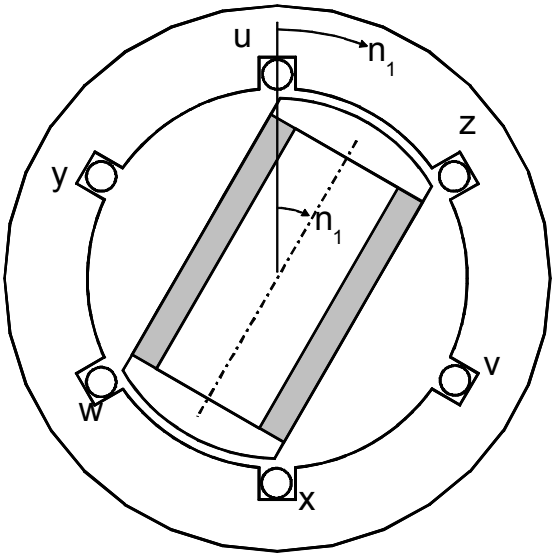

Fig. 127: synchronous machine

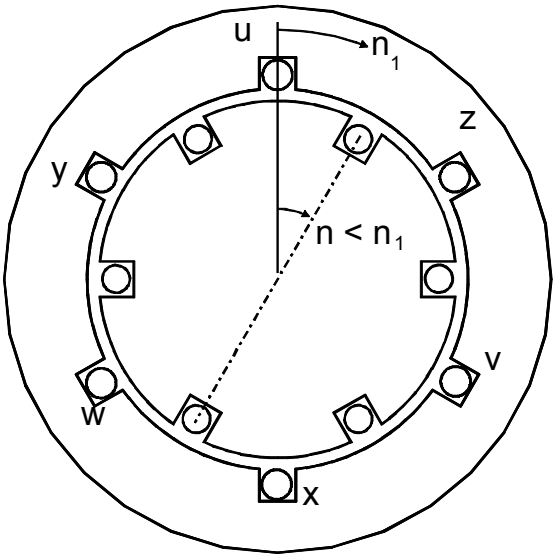

Fig. 128: induction machine

Both synchronous machine and induction machine use the same stator arrangement as a matter of principle. This is composed of insulated iron laminations, provided with a three-phase winding, to create a rotation field revolving with $n_1 = f_1/p$. Both machine types only differ in their rotor design.

Synchronous machines consist of permanent field or electrical excited rotors to follow the stator rotating field synchronous (therefore the name), whereas the rotor of induction machines feature a short-circuit-winding, which is pulled asynchronous by the rotating stator field, due to Lenz's Law.

A combined discussion of voltage and torque generation for both types of three-phase machines in a separate chapter about "rotating field theory" is found reasonable, until both types are discussed in detail later.

6.2 Alternating field

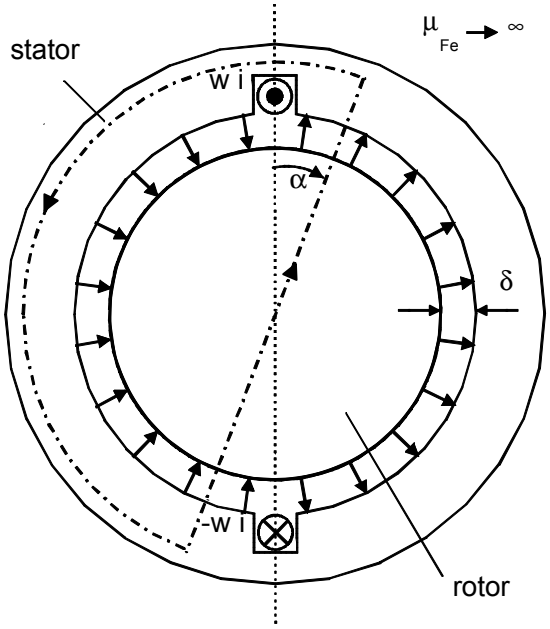

An unwinded rotor enclosed in an arrangement of a stator equipped with 2 opposing slots carrying *w* windings each is shown in Fig. 129.

The according slot-mmf is either $+w\cdot i$ or $-w\cdot i$. Therefore revolution along the dash-dotted line includes an mmf due to $+w\cdot i$ or $-w\cdot i$. Direction assignment is based on Fleming's right-hand-rule.

Fig. 129: unwinded rotor, winded stator

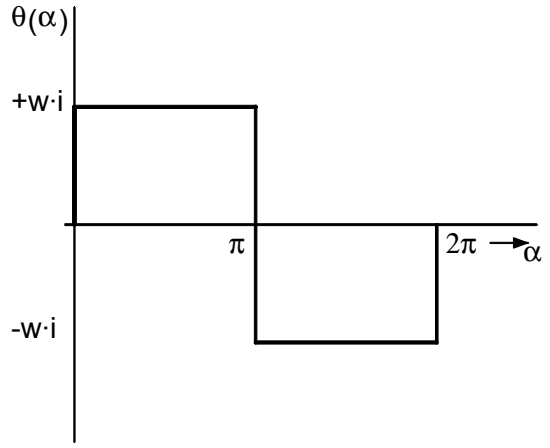

Fig. 130: mmf according to Fig. 130

$$0 < a < p: \qquad q(a) = w\cdot i \tag{6.1}$$

$$p < a < 2\cdot p: \quad q(a) = -w\cdot i \tag{6.2}$$

In case of *i* being alternating current to be stated as $i = \sqrt{2}\cdot I\cdot\cos(w_1\cdot t)$, Ampere's Law being applied over one pole-pitch, neglecting field strength and radial distribution of air gap flux density:

$$q(a) = \oint \vec{H}\cdot d\vec{s} = H(a)\cdot 2\cdot d = \frac{B(a)}{m_0}\cdot 2\cdot d \tag{6.3}$$

spatiotemporal dependent flux density results as follows:

$$0 < a < p \qquad b^w(a,t) = \frac{m_0}{2\cdot d}\cdot q(a) = \frac{m_0}{2\cdot d}\cdot w\cdot\sqrt{2}\cdot I\cdot\cos(w_1\cdot t) \tag{6.4}$$

$$p < a < 2\cdot p \qquad b^w(a,t) = -\frac{m_0}{2\cdot d}\cdot w\cdot\sqrt{2}\cdot I\cdot\cos(w_1\cdot t) \tag{6.5}$$

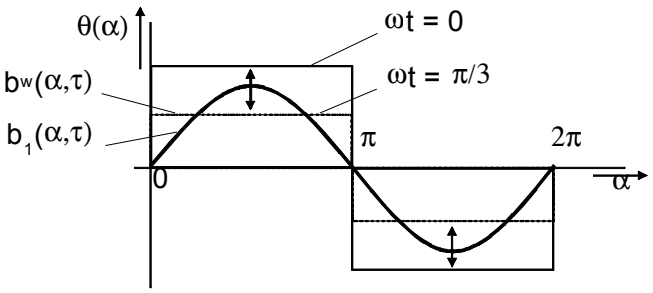

Spatial field distribution and zero crossings remain the same, whereas the field strength amount changes periodically with current frequency. This kind of field is called *alternating field*.

Fig. 131: alternating field distribution

With more than one pole-pair, the process repeats p-times per circumference, the number of windings is distributed on p pole-pairs.

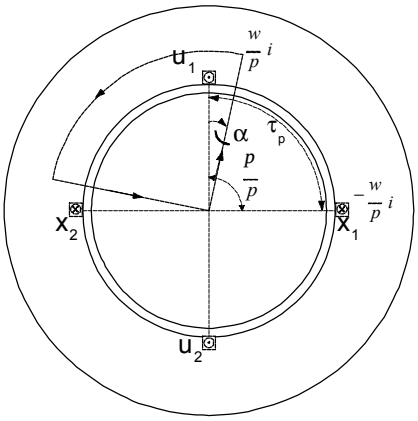

Fig. 132: stator, two pole-pairs

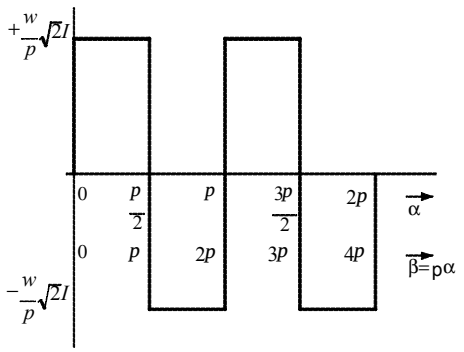

Fig. 133: mmf for two pole-pair stator

The fundamental wave of the square-wave function (Fig. 131 etc.) can be determined by Fourier analysis. This results in an infinite count of single waves of odd ordinal numbers and anti-proportional decreasing amplitude with ordinary numbers. The amplitudes of fundamental waves and harmonics show proportional dependency to the current, zero crossings remain the same. These are called standing wave.

$$b^W(a,t) = \underset{\omega t=0}{\frac{4}{p}\cdot\frac{m_0}{2\cdot d}\cdot\frac{w}{p}\cdot\sqrt{2}\cdot I\cdot\cos(w_1\cdot t)}\cdot\sum_{g'=1}^{\infty}\frac{\sin[(2g'-1)\cdot ap]}{2g'-1} \qquad (6.6)$$

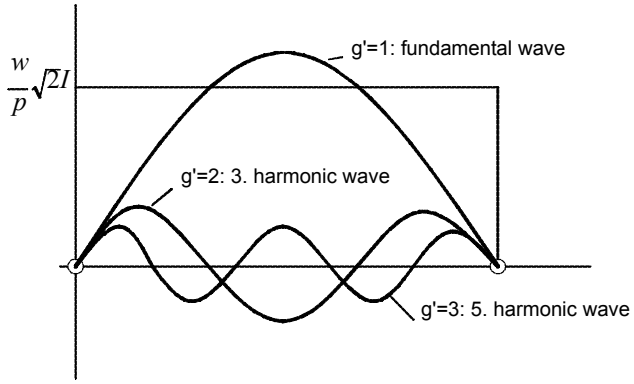

The existence of harmonics is to be attributed to the spatial distributions of the windings. The generating current is of pure sinusoidal form, not containing harmonics.

Fig. 134: fundamental wave, 3rd and 5th harmonics

Important hint: it necessarily needs to be distinguished between

- **wave**: spatiotemporal behaviour,
- **oscillation**: pure time dependent behaviour

Main focus is put on the fundamental wave, which is exclusively significant for voltage generation and torque exertion:

$$b_1^w(a,t) = \frac{4}{p} \cdot \frac{m_0}{2 \cdot d} \cdot \frac{w}{p} \cdot \sqrt{2} \cdot I \cdot \sin(a \cdot p) \cdot \cos(w_1 \cdot t) = B_1^w \cdot \sin(a \cdot p) \cdot \cos(w_1 \cdot t) \tag{6.7}$$

with:

$$B_1^w = \frac{4}{p} \cdot \frac{m_0}{2 \cdot d} \cdot \sqrt{2} \cdot \frac{w}{p} \cdot I \tag{6.8}$$

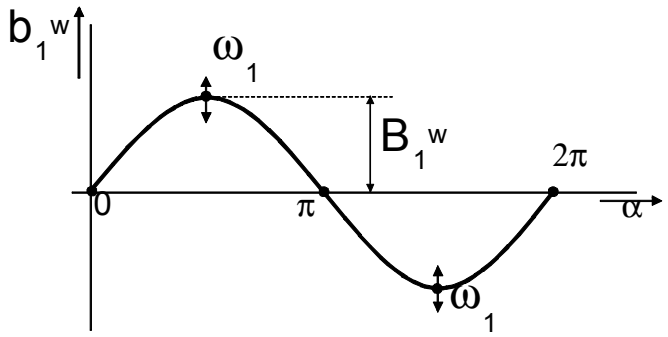

sinusoidal alternating field ≙ standing wave

Fig. 135: sinusoidal wave (as standing wave)

6.3 Rotating field

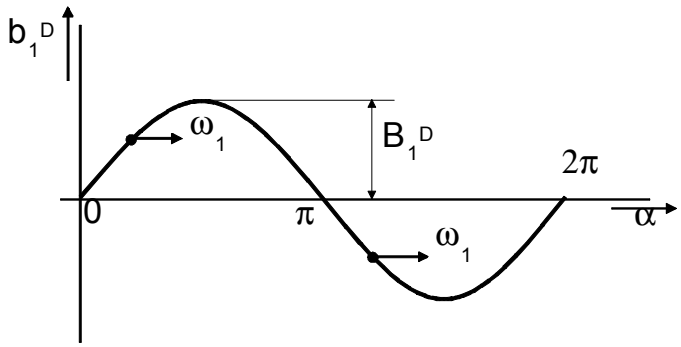

Rotating fields appear as spatial distributed fields of constant form and amount, revolving with angular speed w_1:

progressive wave

Fig. 136: progressive wave

A mathematical formulation is depicted as:

$$b_1^D(a,t) = B_1^D \cdot \sin(a \cdot p - w_1 \cdot t) \tag{6.9}$$

With:

$$a \cdot p - w_1 \cdot t = const \tag{6.10}$$

for any fix point of a curve, the mechanical angle speed of a progressive wave can be calculated:

$$\frac{da}{dt} = \frac{w_1}{p} = \Omega_1 \tag{6.11}$$

with positive α: revolving clockwise (with positive sequence).

A rotating field with:

$$b_1^D(a,t) = B_1^D \cdot \sin(a \cdot p + w_1 \cdot t) \tag{6.12}$$

revolves with a mechanical angular speed of:

$$\frac{da}{dt} = -\frac{w_1}{p} = -\Omega_1 \tag{6.13}$$

with negative α: counter-clockwise (with negative sequence).

A sinusoidal alternating field can be split up into two sinusoidal rotating fields. Their peak value is of half the value as of the according alternating field, their angular speeds are oppositely signed:

$$b_1^w(a,t) = B_1^w \cdot \sin(a \cdot p) \cdot \cos(w_1 \cdot t) = \frac{B_1^w}{2} \cdot \left[\underbrace{\sin(a \cdot p - w_1 \cdot t)}_{positive\ sequence} + \underbrace{\sin(a \cdot p + w_1 \cdot t)}_{negative\ sequence} \right] \tag{6.14}$$

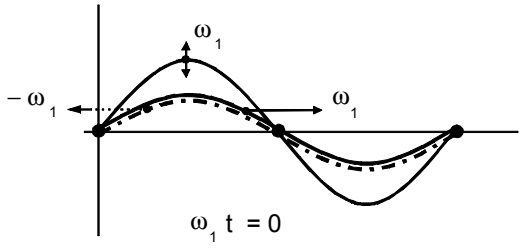

Fig. 137a: alternating field shape

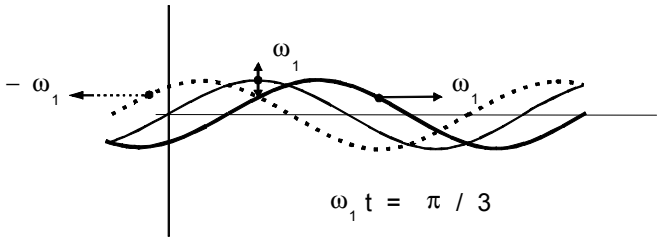

Fig. 137b: split alternating field

This enables a dispartment of rectangular fields (evoked by slot pairs) into clockwise-/counter-clockwise-rotating fields – fields with positive/negative sequence rotational sense:

$$b^W(a,t) = B_1^W \cdot \cos(w_1 \cdot t) \cdot \sum_{g'=1}^{\infty} \frac{\sin[(2g'-1) \cdot ap]}{2g'-1} =$$

$$= \frac{B_1^W}{2} \cdot \left\{ \sum_{g'=1}^{\infty} \underbrace{\frac{\sin[(2g'-1) \cdot ap - w_1 \cdot t]}{2g'-1}}_{positive\ sequence} + \sum_{g'=1}^{\infty} \underbrace{\frac{\sin[(2g'-1) \cdot ap + w_1 \cdot t]}{2g'-1}}_{negativesequence} \right\} \tag{6.15}$$

The angular speed of the single waves amounts:

$$\frac{da}{dt} = \frac{w_1}{p \cdot (2g'-1)} = \Omega_{2g'-1} \qquad \text{clockwise rotation (positive sequence)} \tag{6.16}$$

$$\frac{da}{dt} = \frac{-w_1}{p \cdot (2g'-1)} = -\Omega_{2g'-1} \qquad \text{counter-clockwise rotation (negative sequence)} \tag{6.17}$$

with single wave peak value:

$$B_{2g'-1}^W = \frac{B_1^W}{2g'-1} \tag{6.18}$$

6.4 Three-phase winding

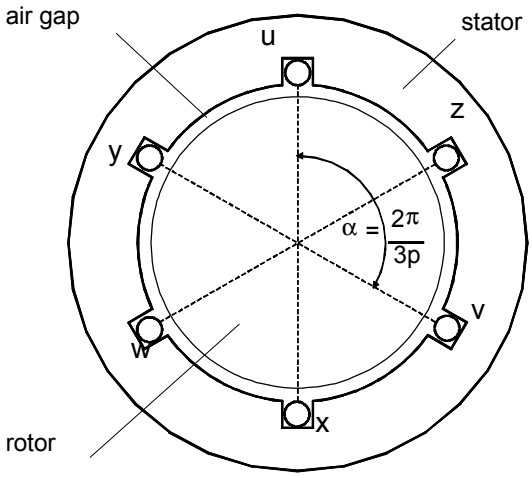

Fig. 138: three-phase winding, stator

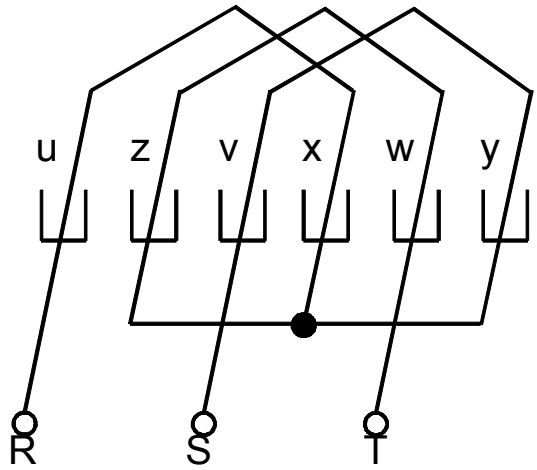

Fig. 139: three-phase winding, star point

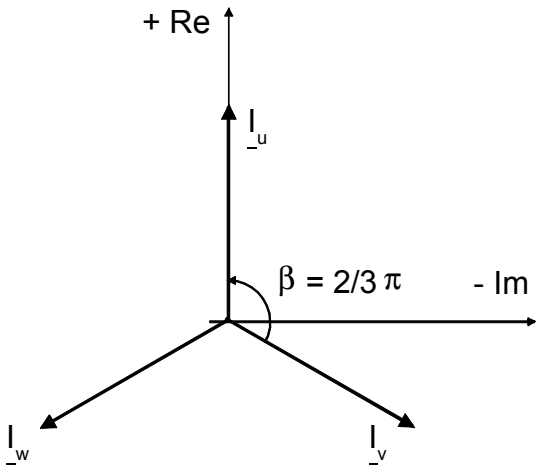

Fig. 140: phase currents, phasor diagram

Most simple arrangement of a three-phase stator consist of:

- core stack composed of laminations with
  - approximately 0,5 mm thickness,
  - mutual insulation

  for a reduction of eddy currents.

- *m=3* phases with spatial displacement of an angle $a = \frac{2 \cdot p}{3 \cdot p}$ against each other. Leads of windings are assigned as *U*, *V*, *W*, whereas line ends are indicated with *X*, *Y*, *Z* (shown in Fig. 139 for star connection).

- The number of pole pairs is *p=1* in Fig. 138. In case of *p*>1, the configuration repeats *p*-times along the circumference.

a : mechanical angle
$b = p \cdot a$: electrical angle

The pole pitch is given as $t_p = \frac{p \cdot D}{2 \cdot p}$

The number of slots per pole and phase is

$$q = \frac{N}{2 \cdot p \cdot m} \overset{!}{=} \text{integer}$$

There are three phases connected due to *U-X*, *V-Y*, *W-Z*, which are supplied by three AC currents, also displaced by a phase shift angle $\frac{2 \cdot p}{3}$:

$$i_U = \sqrt{2} \cdot I \cdot \cos(w_1 \cdot t) \qquad (6.19)$$

$$i_V = \sqrt{2} \cdot I \cdot \cos\left(w_1 \cdot t - \frac{2 \cdot p}{3}\right) \qquad (6.20)$$

$$i_W = \sqrt{2} \cdot I \cdot \cos\left(w_1 \cdot t - \frac{4 \cdot p}{3}\right) \qquad (6.21)$$

An alternating field is created by any of the phases, to be segmented in both positive- and negative sequence rotating field. Only fundamental waves are taken into account.

$$\left.\begin{aligned} b_U &= B_1^w \cdot \sin(a \cdot p) \cdot \cos(w_1 \cdot t) \\ b_V &= B_1^w \cdot \sin\left(a \cdot p - \frac{2 \cdot p}{3}\right) \cdot \cos\left(w_1 \cdot t - \frac{2 \cdot p}{3}\right) \\ b_W &= B_1^w \cdot \sin\left(a \cdot p - \frac{4 \cdot p}{3}\right) \cdot \cos\left(w_1 \cdot t - \frac{4 \cdot p}{3}\right) \end{aligned}\right\} B_1^w = \frac{4}{p} \cdot \frac{m_0}{2 \cdot d} \cdot \frac{w}{p} \cdot \sqrt{2} \cdot I \tag{6.22}$$

$$\begin{aligned} b_U &= \frac{B_1^w}{2} \cdot [\sin(a \cdot p - w_1 \cdot t) + \sin(a \cdot p + w_1 \cdot t)] \\ b_V &= \frac{B_1^w}{2} \cdot \left[\sin(a \cdot p - w_1 \cdot t) + \sin\left(a \cdot p + w_1 \cdot t - \frac{4 \cdot p}{3}\right)\right] \\ b_W &= \frac{B_1^w}{2} \cdot \left[\sin(a \cdot p - w_1 \cdot t) + \underbrace{\sin\left(a \cdot p + w_1 \cdot t - \frac{8 \cdot p}{3}\right)}_{\sum = 0}\right] \end{aligned} \tag{6.23}$$

The total field results from a superposition of the 3 phases at any time. Negative sequence rotating fields eliminate each other, whereas positive sequence fields add up to a sinusoidal rotating field. Its amplitudes are 3/2 times higher than those of single alternating field amplitudes.

$$\begin{aligned} b_1^D(a,t) &= \frac{3}{2} \cdot B_1^w \cdot \sin(a \cdot p - w_1 \cdot t) = B_1^D \cdot \sin(a \cdot p - w_1 \cdot t) \\ B_1^D &\equiv B = \frac{3}{2} \cdot \frac{4}{p} \cdot \frac{m_0}{2 \cdot d} \cdot \frac{w}{p} \cdot \sqrt{2} \cdot I \end{aligned} \tag{6.24}$$

The rotational speed (= synchronous rotational speed) can be determined by taking a look at the zero crossing condition $(a \cdot p - w_1 \cdot t = 0)$:

$$a \cdot p = w_1 \cdot t \Rightarrow \frac{da}{dt} = \frac{w_1}{p} = \frac{2 \cdot p \cdot f_1}{p} = 2 \cdot p \cdot n_1 \Rightarrow n_1 = \frac{f_1}{p} \tag{6.25}$$

The air gap field of multipole rotating field machines revolves with synchronous rotational speed $n_1 = \frac{f_1}{p}$, so that the following speeds occur at 50 Hz:

p	1	2	3	4	5	6	10	20	30
$n_1 / {}^{1}/_{\min}$	3000	1500	1000	750	600	500	300	150	100

Fig. 141: speeds due to number of pole pairs (example: 50 Hz)

Visualization:

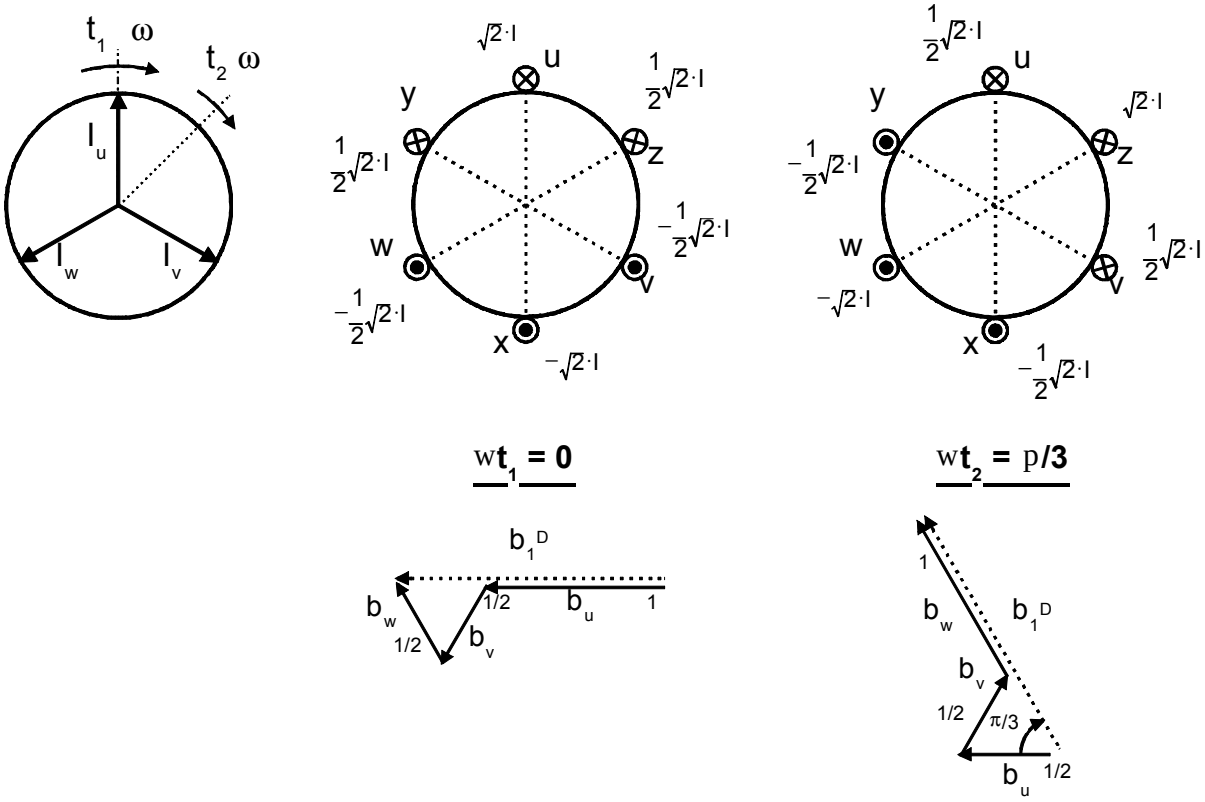

Fig. 142: field shares of phases U, V, W while rotation from $w_1 \cdot t = 0$ through $w_1 \cdot t = \mathrm{p}/3$

If slot mmf harmonics of the three phases are regarded, the total field ensues to:

$$b^D(a,t) = B_1^D \cdot \sum_{g'=-\infty}^{\infty} \frac{\sin\left[(6g+1)\cdot ap - w_1 \cdot t\right]}{6g+1} \tag{6.26}$$

Again, equation 6.26 defines an infinite sum of positive- and negative-sequence single rotating fields with ordinal number 6g+1. Field components with ordinary numbers divisible by three disappear for the case of superposition:

- positive g: 1, 7, 13, 19,... positive sequence
- negative g: -5, -11, -17,... negative sequence

The mechanical angular speed of the single waves amounts:

$$\Omega_{6g+1} = \frac{w_1}{p \cdot (6g+1)} \tag{6.27}$$

as well as the amplitude of single waves:

$$B_{6g+1}^D = \frac{B_1^D}{6g+1} \tag{6.28}$$

Rotational speed as well as the amplitudes of the harmonics decrease with increasing ordinal number.

6.5 Example

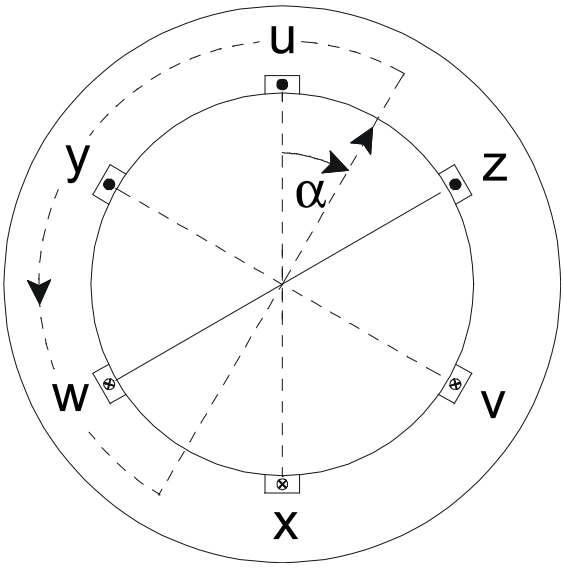

Fig. 143: three-phase stator, rotational angle

with $q_N = \sqrt{2} I \frac{w}{p}$ (6.29)

we get

$$q_u = q_N \cos(wt) \tag{6.30}$$

$$q_v = q_N \cos\left(wt - \frac{2p}{3}\right) \tag{6.31}$$

$$q_w = q_N \cos\left(wt - \frac{4p}{3}\right) \tag{6.32}$$

Determination of slot mmf for different moments (temporal)

- quantity of slot mmf is applied over the circumference angle.
- line integrals provide enveloped mmf, dependent on the circumference angle.
- total mmf is shaped like a staircase step function, being constant between the slots. At slot edges, with slots assumed as being narrow, the total mmf changes about twice the amount of the slot mmf.

The air gap field results from the total mmf:

$$B(a,t) = \frac{m_0}{2d} \cdot q(a,t) \tag{6.33}$$

The fundamental wave runs to the right at speed $\frac{w}{p}$, harmonics run to both right and left, at speed $\frac{w}{p(6g+1)}$. Amplitudes of fundamental waves and harmonics remain constant. The shape of the air gap field changes periodically at times $wt = 0, \frac{p}{6}, \frac{p}{3}, \ldots$ between both extrema. The change of shape is based on the different rotational speeds of fundamental wave and harmonics and hence different results of their addition.

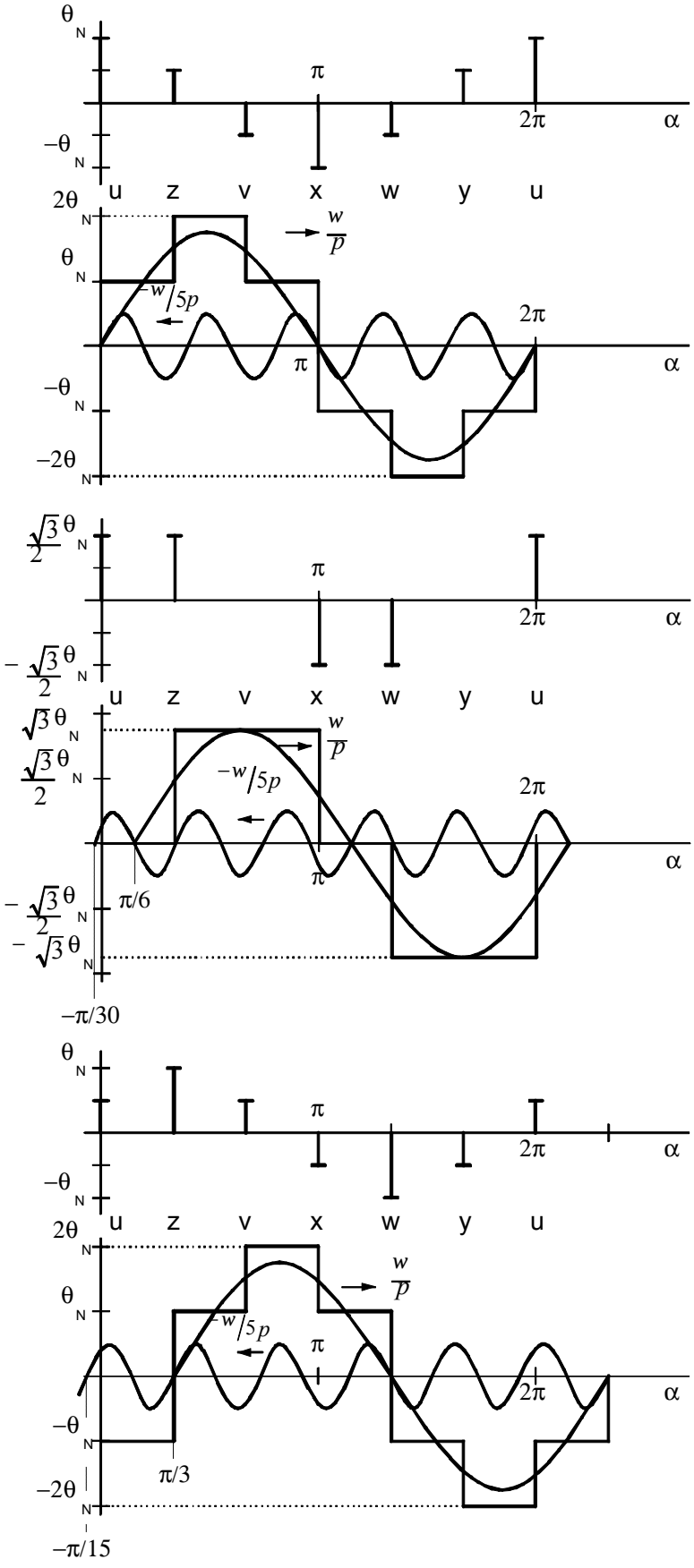

$wt = 0$

$q_u = q_N$

$q_v = -\frac{q_N}{2}$

$q_w = -\frac{q_N}{2}$

$wt = \frac{p}{6}$

$q_u = \frac{\sqrt{3}}{2} q_N$

$q_v = 0$

$q_w = -\frac{\sqrt{3}}{2} q_N$

$wt = \frac{p}{3}$

$q_u = \frac{q_N}{2}$

$q_v = \frac{q_N}{2}$

$q_w = -q_N$

Fig. 144: mmf, sequence

6.6 Winding factor

If *w* windings per phase are not placed in two opposing slots, but are moreover spread over more than one slot (zone winding) and return conductors are returned under an electric angle smaller than < *180°*, the effective number of windings appears smaller than it is in real:

number of slots per pole and phase

$$q = \frac{N}{2 \cdot p \cdot m} \geq 1 \tag{6.34}$$

chording

$$\frac{5}{6} < \frac{s}{t} < \frac{6}{7} \tag{6.35}$$

resulting number of windings

$$w_{res} \leq w \tag{6.36}$$

This is taken into account, introducing the winding factor x :

$$x \leq 1: \quad w_{res} = w \cdot x \tag{6.37}$$

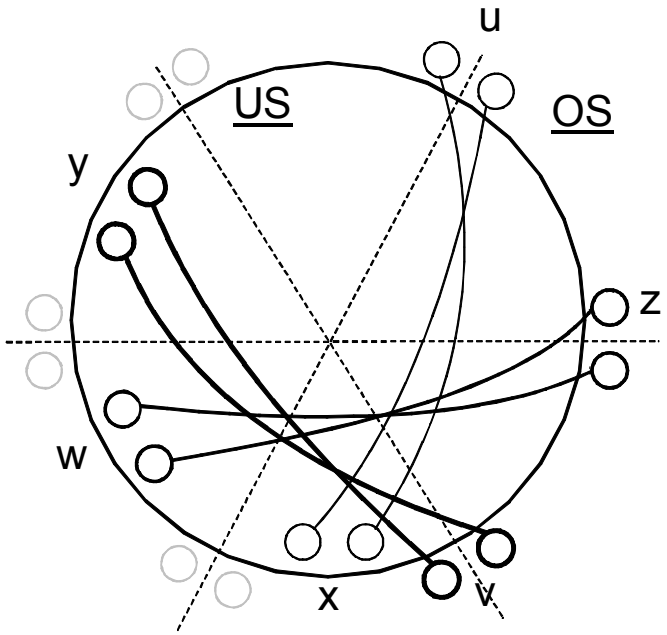

Fig. 145: three-phase winding, chording

This means is utilized for a supression of harmonics, which cause parasitic torques and losses, influencing proper function of a machine..

Actually there is no machine with $q = 1$. Only zoning and chording enable disregarding harmonics.

6.6.1 Distribution factor

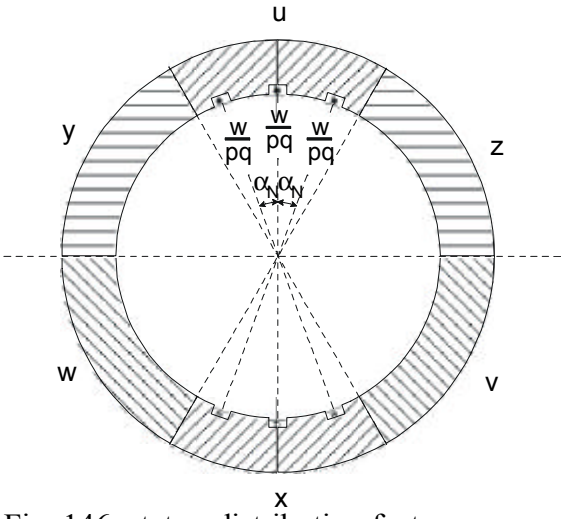

Fig. 146: stator, distribution factor

All w/p windings per pole and phase are distributed over q slots. Any of the w/pq conductors per slot show a spatial displacement of.

$$a_N = \frac{2p}{N} = \frac{p}{p \cdot m \cdot q} \tag{6.38}$$

against each other. This leads to an electrical displacement of

$$b_N = p \cdot a_N = \frac{p}{m \cdot q} \tag{6.39}$$

The resulting number of windings w_{res} per phase is computed by geometric addition of all q partial windings w/pq. The vertices of all q phasors per phase, being displaced by β_N (electrically), form a circle. The total angle per phase adds up to q β_N.

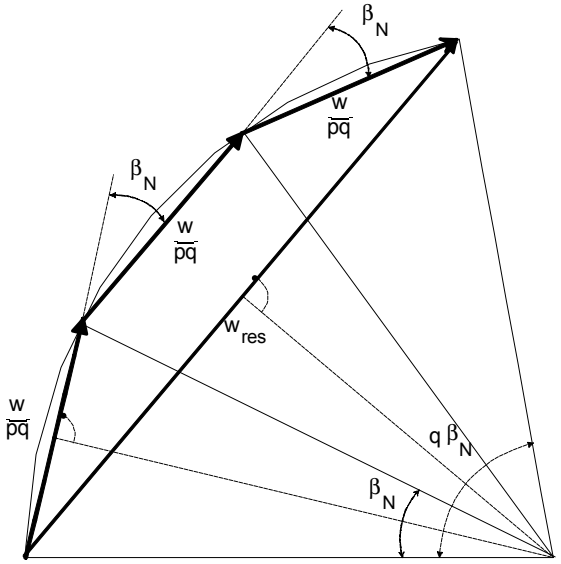

Fig. 147: displaced windings

Circle radius:

$$r = \frac{\frac{1}{2} \cdot \frac{w}{p \cdot q}}{\sin\left(\frac{b_N}{2}\right)} \tag{6.40}$$

chord line:

$$w_{res} = 2 \cdot r \cdot \sin\left(\frac{q \cdot b_N}{2}\right) \tag{6.41}$$

Therefore follows for the resulting number of windings:

$$w_{res} = \frac{w}{p} \frac{\sin\left(\frac{q \cdot b_N}{2}\right)}{q \cdot \sin\left(\frac{b_N}{2}\right)} \tag{6.42}$$

The ratio

$$\frac{w_{res}}{\frac{w}{p}} = \frac{\sin\left(\frac{q \cdot b_N}{2}\right)}{q \cdot \sin\left(\frac{b_N}{2}\right)} \tag{6.43}$$

is called *distribution factor*.

Rotating field windings feature:

$$b_N = \frac{p}{3 \cdot q} \tag{6.44}$$

which leads to

$$x_Z = \frac{\sin\frac{p}{6}}{q \cdot \sin\frac{p}{6 \cdot q}}, \tag{6.45}$$

considering the fundamental wave.

Regarding harmonics, the electrical angle β_N needs to be multiplied (6g+1)-times the basic value, with (6g+1) being the harmonic ordinal number. Then follows for the harmonic distribution factor:

$$x_{Z,(6g+1)} = \frac{\sin\left[\frac{p \cdot (6g+1)}{6}\right]}{q \cdot \sin\left[\frac{p}{6 \cdot q} \cdot (6g+1)\right]}. \tag{6.46}$$

Purpose: The purpose of utilizing zone winding is to aim

- slot mmf fundamental waves adding up
- harmonics compensating each other, as they suppose to do.

Example for q = 3

Figure series 148a-c illustrates how different distribution factors (abbrev.: df) accomplish for different g:

$g = 0$

$6g + 1 = 1$

$b_{N1} = \frac{p}{3 \cdot 3} \hat{=} 20°$

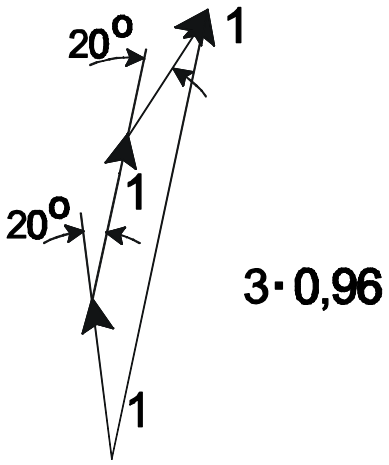

Fig. 148a: df for g=0

$g = 1$

$6g + 1 = 7$

$b_{N7} = 140°$

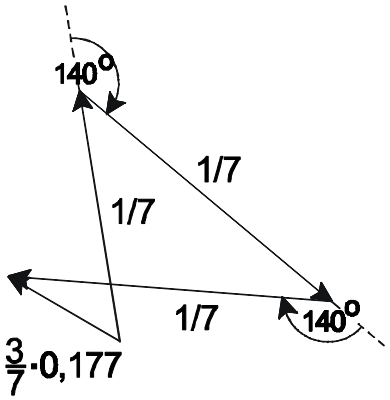

Fig. 148b: df for g=1

$g = -1$

$6g + 1 = -5$

$b_{N-5} = -100°$

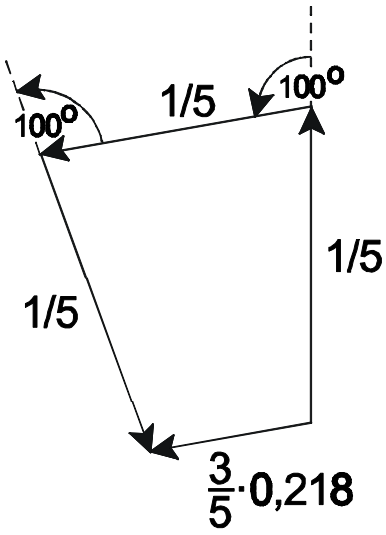

Fig. 148c:df for g=-1

$$x_{Z1} = \frac{\sin\frac{p}{6}}{3\sin\frac{p}{18}} = 0.960$$

$$x_{Z7} = \frac{\sin\frac{p}{6}7}{3\sin\frac{p}{18}7} = -0.177$$

$$x_{Z-5} = \frac{\sin\frac{p}{6}(-5)}{3\sin\frac{p}{18}(-5)} = 0.218$$

See table below for a list of the distribution factor for the fundamental wave:

q	1	2	3	4	...	∞
x_{Z1}	1	0.966	0.960	0.958		0.955

6.6.2 Pitch factor

If windings are not implemented as diametral winding, but as chorded winding, return- and line conductor are not displaced by an entire pole pitch τ_p (equal to 180° electrical), but only by an angle $s < \tau_p$, being < 180° (el.). Mentioned stepping s/τ_p can only be utilized for entire slot pitches $\tau_N = 2\pi/N$.

In practice the windings are distributed over two layers. Line conductors are placed into the bottom layer, whereas return conductors are integrated into the top layer. That arrangement complies with a superposition of two winding systems of halved number of windings, being displaced by an angle α_S (mech.).

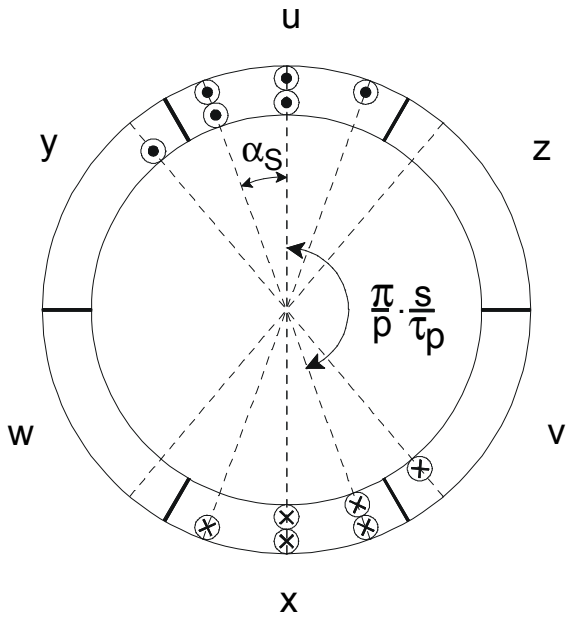

Fig. 149: three-phase winding, chording

This leads to an electrical displacement of $\beta_S = p\alpha_S$. Both fractional winding systems add up to the resulting number of windings.

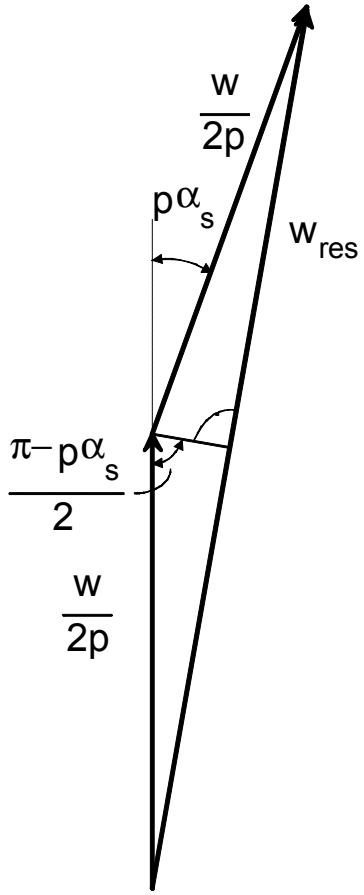

Fig. 150: angle displacement

$$a_S = \frac{p}{p}\left(1 - \frac{s}{t_p}\right) \tag{6.47}$$

$$w_{res} = \frac{w}{p} \cdot \sin\left(\frac{p - p \cdot a_S}{2}\right) = \frac{w}{p} \cdot \sin\left(\frac{p}{2} \cdot \frac{s}{t_p}\right) \tag{6.48}$$

The ratio

$$x_S = \frac{w_{res}}{\frac{w}{p}} = \sin\left(\frac{p}{2} \cdot \frac{s}{t_p}\right) \tag{6.49}$$

is called *pitch factor* (or *chording factor*).

Considering harmonic waves, the electric angle β_S needs to be multiplied by times the ordinal number, which leads to the harmonic's pitch factor:

$$x_{S,(6g+1)} = \sin\left((6g+1)\frac{p}{2}\cdot\frac{s}{t_p}\right) \tag{6.50}$$

The effect of using chorded windings is based on a clever choice of the ratio $\frac{s}{t_p}$, leading to a mutual elimination of the 5th and 7th harmonics of primary and secondary side, so that they disappear for an outside view.

e.g.:

$$\frac{s}{t_p} = \frac{4}{5} \qquad x_{S5} = 0$$

$$\frac{s}{t_p} = \frac{6}{7} \qquad x_{S7} = 0$$

It is proven useful to choose a median value (e.g. 5/6) in order to damp 5th and 7th harmonics at the same time.

Then follows:

- $x_{S1} = 0.966$
- $x_{S5} = 0.259$
- $x_{S7} = 0.259$

6.6.3 Resulting winding factor

The resulting winding factor for three-phase windings results from the multiplication of zone winding factor and chording factor.

- fundamental wave:

$$x = x_Z \cdot x_S = \frac{\sin\frac{p}{6}}{q \cdot \sin\frac{p}{6 \cdot q}} \cdot \sin\left(\frac{s}{t} \cdot \frac{p}{2}\right) \tag{6.51}$$

- harmonic waves:

$$x_{(6g+1)} = x_{Z,(6g+1)} \cdot x_{S,(6g+1)} = \frac{\sin\left[\frac{p \cdot (6g+1)}{6}\right]}{q \cdot \sin\left[\frac{p}{6 \cdot q} \cdot (6g+1)\right]} \cdot \sin\left((6g+1)\frac{p}{2} \cdot \frac{s}{t_p}\right) \tag{6.52}$$

With regard to the winding factor, a mathematic formulation for a rotating field generally appears as:

$$b^D(a,t) = \frac{3}{2} \cdot \frac{4}{p} \cdot \frac{m_0}{2 \cdot d} \cdot \frac{w}{p} \cdot \sqrt{2} \cdot I \cdot \sum_{g'=-\infty}^{\infty} \frac{x_{(6g+1)} \cdot \sin\left[(6g+1) \cdot ap - w_1 \cdot t\right]}{6g+1} \tag{6.53}$$

Assumption for the fundamental wave:

$$b_1^D(a,t) = B_1^D \cdot \sin(a \cdot p - w_1 \cdot t) \tag{6.54}$$

with

$$B_1^D = \frac{3}{2} \cdot \frac{4}{p} \cdot \frac{m_0}{2 \cdot d} \cdot \frac{w}{p} \cdot x \cdot \sqrt{2} \cdot I \tag{6.55}$$

6.7 Voltage induction caused by influence of rotating field

Voltage in three-phase windings revolving at variable speed, induced by a rotating field is subject to computation in the following:
Spatial integration of the air gap field results in the flux linkage of a coil. Induced voltage ensues by derivation of the flux linkage with respect to time. Using the definition of slip and a transfer onto three-phase windings, induced voltages in stator and rotor can be discussed. The following considerations are made only regarding the fundamental wave.

6.7.1 Flux linkage

The air gap field is created in the three-phase winding of the stator, characterized by the number of windings w_1 and current I_1:

$$b_1^D(a,t) = B_1^D \cdot \sin(ap - w_1 t) \tag{6.56}$$

$$B_1^D = \frac{3}{2}\frac{4}{p}\frac{m_0}{2d}\frac{w_1}{p}x_1\sqrt{2}I_1 \tag{6.57}$$

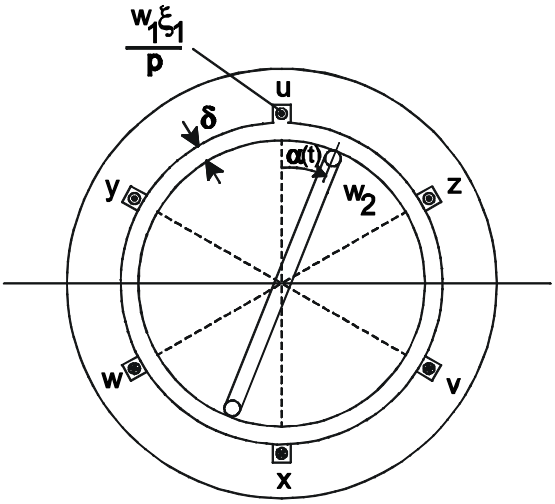

Fig. 151: three-phase winding

First of all, only one single rotor coil with number of windings w_2 and arbitrary position α (angle of twist) is taken into account.
Flux linkage of the rotor coil results from spatial integration of the air gap flux density over one pole pitch.

$$y_2(a,t) = w_2 f_2(a,t) = w_2 \int_0^{tp} b_1^D(a,t)\cdot l \cdot \mathrm{d}x \tag{6.58}$$

$$\mathrm{d}x = \frac{D}{2}\cdot \mathrm{d}a \tag{6.59}$$

$$\begin{aligned} y_2(a,t) &= w_2 \int_a^{a+p/p} b_1^D(a,t)\cdot l \cdot \frac{D}{2}\cdot da = w_2 \cdot l \cdot \frac{D}{2}\int_a^{a+p/p} B_1^D \sin(ap - w_1 t)\mathrm{d}a \\ &= w_2 \frac{l\cdot D}{p}\cdot B_1^D \cdot \cos(ap - w_1 t) \end{aligned} \tag{6.60}$$

fundamental wave of air gap flux:

$$f_1 = \frac{l\cdot D}{p}\cdot B_1^D \tag{6.61}$$

flux linkage of the rotor coil:

$$y_2 = w_2 \cdot f_1 \cdot \cos(ap - w_1 t) \tag{6.62}$$

6.7.2 Induced voltage, slip

Induced voltage in a rotor coil of arbitrary angle of twist $a(t)$, which is flowed through by the air gap flux density $b_1^D(a,t)$, computes from variation of the flux linkage with time.
Described variation of flux linkage can be caused by both variation of currents $i_u(t)$, $i_v(t)$, $i_w(t)$ with time, inside the exciting three-phase winding and also by rotary motion $a(t)$ of the coil along the air gap circumference.

$$u_{i2}(a,t) = -\frac{dy_2(a,t)}{\mathrm{d}t} = -\frac{\partial y_2(a,t)}{\partial a}\frac{\mathrm{d}a}{\mathrm{d}t} - \frac{\partial y_2(a,t)}{\partial t} \tag{6.63}$$

$$u_{i2} = w_2 f_1 \sin(ap - w_1 t)\cdot\left(p\frac{\mathrm{d}a}{\mathrm{d}t} - w_1\right) \tag{6.64}$$

mechanical angular speed of the rotor:

$$\frac{\mathrm{d}a}{\mathrm{d}t} = \Omega = 2pn \tag{6.65}$$

rotational speed of the air gap field:

$$\Omega_1 = \frac{w_1}{p} = 2pn_1 \tag{6.66}$$

definition of the *slip*:

$$s = \frac{\Omega_1 - \Omega}{\Omega_1} = \frac{n_1 - n}{n_1} \tag{6.67}$$

Slip is the referenced differential speed between stator rotating field and rotor. Rotational speed of the stator rotating field is taken as reference value.

The rotational speed of the stator field fundamental wave is called synchronous speed.

$$n_1 = \frac{\Omega_1}{2p} = \frac{\left(\frac{w_1}{p}\right)}{2p} = \frac{\left(\frac{2pf_1}{p}\right)}{2p} = \frac{f_1}{p} \tag{6.68}$$

As per 6.67, slip $s=0$ applies at synchronous speed, whereas $s=1$ applies for standstill. Therefore follows for the induced voltage of the rotor winding:

$$\begin{aligned} u_{i2}(a,t) &= w_2 f_1 \sin(ap - w_1 t)\cdot\frac{p\Omega - w_1}{w_1} w_1 \\ &= -s\cdot w_1 \cdot w_2 f_1 \sin(ap - w_1 t) \end{aligned} \tag{6.69}$$

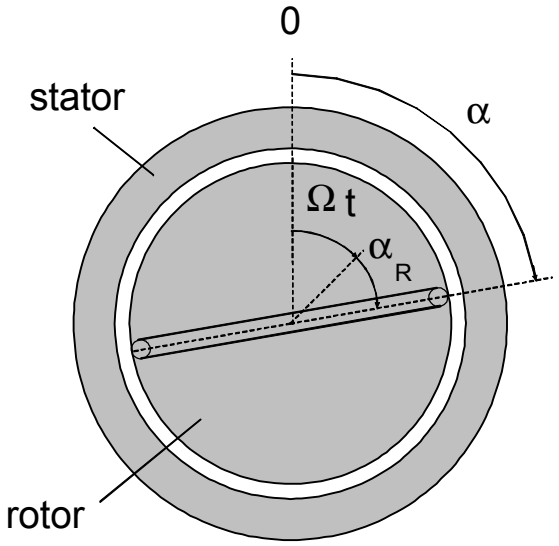

Fig. 152: rotor position, rotation angle

Spatial position of the rotor coil can also be depicted as:

$$a(t) = a_R + \Omega t \tag{6.70}$$

Therefore follows for the induced voltage in the rotor coil:

$$\begin{aligned} u_{i2}(a,t) &= -s \cdot w_1 \cdot w_2 f_1 \sin(a_R p + \Omega t \cdot p - w_1 t) \\ &= -s \cdot w_1 \cdot w_2 f_1 \sin\left(a_R p - \frac{w_1 - p\Omega}{w_1} w_1 t\right) \\ &= -s \cdot w_1 \cdot w_2 f_1 \sin(a_R p - s \cdot w_1 t) \end{aligned} \tag{6.71}$$

- Some aspects regarding induced voltage dependencies are listed below:
- the amplitude of the induced voltage is proportional to the line frequency of the stator *and* to the according slip.
- frequency of induced voltage is equal to slip frequency.
- at rotor standstill (*s=1*), frequency of the induced voltage is equal to line frequency.
- when rotating ($s \neq 1$), voltage of different frequency is induced by the fundamental wave of the stator windings.
- no voltage is induced into the rotor at synchronous speed (*s=0*).
- phase displacement of voltages to be induced into the rotor is only dependent from the spatial position of the coil, represented by the (elec.) angle $a_R p$.

Is a rotor also equipped with a three-phase winding, instead of a single coil - similar to the stator arrangement – with phases being displaced by a mechanical angle $a_R = (k-1)\frac{2p}{3p}$ (k=1,2,3), a number of slots per pole and phase greater than 1 (q>1) and the resulting number of windings $w_2\xi_2$, then follows for the induced voltage of single rotor phases:

$$u_{i2k}(t) = s \cdot w_1 \cdot w_2 x_2 f_1 \sin\left(s \cdot w_1 t - \frac{2p}{3}(k-1)\right) \tag{6.72}$$

For s=1, equation 6.72 applies for induced voltages in stator windings using $w_1 x_1$:

$$u_{i1K}(t) = w_1 w_1 x_1 f_1 \sin\left(w_1 t - \frac{2p}{3}(k-1)\right) \tag{6.73}$$

The rms values of induced voltages in stator and rotor windings ensue to:

$$U_{i1} = w_1 \cdot w_1 x_1 \cdot \frac{f_1}{\sqrt{2}} \tag{6.74}$$

$$U_{i2} = s w_1 \cdot w_2 x_2 \cdot \frac{f_1}{\sqrt{2}} \tag{6.75}$$

$$\frac{U_{i1}}{U_{i2}} = \frac{w_1 x_1}{w_2 x_2} \cdot \frac{1}{s} \tag{6.76}$$

Voltages behave like effective number of windings and relative speed.

6.8 Torque of two rotating magneto-motive forces

As fulfilled previous considerations, only the fundamental waves of the effects caused by the air gap field are taken into account.

Rotating mmf q_1^D, caused in stator windings, is revolving with $\frac{w_1}{p_1}$:

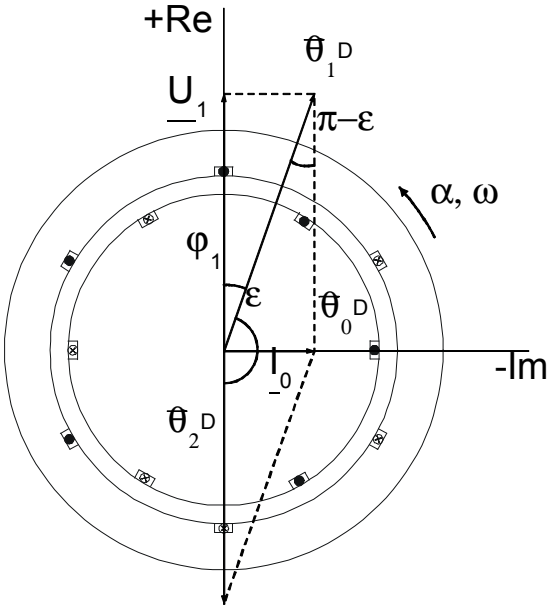

Fig. 153: space vector representation for θ
time vector representation for $\underline{U}, \underline{I}$.

$$q_1^D(a,t) = q_1^D \sin(a p_1 - w_1 t) \tag{6.77}$$

$$q_1^D = \frac{3}{2}\frac{4}{p}\frac{w_1 x_1}{p_1}\sqrt{2} I_1 \tag{6.78}$$

An according rotating mmf is evoked in the rotor windings q_2^D, revolving with $\frac{w_2}{p_2}$ and being displaced by a lagging angle ε:

$$q_2^D(a,t) = q_2^D \sin(a p_2 - w_2 t - e p_2) \tag{6.79}$$

$$q_2^D = \frac{3}{2}\frac{4}{p}\frac{w_2 x_2}{p_2}\sqrt{2} I_2 \tag{6.80}$$

Initially no assumptions are made for the number of pole pairs, angular frequency and phase angle of rotating magneto-motive forces of stator- and rotor.

With appliance of Ampere's law, the resulting air gap field calculates from superimposing of both rotating magneto-motive forces of stator and rotor:

$$b^D(a,t) = \frac{m_0}{2d} \underbrace{\left(q_1^D(a,t) + q_2^D(a,t)\right)}_{q_0(a,t)} \tag{6.81}$$

The magnetic energy in the air gap ensues to:

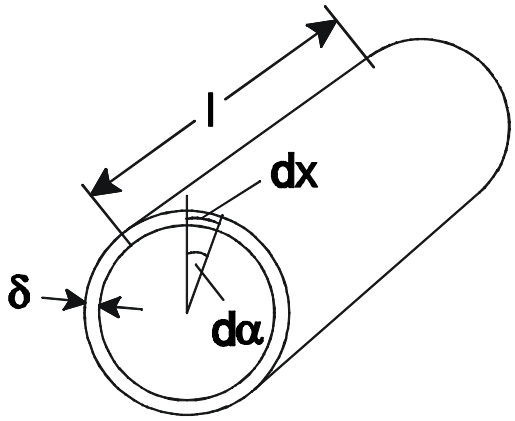

Fig. 154: dimension, air gap surface

$$W_m = \int_V \frac{B^2(a,t)}{2m_0} \mathrm{d}V \tag{6.82}$$

$$\mathrm{d}V = l d \mathrm{d}x = l d \frac{D}{2} \mathrm{d}a \tag{6.83}$$

Torque computes from the derivation of the magnetic energy with the relative mechanical displacement ε of both rotating fields against each other:

$$M = \frac{\partial W_m}{\partial e} = \frac{\partial}{\partial e} \int_0^{2p} \frac{B^2(a,t)}{2m_0} l d \frac{D}{2} \mathrm{d}a \tag{6.84}$$

Derivation with regard to chain rule (math.):

$$\frac{\partial}{\partial e} B^2(a,t) = 2B(a,t) \frac{\partial B(a,t)}{\partial e} = 2\left(\frac{m_0}{2d}\right)^2 \left(q_1^D(a,t) + q_2^D(a,t)\right) \frac{\partial q_2^D(a,t)}{\partial e} \tag{6.85}$$

Only $q_2^D(a,t)$ is a function of ε, $q_1^D(a,t)$ is independent from ε.

Replacing variables:

$$M = \frac{l d D}{4m_0} 2\left(\frac{m_0}{2d}\right)^2 \int_0^{2p} \left[q_1^D \sin(ap_1 - w_1 t) + q_2^D \sin(ap_2 - w_2 t - ep_2)\right] q_2^D \left[-p_2 \cos(ap_2 - w_2 t - ep_2)\right] \mathrm{d}a \tag{6.86}$$

Equation 6.86 can be modified and simplified by appliance of trigonometric relations.

With regard to the validity of:

$$\int_0^{2p} \sin x \cos x \, \mathrm{d}x = 0 \tag{6.87}$$

equation 6.86 simplifies to:

$$M = \frac{-p_2 l D m_0}{4 \cdot 2d} q_1^D q_2^D \int_0^{2p} \sin(ap_1 - w_1 t) \cos(ap_2 - w_2 t - ep_2) \mathrm{d}a \tag{6.88}$$

with:

$$\sin x \cos y = \frac{1}{2}\left(\sin(x+y)+\sin(x-y)\right) \tag{6.89}$$

follows:

$$M = \frac{-p_2 l D m_0}{4 \cdot 2d} \frac{q_1^D q_2^D}{2} \int_0^{2p} \underbrace{\left(\sin\left[(p_1+p_2)a-(w_1+w_2)t-ep_2\right]\right.}_{x_1} + \underbrace{\left.\sin\left[(p_1-p_2)a-(w_1-w_2)t+ep_2\right]\right)}_{x_2} \mathrm{d}a \tag{6.90}$$

in general:

$$\int_0^{2p} \sin(nx+j)\,dx = \begin{cases} 0 & \text{für} \quad n \neq 0 \\ 2p \sin j & \text{für} \quad n = 0 \end{cases} \tag{6.91}$$

Since p_1 and p_2 are integer numbers, x_1 is always equal to zero and x_2 is only unequal to zero, if $p_1 = p_2 = p$.

Therefore the number of pole pair of stator and rotor must agree, in order to create torque at all.

With this assumption follows:

$$M = \frac{-plDm_0}{4 \cdot 2d} \frac{q_1^D q_2^D}{2} 2p \sin\left[-(w_1-w_2)\,t+ep\right] \tag{6.92}$$

A time-variant sinusoidal torque with average value equal to zero appears which is called *oscillation torque*. Only if angular frequencies of the exciting currents agree, which means $\omega_1=\omega_2=\omega$ and therefore speed of rotation of stator and rotor rotating field agree (at equal number of pole pairs), a time-constant torque derives for $e \neq 0$:

$$M = \frac{plDm_0}{4 \cdot 2d} p q_1^D q_2^D \sin(-ep) \tag{6.93}$$

As to be seen in equation 6.93 the torque of two magneto-motive forces is porportional to their amplitudes and the sine-value of the enclosed angle.

- M = maximum for $e = \frac{p}{2p}$
- $M = 0$ for $\varepsilon = 0$

Magneto-motive force q_0^D reflects the geometrical sum of stator and rotor mmf, which complies with the resulting air gap field.

$$\vec{q}_0^D = \vec{q}_1^D + \vec{q}_2^D = \frac{2d}{m_0} B_1^D \tag{6.94}$$

The appliance of the sine clause leads to:

$$\frac{q_2^D}{\sin\left(\frac{p}{2} - j_1\right)} = \frac{q_0^D}{\sin(p - e)} \tag{6.95}$$

then follows:

$$-q_2^D \sin e = q_0^D \cos j_1 = \frac{2d}{m_0} B_1 \cos j_1 \tag{6.96}$$

Inserted into the torque equation finally results in:

$$\begin{aligned} M &= \frac{plDp}{4} q_1^D B_1^D \cos j_1 = \frac{plDp}{4} \frac{3}{2} \frac{4}{p} \frac{w_1 x_1}{p} \sqrt{2} I_1 B_1^D \cos j_1 \\ &= \frac{3p}{w_1} w_1 w_1 x_1 \frac{f_1}{\sqrt{2}} I_1 \cos j_1 = \frac{3U_1 I_1 \cos j_1}{\Omega_1} = \frac{P_D}{\Omega_1} \end{aligned} \tag{6.97}$$

Displacement between U_1 und I_1 is represented by φ_1.
The voltage phasor U_1 is orientated in the direction of the +Re-axis (real) whereas I_0 is orientated in direction of the –Im-axis (imaginary), for complex coordinate presentation.

6.9 Frequency condition, power balance

If stator windings of rotating field machines are fitted with a number of pole pairs p, supplied by a balanced three-phase system of frequency f_1, a rotating field is evoked in the air gap, revolving with synchronous speed $n_1 = f_1 / p$.

If n may be rotor speed, then follows for the relative speed between stator rotating field and rotor speed $n_2 = n_1 - n$.

If rotor slots are also fitted with symmetrical three-phase windings (number of pole pairs p, currents with slip frequency $f_2 = p \cdot n_2$ are induced into the rotor. Those currents likewise create a rotating field, revolving relatively to the rotor speed at speed $n_2 = f_2 / p$.

The rotating field, caused by rotor currents features a rotational speed $n_2 + n = n_1$, according to the stator field. This necessity is called frequency condition.

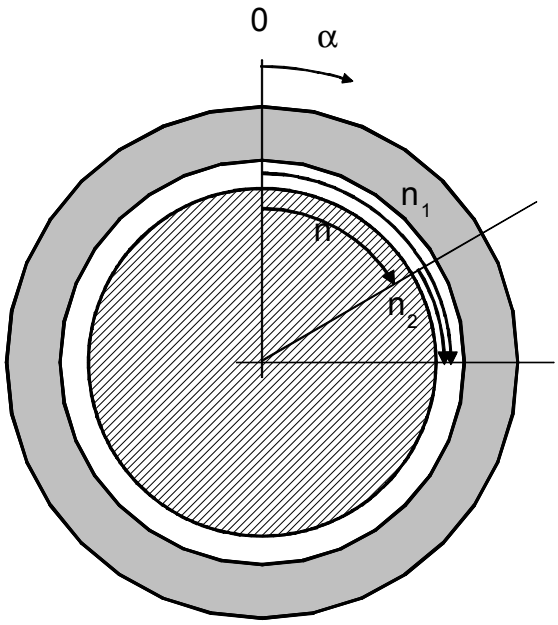

Fig. 155: speed overview

Stator field and rotor field show the same rotational speed, same number of pole pairs assumed. That means they are steadfastly to each other, which is the basic assumption for the creation of time-constant torque.

If the described frequency condition is fulfilled for every possible speeed, the behaviour is called “asynchronous”. That case is characterized by rotor frequencies to adjust according to their rotational speeds.

Is the frequency condition only fulfilled at one speed n_1, the machine shows synchronous behaviour. In this case, rotor frequency is defined fix, e. g. $f_2 = 0$.

slip:

$$s = \frac{n_1 - n}{n_1} = \frac{n_2}{n_1} = \frac{f_2}{f_1} \tag{6.98}$$

slip frequency:

$$f_2 = s \cdot f_1 \tag{6.99}$$

rotor speed:

$$n = n_1 \cdot (1 - s) \tag{6.100}$$

If rotating field machines are directly supplied by three-phase lines, the accepted active power, less occurring copper losses in windings is equal to the air gap power:

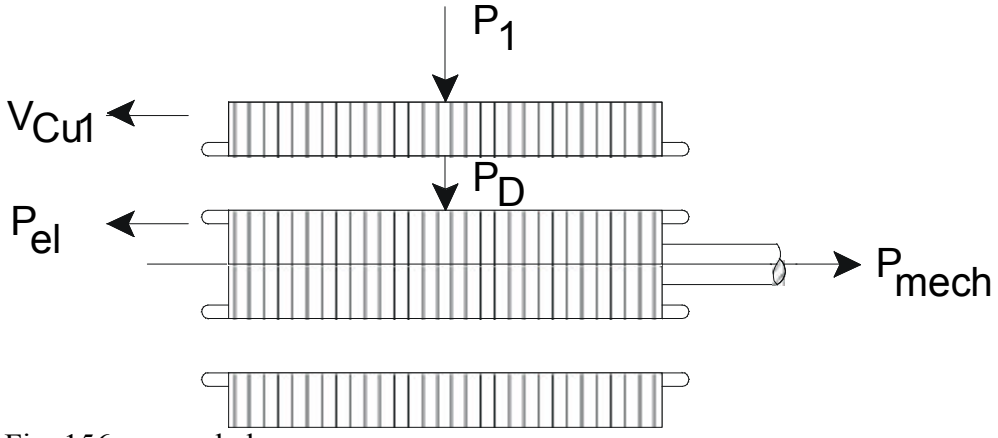

Fig. 156: power balance

$$P_D = P_1 - V_{Cu1} \tag{6.101}$$

Air gap power is converted inside the air gap:

$$P_D = 3 \cdot U_{i1} \cdot I_1 \cdot \cos j_1 = M \cdot 2p \cdot n_1 \tag{6.102}$$

exerted power on shaft:

$$P_{mech} = M \cdot 2p \cdot n = M \cdot 2p \cdot (1-s) \cdot n_1 = (1-s) \cdot P_D \tag{6.103}$$

The difference of air gap power less mechanical power on the shaft is converted to heat losses inside the rotor windings:

$$P_{el} = P_D - P_{mech} = P_D - (1-s) \cdot P_D = s \cdot P_D \tag{6.104}$$

6.10 Reactances and resistance of three-phase windings

The magnetizing reactance of a three-phase winding computes from the induced voltage in no-load case:

$$X_{1h} = \frac{U_i}{I_1} \tag{6.105}$$

with

$$U_i = w_1 w_1 x_1 \frac{f_1}{\sqrt{2}} \tag{6.106}$$

$$f_1 = \frac{lD}{p} B_1 \tag{6.107}$$

$$B_1 = \frac{m_0}{2d} \frac{3}{2} \frac{4}{p} \frac{w_1 x_1}{p} \sqrt{2} I_1 \tag{6.108}$$

follows

$$X_{1h} = w \frac{3}{2} m_0 \left(\frac{w_1 x_1}{p} \right)^2 \frac{2}{p} \frac{lD}{d} \tag{6.109}$$

The leakage reactance of three-phase windings results from a superposition of three effects, being independently calculable:

- end winding leakage
- slot leakage
- harmonic leakage

} $\Sigma = X_{1\sigma}$

Same conditions apply for the rotor leakage reactance. Detailed discussion is to be found in literature as given.

The total reactance of a three-phase winding results in:

$$X_1 = X_{1h} + X_{1s} \tag{6.110}$$

to be measured in no-load operation, $I_2=0$, $f_1=f_{1N}$, $R_1=0$:

$$X_1 = \frac{U_1}{I_0} \tag{6.111}$$

The phase resistance of three-phase windings can be determined by basically considering geometric dimensions and specific material parameters:

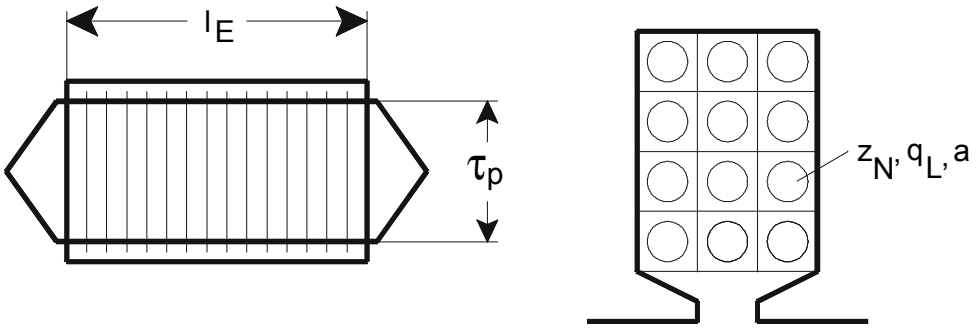

Fig. 157: windings, geometric dimensions

with an approximate length of windings of

$$l_m \approx 2\left(l_E + t_p\right) \tag{6.112}$$

and the number of windings per phase:

$$w = \frac{N\,{}^{z_N}\!/_{a}}{2m} \tag{6.113}$$

Then follows for the resistance per phase at working temperature:

$$R = r\,\frac{wl_m}{aq_l}\left[1 + a\left(T - 20K\right)\right] \tag{6.114}$$

with copper temperature coefficient:

$$a = \frac{0.004}{K} \tag{6.115}$$

The maximum overtemperature in nominal operation depends on the insulation class (VDE):

e. g.: A: 105°C (enamelled wire)
F: 155°C (foil insulation)

7 Induction machine

7.1 Design, method of operation

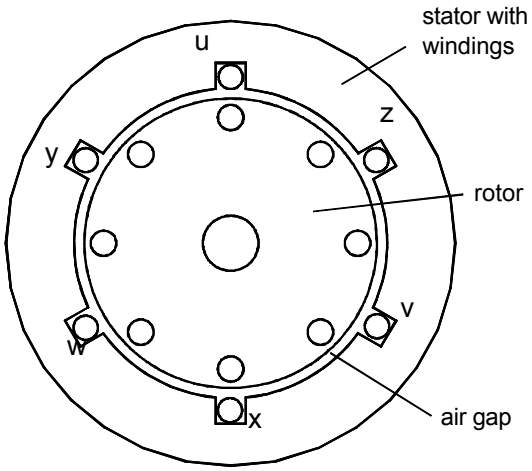

Fig. 158: induction machine, design

Induction machines state the most import type of three-phase machines, to be mainly used as motor. Stator and rotor are composed of slotted iron laminations that are stacked to form a core. A symmetric three-phase winding is placed in the stator slots, which is connected to a three-phase system in either star- or delta-connection. Rotor slots also contain a symmetric three-phase winding or a squirrel-cage-winding, to be short-circuited.

Most simplified induction machine consists of 6 stator slots per pole pair – one per line and one per return conductor each. Usual windings are designed with a number of pole pairs greater than one p > 1, which are distributed on more than one slot q > 1.

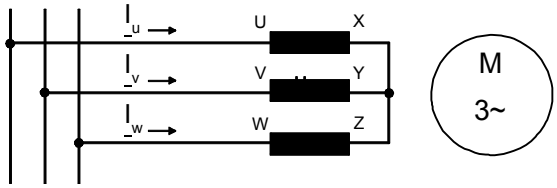

Fig. 159: induction machine, power supply

If induction machines are supplied by three-phase networks of frequency f_1, balanced currents occur, to create a rotating field inside the air gap, revolving with synchronous rotational speed n_1. This rotating field induces currents of frequency f_2 inside the conductors of the rotor windings. This again creates another rotating field, revolving with differential speed n_2 relatively towards the rotor speed n and relatively towards the stator field with $n_1 = n + n_2$, which fulfils the frequency condition. Due to Lenz's Law, rotor currents counteract their origin, which is based on relative motion between stator and rotor. As a consequence rotor currents and stator rotating field, which revolves with synchronous speed, create torques driving the rotor in direction of the stator rotating field and trying to adapt their speed to that of the stator rotating field. Since the induction effect would disappear in case of not having any relative motion between rotor and stator field, the rotor is actually not able to reach stator field rotational speed. Rotors show a certain amount of slip s against the stator rotating field – their method of running is called asynchronous. Therefore this kind of machine is called induction machine (asynchronous machine). The higher the torque, demanded by the rotor, the greater the amount of slip.

Synchronous speed:	$n_1 = \frac{f_1}{p}$	(7.1)
rotor speed:	n	(7.2)
slip:	$s = \frac{n_1 - n}{n_1} = \frac{f_2}{f_1}$	(7.3)

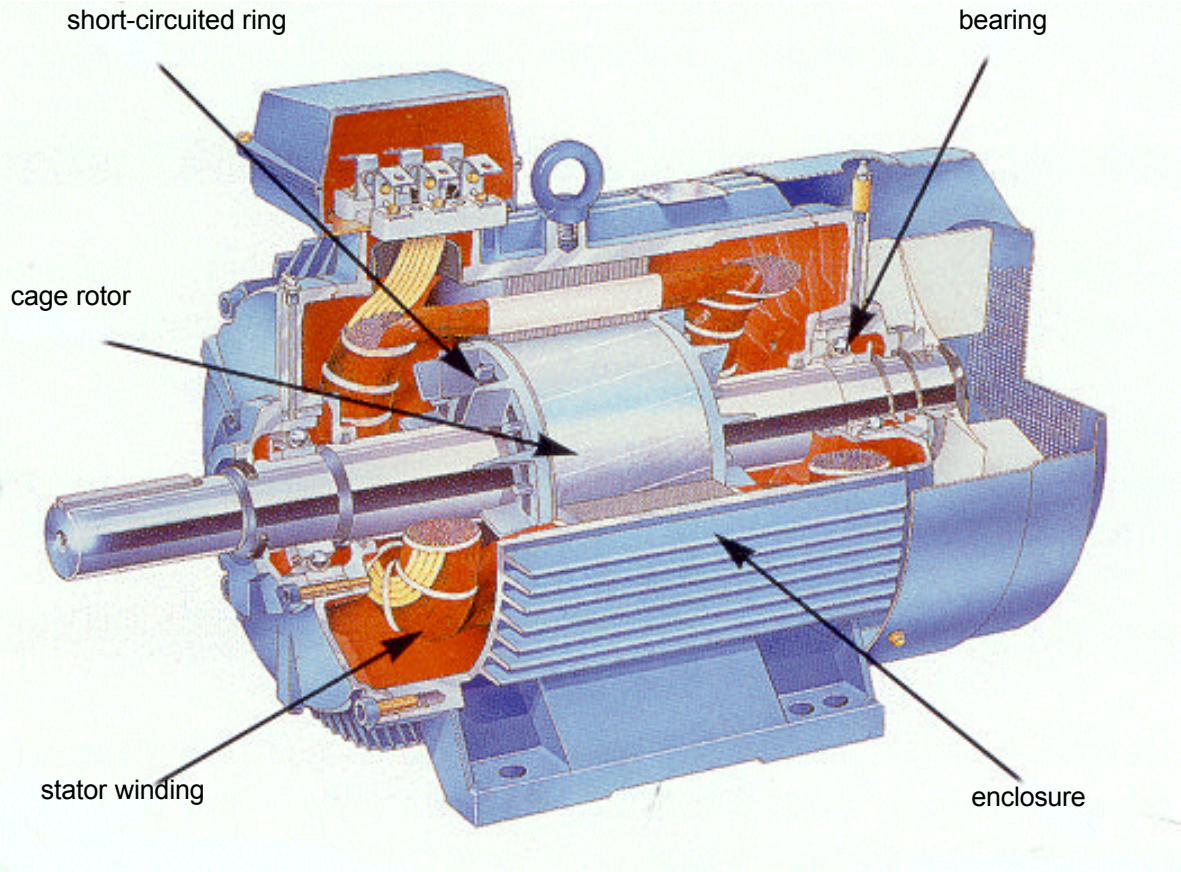

Fig. 160: induction machine, general design

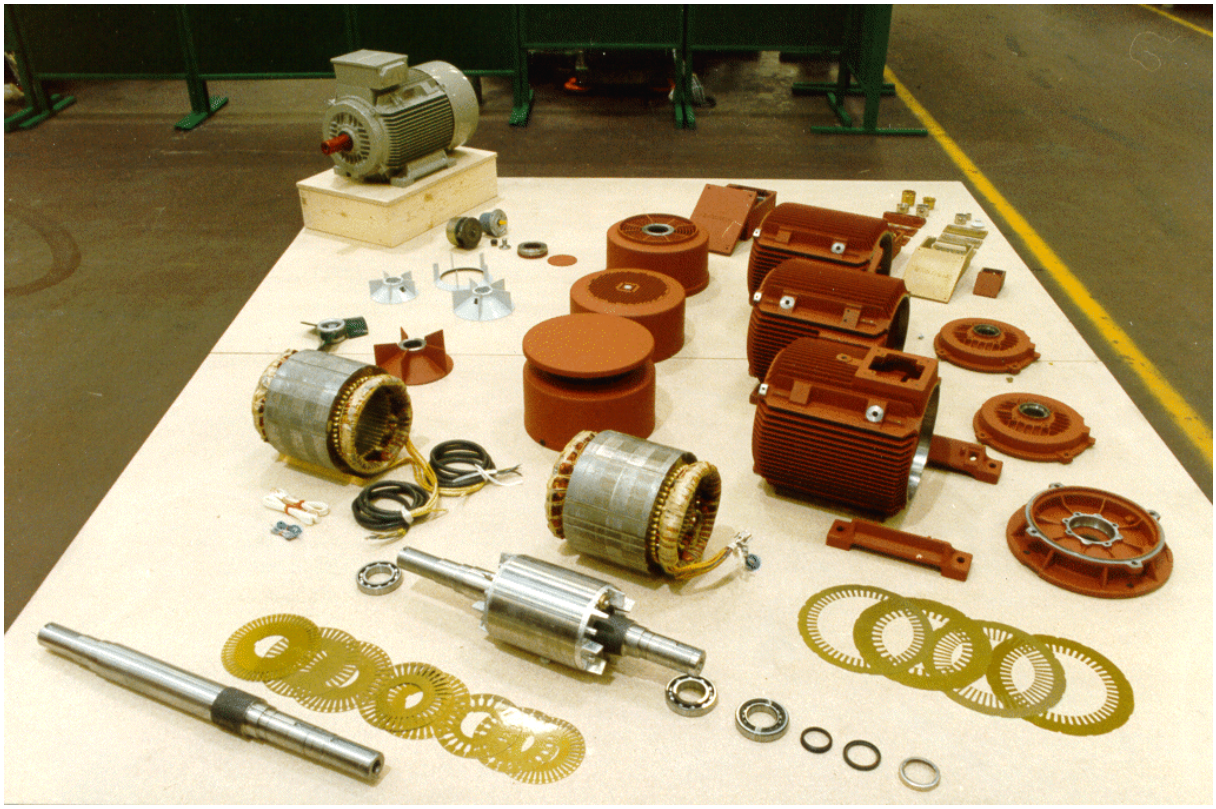

Fig. 161: induction machine, unassembled parts

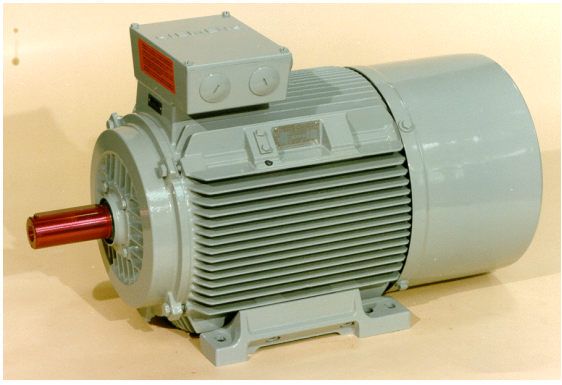

Fig. 162a: induction motor, power: 30 kW

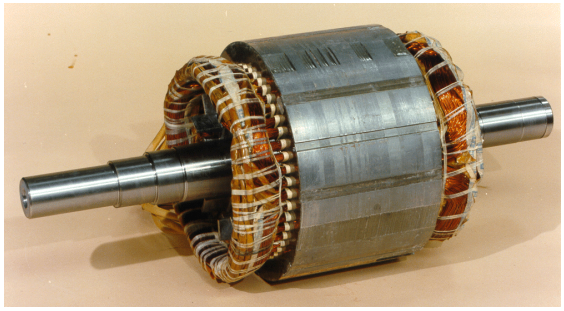

Fig. 162b: same machine, rotor only

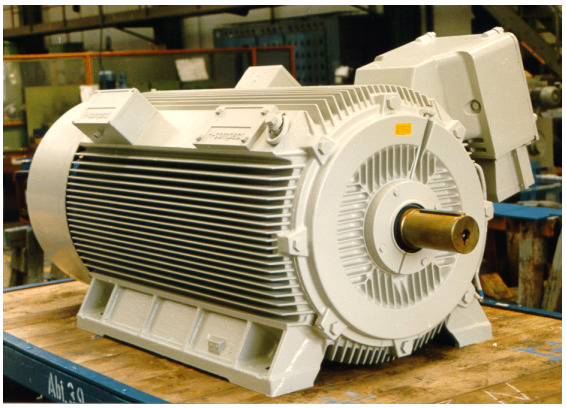

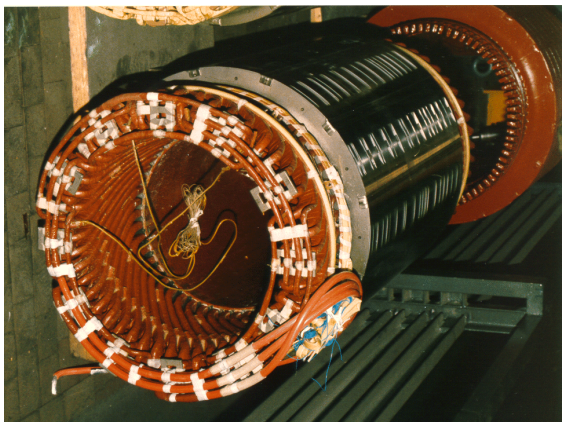

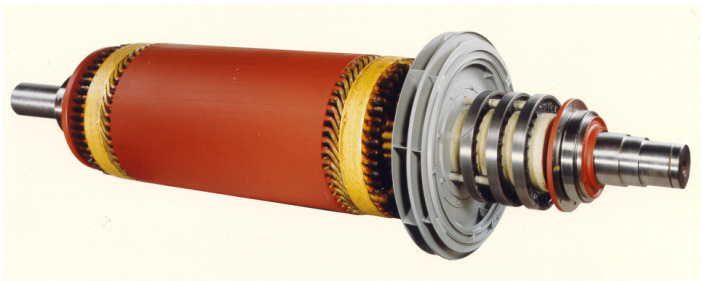

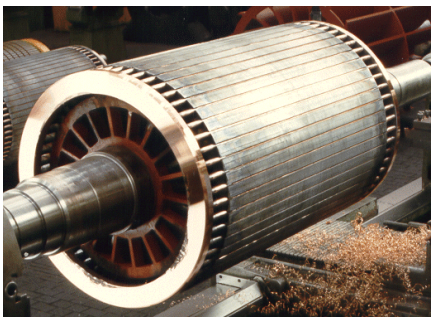

Fig. 163a-d: high-voltage induction motor, power: 300 kW (Siemens) - case with shaft (upper left), stator (upper right), slip-ring rotor (lower left), squirrel-cage rotor (lower right)

Induction machines are either equipped with

- slip-ring rotors, or with
- squirrel-cage rotors.:

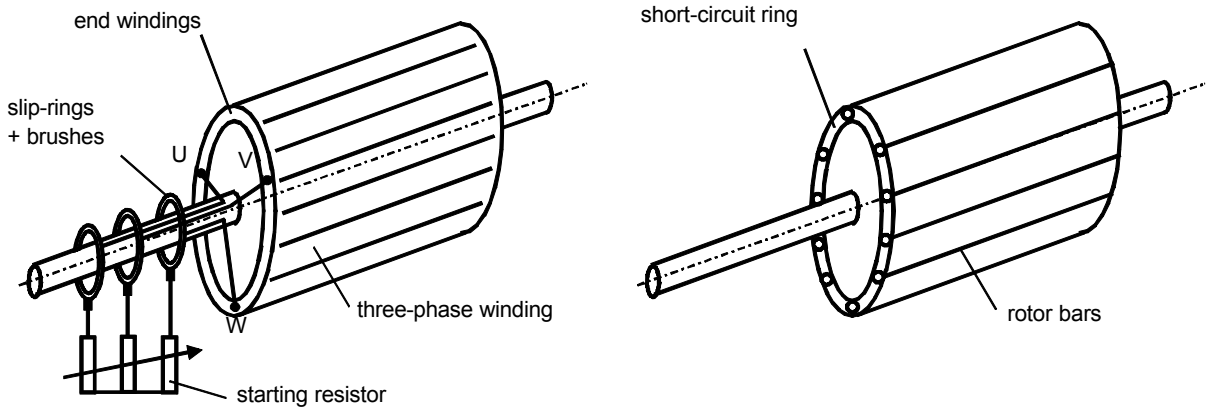

Fig. 164: induction machine, rotor type overview

- induction machines with slip-ring rotor consist of three-phase windings with a number of phases $m_2 = 3$, similar to their stator. End windings are outside the cylindrical cage connected to slip rings. Rotor windings are short-circuited either directly or via brushes using a starting resistor or can be supplied by external voltage, which are means to adjust rotational speed.

- Squirrel-cage rotors are composed of separate rotor bars to form a cylindrical cage. Their end windings are short-circuited using short-circuit-rings at their end faces. The number of phases is $m_2 = N_2$. This type of construction does not admit any access to the rotor windings while operating, which results in a missing opportunity to directly influence the operational behaviour. Large machines feature copper rotor bars and short-circuit-rings whereas die-cast aluminium cages are used for small power machines.

The following considerations apply for both slip-ring rotor machines as well as squirrel-cage rotor machines.

7.2 Basic equations, equivalent circuit diagrams

Stator and rotor of considered induction machines are to be fitted with balanced three-phase windings. This assumption permits a single-phase consideration.

Each of the windings of stator and rotor feature a resistance, R_1 for the stator and R_2 for the rotor, as well as a self inductance L_1 (stator) and L_2 (rotor).

Stator- and rotor winding are magnetically coupled by their common mutual inductance M.

Since currents in stator windings are of frequency f_1, whereas currents in rotor windings are of frequency f_2, certain conditions apply for operation at rotational speed n:

- stator induces into the rotor with frequency f_2,
- rotor induces into the stator with frequency f_1,

which leads to the equivalent circuit diagram as shown in Fig. 165:

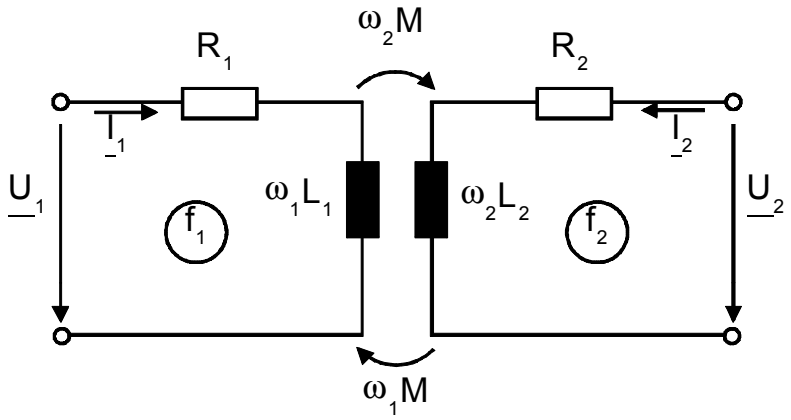

Fig. 165: induction machine, ecd, galvanic separated

According voltage equations:

$$\underline{U}_1 = R_1 \cdot \underline{I}_1 + j \cdot w_1 \cdot L_1 \cdot \underline{I}_1 + j \cdot w_1 \cdot M \cdot \underline{I}_2 \tag{7.4}$$

$$\underline{U}_2 = R_2 \cdot \underline{I}_2 + j \cdot w_2 \cdot L_2 \cdot \underline{I}_2 + j \cdot w_2 \cdot M \cdot \underline{I}_1 \tag{7.5}$$

Rotor quantities are now transferred into stator quantities, i.e. voltage U_2^* and current I_2^* of frequency f_1 are to be used for steady oriented stator windings, evoking the same effect as voltage U_2 and current I_2 in revolving rotor windings. Power invariant transformation, introducing a transformation ratio $\ddot{u}$ is utilized to aim the described transfer.

$$\underline{U}_2^* = \ddot{u} \cdot \underline{U}_2 \quad , \qquad \underline{I}_2^* = \frac{\underline{I}_2}{\ddot{u}} \tag{7.6}$$

Voltage equations (7.4-7.5) expand to:

$$\underline{U}_1 = R_1 \cdot \underline{I}_1 + j \cdot w_1 \cdot \left(L_1 - \ddot{u} \cdot M \right) \cdot \underline{I}_1 + j \cdot w_1 \cdot \ddot{u} \cdot M \cdot \left(\frac{\underline{I}_2}{\ddot{u}} + \underline{I}_1 \right) \tag{7.7}$$

$$\ddot{u} \cdot \underline{U}_2 = \ddot{u}^2 \cdot R_2 \cdot \frac{\underline{I}_2}{\ddot{u}} + j \cdot w_2 \cdot \left(L_2 \cdot \ddot{u}^2 - \ddot{u} \cdot M \right) \cdot \frac{\underline{I}_2}{\ddot{u}} + j \cdot w_2 \cdot \ddot{u} \cdot M \cdot \left(\underline{I}_1 + \frac{\underline{I}_2}{\ddot{u}} \right) \tag{7.8}$$

with a reasonable choice of $\ddot{u}$ as:

$$\ddot{u} = \frac{L_1}{M} = \frac{w_1 \cdot x_1}{w_2 \cdot x_2} \cdot \left(1 + s_1 \right) \tag{7.9}$$

With that, disappearance of the leakage inductance on the primary side is achieved, the transformation ratio $\ddot{u}$ can be measured as the ratio of no-load voltages in standstill operation.

In analogy to transformers we find (see chapter 3):

$$R_2^* = \ddot{u}^2 \cdot R_2 = (1+s_1)^2 \cdot \left(\frac{w_1 \cdot x_1}{w_2 \cdot x_2}\right)^2 \cdot R_2 = (1+s_1)^2 \cdot R_2' \tag{7.10}$$

$$\begin{aligned} L_2^* &= \ddot{u}^2 \cdot L_2 - \ddot{u} \cdot M = (1+s_1)^2 \cdot \left(\frac{w_1 \cdot x_1}{w_2 \cdot x_2}\right)^2 \cdot (1+s_2) \cdot L_{2h} - (1+s_1) \cdot \left(\frac{w_1 \cdot x_1}{w_2 \cdot x_2}\right) \cdot M = \\ &(1+s_1) \cdot (1+s_2) \cdot L_1 - L_1 = \left(\frac{1}{1-s} - 1\right) \cdot L_1 = \frac{s}{1-s} \cdot L_1 \end{aligned} \tag{7.11}$$

with the total leakage factor:

$$s = 1 - \frac{1}{(1+s_1) \cdot (1+s_2)} \tag{7.12}$$

Then follows for the voltage equations:

$$\underline{U}_1 = R_1 \cdot \underline{I}_1 + j \cdot w_1 \cdot L_1 \cdot \underline{I}_0 \tag{7.13}$$

$$\underline{U}_2^* = R_2^* \cdot \underline{I}_2^* + j \cdot w_2 \cdot L_2^* \cdot \underline{I}_2^* + j \cdot w_2 \cdot L_1 \cdot \underline{I}_0 \tag{7.14}$$

$$\underline{I}_0 = \underline{I}_1 + \underline{I}_2^* \tag{7.15}$$

The appearance of different frequencies in stator and rotor is displeasing. This issue can be formally eliminated, if the rotor voltage is multiplied by $\frac{w_1}{w_2} = \frac{1}{s}$. Reactances are to be transferred onto the stator side:

$$X_1 = w_1 \cdot L_1 \qquad , \qquad X_2^* = w_1 \cdot L_2^* \tag{7.16}$$

which finally leads to:

$$\underline{U}_1 = R_1 \cdot \underline{I}_1 + j \cdot X_1 \cdot \underline{I}_0 \tag{7.17}$$

$$\frac{\underline{U}_2^*}{s} = \frac{R_2^*}{s} \cdot \underline{I}_2^* + j \cdot X_2^* \cdot \underline{I}_2^* + j \cdot X_1 \cdot \underline{I}_0 \tag{7.18}$$

$$\underline{I}_0 = \underline{I}_1 + \underline{I}_2^*$$

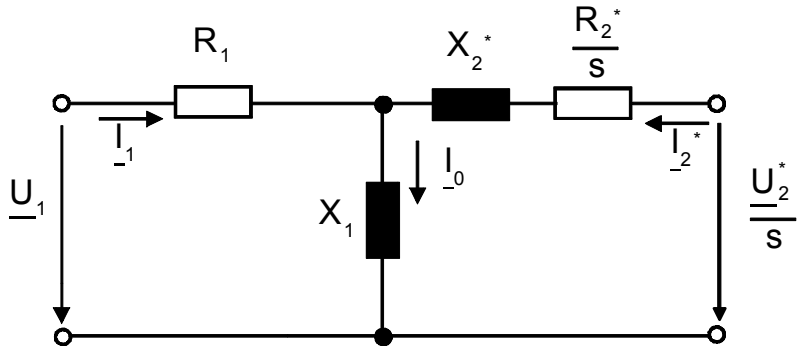

Fig. 166: induction machine, general ecd

All occurring variables of the ecd shown in Fig. 166 are considered at frequency f_1. Operational behaviour of induction machines can be completely described using the ecd shown in Fig. 166. It is purposively used for operation with constant stator flux linkage, which means system supply with constant voltage and frequency.

The chosen transformation ratio $\ddot{u}$ can be measured on the primary side at no-load an standstill on secondary side – neglecting stator winding copper losses. Then follows with:

$$I_2 = 0,$$
$$s = 1,$$
$$R_1 = 0$$

for no-load voltages:

$$U_1 = U_{20}^* = \ddot{u} \cdot U_{20} = \frac{w_1 \cdot x_1}{w_2 \cdot x_2} \cdot (1 + s_1) \cdot U_{20} \tag{7.19}$$

$$\ddot{u} = \frac{U_1}{U_{20}} = \frac{w_1 \cdot x_1}{w_2 \cdot x_2} \cdot (1 + s_1) \tag{7.20}$$

Operating with constant rotor flux linkage, which means field-oriented control, an ecd is to be utilized with tranformation ratio of:

$$\ddot{u} = \frac{w_1 \cdot x_1}{w_2 \cdot x_2} \cdot \frac{1}{(1 + s_2)} \tag{7.21}$$

which makes the rotor leakage inductance disappear (without derivation):

$$\underline{U}_1 = R_1 \cdot \underline{I}_1 + j \cdot s \cdot X_1 \cdot \underline{I}_1 + j \cdot (1 - s) X_1 \cdot \underline{I}_0 \tag{7.22}$$

$$\frac{\underline{U}_2^+}{s} = \frac{R_2^+}{s} \cdot \underline{I}_2^+ + j \cdot (1 - s) \cdot X_1 \cdot \underline{I}_0 \tag{7.23}$$

$$\underline{I}_0 = \underline{I}_1 + \underline{I}_2^+$$

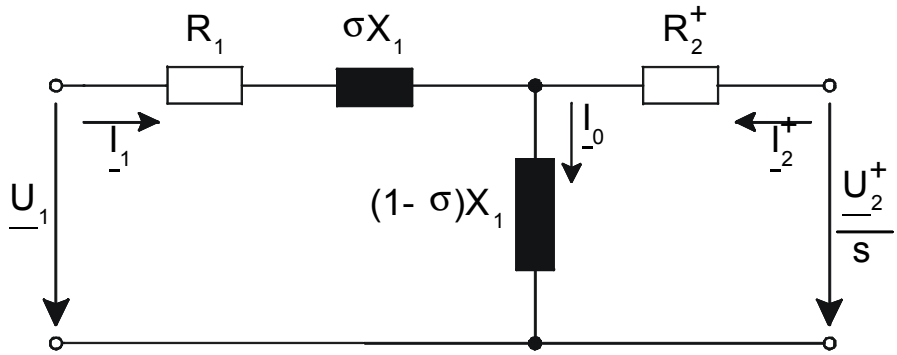

Fig. 167: induction machine, ecd for constant rotor flux linkage

Transformation ratio *ü* can be measured on secondary side at no-load and standstill on primary side.

With the non-measurable transformation ratio:

$$\ddot{u} = \frac{w_1 \cdot x_1}{w_2 \cdot x_2} \tag{7.24}$$

which complies with the effective number of windings, a T-form ecd derives for induction machines. This type of ecd is similar to those of transformers (as discussed in chapter 3), but of minor importance when considering operational behaviour (also without derivation):

$$\underline{U}_1 = R_1 \cdot \underline{I}_1 + j \cdot X_{1s} \cdot \underline{I}_1 + j \cdot X_{1h} \cdot \underline{I}_0 \tag{7.25}$$

$$\frac{\underline{U}_2'}{s} = \frac{R_2'}{s} \cdot \underline{I}_2' + j \cdot X_{2s}' \cdot \underline{I}_2' + j \cdot X_{1h} \cdot I_0 \tag{7.26}$$

$$\underline{I}_0 = \underline{I}_1 + \underline{I}_2'$$

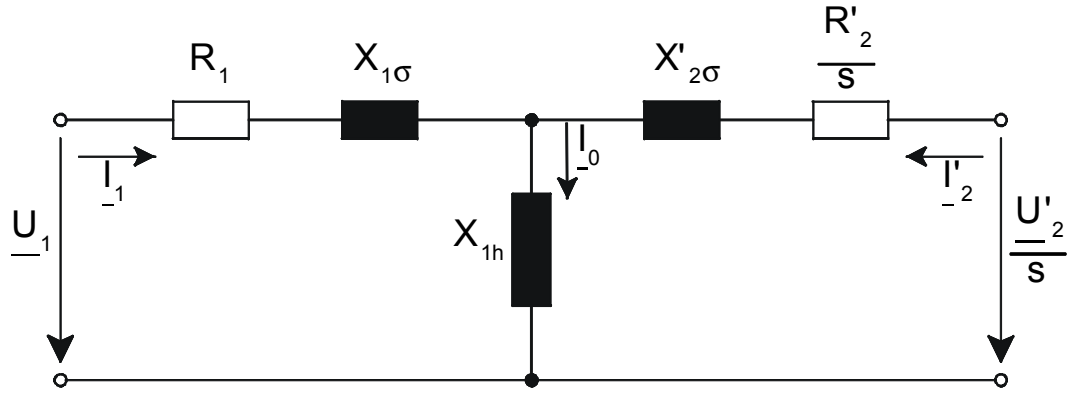

Fig. 168: induction machine, T-ecd

Please note:

- all types of ecd are physically identical and lead to same results
- a suitable choice of the transformation ratio is a question of expedience

Stator winding resistance R_1 is usually neglected for machines at line frequency f_l = 50 Hz:

$$R_1 = 0 \tag{7.27}$$

Rotor windings of slip-ring rotors are usually short-circuited by slip-rings and brushes, same as squirrel-cage rotors. As long as current displacement (skin effect, proximity effect) can be neglected for squirrel-cage rotors, the operational behaviour of both types are alike:

$$U_2^* = 0 \tag{7.28}$$

With equation 7.28, voltage equations for induction machines ensue to:

$$\underline{U}_1 = j \cdot X_1 \cdot \underline{I}_0 \tag{7.29}$$

$$\underline{U}_1 = -\frac{R_2^*}{s} \cdot \underline{I}_2^* - j \cdot X_2^* \cdot \underline{I}_2^* \tag{7.30}$$

$$\underline{I}_0 = \underline{I}_1 + \underline{I}_2^*$$

which leads to a simple ecd, to consist of only 3 elements, shown in Fig. 169. This ecd is taken as a basis for the investigation of the operational behaviour of induction machines in the following.

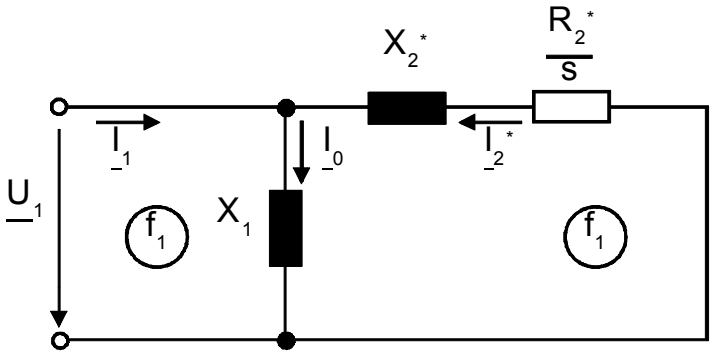

Fig. 169: induction machine, simplified ecd

The according phasor diagram can be drawn by using the voltage equations above.

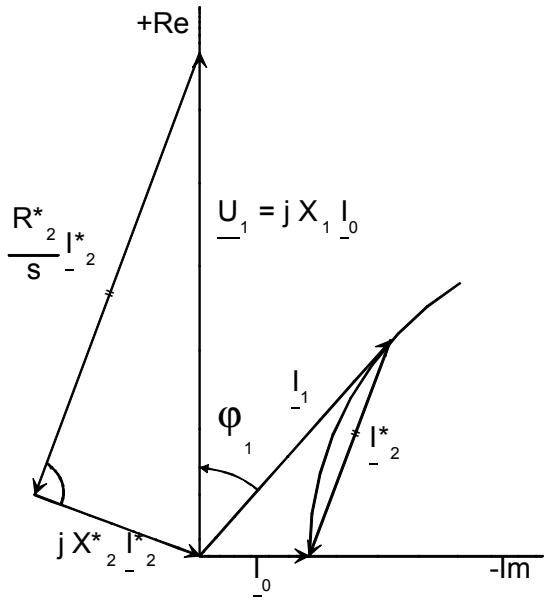

Fig. 170: induction machine, phasor diagram

7.3 Operational behaviour

7.3.1 Power balance

A power balance is established for the definition of power:

absorbed active power is defined as:

$$P_1 = 3 \cdot U_1 \cdot I_1 \cdot \cos j_1 . \tag{7.31}$$

Since no losses occur in stator windings ($R_1 = 0$ assumed), the entire absorbed active power is transmitted over the air gap to appear as air-gap power for the rotor:

$$P_D = P_1 = 3 \cdot \frac{R_2^*}{s} \cdot \underline{I}_2^{*2} . \tag{7.32}$$

In described equivalent circuit diagrams, the air gap power is represented by the active power to be converted in the R_2^*/s -resistor. No copper losses occur for the rotor resistance R_2 itself:

$$P_{el} = 3 \cdot R_2 \cdot \underline{I}_2^2 = 3 \cdot R_2^* \cdot \underline{I}_2^{*2} = s \cdot \left(3 \cdot \frac{R_2^*}{s} \cdot \underline{I}_2^{*2} \right) = s \cdot P_D . \tag{7.33}$$

With that fact, the mechanical power of induction machines to be exerted on the shaft ensues to the difference of air gap power and rotor copper losses:

$$P_{mech} = P_D - P_{el} = (1-s) \cdot P_D . \tag{7.34}$$

7.3.2 Torque

Based on the simplified ecd follows for the current in a short circuited rotor:

$$\underline{I}_2^* = \frac{-\underline{U}_1}{\frac{R_2^*}{s} + j \cdot X_2^*}, \quad I_2^{*2} = \frac{U_1^2}{\left(\frac{R_2^*}{s} \right)^2 + X_2^{*2}}, \tag{7.35}$$

which makes it possible to describe torque M as a function of slip s:

$$M = \frac{P_{mech}}{2 \cdot p \cdot n} = \frac{(1-s) \cdot P_D}{2 \cdot p \cdot n_1 (1-s)} = \frac{P_D}{2 \cdot p \cdot n_1} = \frac{1}{2 \cdot p \cdot \frac{f_1}{p}} \cdot 3 \cdot \frac{R_2^*}{s} \cdot \frac{U_1^2}{\left(\frac{R_2^*}{s} \right)^2 + X_2^{*2}}$$

$$= \frac{3 \cdot p}{w_1} \cdot \frac{U_1^2 / X_2^*}{\frac{R_2^*}{s \cdot X_2^*} + \frac{s \cdot X_2^*}{R_2^*}} \tag{7.36}$$

Torque reaches its peak value in case of the denominator is minimum. The denominator is to be differentiated after *s* and to be set = 0:

$$-\frac{1}{s^2}\cdot\frac{R_2^*}{X_2^*}+\frac{X_2^*}{R_2^*}=0 \qquad \Rightarrow \qquad s=\pm\frac{R_2^*}{X_2^*}. \tag{7.37}$$

The amount of slip to occur at maximum torque is called *breakdown slip*:

$$s_{kipp}=\frac{R_2^*}{X_2^*}\approx 0{,}1\cdots 0{,}2 \tag{7.38}$$

with the according *breakdown torque*, being the maximum torque value:

$$M_{kipp}=\frac{3\cdot p}{w_1}\cdot\frac{U_1^2}{2\cdot X_2^*} \tag{7.39}$$

The *Kloss Equation* (7.40) derives from a reference of the actual torque on to the maximum value and a replacement of R_2^*/X_2^* by s_{kipp} (note: index *kipp* means *breakdown*):

$$\boxed{\frac{M}{M_{kipp}}=\frac{2}{\frac{s_{kipp}}{s}+\frac{s}{s_{kipp}}}} \tag{7.40}$$

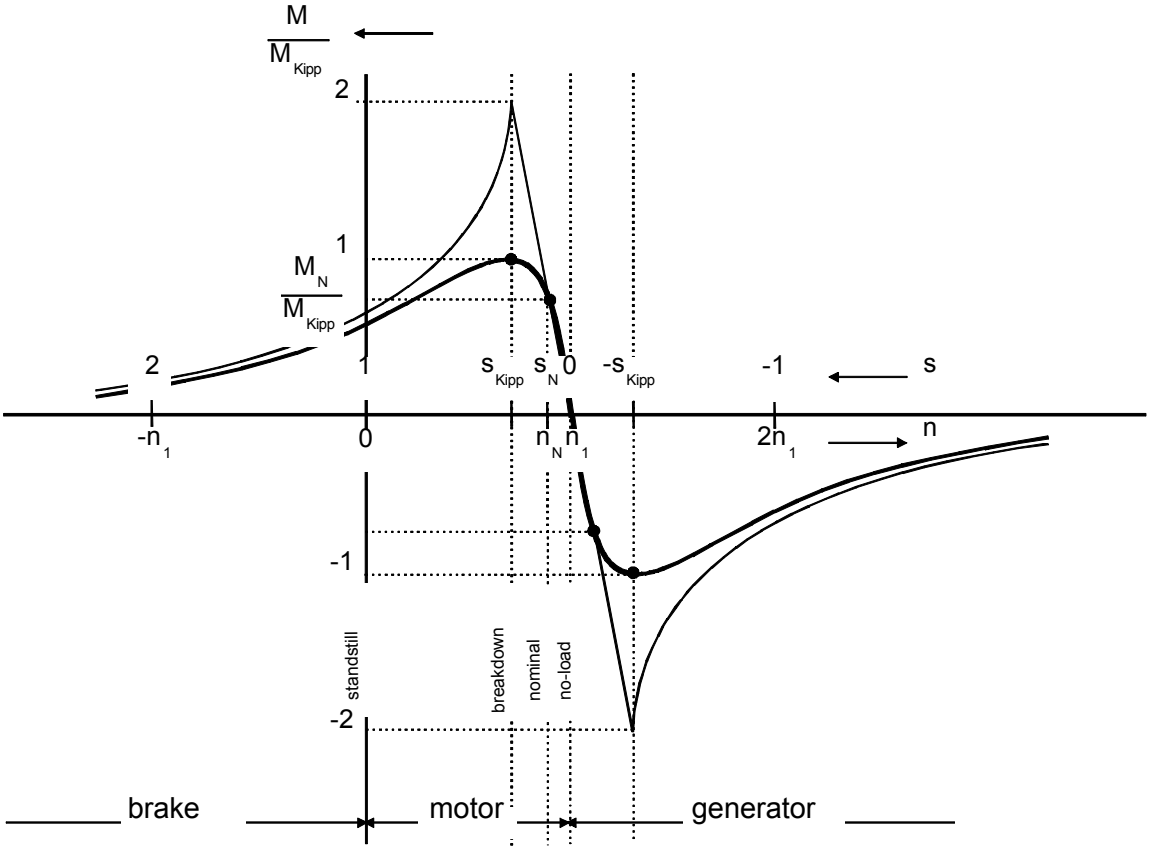

Fig. 171: induction machine, torque/speed diagram

Characteristics $M = f(s)$ or $M = f(n)$ can be drawn as in Fig. 171 and be also discussed with equation 7.40. Typical slip ranges are:

$$s << s_{kipp}: \quad \frac{M}{M_{kipp}} = \frac{2}{s_{kipp}/s} = 2 \cdot \frac{s}{s_{kipp}} \quad \text{straight line,} \tag{7.41}$$

$$s >> s_{kipp}: \quad \frac{M}{M_{kipp}} = \frac{2}{s/s_{kipp}} = 2 \cdot \frac{s_{kipp}}{s} \quad \text{hyperbola,} \tag{7.42}$$

$$s = s_{kipp}: \quad \frac{M}{M_{kipp}} = 1 \quad \text{point.} \tag{7.43}$$

Induction machines can be operated in 3 different modes:

- motor (rotor revolves slower than rotating field):

  $$M > 0, n > 0, 0 < s < 1, \tag{7.44}$$

- generator (rotor revolves faster than rotating field):

  $$M < 0, n > n_1, s < 0, \tag{7.45}$$

- brake (rotor revolves against rotating field):

  $$M > 0, n < 0, s > 1. \tag{7.46}$$

7.3.3 Efficiency

The efficiency of induction machines at nominal operation, with neglection of stator copper losses ($R_1 = 0$), computes to:

$$h_N = \frac{P_{ab}}{P_{auf}} = \frac{P_{mechN}}{P_{DN}} = \frac{(1 - s_n) \cdot P_{DN}}{P_{DN}} = 1 - s_N \tag{7.47}$$

The nominal slip s_n is supposed to be kept as small as possible, in order to achieve proper nominal efficiency. Usual amounts for nominal slips are:

$$s_N \approx 0{,}05 \cdots 0{,}01 \tag{7.48}$$

which leads to effiencies

$$h_N = 0.95...0.99 \tag{7.49}$$

When taking stator copper losses and hysteresis losses into account, real applications actually show lower efficiency amounts between approx. 0,8 and 0,95.

7.3.4 Stability

An important condition is to be requested for both motor and generator operation: in which range does the machine show stable operational behaviour? That leads to:

$$\frac{dM_{Motor}}{dn} < \frac{dM_{Last}}{dn} = 0\,, \tag{7.50}$$

meaning load torque must be of greater value than motor torque at increasing speed.

Assuming

$$M_{Last} = const \qquad \text{i.e.} \qquad \frac{dM_{Last}}{dn} = 0 \tag{7.51}$$

and taking into account, that in cause of

$$n = (1 - s) \cdot n_0 \tag{7.52}$$

follows:

$$dn = -n_0 \cdot ds\,, \tag{7.53}$$

a stability condition of induction machines ensues to:

$$\frac{dM_{Motor}}{ds} > 0 \quad \text{bzw.} \qquad \frac{dM_{Motor}}{dn} < 0\,, \tag{7.54}$$

which is given for

$$-s_{kipp} < s < s_{kipp} \tag{7.55}$$

These considerations leads to the assignment *breakdown torque*, because if the load exceeds the breakdown torque, the rotor falls into standstill (motion breaks down), whereas it runs away at oversized driving torque (running away may lead to destruction $\Rightarrow$ break-down). Therefore a certain overload factor is required for induction machines:

$$\frac{M_{kipp}}{M_N} > 1{,}5 \tag{7.56}$$

7.4 Circle diagram (Heyland diagram)

7.4.1 Locus diagram

Circle diagram of induction machines means locus diagram of their stator current.

Preconditions:

- U_1 wird in reelle Achse gelegt,
- der Läufer ist kurzgeschlossen,
- $R_1 = 0$.

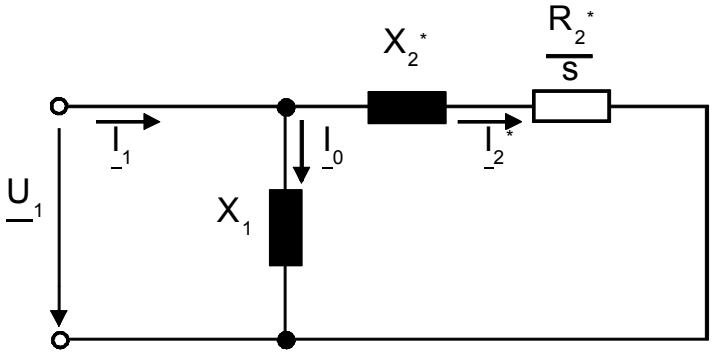

Fig. 172: induction machine, ecd, short circuited (secondary)

From voltage equations derives:

$$\underline{I}_0 = \frac{U_1}{j \cdot X_1} = const\,, \tag{7.57}$$

$$\underline{I}_2^* = \frac{U_1}{\frac{R_2^*}{s} + j \cdot X_2^*}\,. \tag{7.58}$$

Then follows for the stator current:

$$\underline{I}_1 = \underline{I}_0 + \underline{I}_2^* = \underline{I}_0 + \frac{U_1}{\frac{R_2^*}{s} + j \cdot X_2^*}\,. \tag{7.59}$$

Minimum current applies for $s = 0$ $\left(n = n_1\right)$: ideallized no-load case

$$\underline{I}_1 = \underline{I}_0 = \frac{U_1}{j \cdot X_1} \qquad \text{(located on } -j\text{-axis)} \tag{7.60}$$

Maximum current appears for $s = \infty \left(n = \infty\right)$: idealized short-circuit:

$$\frac{R_2^*}{s} = 0\,,$$

the ideal short-circuit reactance derives from a parallel connection of X_1 and X_2^*:

$$X_K = \frac{X_1 \cdot X_2^*}{X_1 + X_2^*} = \frac{X_1 \cdot X_1 \cdot \frac{s}{1-s}}{X_1 + X_1 \cdot \frac{s}{1-s}} = s \cdot X_1 . \tag{7.61}$$

That leads to an appraisalof the short-circuit current as:

$$\underline{I}_1 = \frac{U_1}{j \cdot s \cdot X_1} = \underline{I}_\infty >> \underline{I}_0 \text{ (located on } -j\text{-axis)} \tag{7.62}$$

The locus diagram of I_1 forms a circle (not subject to derivation), whose center-point is also located on the $-j$-axis, diameter ensues to ($\underline{I}_\infty - \underline{I}_0$)

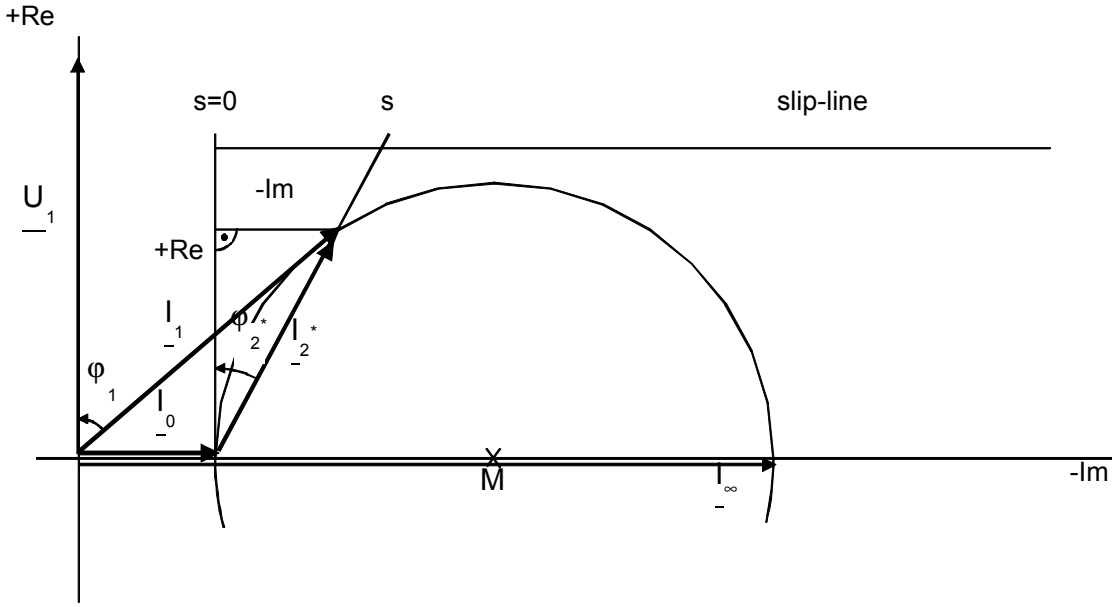

Fig. 173: induction machine, locus diagram

7.4.2 Parametrization

The tangent function is to be applied for the rotor current angle for parameter assignment:

$$\tan j_2^* = \frac{\mathrm{Im}\{\underline{I}_2^*\}}{\mathrm{Re}\{\underline{I}_2^*\}} = \frac{X_2^*}{R_2^*} \cdot s = \frac{s}{s_{kipp}} \sim s , \tag{7.63}$$

which is a linear function of s and can therefore be utilized for construction purpose of the slip-line.

A tangent to the circle is to be drawn at I_0, intersected by a line in parallel the $-j$-axis.
This line is called slip-line, which terminates at the intersection with the extension of the current phasor I_2. This line is divided linearly because of is proportional to the slip.
Besides the no-load point, a second point on the circle graph must be known, in order to define a parametrization.

If the ohmic stator winding resistance needs to be taken into account, to apply for low power machines and power converter supply at low frequencies, an active partition is added to the circle of the locus diagram, which differs for location of center point and parameter assignment – not supposed to be discussed further.

7.4.3 Power in circle diagram

The opportunity to easily determine the current value for any given operational point is not the only advantage of the circle diagram of induction machines. Apart from that, it is possible to directly read off torque value M and air gap power P_D, mechanical power P_{mech} and elektrical power P_{el} as distances to appear in the circle diagram.

If R_1 is equal to zero $(R_1 = 0)$, the entire absorbed active power is equal to the air gap power P_D, to be transferred across the air gap.

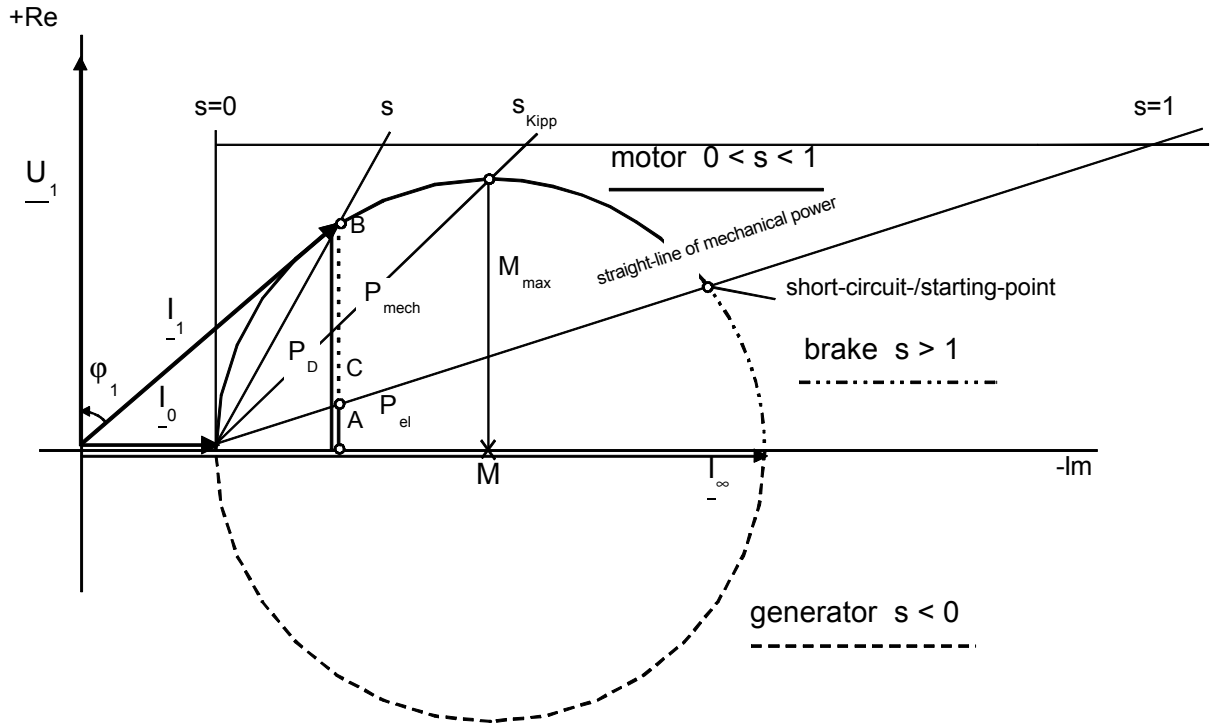

Fig. 174: induction machine, circle diagram, torques and powers

Geometric interdependences for air gap power and torque derive from Fig. 174:

$$P_D = P_1 = 3 \cdot U_1 \cdot I_1 \cdot \cos j_1 = 3 \cdot U_1 \cdot I_{1w} = c_p \cdot \overline{AB}\,, \tag{7.64}$$

$$M = \frac{P_D}{2 \cdot p \cdot n_1} = c_M \cdot \overline{AB}\,, \tag{7.65}$$

as well as (intercept theorem):

$$\frac{\overline{AB}}{\overline{AC}} = \frac{1}{s} \qquad \Rightarrow \qquad \overline{AC} = s \cdot \overline{AB}\ ,\ \overline{BC} = (1-s) \cdot \overline{AB}\,. \tag{7.66}$$

The leg $\overline{AB}$ is subdivided due to the ratio $s/(1-s)$, so that:

$$P_{el} = s \cdot P_D = c_P \cdot \overline{AC}, \tag{7.67}$$

$$P_{mech} = (1-s) \cdot P_D = c_P \cdot \overline{BC}. \tag{7.68}$$

The straight-line to run through points $s = 0$ and $s = 1$ on the circle is called *straight-line of mechanical power* (see Fig. 174).

7.4.4 Operating range, signalized operating points

The three operating ranges of induction machines are to be found in the according circle diagram as:

- motor: for: 0< s < 1,
- braking: for: 1 < s < ∞,
- generator: for: s < 0.

Five signalized operating points need to be mentioned:

- **no-load**: $s = 0,\ n = n_1$ (7.69)

  No-load current

  $$I_0 = \frac{U_1}{X_1} \tag{7.70}$$

  is placed on the *–Im*-axis and is supposed to be kept small with regard to the absorbed reactive power of induction machines. Since the total reactance X_1 is inverse proportional to the air gap width, this width is also supposed to be kept small. Mechanical limits may be reached when considering shaft deflection and bearing clearance:

  $$d \geq 0.2mm + \frac{D}{1000}. \tag{7.71}$$

  Practical applications show a ratio as of:

  $$\frac{I_0}{I_{1N}} = 0.25...0.5. \tag{7.72}$$

- **breakdown**: $s_{kipp} = \frac{R_2^*}{X_2^*}$. (7.73)

  At this point, maximum torque is exerted on the shaft of induction machines. This point describes the peak value of the circle, real- and imaginary part of I_2^* are equal, so that $\tan j_2^* = 1$.

- **short-circuit- or starting-point**: $s = 1$, $n = 0$ (7.74)

  When starting, short-circuit currents I_{1k} occurs, which is multiple the nominal current I_{1N} and therefore needs to be limited, due to approximately:

  $$I_{1K} = 5...8 \cdot I_{1N}.$$ (7.75)

- **ideal short-circuit**: $s = \infty$, $n = \infty$

  Maximum current value to theoretically appear – also located on the –*Im*-axis.

  $$I_\infty = \frac{U_1}{s \cdot X_1} = \frac{I_0}{s}.$$ (7.76)

  Practical values are aimed as:

  $$s = 0.03...0.1$$
  $$\frac{I_\infty}{I_{1N}} = 5...8 \quad .$$

- **optimum operational point**:

  The nominnal point is to be chosen in the way, to maximize $\cos j_1$. This case is given, if the nominal currents ensues to a tangent to the circle. A better value of $\cos j_1$ can not be achieved. The optimum point is not always kept precisely in practical applications.

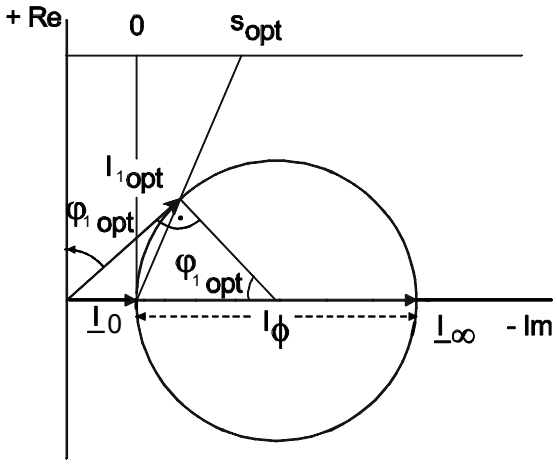

Fig. 175: induction mach., optimum point

If the nominal point is set equal to the optimum point follows:

$$\cos j_{1opt} = \frac{\frac{I_\varnothing}{2}}{\frac{I_\varnothing}{2} + I_0} = \frac{\frac{1}{2} \cdot (I_\infty - I_0)}{\frac{1}{2} \cdot (I_\infty + I_0)} = \frac{1-s}{1+s},$$ (7.77)

with practical values:

$$\cos j_1 \approx 0.8...0.9.$$ (7.78)

7.4.5 Influence of machine parameters

Influences of machine parameters on the circle diagram are subject to discussion in the following.

No-load current is given as:

$$I_0 = \frac{U_1}{X_1}. \tag{7.79}$$

The ideal short-circuit current approximately amounts:

$$I_\infty = \frac{U_1}{s \cdot X_1} = \frac{I_0}{s}. \tag{7.80}$$

Parameter assignment is based on:

$$\tan j_2^* = \frac{X_2^*}{R_2^*} \cdot s. \tag{7.81}$$

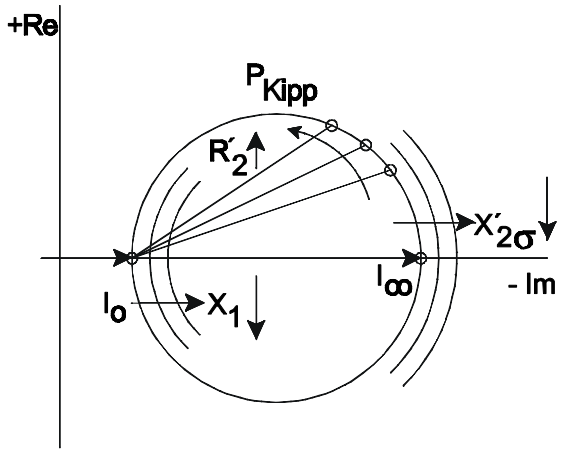

Fig. 176: parameter variation, effects

Conceivable alternatives may be:

- X_1 decreased, caused by a wider air gap $\Rightarrow I_0$ increases
- X_K decreased, caused by skin-/ proximity-effect $\Rightarrow I_\infty$ increases
- R_2^* decreased, caused by skin-/ proximity-effect $\Rightarrow P_K$ approaches the breakdown point at P_{Kipp}

7.5 Speed adjustment

Most important opportunities for speed adjustment of induction machines can be taken from the basic equation (7.81):

$$n = \frac{f_1}{p} \cdot (1 - s) \tag{7.82}$$

7.5.1 Increment of slip

An increment of slip can be achieved by looping starting resistors into the rotor circuit of slip-ring machines.

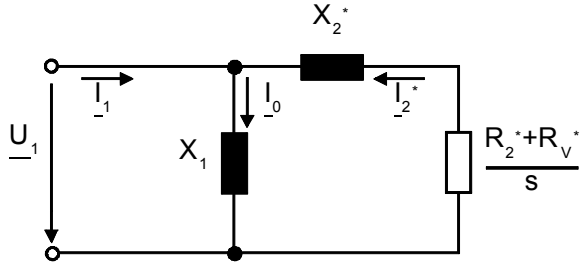

Fig. 177: induction mach., starting resistor

$$\underline{I}_0 = \frac{U_1}{j \cdot X_1} = const\,|_{R_2^*} \tag{7.83}$$

$$\underline{I}_\infty = \frac{\underline{I}_0}{s} = const\,|_{R_2^*} \tag{7.84}$$

$$M_{kipp} = \frac{3 \cdot p}{w} \cdot \frac{U_1^2}{2 \cdot X_2^*} = const\,|_{R_2^*} \tag{7.85}$$

The circle of the locus diagram remains the same in case of an increased rotor resistor, realized by adding R_V to R_2 – only the slip-parametrization differs.

- without R_v^*: $\tan \varphi_2^* = \frac{X_2^*}{R_2^*} \cdot s_1$ (7.86)

- with R_v^*: $\tan \varphi_2^* = \frac{X_2^*}{R_2^* + R_v^*} \cdot s_2$ (7.87)

In order to achieve the same point on the circle diagram, both $\tan \varphi_2^*$ values need to be the same:

$$\frac{R_2^*}{s_1} = \frac{R_2^* + R_V^*}{s_2} \tag{7.88}$$

and therefore:

$$s_2 = s_1 \cdot \left(1 + \frac{R_V}{R_2^*}\right) \tag{7.89}$$

The same circle point and therefore the same amount of torque is achieved for a slip value s_2 when adding R_V^* to the rotor circuit as for slip value s_1. This enables starting with breakdown torque (=maximum torque).

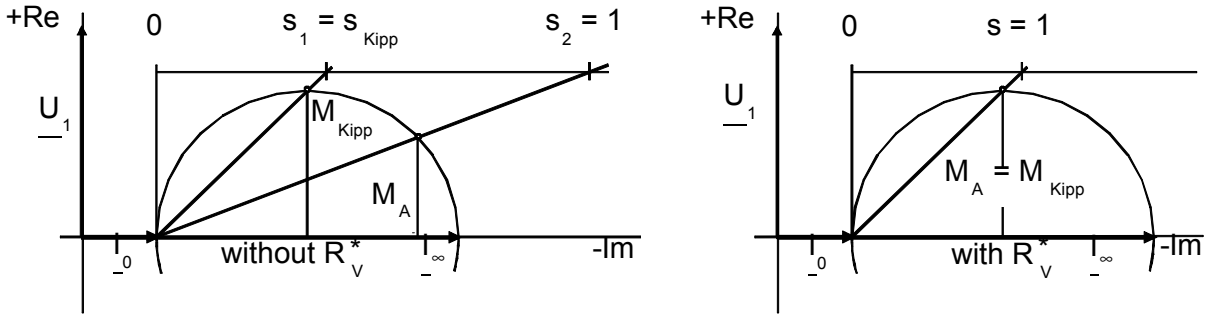

Fig. 177 a/b: induction machine, circle diagram without/with starting resistor

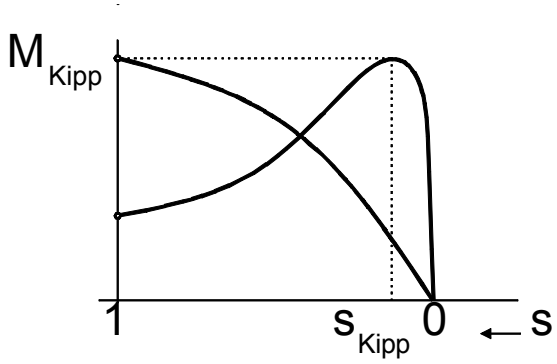

Fig. 178:

Example:

$$s_1 = s_{kipp},\ s_2 = 1 \tag{7.90}$$

$$\frac{R_2^*}{s_{kipp}} = \frac{R_2^* + R_v^*}{1} \rightarrow R_v^* = R_2^* \cdot \left(\frac{1}{s_{kipp}} - 1 \right) \tag{7.91}$$

Disadvantage of this method: additional losses caused by the additional resistor R_V, the efficiency $h = 1 - s$ decreases.

No-load speed remains the same as of operation without starting resistor.

7.5.2 Variating the number of pole pairs

Speed adjustment can also be achieved for squirrel-cage machines by changing the poles, because this type is not bound to a certain number of poles. This is realized utilizing either two separate three-phase windings of different number of poles to be implemented into the stator, with only one of them being used at a time or a change-pole winding, called *Dahlander winding*. The latter enables speed variation due to a ratio of 2:1 by reconnecting two winding groups from series to parallel connection. Speed variation can only be performed in rough steps.

7.5.3 Variation of supply frequency

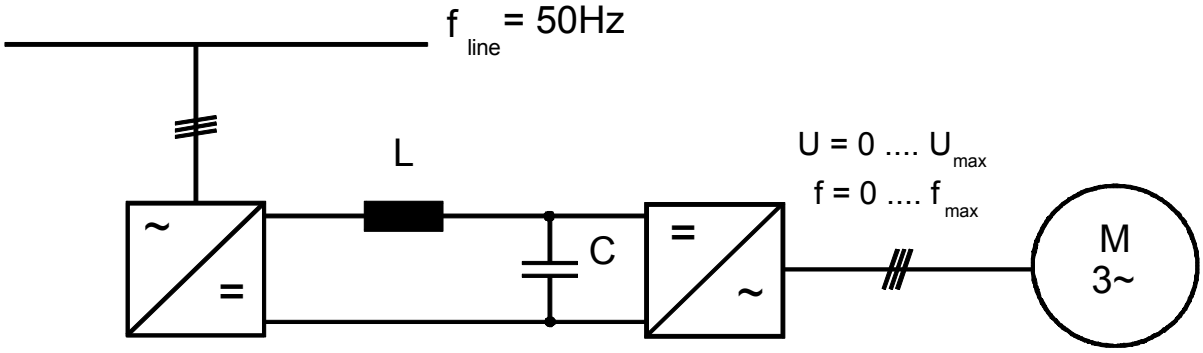

Fig. 179: power system set, power supply, AC/DC – DC/AC converters, three-phase machine

Power converters are required fort his method of speed adjustment. Power is taken from the supplying system, then rectified and transferred to the inverter block via its DC-link. The inverter takes over speed control of the induction machine, supplying with varable frequency and voltage.

The characteristic circle diagram needs to be discussed for variable frequencies:

On the one hand, the circle is partially defined by:

$$I_0 = \frac{U_1}{X_1} \sim \left(\frac{U_1}{f_1} \right) \tag{7.92}$$

and on the other hand by

$$I_\infty = \frac{I_0}{s} \sim \left(\frac{U_1}{f_1} \right). \tag{7.93}$$

If the supplying voltage is variated proportionally to the line frequency, the according circle size remains the same and therefore also its breakdown torque

$$M_{kipp} = \frac{3 \cdot p}{w_1} \cdot \frac{U_1^2}{2 \cdot X_2^*} \sim \left(\frac{U_1}{f_1} \right)^2, \tag{7.94}$$

but the parametrization differs due to:

$$\tan j_2^* = \frac{X_2^*}{R_2^*} \cdot s \sim s \cdot f_1 = f_2 . \tag{7.95}$$

Any rotor frequency is assigned to a circle point. The short-circuit operational points approaches the no-load point with decreasing frequency.

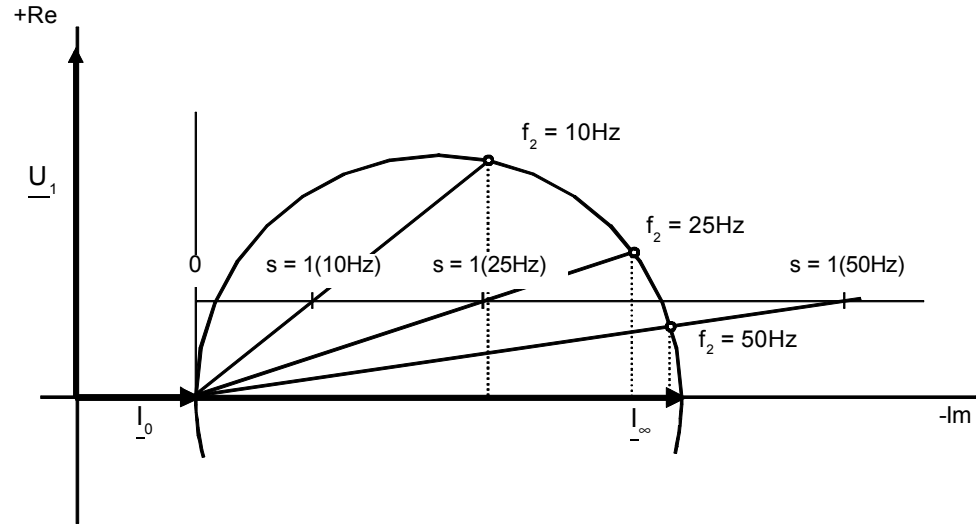

Fig. 180:circle diagram for $\frac{U_1}{f_1} = const , R_1 = 0$

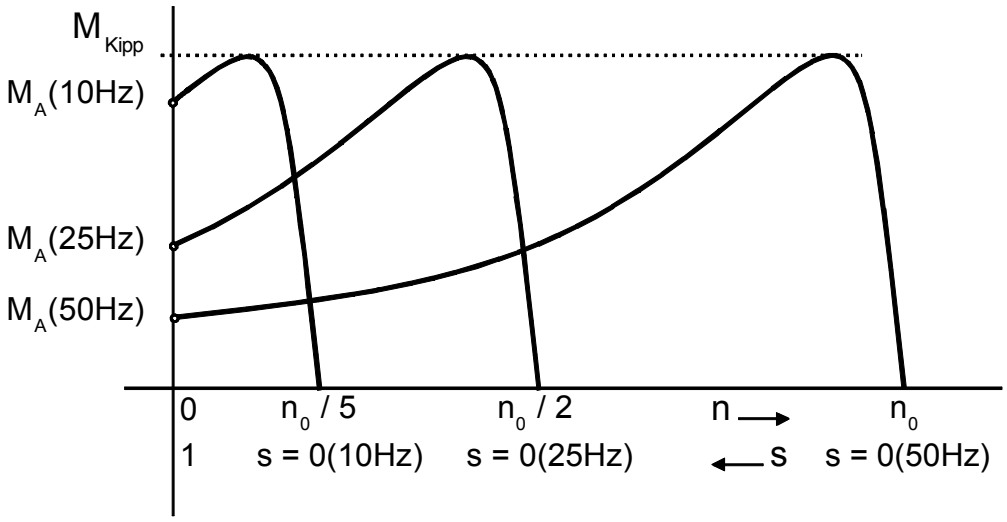

Fig. 181: torque-speed-characteristic for $\frac{U_1}{f_1} = const , R_1 = 0$

The mode of operation keeping $\frac{U_1}{f_1} = const$ is called operation with *constant stator flux linkage*. For instance constant no-load stator flux linkage ensues to:

$$\Psi_{10} = L_1 \cdot I_{10} = L_1 \cdot \frac{U_1}{w_1 \cdot L_{10}} \sim \frac{U_1}{f_1} = const \tag{7.96}$$

7.5.4 Additional voltage in rotor circuit

Double supplied induction machines are based on feeding slip-ring-rotors with slip-frequent currents.

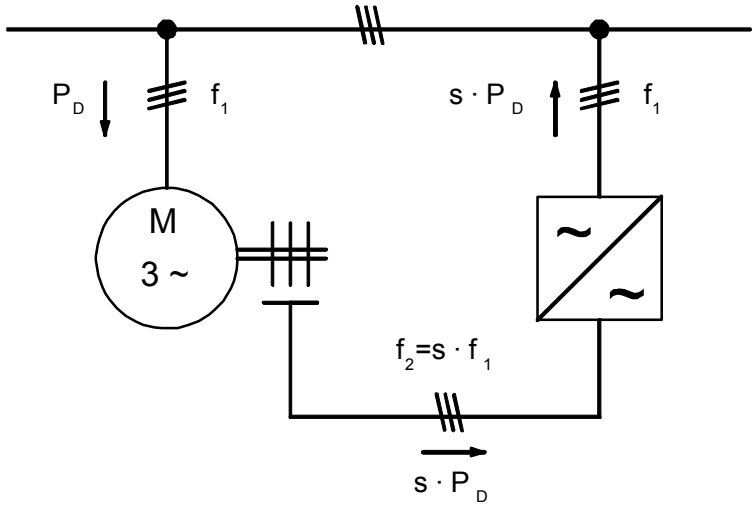

Fig. 182: ecd for additional voltage in rotor circuit

Slip power $s \cdot P_D$ is taken from (or fed to) the slip-rings of the machine and supplied to (or taken from) the line using an inverter. Therefore slip is increased or decreased, an almost lossless speed adjustment is possible - „under-synchronous or over-synchronous inverter cascades“.
The power inverter necessarily only needs to be designed for slip power.

7.6 Induction generator

The bottom part of the circle diagram covers generator mode of induction machines at three-phase supply. Over-synchronous speed $(s < 0)$ is to be achieved by accordant driving in order to work as generator. The reversal of the energy flow direction is regarded in the ecd with appliance of $R_2^*/s < 0$ and therefore a reversal from sink towards source.

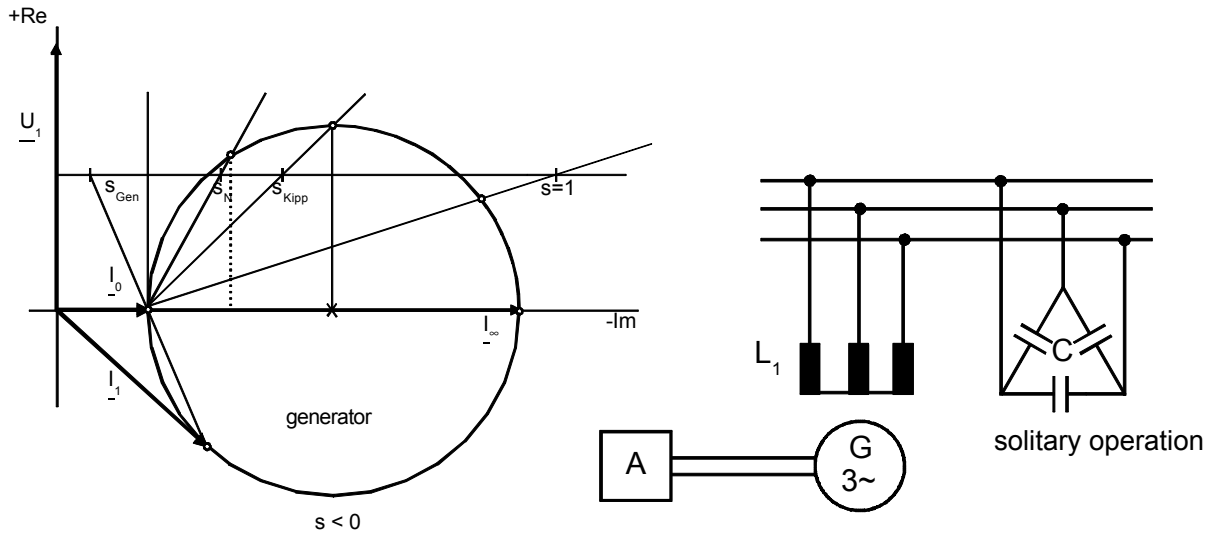

Fig. 183: induction generator, operational range, ecd

The stator current reactive component direction remains the same at changeover from motor to generator mode. Thus induction machines are not able to autonomously excite required magnetizing current, but need to be supplied by external sources. Since synchronous generators are able to provide lagging reactive power, mains operation appears trouble-free. If induction machines are supposed to operate in solitary operation without mains connection (e.g. auxiliary power supplies, alternator in automotive applications, etc.), capacitor banks need to be connected in parallel for coverage of required reactive power.

Besides described application samples, maintenance-free induction machines in solitary operation are utilized for run-of-river power stations as well as for wind-energy generators.

Similar to DC machines, self excitation is possible for inductions machines in solitary operation as well. Saturation dependent machine reactance and external capacitors form a resonating circuit, which is excited to oscillate by current peak or remanence magnetism for actuated rotors.

A stable operating point ensues for $U_C = U_0$ at the intersection of no-load characteristic and capacitor characteristic. The amount of no-load voltage can be adjusted by the choice of the utilized capacitor value.

The no-load characteristic $U_0 = f(I_m)$ applies for constant speed without load $\Rightarrow$ $I_{\text{wirk}} = 0$, whereas the capacitor characteristic $U_C = \dfrac{I_m}{wC}$ complies with the reactive voltage drop along the capacitor, to be connected in parallel.

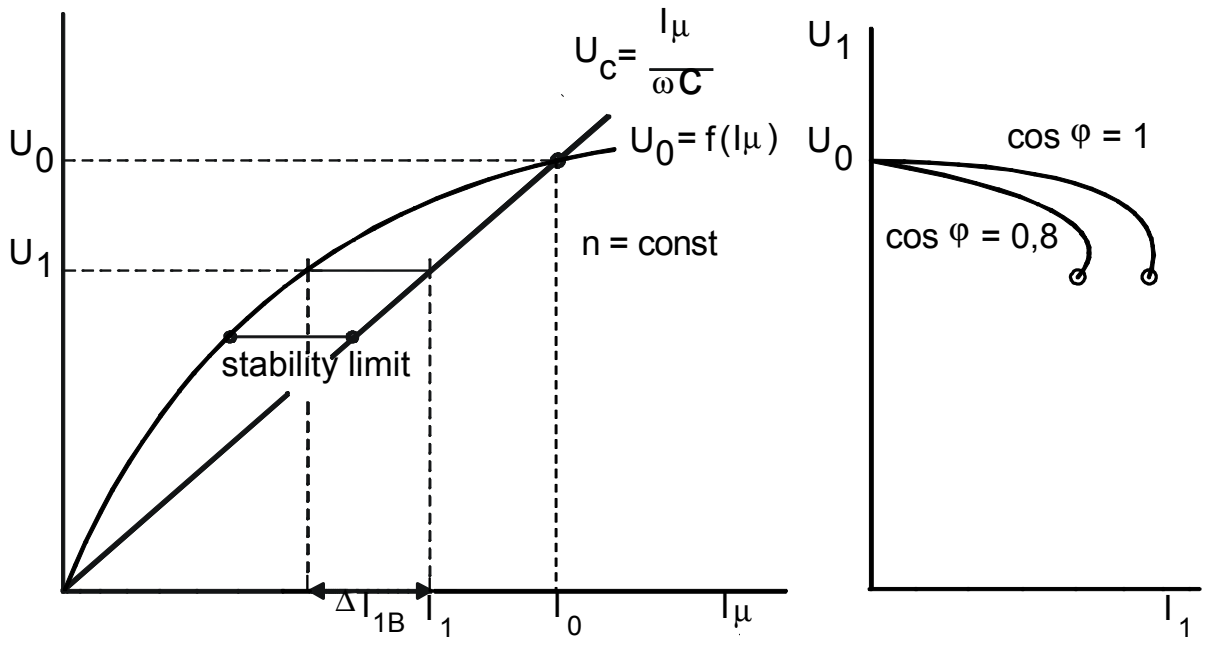

Fig. 184: induction generator, intersection of no-load and capacitor characteristics

If the machine is loaded with active current I_1, the required reactive current amount increased about ΔI_{1B}. Since the capacitor is not able to provide more reactive current in real, voltage drops until U_1. Therefore the machine load can be increased until the stability limit is reached, which means, an additional reactive current demand can not be covered.
The according load characteristics $U_1 = f(I_1)$ take after those of entirely excited DC shunt generators.

7.7 Squirrel-cage rotors

7.7.1 Particularities, bar current – ring current

Induction machines with squirrel-cage rotors are most utilized type of electrical machine. Its special design is simpler, more robust and apart from that also cheaper than slip-ring rotors. Squirrel cage rotors can be used, if the power supply is able to get along with breakaway starting currents of 4 ... 7 I_N and admissible heating is not going to be exceeded.

In its simplest form squirrel cage rotors consist of bars, placed in slots, to count the same number as the number N_2 of rotor slots. At the rotor front end, cage bars are interconnected with short-circuit rings. The arrangement is generally called *cage rotor* and because their alikeness usually known as *squirrel cage rotor*.

Either blank copper bars are sandwiched into uninsulated slots of the rotor laminations stack, to be short-circuited by conducting rings at the front ends as described or alternatively die-cast aluminium cages are implemented, usually for low-power machines.

Cage windings can be understood as polyphase winding of N_2 phases, with any of the bars to consist of single bars. This assumption appears perspiciuous as soon as single bars are added up to short-circuited ring-windings, whose one side reaches trough the armature (Fig. 185a). This leads to a symmetrical polyphase winding with N_2 short-circuited phase windings. The total sum of induced currents by sinusoidal rotating fields is supposed to be equal to zero at any moment of time. Thus return conductors through the interior of the armature can be spared if all bars at both ends of the rotor are connected in one electrical node each (Fig. 185b). The only item of squirrel-cage rotors to differ from the described winding principle is a substitution of node points by ring conductors, which can be displayed by a resistor to be connected as N_2-angle (Fig. 185c).

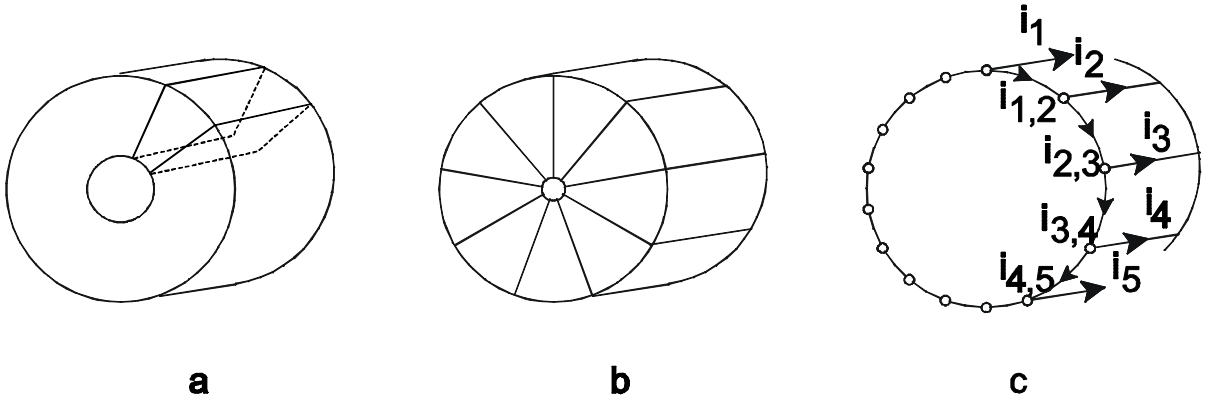

Fig. 185: development of squirrel-cage rotors

The number of turns w_2 of cage windings with m_2 phases = N_2 bars ensues to:

$$w_2 = \frac{N_2 z_N}{2 m_2 a} = \frac{1}{2} \qquad (z_N = 1, a = 1) \tag{7.97}$$

with the winding factor for the fundamental wave:

$$x_2 = 1. \tag{7.98}$$

Squirrel-cage rotors do not feature certain number of poles, but as an effect of the induction evoked by the stator, it takes over the number of stator poles.

This leads to the fundamental wave of the rotor mmf:

$$q_2^D = \frac{m_2}{2}\frac{4}{p}\frac{w_2 x_2}{p}\sqrt{2}I_2 = \frac{N_2}{2}\frac{4}{p}\frac{\frac{1}{2}\cdot 1}{p}\sqrt{2}I_{Stab} = \frac{\sqrt{2}}{p}\frac{N_2}{p}I_{Stab}, \tag{7.99}$$

with $I_2 = I_{Stab}$ being current per rotor bar.

The amount of ring current is now supposed to be subject to investigations:

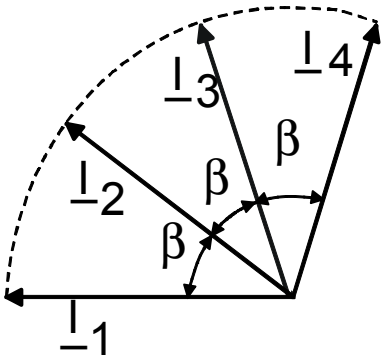

Fig. 186: bar currents

Bar currents are displaced ofan electric angle β against each other:

$$b = pa = \frac{p2p}{N_2}. \tag{7.100}$$

First Kirchhoff's Law applies for the dependence of bar- and ring currents:

$$I_{01} = I_1 + I_{12} \tag{7.101}$$
$$I_{12} = I_2 + I_{23} \tag{7.102}$$
$$I_{23} = I_3 + I_{34} \tag{7.103}$$
$$I_{34} = I_4 + I_{45} \tag{7.104}$$

which can be displayed by a phasor diagram due to Fig. 187.

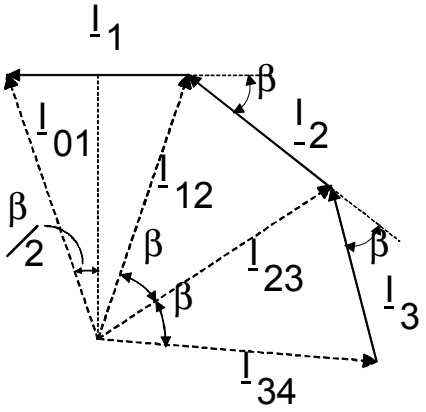

Fig. 186: phasor diagram of bar and ring currents

Phase displacement of bar currents is equal to phase displacement of ring currents, so that generally follows:

$$I_{Ring} = \frac{I_{Stab}/2}{\sin\frac{b}{2}} = \frac{I_{Stab}}{2\sin\frac{pp}{N_2}} \tag{7.105}$$

This leads to the evaluation $I_{Ring} >> I_{Stab}$ - short-circuit rings need to be necessarily design to stand high ring currents with damage. Squirrel-cage machines with low number of poles in particular require large ring cross section compared to bar diameters.

Note: On the one hand, squirrel cage rotors adapt to various number of stator poles, but they can not be utilized for different a number of poles on the other hand – founded by reasons of dimensioning (see above).

7.7.2 Current displacement (skin effect, proximity effect)

The basic effect of current displacement and the opportunity to utilize it for an improvement of the start-up behaviour of squirrel-cage motors is subject of discussion in the following.

For a better understanding only a single slot of typical squirrel-cage motors, shown in Fig. 187, is part of investigation. Assumptions as the conductor to completely fill out the slot and current density to be constant over cross-section area in case of DC current supply and no current displacement, are made for simplification reasons. Appliance of Ampere's Law on the conductor shows linear rise of flux density inside the slot, neglect of the magnetic voltage drop in iron parts assumed.

$$q = \oint \vec{H}\mathrm{d}\vec{s}\,, \quad m_{Fe} \to \infty$$

$$q(x) = S_N b_N x = H(x)\cdot b_N = \frac{B(x)}{m_0} b_N \tag{7.106}$$

$$B(x) = m_0 \frac{S_N b_N}{b_N} x \frac{h_N}{h_N} = m_0 \frac{I_=}{b_N}\frac{x}{h_N} = B_{\max}\frac{x}{h_N} \tag{7.107}$$

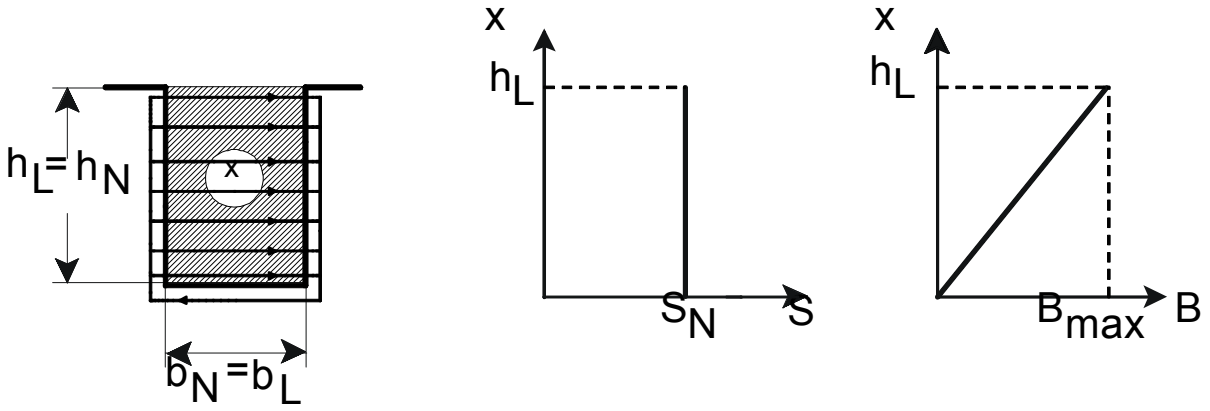

Fig. 187: conductor bar run of current density and flux density

DC current: $S(x) = S_N = \frac{I_=}{h_L b_L}$; $B(x) = B_{\max}\frac{x}{h_N}$; $B_{\max} = \frac{m_0 I_=}{b_N}$

In case of AC current supply, flowing bar current is displaced towards the air gap the more its frequency rises. The effect is called current displacement, it is caused by the slot leakage field. Model: if a solid conductor bar is assumed as stacked partial conductors, placed one upon another, lower layers are linked with higher leakage flux than upper layers, which means lower partial coils feature higher leakage inductance than upper partial coils. In case of flowing AC current, back-e.m.f. into separate zones is induced by the slot leakage field. ($L_s \cdot \frac{\mathrm{d}i}{\mathrm{d}t}$). The amount of back-e.m.f. increases from top to bottom of the conductor (-layers), which counteract their creating origin (Lenz`s Law). As a consequence of this, eddy currents of uneven distribution develop, whose integration over the conductor cross section area is equal to zero, but create single-sided current displacement towards the slot opening.

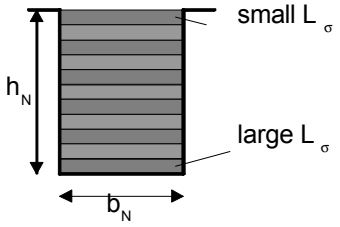

$L_s \sim \frac{h_N}{b_N}$

Fig. 188: leakage inductance values

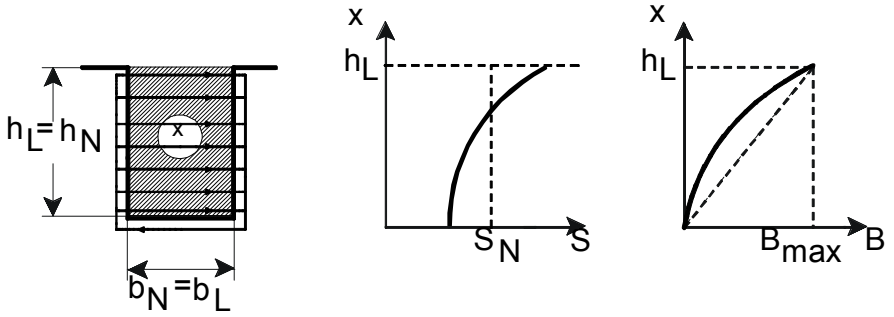

Fig. 189a-c: conductor in slot, dimensions (a), current density (b), flux density (c)

AC current: $b_N \int S(x)\mathrm{d}x = I$; $B_{\max} = \frac{m_0 I\sqrt{2}}{b_N}$; $\sqrt{2}I \hat{=} I_=$

Layer thickness on which current flow is reduced to amounts:

$$d = \sqrt{\frac{2r}{wm_0}} = \frac{1}{\sqrt{pfkm_0}}. \qquad (7.108)$$

Symbol δ is used for penetration depths, e.g. results for copper with $r = \frac{1}{57}\frac{\Omega mm^2}{m}$ and line frequency 50 Hz: δ = 1cm.

In order to illustrate the effect of current displacement, the following pictures show field distribution of an induction machine at different frequencies, calculated with Finite Element Method (FEM).

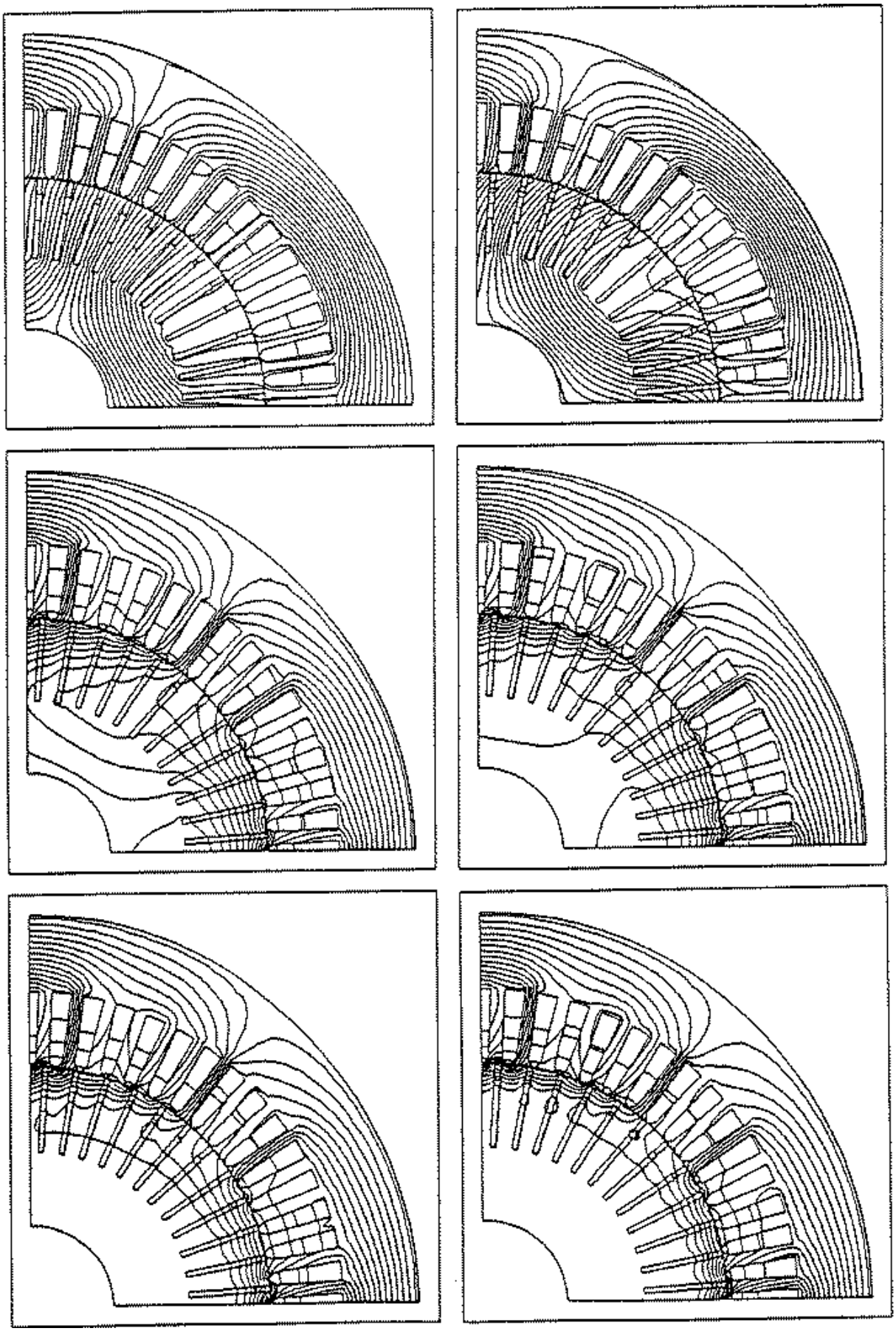

Fig. 190: induction machine, field distribution at f_s = 0.1 Hz, 0.5 Hz, 5 Hz, 10 Hz, 20 Hz, 50 Hz (top left through bottom right)

Current displacement is the cause for increased AC resistance of conductors in contrast to their DC restance. This results in increased copper losses to occur in rotor conductors:

$$P_V = r\int_V S^2(x)\mathrm{d}V = I^2 R_2(s) \tag{7.109}$$

$$R_2(s) = K_R(s)R_2 \tag{7.110}$$

$$K_R(0) = 1; \qquad K_R(1) \approx 3\ldots5 \tag{7.111}$$

(for calculation of K_R please see additional literature)

Current displacement reduces flux density in rotor conductors, solely the slot opening shows same maximum values as in the DC case. This effect leads to a reduction of the leakage inductances:

$$W_m = \frac{1}{2m_0}\int_V B^2(x)\mathrm{d}V = \frac{1}{2}I^2 L_{2sN}(s) \tag{7.112}$$

$$L_{2sN}(s) = K_I(s)L_{2sN} \tag{7.113}$$

$$K_I(0) = 1; \qquad K_I(1) = 0{,}25\ldots0{,}4 \tag{7.114}$$

(for calculation of K_I please see additional literature)

Usually current displacement is an unwanted effect for electrical machines in general, because of the described additional losses in rotor bars – with increased heating and deteriorated efficiency as a consequence. In order to avoid this, conductor cross sections of large machines are partitioned and additionally transposed.

Current displacement is merely used for induction machines for improvement of start-up behaviour. Different forms of rotor bars appear for optimizing purposes.

- deep-bar rotor,

  subdivided into:

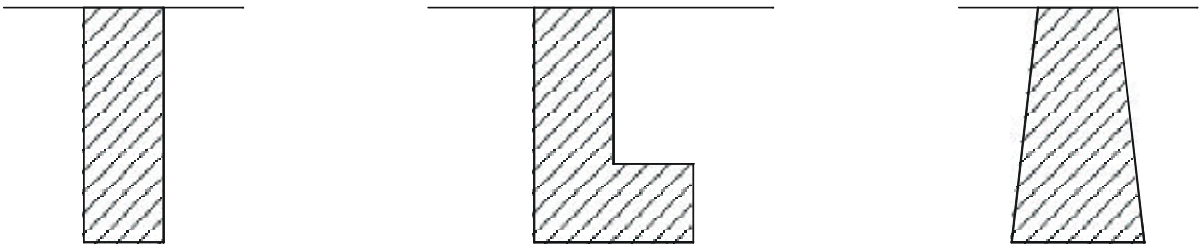

Fig. 192: deep-bar slot L-slot spline slot

Material: aluminium die-cast, copper bars

Frequency of rotor currents is equal to line frequency at the moment of actuation. Current displacement appears in rotor bars. That enlarges R_2' and lessens X_{2s}'. The amplification of R_2' moves the short-circuit operational point towards the breakdown point, a reduction of X_{2s}' enlarges the circle diameter.

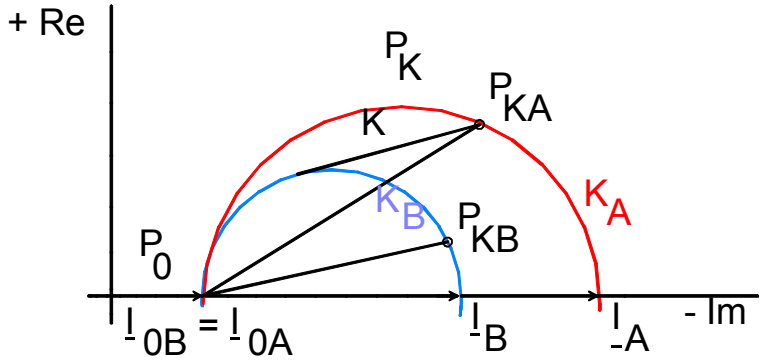

Fig. 193: variance of the circle form at parameter change

- s = 1: X_1, X_{2s}' small, R_2' large
- $s \to 0$: X_1, X_{2s}' large, R_2' small

The influence of current displacement decreases with increasing speed of the motor, until it disappears near the nominal point. The course of the locus diagram K can be developed from start-up diagram K_A and operation diagram K_B. Strictly speaking, any operational point requires an own according circuit diagram.

- twin-slot-cage rotor

Double-slot rotors as well as double-cage rotors form the category of twin-slot-cage rotors:

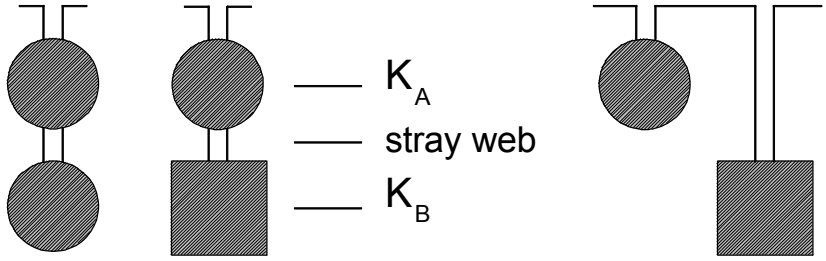

Fig. 194: double-slot double-cage

Material: starting cage: brass, bronze; operation cage: copper

Revealing design is made possible by using two different cages.

The starting cage features a large active resistance and low leakage reactance, whereas the operation cage oppositely shows low active resistance and large leakage resistance. At start-up the rotor current predominantly flows inside the starting cage, caused by the high leakage reactance of the operation cage. The start-up torque is raises caused by the high active resistance of the starting cage. In nominal operation with low rotor frequency, the rotor current splits with reciprocal ratio of the active resistances and therefore principally flows in the operation cage. Low nominal slip accompanied by reasonable efficiency ensues due to the small active resistance.

The according ecd shows both cages to be connected in parallel:

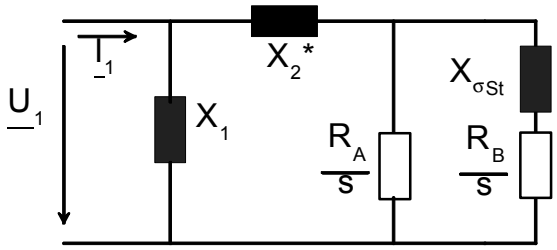

Fig. 195: twin-slot cage machine, ecd

- Leakage of operation cage is elevated about the partition of the leakage segment $X_{\sigma S}$.
- Stator- and slot leakage are contained in reactance X.
- R_1 neglected, R_A large, R_B small

The following diagram shows locus diagrams of starting cage and operation cage:

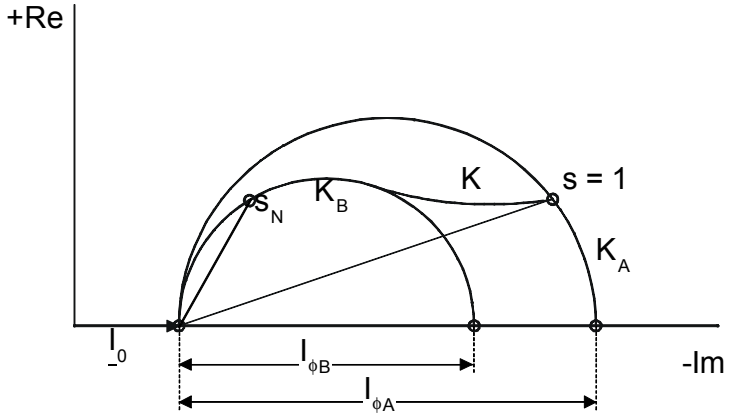

Fig. 196: locus diagrams of different cage types

A comparison of current and torque course over rotational speed for different rotor types is illustrated in Fig. 197:

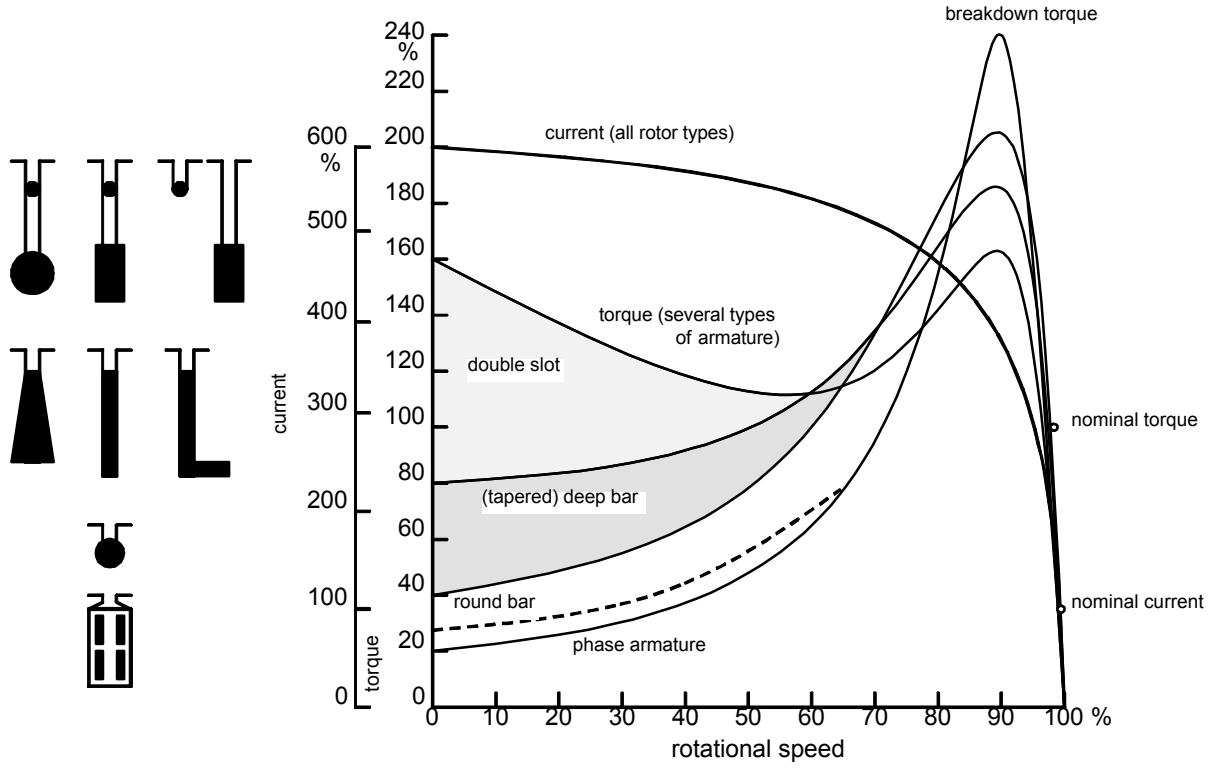

Fig. 197: torque/speed characteristics for different rotor types

7.8 Single-phase induction machines

7.8.1 Method of operation

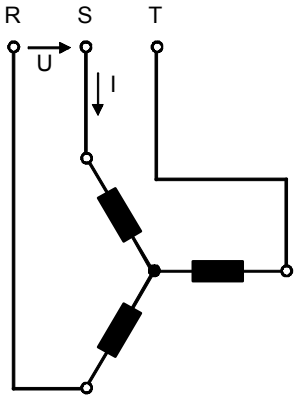

Are three-phase induction machines connected to a balanced three-phase system, their stator windings create a circular rotating field.

In case of one phase being disconnected from the mains, the remaining two phases form a resulting AC winding, creating an AC field. This AC field can be split up into two counterrotating circular fields.

Fig. 198: single-phase induction machine, ecd

The first field, to rotate in direction of the rotor shows a slip due to:

$$s = \frac{n_1 - n}{n_1}, \tag{7.115}$$

whereas the slip of the counter rotor motion rotating field ensues to:

$$s = \frac{-n_1 - n}{-n_1} = 2 - s \tag{7.116}$$

- Concurrent stator field and the concurrent rotor field as well as the counterrotating stator field and the counterrotating rotor field form constant torque each.
- Concurrent stator field and the counterrotating rotor field as well as the counterrotating stator field and the concurrent rotor field create pulsating torque with average value equal to zero.

The effect of both rotating fields with opposing motion directions on the rotor can be understood as a machine set to consist of two equal three-phase machines exerting opposite rotational speed directions on one shaft.

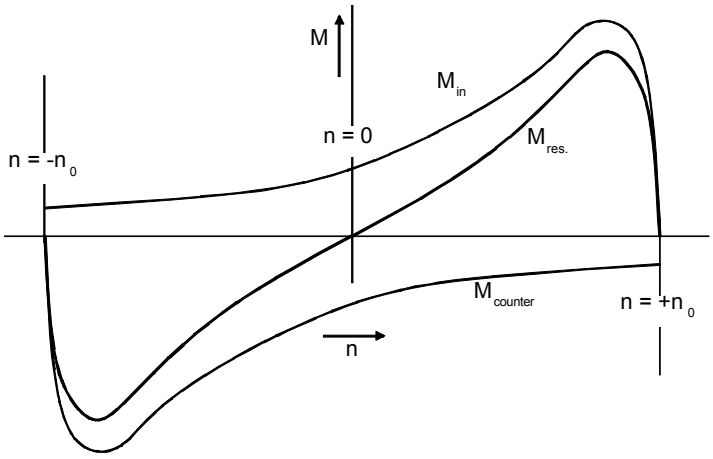

Fig. 199: machine set: torque/speed diagram

Both torque partitions equalize each other in standstill. Single-phase induction machines fail to exert torque on the shaft, so that they are unable to start on their own!

Different reactions occur in operation, caused by different slip values. The counterrotating field is vigorously damped at $s \to 2$, whereas the concurrent field is barely influenced at $s \to 0$.

This leads to elliptical rotating field. If single-phase induction machines are pushed to speed with external means (hand-start), the resulting torque value is unequal to zero, the rotor accelerates independently and can be loaded.

7.8.2 Equivalent circuit diagram (ecd)

The equivalent circuit diagram of single-phase operated induction machines and be derived with appliance of the method of symmetrical components:

due to circuit diagram follows:

$\underline{I}_u = -\underline{I}_v = \underline{I}; \qquad \underline{I}_w = 0$

With transformation into symmetrical components:

$$\begin{pmatrix} \underline{I}_m \\ \underline{I}_g \\ \underline{I}_0 \end{pmatrix} = \frac{1}{3}\begin{pmatrix} 1 & \underline{a} & \underline{a}^2 \\ 1 & \underline{a}^2 & \underline{a} \\ 1 & 1 & 1 \end{pmatrix}\begin{pmatrix} \underline{I}_u \\ \underline{I}_v \\ \underline{I}_w \end{pmatrix} = \begin{pmatrix} \frac{(1-\underline{a})}{3} I \\ \frac{(1-\underline{a}^2)}{3} I \\ 0 \end{pmatrix}. \tag{7.117}$$

The relation between $\underline{U}$ and $\underline{I}$ is regarded for induction machines including the slip-dependent motor impedance $\underline{Z}(s)$.

Then ensues for the positive-sequence system:

$$\underline{U}_m = \underline{Z}_m \underline{I}_m = \underline{Z}(s)\frac{(1-\underline{a})}{3}\underline{I}, \tag{7.118}$$

whereas for the negative-sequence system follows:

$$\underline{U}_g = \underline{Z}_g \underline{I}_g = \underline{Z}(2-s)\frac{(1-\underline{a}^2)}{3}\underline{I}. \tag{7.119}$$

No zero-sequence system applies.

Inverse transformation:

$$\underline{U}_u = \underline{U}_m + \underline{U}_g + \underline{U}_0 \tag{7.120}$$

$$\underline{U}_v = \underline{a}^2\underline{U}_m + \underline{a}U_g + \underline{U}_0 \tag{7.121}$$

$$\begin{aligned} \sqrt{3}\underline{U} &= \underline{U}_u - \underline{U}_v = \underline{U}_m(1-\underline{a}^2) + U_g(1-\underline{a}) \\ &= \underline{Z}(s)\frac{(1-\underline{a})}{3}\underline{I}(1-\underline{a}^2) + \underline{Z}(2-s)\frac{(1-\underline{a}^2)}{3}\underline{I}(1-\underline{a}) \\ &= [\underline{Z}(s) + \underline{Z}(2-s)]\underline{I} = \underline{U}_I + \underline{U}_{II} \end{aligned} \tag{7.122}$$

Figure 200 illustrates the ecd for single-phase operation. The ohmic resistance of the stator winding needs to be taken into account for machines of low power. Reactances of the three-phase windings remain the same for single-phase operation.

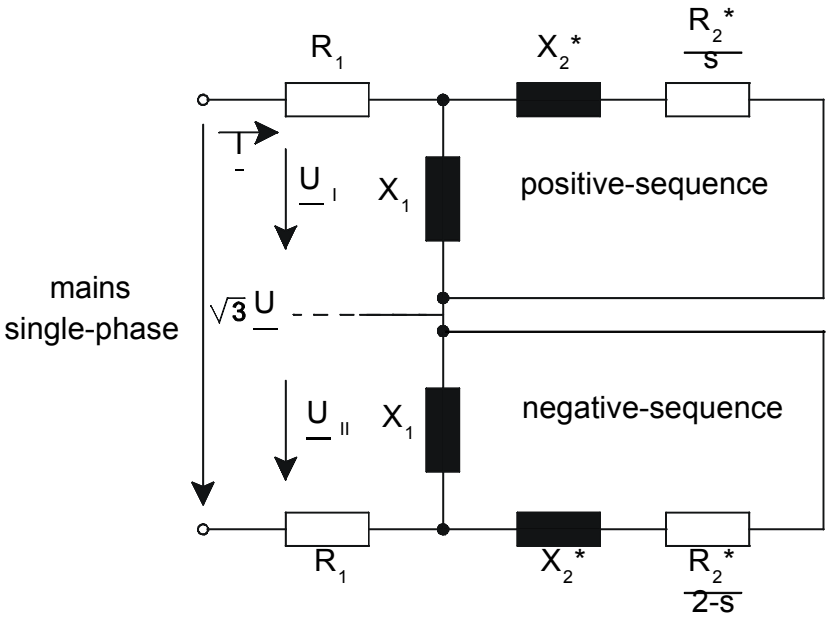

Fig. 200: induction machine in single-phase operation, ecd

Then follows for the current amount in single-phase operation:

$$\underline{I} = \frac{\sqrt{3}\underline{U}}{\underline{Z}(s) + \underline{Z}(2-s)} \tag{7.123}$$

Impedance values of positive- and negative sequence system can be taken from the circuit diagram in balanced operation for arbitrary operational points *s*.

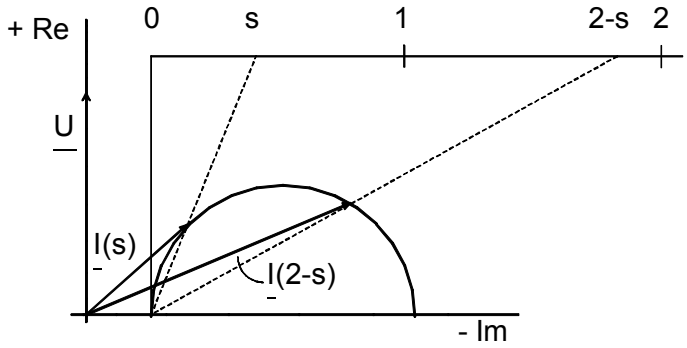

Fig. 201: balanced operation, circuit diagram

$$\underline{Z}(s) = \frac{\underline{U}}{\underline{I}(s)} \tag{7.124}$$

$$\underline{Z}(2-s) = \frac{\underline{U}}{\underline{I}(2-s)} \tag{7.125}$$

Phase current in single-phase operation can be approximated in the proximity of low slip values by:

$$I_{1Ph} = \frac{\sqrt{3}U}{|Z(s)+Z(2-s)|} \approx \frac{\sqrt{3}U}{Z(s)} = \sqrt{3}I_{3Ph}, \tag{7.126}$$

that means: if one phase is disconnected in normal operation at three-phase system, the motor continues running, the current absorbtion increases between no-load an nominal operation about factord $\sqrt{3}$. This may lead to thermal overload.

Phase current for single-phase operation in standstill amounts:

$$I_{1Ph} = \frac{\sqrt{3}U}{2Z(1)} = \frac{\sqrt{3}}{2} I_{3Ph} \tag{7.127}$$

The according short-circuit current is slightly below that in three-phase operation.

7.8.3 Single-phase induction machine with auxiliary phase winding

If single-phase induction motors are supposed to exert start-up torques, the appliance of an at least elliptical rotating field is mandatory.

This requires an auxiliary phase winding (*h*), which is displaced from the main winding (*H*) by a spatial angle *e* and fed by currents being displaced by electrical phase angle *j*.

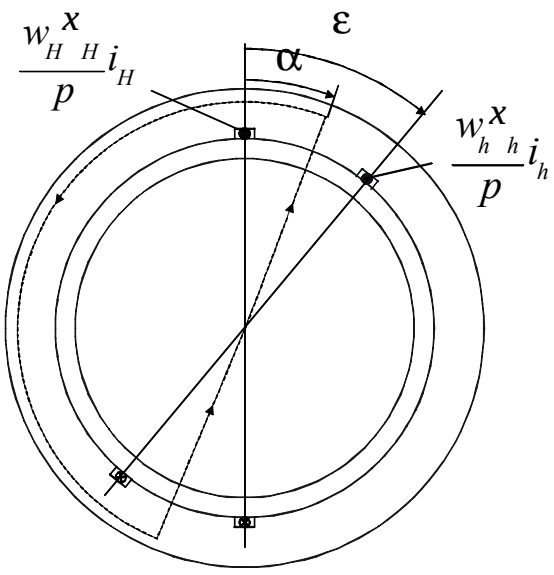

Fig. 202: auxiliary winding, design

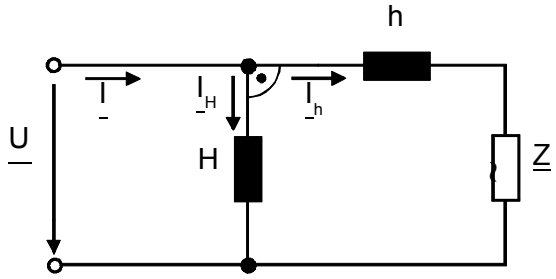

Fig. 203: machine with aux. winding, ecd

Optimized solution would be:

$$e = \frac{p}{2p} \text{ and } j = \frac{p}{2} \text{ as well as } w_h \cdot x_h = w_H \cdot x_H ,$$

that means spatial displacement of the coils and temporal displacement of the currents of 90° and also the same number of windings for main and auxiliary phase. A circular rotating field accrues based on these conditions. Due to cost reasons, in practical auxiliary phases are designed for lower efforts and with a smaller temporal displacement of the currents. This effects in an elliptical rotating field.

Current displacement of main phase current I_H and auxiliary phase current I_h is achieve by utilization of an impedance in the auxiliary phase circuit.

Different opportunities exist:

1. capacitor: optimum solution; high initial torque
   - start-up capacitor, switch-off by centrifugal switch
   - running capacitor for improvement of h and $\cos j$
2. inductance
   - expensive and heavy weighted, low initial torque
3. resistance
   - cheap, low initial torque
   - switch-off after start-up, because occurence of additional losses

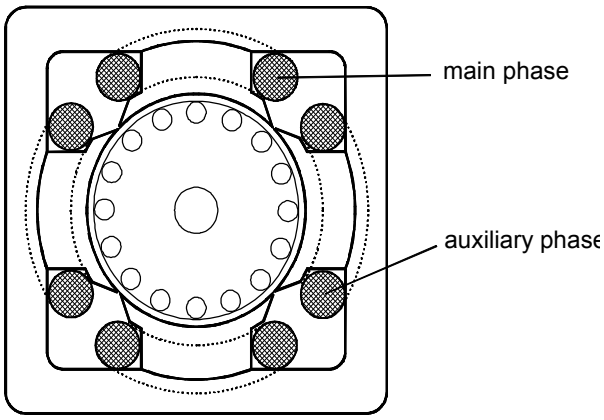

Fig. 204: single-phase iduction machine

Technical realization:

Fig. 204 illustrates a two-pole motor with distinctive poles and two-phase stator winding, with each phase to consist of two coils each. Its mass production is cheap doing it that way.

Appliance: low-power drive systems for industry, trade, agriculture and household applications.

7.8.4 Split-pole machine

Split-pole machines are basically induction machines with squirrel cage rotors to consist of two totally different stator windings. The main phase windings are arranged on one or more distinctive poles with concentrated coils, to be operated at single-phase systems. The auxiliary winding, to be realized as short-circuit winding, encloses only parts of the pole and is fed by induction (transformer principle) by the main windings. Spatial displacement of the auxiliary winding is achieved by constructive means whereas temporal displacement is achieved by induction feeding. That suffices to create an elliptical rotating field.

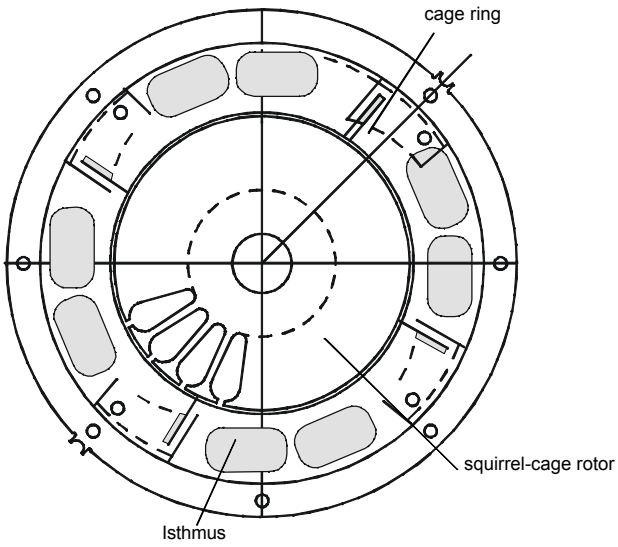

Fig. 205: split-pole motor, design

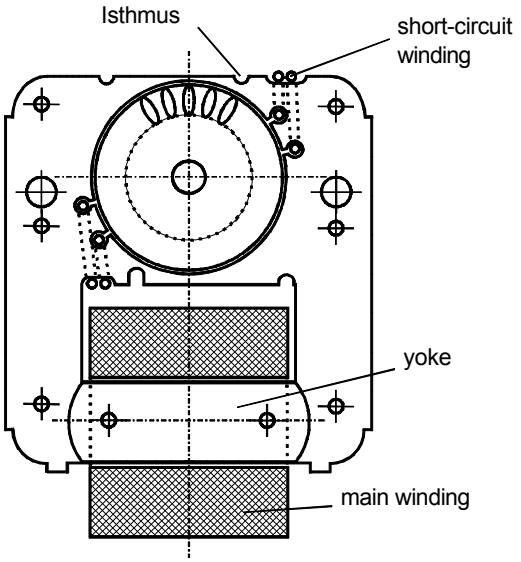

Fig. 206: ditto, asym. partial cross-section

In practical there is both symmetrical and asymmetrical cross section, to be displayed in Fig. 205 and 206.

Split-pole machines feature unreasonable efficiencies, because of their losses to occur in the copper short-circuit ring and their counterrotating rotating fields as well as low initial torque. Despite low production costs and simple design, split-pole motors are only utilized for low power applications (below 100W) for discussed reasons.

Appliance: low cost drive applications in household and consumer goods.

8 Synchronous machine

8.1 Method of operation

Synchronous machines (SYM) are most important electric generator and is therefore mainly used in generator mode.

Same as induction machines, synchronous machines belong to the category of rotating field machines, solely their rotor windings are fed with DC current. Voltage equation and equivalent circuit diagram can be derived from those of induction machines.

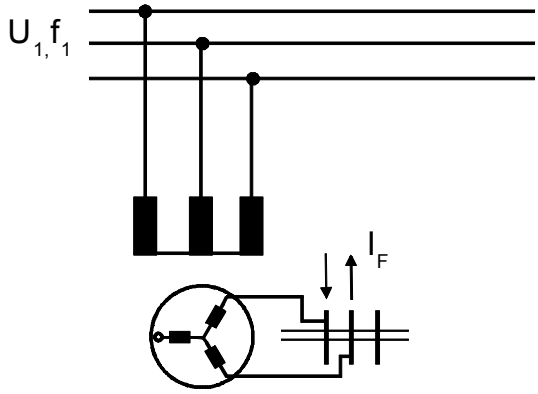

Fig. 207: synchronous machine, connection

The stator arrangement consists of a three-phase winding, to be connected to mains of constant voltage U_1 and frequency f_1.

Initially the rotor may also consist of a three-phase winding of the same number of pole-pairs, to be connected to slip-rings.

DC current is fed between both slip-rings, called exciter current. Therefore the rotor current frequency f_2 is equal zero.

Synchronous machines are solely able to create time-constant torque (unequal zero) if the frequency condition applies:

$$f_2 = s \cdot f_1 \tag{8.1}$$

with $f_2 = 0$ and $f_1 = f_{Netz}$ follows:

$$s = 0 \quad \text{and} \quad n = n_1 = \frac{f_1}{p}. \tag{8.2}$$

For stationary operation, the rotor exclusively revolves at synchronous speed n_1, where the assignment as „synchronous machine" derives from. Pulsating torques emerge at any other speeds $n \neq n_1$, with mean values equal zero.

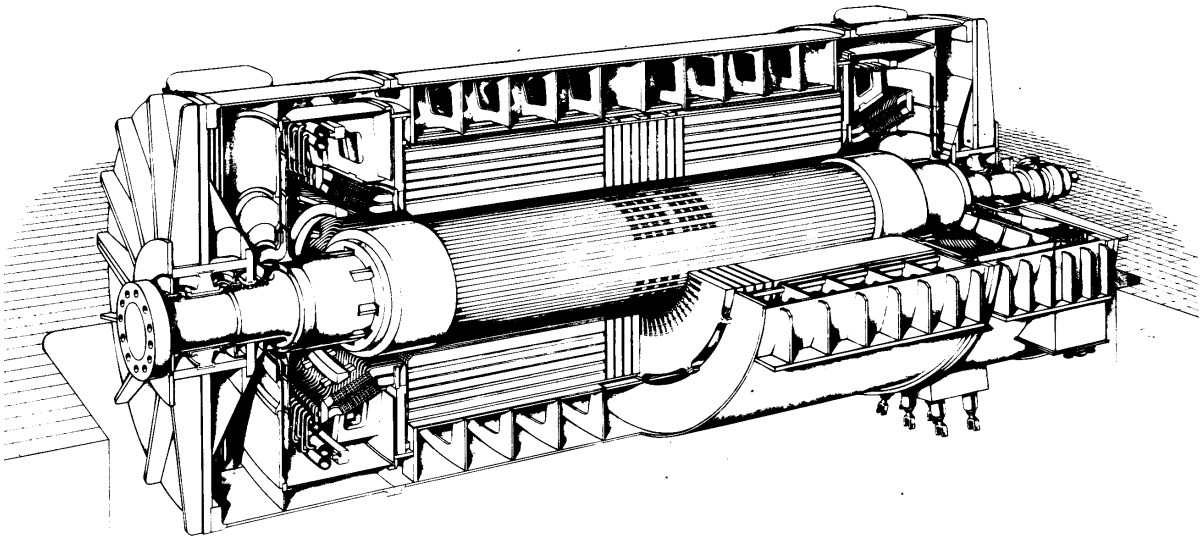

Fig. 208: Turbogenerator, 1200 MVA (ABB)

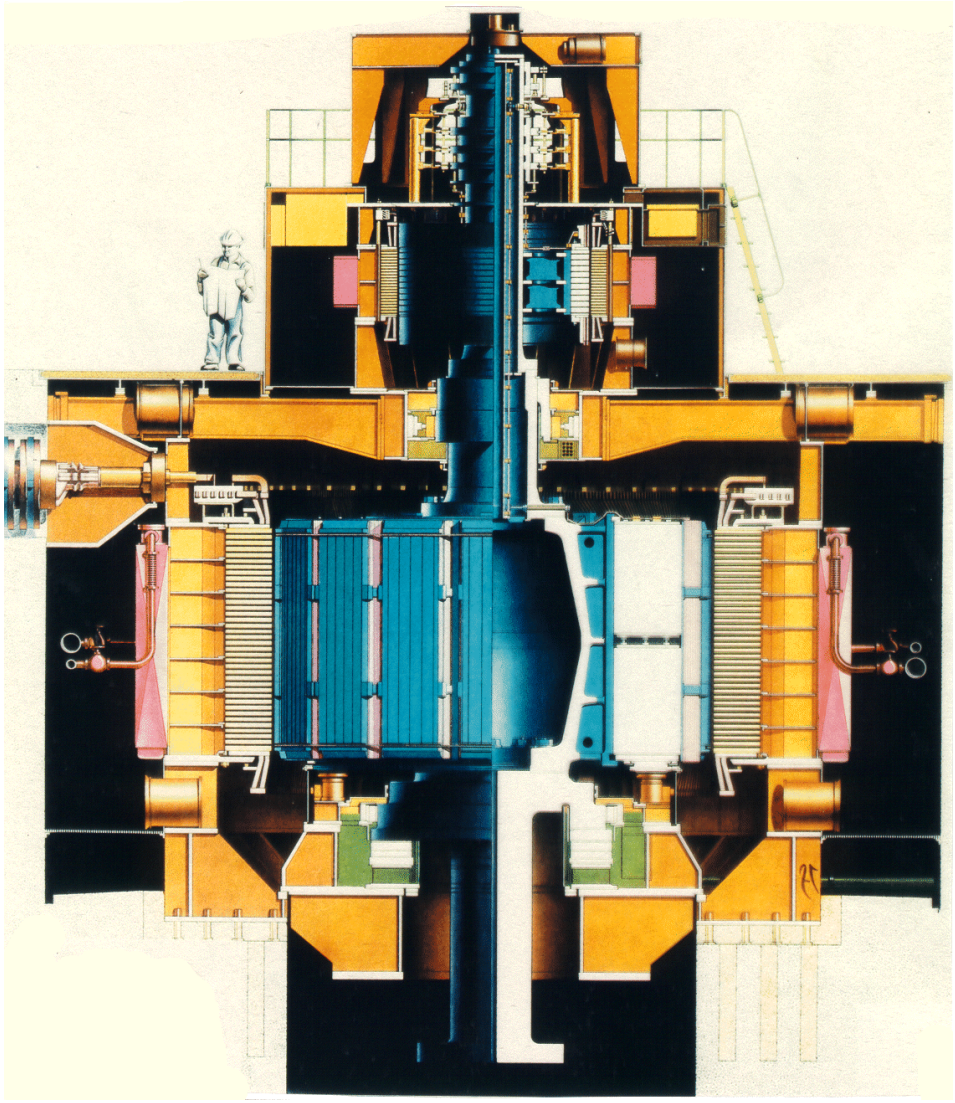

Fig. 209: hydro-electric generator, 280 MVA (ABB)

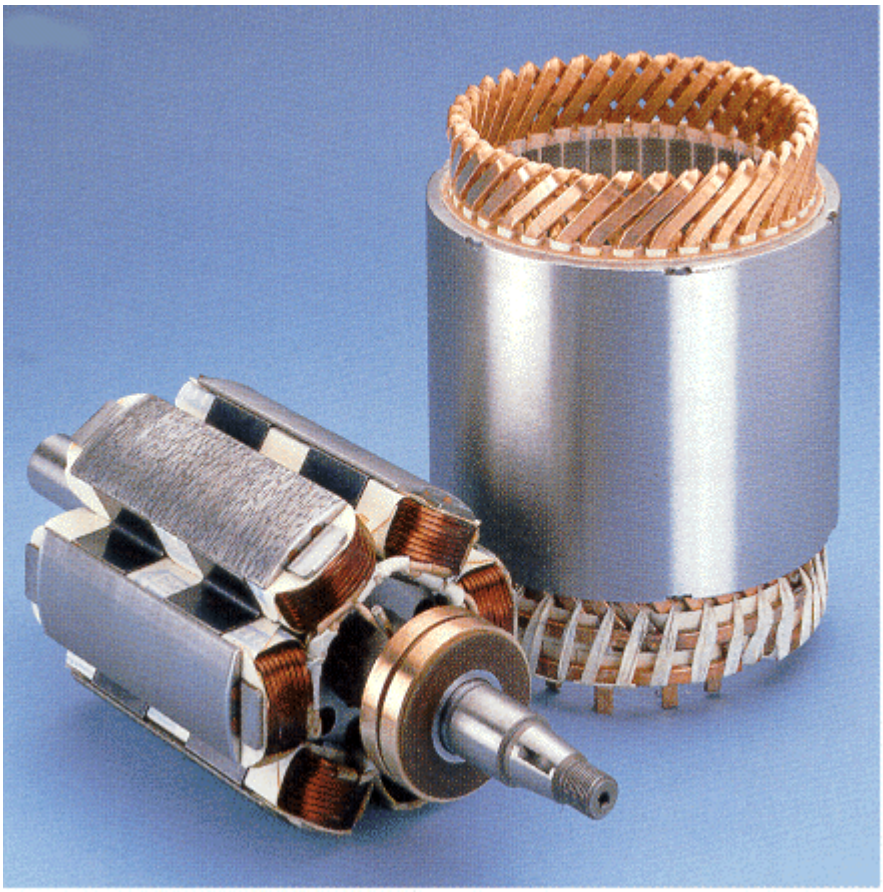

Fig. 210: synchronous generator for vehicle network applications, 5 kVA

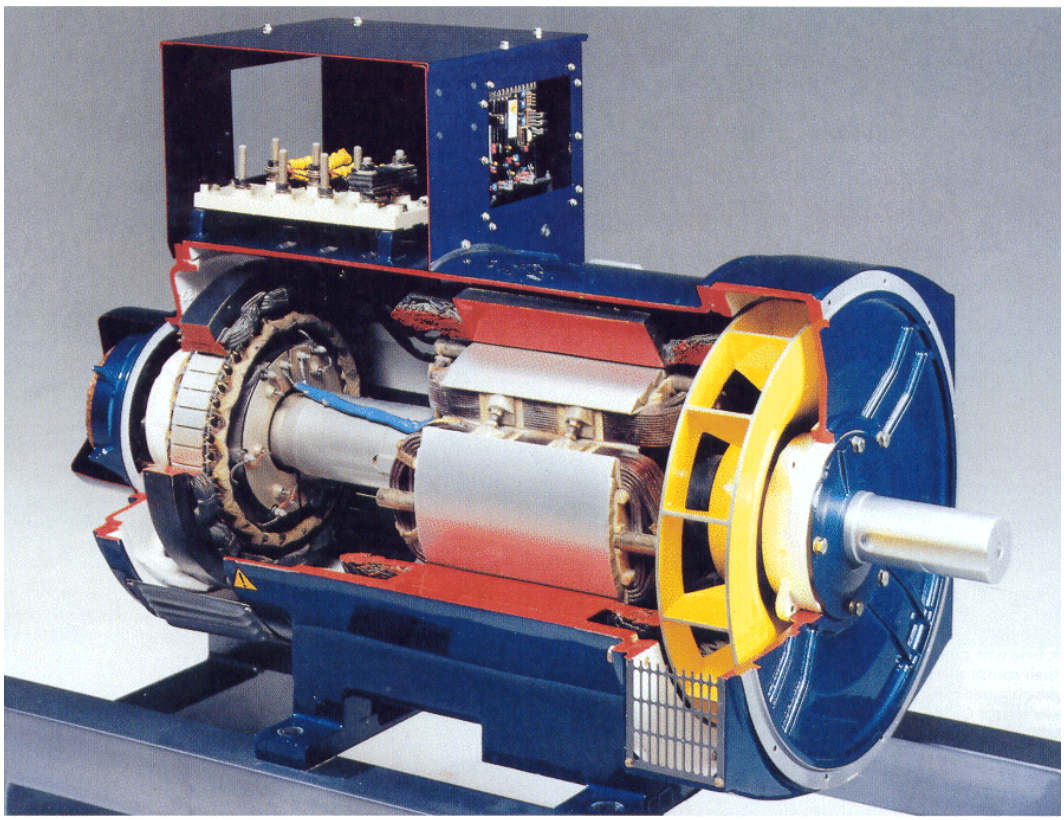

Fig. 211: sync. generator with stationary field exciter machine, revolving rectifiers, 30 kVA

8.2 Mechanical construction

Stators of synchronous machines show the same design as induction machines in principle. Those stators basically consist of insulated lamination stacks, fitted with slots and three-phase windings being placed into.

Rotor windings are supplied by DC current. Since f_2 is equal zero ($f_2 = 0$), the rotor can be implemented as solid unit. Due to different rotor types, two machine types are distinguished:

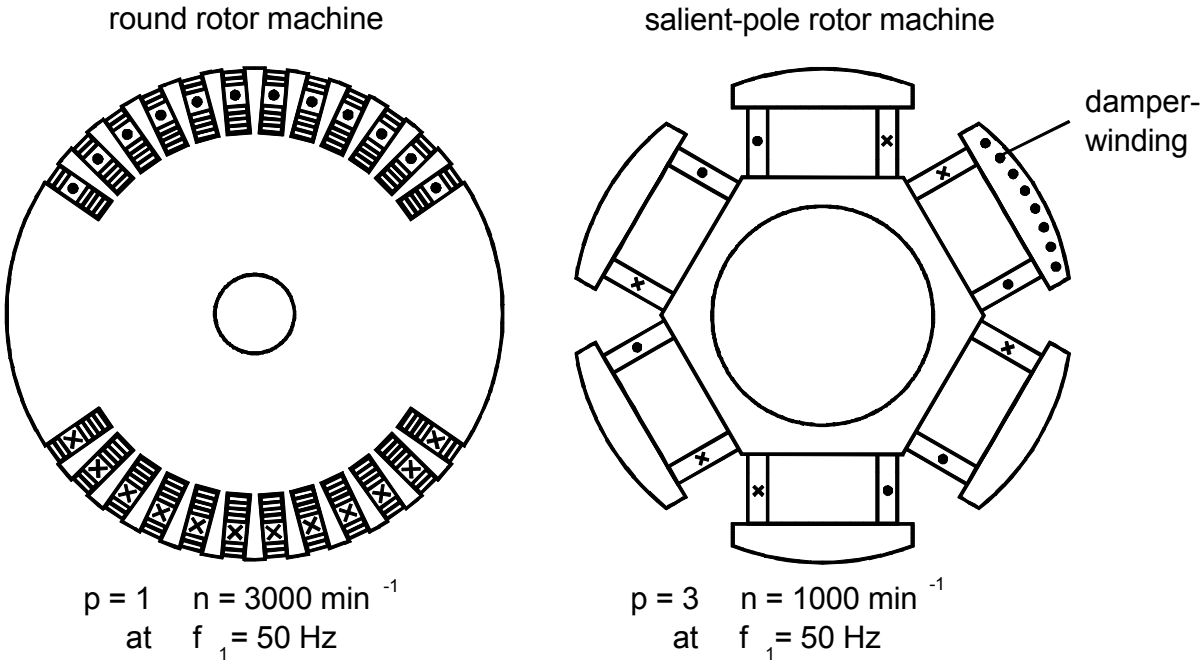

Fig. 212: rotor designs of both machine types: round rotor (left), salient-pole rotor (right)

Two-pole turbo-alternators with round-rotor are used as generator to be driven by gas- or steam-turbines and designed for power ranges up to 1800 MVA per unit. In order to accommodate with high centrifugal stress, the (stretched) rotor is modelled as solid steel cylinder, which is slotted only at 2/3 of the total circumference. End turns of the concentric exciter windings are held on their position with non-magnetic caps. Stator and rotor in machines designed for high power applications are directly cooled with water or hydrogen. Current supply is realized slip-ring-less as stationary field exciter machine with revolving rectifiers. Damper windings are implemented as conductive slot-cotters and pole-caps.

Salient-pole rotor synchronous machines with distinctive single poles are either utilized for generators at low speed such as water turbine applications or as low-speed motor in the field of material handling and conveying. A power range up to 800 MVA per unit is achieved with this type of rotors; a number of pole-pairs up to p=30 is usual. The latter leads to wide armature diameters and short iron lengths. Exciter windings are arranged on solid poles similar to typical DC machine arrangements. Damper windings appear as pole-grids.

8.3 Equivalent circuit diagram, phasor diagram

Based on the equivalent circuit diagram of induction machines with slip-ring rotors an direction assignment due to EZS is chosen for the stator, since synchronous machines are mainly used as generator. Simply the direction of the voltage phasor U_1 is reversed. Using voltage U_2^*/s on the secondary side, supply with DC current is regarded.

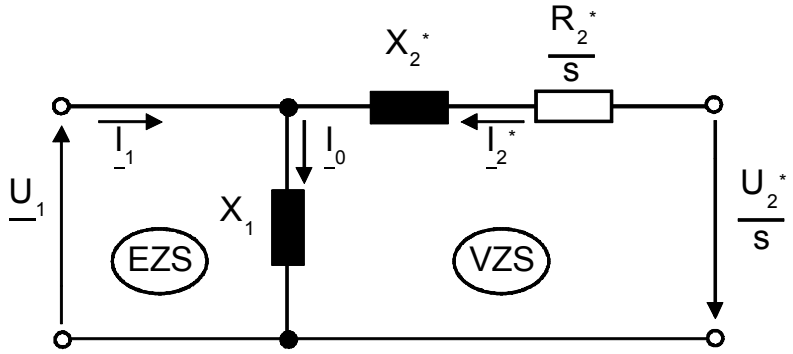

Fig. 213: ecd based on induction machine

The following voltage equations derive from Fig. 212::

$$\underline{U}_1 + j \cdot X_1 \cdot \left(\underline{I}_1 + \underline{I}_2^* \right) = 0 \tag{8.3}$$

$$\frac{\underline{U}_2^*}{s} = \underline{I}_2^* \cdot \left(\frac{R_2^*}{s} + j \cdot X_2^* \right) + j \cdot X_1 \left(\underline{I}_1 + \underline{I}_2^* \right) \tag{8.4}$$

Since a division by $s = 0$ must not be performed, the rotor voltage equation needs to be multiplied by s and reformed:

$$\underline{U}_1 + j \cdot X_1 \cdot \underline{I}_1 = -j \cdot X_1 \cdot \underline{I}_2^* \tag{8.5}$$

$$\underline{U}_2^* = \underline{I}_2^* \cdot R_2^* + s \cdot j \cdot X_2^* \cdot \underline{I}_2^* + s \cdot j \cdot X_1 \left(\underline{I}_1 + \underline{I}_2^* \right) \tag{8.6}$$

Synchronous generated internal voltage is due to EZS defined as:

$$\underline{U}_p = -j \cdot X_1 \cdot \underline{I}_2^* \tag{8.7}$$

regarding $s = 0$ leads to:

$$\underline{U}_1 + j \cdot X_1 \cdot \underline{I}_1 = \underline{U}_p \tag{8.8}$$

$$\underline{U}_2^* = \underline{I}_2^* \cdot R_2^* \tag{8.9}$$

I_2^* complies with the exciter current I_F, being converted to a stator side measure. An arbitrary current I_2 of line frequency flowing in stator windings would cause exactly the same air gap field as a DC current I_F in revolving rotor windings. The rotor voltage equation is trivial and therefore not subject of further discussions, so that the stator voltage equation needs to be regarded. Feedback of the revolving rotor (also known as magnet wheel) on the stator is contained in the synchronous generated internal voltage U_p.

Synchronous generated internal voltage U_P can be directly measured as induced voltage at the machine terminals with excitation I_F in no-load with $I_1 = 0$ at synchronous speed $n = n_1$. The typical no-load characteristic $U_P = f(I_F)$ shows non-linear behavior, caused by saturation effects, which are not taken into account at this point.

Since only one voltage equation is used in the following, formerly used indices may be dropped. Copper losses in stator windings can be neglected for synchronous machines, which leads to $R_1 = 0$. The general equivalent circuit diagram for synchronous machines as shown in Fig. 214 enables the description of its operational behavior completely.

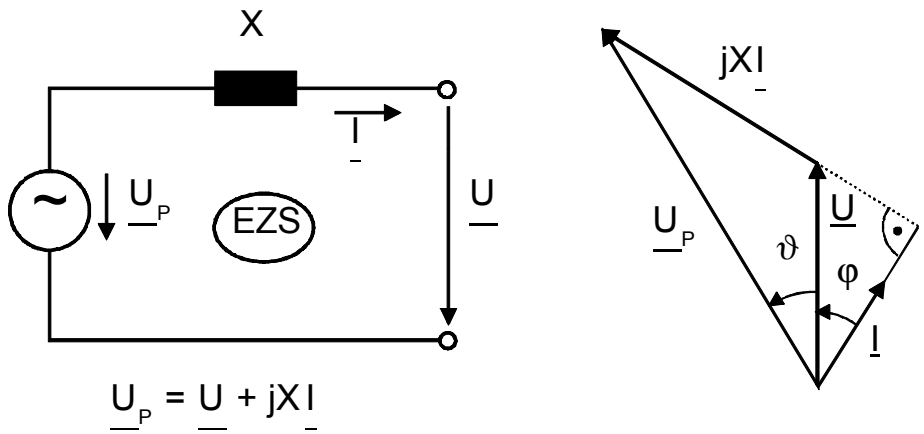

Fig. 214: synchronous machine, simplified ecd, phasor diagram

In order to represent particular operation conditions or ranges, the according phasor diagram can be determined based on the voltage equation. Figure 214 illustrates such a phasor diagram for generator operation with active power and inductive reactive power output, using a notation defining:

- φ as phase angle between current and voltage.
- ϑ as rotor displacement angle, describing the phase relation of the synchronous generated internal voltage U_P towards the terminal voltage U. It corresponds with the position of the magnet wheel in relation to the resulting air-gap field. The rotor displacement angle is ϑ positive in generator mode and negative for motor operation. Hence follows ϑ = 0 for no-load or mere reactive load.
- $y = J + j$ as load angle. Exciter magnetomotive force is
  - $\frac{p}{2} + y$ ahead of armature magnetomotive force in generator mode,
  - $\frac{p}{2} - y$ behind of armature magnetomotive force in motor operation.

8.4 No-load, sustained short circuit

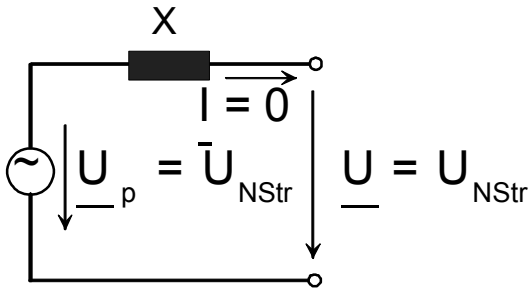

Fig. 215: SYM, ecd for no-load

Nominal voltage U_N (shown as U_{NStr} in Fig. 215) can be measured at the terminals in no-load operation ($I=0$) at synchronous speed n_1 if no-load exciter current I_{F0} applies.

$$U_P = U_{NStr} \quad \text{for} \quad I_F = I_{F0} \quad \text{and} \quad n = n_1$$

with:

$$U_{NStr} = \frac{U_N}{\sqrt{3}} \tag{8.10}$$

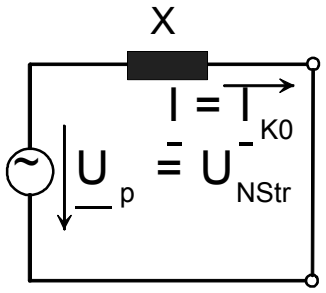

Fig. 216: SYM, sustained short circuit

Are synchronous machines short-circuited at no-load exciter current I_{F0} and synchronous speed n_1, a sustained short-circuit current I_{K0} flows after dynamic initial response.

$$I = I_{K0} = \frac{U_{NStr}}{X} \quad \text{for} \quad I_F = I_{F0} \quad \text{and} \quad n = n_1 \tag{8.11}$$

An important means to describe synchronous machines is the *no-load-short-circuit-ratio* K_C:

$$K_C = \frac{I_{K0}}{I_N} = \frac{U_{NStr}}{XI_N} = \frac{1}{x} \tag{8.12}$$

K_C is defined as the reciprocal of the reactance X, being refered onto the nominal impedance.

The value of K_C can either be measured at sustained short-circuit with no-load excitation or at nominal voltage supply U_N and no-load speed n_1, unexcited rotor assumed. Sustained short-circuit current I_{K0} occurs for both cases.

Latter case is illustrated in Fig. 217:

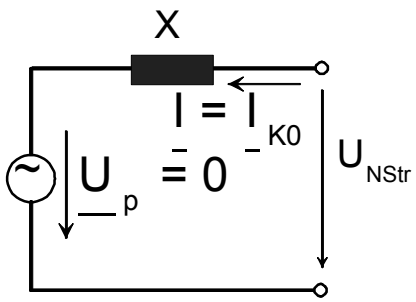

Fig. 217: SYM, unexcited rotor

$$U = U_{Nstr}\,,\ n = n_1\,,\ I_F = 0$$

$$I = \frac{U_{NStr}}{X} = I_{K0} \tag{8.13}$$

$$K_C = \frac{I_{K0}}{I_N} \tag{8.14}$$

Sustained short-circuit current I_{K0} in synchronous machines corresponds with the no-load current I_0 in induction machines.

Whereas induction machines fetch required reactive power for according magnetization from the mains, the air-gap of synchronous machines can be chosen wider, since magnetization is achieved by DC excitation of the rotor. This leads to reduced armature reaction of the reactance *X* and the overload capability – the ratio of breakdown torque and nominal torque – increases.

$$\frac{I_{K0}}{I_N} = K_C = \frac{1}{x} = \begin{cases} 0{,}4 \ldots 0{,}7 & \text{for turbo generators} \\ 0.8 \cdots 1{,}5 & \text{for salient - pole generators} \end{cases} \tag{8.15}$$

$$\frac{I_0}{I_N} = \frac{1}{x} = 0{,}2 \ldots 0{,}5 \quad \text{for induction machines} \tag{8.16}$$

8.5 Solitary operation

8.5.1 Load characteristics

Synchronous machines in solitary operatation are used for e.g. wind farms or hydro-electric power plants. This case is defined as the mode of operation of separately driven synchronous machines in single operation loaded with impedances working

Terminal voltage depends on amount and phase angle of the load current, constant excitation assumed.

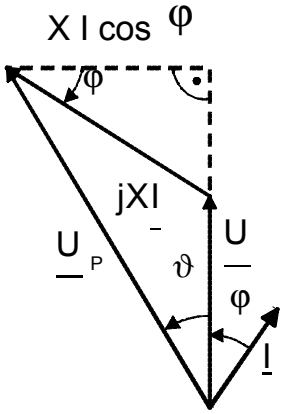

Fig. 218: SYM, phasor diagram

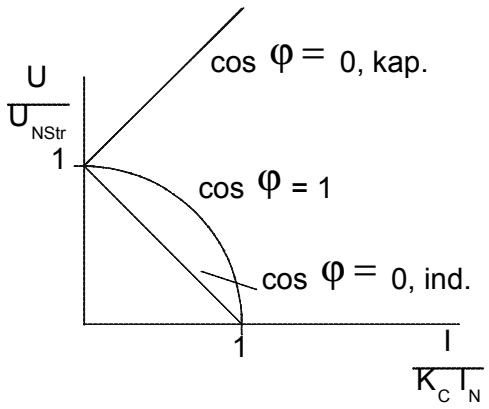

Fig. 219: SYM, load characteristics

Phasor diagram (Fig. 218) provides:

$$\left(U + XI \sin j\right)^2 + \left(XI \cos j\right)^2 = U_p^2 \tag{8.17}$$

In no-load excitation $I_F = I_{F0}$ at synchronous speed $n = n_1$ applies $U_p = U_{NStr}$.

$$U^2 + 2UXI \sin j + \left(XI\right)^2 = U_{NSTr}^2 \tag{8.18}$$

$$\left(\frac{U}{U_{NStr}}\right)^2 + 2\frac{U}{U_{NStr}}\frac{XI}{U_{NStr}}\sin j + \left(\frac{XI}{U_{NStr}}\right)^2 = 1 \tag{8.19}$$

$$\left(\frac{U}{U_{NStr}}\right)^2 + 2\frac{U}{U_{NStr}}\frac{I}{K_C I_N}\sin j + \left(\frac{I}{K_C I_N}\right)^2 = 1 \tag{8.20}$$

These dependencies are called *load characteristics.*

$$U = f\left(I\right) \text{ für } I_F = I_{F0} \text{ und } n = n_1 \tag{8.21}$$

Similar to transformer behavior, terminal voltage decreases with increasing inductive-ohmic load, whereas it increases at capacitive load.

8.5.2 Regulation characteristics

In order to provide constant terminal voltage, the exciter current needs to be adjusted according to amount and phase angle of the load current.

Based on the phasor diagram, with $U = U_{NStr}$, $n = n_1$ ensues

$$U_P^2 = U_{NStr}^2 + 2U_{NStr} XI \sin j + (XI)^2 \tag{8.22}$$

so that follows:

$$\frac{U_P}{U_{NStr}} = \frac{I_F}{I_{F0}} = \frac{\sqrt{U_{NStr}^2 + 2U_{NStr} XI \sin j + (XI)^2}}{U_{NStr}} = \sqrt{1 + 2\sin j \frac{I}{K_C I_N} + \left(\frac{I}{K_C I_N}\right)^2} \tag{8.23}$$

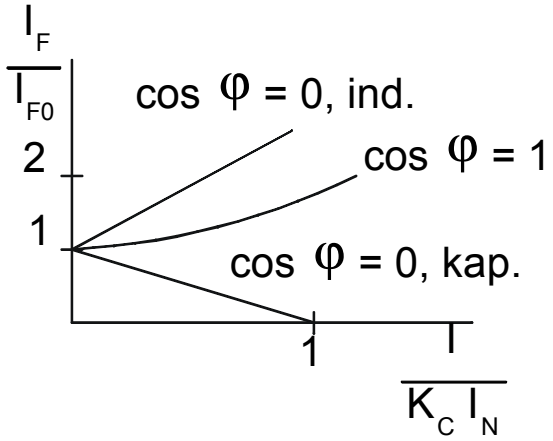

Fig. 220: SYM, regulation characteristics

These are called „*regulation characteristics*“

$$I_F = f(I) \tag{8.24}$$

for

$$U = U_{NStr} \text{ and } n = n_1$$

It is to be seen, that excitation needs to be increased for inductive-ohmic load, since voltage would drop. Excitation needs to be decreased for capacitive load, caused by occuring voltage gain.

This dependency of exciter current on load current and load angle also applies for constant voltage network supply, since $U = U_{NStr}$.

8.6 Rigid network operation

8.6.1 Parallel connection to network

Rigid networks mean constant-voltage constant-frequency systems. Synchronous machines can require synchronization conditions to be fulfilled to be connected to networks of constant voltage and constant frequency.

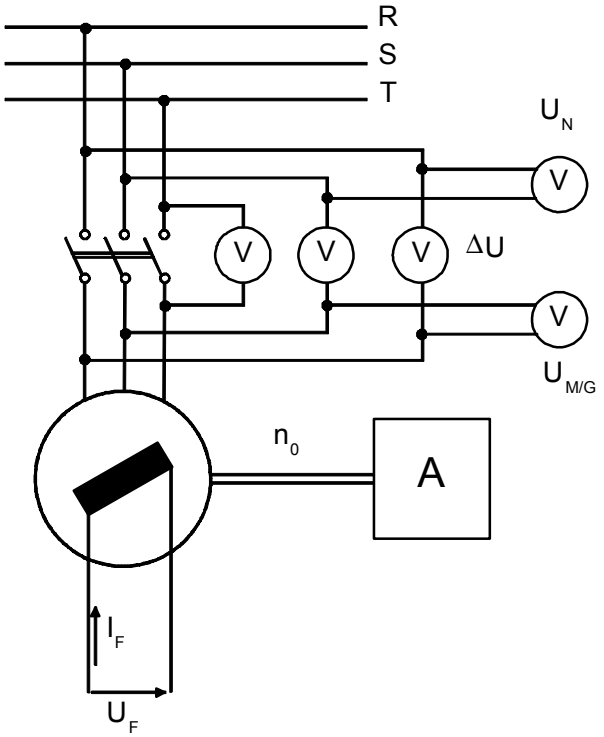

Fig. 221: SYM, rigid network operation

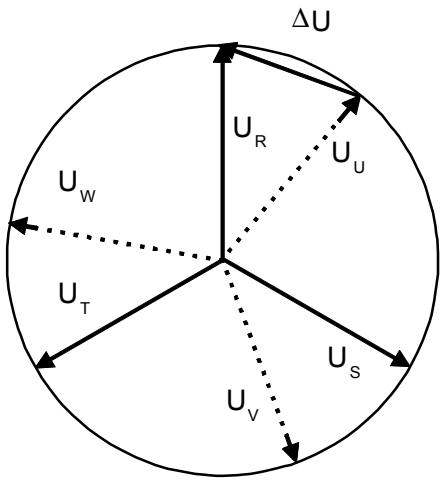

Fig. 222: synchronization conditions

1. Synchronous machine needs to be driven at synchronous speed: $n = n_1$

2. Exciter current I_F of the synchronous machine needs to be set in the way that generator voltage is equal to the mains voltage: $U_M = U_N$.

3. Phase sequence of terminal voltages of generator and network need to match: *RST* - *UVW*

4. Phase angle of both voltage systems generator and network need to be identical, which means a disappearance of voltage difference at terminals being connected: $\Delta U = 0$.

If synchronization conditions are not fulfilled, connection of the unsynchronized synchronous machine to the mains results in torque pulsations and current peaks.

8.6.2 Torque

Effective torque exerted on the shaft derives from transmitted air-gap power divided by synchronous speed. Neglecting stator copper losses, the absorbed active power is equal to the air-gap power.

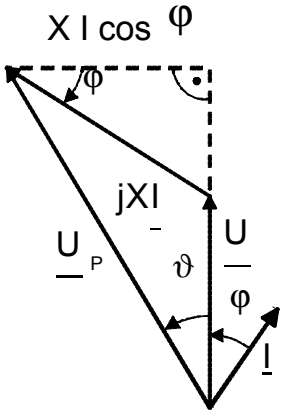

Fig. 223: SYM, phasor diagram

$$M = \frac{P_D}{\Omega_1} = \frac{3 \cdot U \cdot I \cdot \cos j}{\frac{w_1}{p}} \tag{8.25}$$

as given in the phasor diagram:

$$X \cdot I \cdot \cos j = U_p \cdot \sin J \tag{8.26}$$

$$I \cdot \cos j = \frac{U_p}{X} \sin J \tag{8.27}$$

Then follows for the applicable torque on the shaft:

$$M = \frac{3 \cdot p}{w} \cdot \frac{U \cdot U_p}{X} \sin J = M_{kipp} \cdot \sin J \tag{8.28}$$

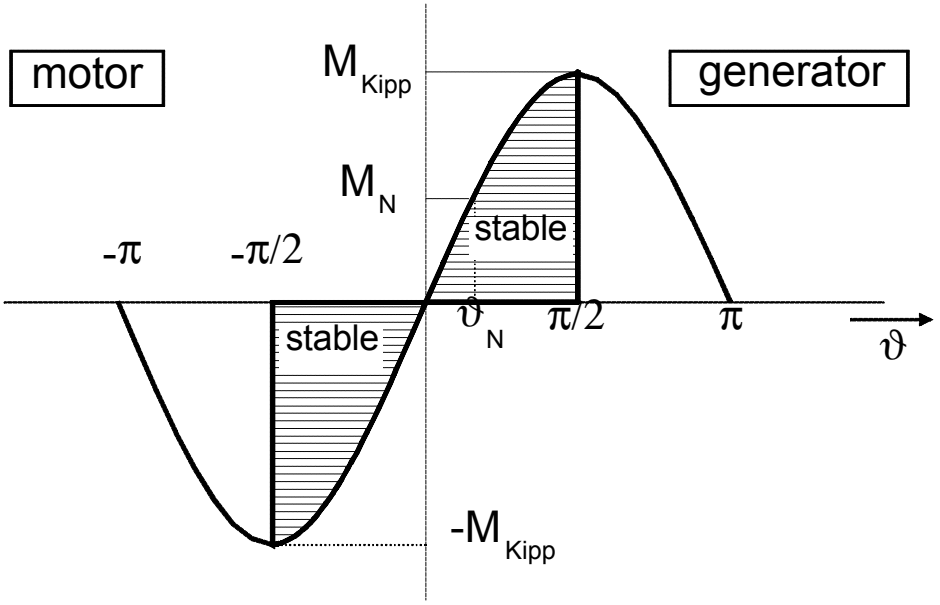

Fig. 224: SYM, range of operation

The torque equation (8.28) solely applies for stationary operation with $I_F = \text{const}$ and $n = n_1$.

If the load increases slowly, torque and angular displacement increases also, until breakdown torque is reached at $J = \pm\frac{p}{2}$ and the machine falls out of step – means standstill in motor operation and running away in generator mode. High pulsating torques and current peaks occur as a consequence of this. In this case machines need to be disconnected from the mains immediately.

Overload capability, the ratio of breakdown torque and nominal torque, only depends on no-load-short-circuit-ratio K_C and power factor.
Die Überlastfähigkeit, das Verhältnis Kippmoment zu Nennmoment, hängt nur vom Leerlauf-Kurzschlußverhältnis und dem Leistungsfaktor ab. Nominal operation features:

$$\frac{M_{kipp}}{M_N} = \frac{\frac{3p}{w_1}\frac{U_{NStr}U_P}{X}}{\frac{3p}{w_1}U_{NStr}I_N\cos j_N} = \frac{U_P}{U_{NStr}}\frac{K_C}{\cos j_N}, \tag{8.29}$$

with synchronous generated voltage dependency:

$$\frac{U_P}{U_{NStr}} = \sqrt{1+\frac{2\sin j_N}{K_C}+\frac{1}{K_C^2}} \tag{8.30}$$

Then follows for the overload capability of synchronous machines:

$$\frac{M_{Kipp}}{M_N} = \frac{1}{\cos j_N}\sqrt{K_C^2+2K_C\sin j_N+1}\,. \tag{8.31}$$

The higher K_C or the lower X, the higher ensues the overload capability.

A ratio of at least $\frac{M_{Kipp}}{M_N} > 1{,}6$ is reasonable for stabile operation. A measure for stability in stationary operation is the synchronizing torque:

$$M_{syn} = \frac{\mathrm{d}M}{\mathrm{d}J} = M_{Kipp}\cos J \geq 0 \tag{8.32}$$

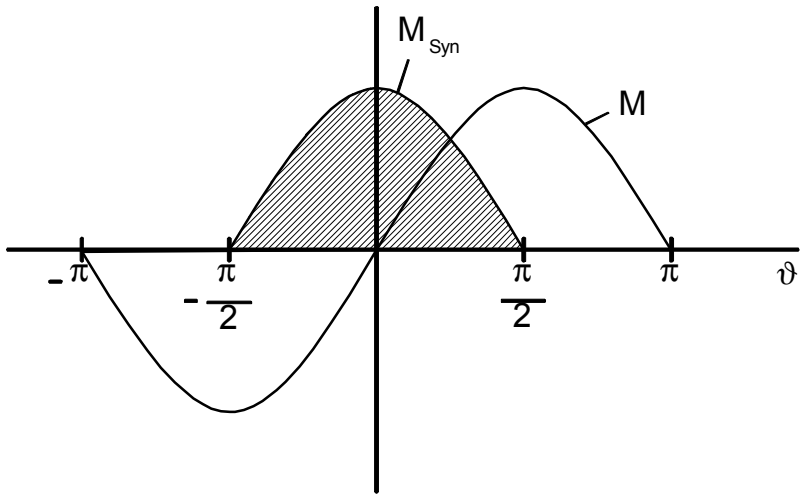

Fig. 225: SYM, synchronizing torque

The higher $\frac{\mathrm{d}M}{\mathrm{d}J}$, the higher appears the back-leading torque M_{syn} after load impulse. The lower ϑ, the more stabile the point of operation.

8.6.3 Operating ranges

Synchronous machines in rigid network operation can be driven in any of the 4 quadrants. The according mode of operation is characterized by the corrsponding phase angle of the stator current, if terminal voltage is assumed to be placed on the real axis.

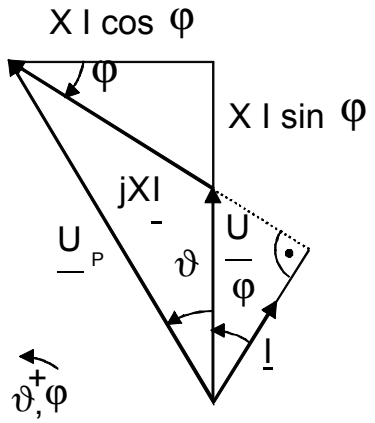

Fig. 226: SYM, phasor diagram

Phasor diagram (Fig. 226) offers a stator diagram, to be split into components:

- active current: $I \cdot \cos j = \frac{U_p}{X} \cdot \sin J$ (8.33)
- reactive current: $I \cdot \sin j = \frac{U_p \cdot \cos J - U}{X}$ (8.34)

Four ranges ensue for EZS description, whose characteristical phasor diagrams are shown below:

$I \cdot \cos j > 0 \quad (J > 0)$ active power output (generator)

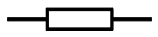

$I \cdot \cos j < 0 \quad (J < 0)$ active power input (motor)

$I \cdot \sin j > 0 \quad (U_p \cdot \cos J > U)$ reactive power output (over excited), machine acts like capacitor

$I \cdot \sin j < 0 \quad (U_p \cdot \cos J < U)$ Reactive power input (under excited), machine works like reactance coil

Fig. 227 a-d: operating ranges and according phasor diagrams

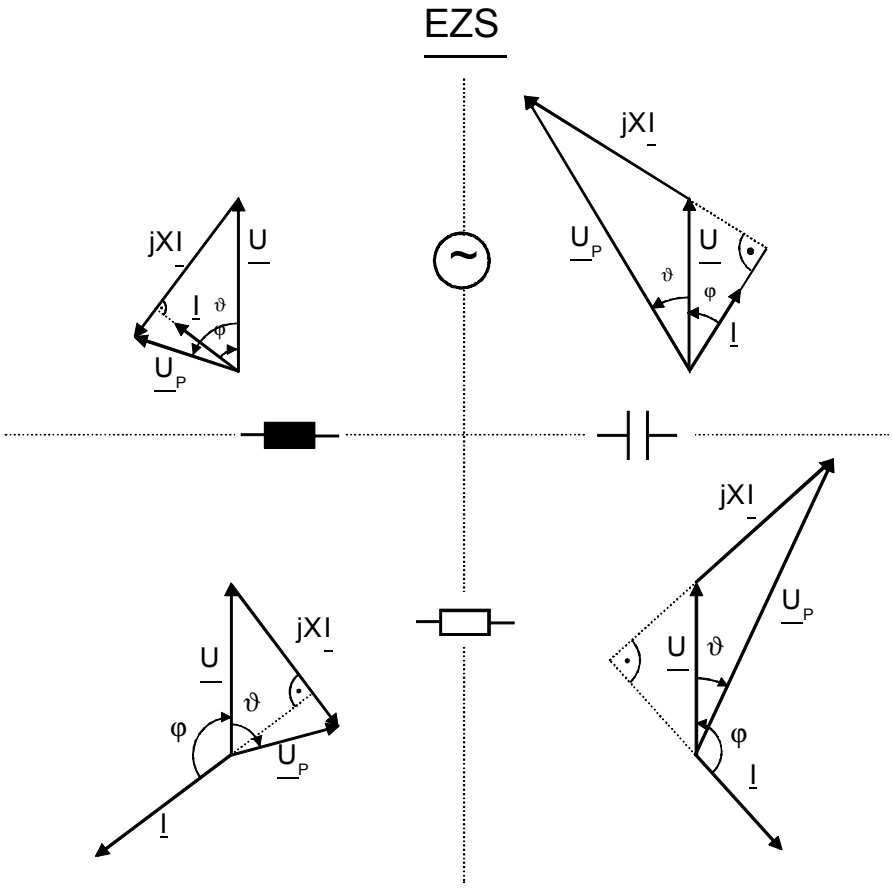

Fig. 228: operating ranges and accordant machine behavior

- Active power proportion is defined by either the driving torque of e.g. turbines in generator mode or by resistance torque of load in motor operation.
- Reactive power is independent from load but solely depending on excitation; as a consequence reactive power output derives from over excitation whereas reactive power input arises from under excitation.
- border case: *synchronous compensator mode*

Synchronous machines are sometimes utilized for mere reactive power generators in synchronous compensator mode for close-by satisfaction of inductive reactive power demands of transformers and induction machines in order to relieve this from supplying networks.

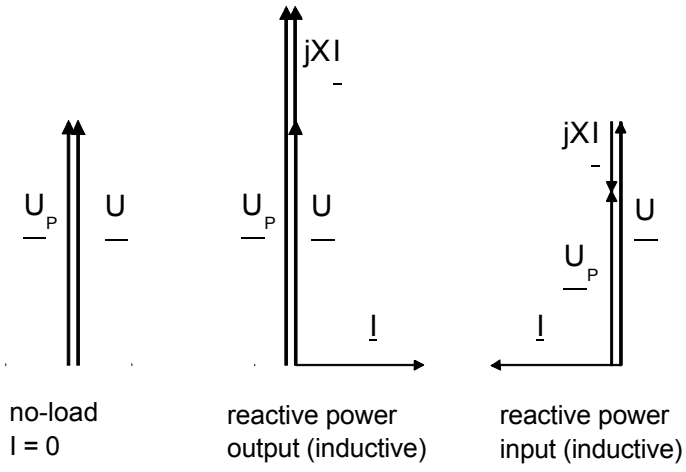

Fig. 229: SYM, phasor diagram of synchronous compensator mode

8.6.4 Current diagram, operating limits

Based on the general voltage equation of synchronous machines:

$$\underline{U}_P = \underline{U} + jX\underline{I} \tag{8.35}$$

ensues with $\underline{U}_P = U_P e^{jJ}$ and $\underline{U} = U_{NStr}$ for current $\underline{I}$:

$$\underline{I} = \frac{U_P e^{jJ} - U_{NStr}}{jX} = j\frac{U_{NStr}}{X} - je^{jJ}\frac{U_P}{X} \tag{8.36}$$

$$\frac{\underline{I}}{I_N} = j\frac{U_{NStr}}{I_N X} - je^{jJ}\frac{U_P}{U_{NStr}}\frac{U_{NStr}}{I_N X} \tag{8.37}$$

and with $K_C = \frac{U_{NStr}}{XI_N}$ as well as $\frac{U_P}{U_{NStr}} = \frac{I_F}{I_{F0}}$ follows:

$$\frac{\underline{I}}{I_N} = jK_C - je^{jJ}K_C\frac{I_F}{I_{F0}} \tag{8.38}$$

With knowledge of equation 8.38 the current diagram of synchronous machines can be established. No-load-short-circuit-ratio K_C is contained as the only effective parameter. Operating limits within the accordant machine can be driven are also marked.

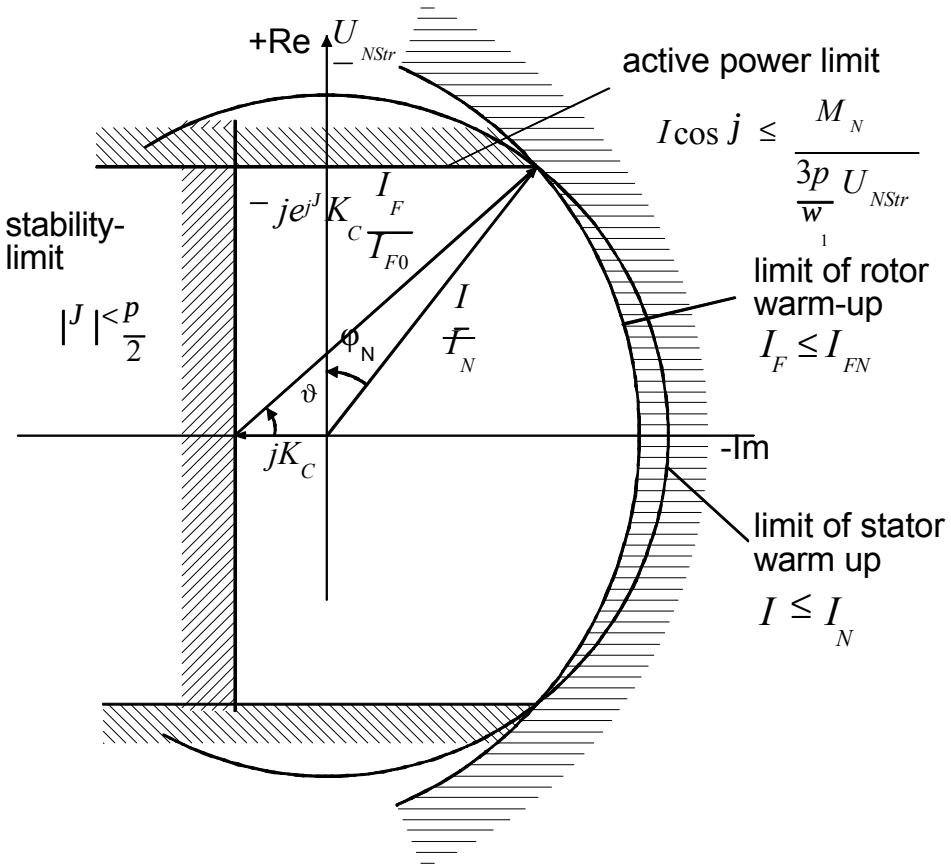

Fig. 230: SYM, current diagram, operating limits

8.7 Synchronous machine as oscillating system, damper windings

8.7.1 without damper windings

Torque balance applies: driving torque M_A minus shaft torque M_W is equal to acceleration torque M_B:

$$M_A - M_W = M_B \tag{8.39}$$

Driving torque M_A of the turbine equals acting torque in stationary operation:

$$M_A = M_{Kipp} \sin J_N \tag{8.40}$$

$$M_{Kipp} = \frac{3p}{w_1} \frac{U_{NStr} U_P}{X} \tag{8.41}$$

Shaft torque M_W of synchronous machines computes from:

$$M_W = M_{Kipp} \sin J \tag{8.42}$$

Acceleration torque M_B ensues to:

$$M_B = J \frac{\mathrm{d}\Omega}{\mathrm{d}t} \tag{8.43}$$

with J representing masss moment of inertia of all rotating masses, and the machine to be driven at nominal speed.

$$\Omega = 2pn_1 + \frac{\mathrm{d}J \diagup p}{\mathrm{d}t} \tag{8.44}$$

Thus the following differential equation can be established:

$$M_{Kipp} \sin J_N - M_{Kipp} \sin J = J \frac{\mathrm{d}\Omega}{\mathrm{d}t} = \frac{J}{p} \frac{\mathrm{d}^2 J}{\mathrm{d}t^2} \tag{8.45}$$

The electrical angle ϑ may slightly vary in the proximity of the operating point:

$$J = J_N + \Delta J \tag{8.46}$$

Then follows:

$$\frac{\mathrm{d}J}{\mathrm{d}t} = \frac{\mathrm{d}\Delta J}{\mathrm{d}t} \text{ and } \frac{\mathrm{d}^2 J}{\mathrm{d}t^2} = \frac{\mathrm{d}^2 \Delta J}{\mathrm{d}t^2}. \tag{8.47}$$

The differential equation is linearized by Taylor development with abort after the first step:

$$f(x+h) = f(x) + \frac{f'(x)}{1!}h + \ldots \tag{8.48}$$

$$\sin J = \sin\left(J_N + \Delta J\right) = \sin J_N + \Delta J \cos J_N \tag{8.49}$$

That dodge and the differential equation as such leads to:

$$M_{Kipp} \sin J_N - M_{Kipp}\left(\sin J_N + \Delta J \cos J_N\right) = \frac{J}{p}\frac{\mathrm{d}^2 \Delta J}{\mathrm{d}t^2} \tag{8.50}$$

$$\frac{J}{p}\frac{d^2 \Delta J}{dt^2} + M_{Kipp} \cos J_N \Delta J = 0 \tag{8.51}$$

Synchronizing torque for the operating point is defined as:

$$M_{Kipp} \cos J_N = M_{SyncN} \tag{8.52}$$

so that:

$$\frac{d^2 \Delta J}{dt^2} + \frac{M_{syncN}}{J/p} \Delta J = 0 \tag{8.53}$$

Solution for the differential equation is provided by a harmonic, undamped oscillation:

$$\Delta J = \sin \Omega_{eN} t \tag{8.54}$$

with mechanical natural frequency:

$$\Omega_{eN} = 2pf_{eN} = \sqrt{\frac{M_{SyncN}}{J/p}} \hat{=} \sqrt{\frac{c}{m}} \tag{8.55}$$

Synchronizing torque complies with spring stiffness, the reduced mass moment of inertia of the rotating mass. The frequency of the mechanical oscillation approximately amounts in the range of f_{eN} = 1 ... 2 Hz.

Pulsating oscillations may occur, caused by electric or mechanic load changes, to come along with current fluctuations. Two or more generators may activate each other in network interconnection. Machines with irregular torque in particular, such as diesel engines or reciprocating compressors may initiate oscillations with pulsations up to severe values, if activation is close to natural frequency.

8.7.2 with damper winding

In order to damp natural oscillations, all synchronous machines are equipped with damper windings in any case. The effect of damper windings is similar to the effect of the squirrel cage in induction machines.

Salient-pole machines: bars are placed in slotted poles, to be short circuited with short-circuit rings at their ends. If those short-circuit rings merely consist of segments of a circle the arrangemnet is called *pole damping grid* estehen die Ringe nur aus Kreissegmenten, so spricht man von einem Polgitter. Solid poles also act damping.

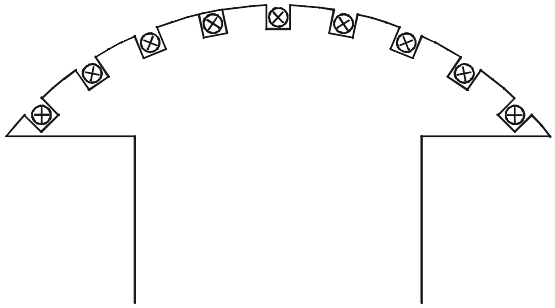

Fig. 231: SYM, damper windings

Turbo generators: damper bars are placed ahead of exciter windings inside rotor slots to be short-circuited at their ends. Also slot wedges can be utilized as damper bars. Solid rotors amplify the damping effect.

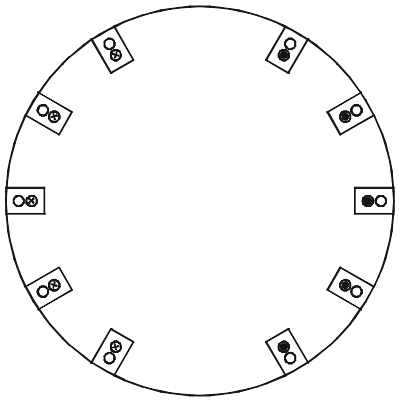

Fig. 232: SYM, damper windings

The effect of damper windings derives from the Kloß-Equation:

$$\frac{M_D}{M_{kippAsyn}} = \frac{-2}{\frac{s}{s_{kipp}} + \frac{s_{kipp}}{s}} \tag{8.56}$$

$$M_{kippAsyn} = \frac{3p}{w_1}\frac{U_1^2}{2X_2^*} \tag{8.57}$$

$$s_{kipp} = \frac{R_2^*}{X_2^*} \tag{8.58}$$

Damping torque shows a braking effect – therefore signed negative.
Close to synchronous speed the slip ratio applies as:

$$\frac{s}{s_{kipp}} << \frac{s_{kipp}}{s} \tag{8.59}$$

so that the damping torque component ensues to:

$$M_D = -M_{kippAsyn}\frac{2s}{s_{kipp}}. \tag{8.60}$$

Slip is to be described as:

$$s = \frac{\Omega_1 - \Omega}{\Omega_1} = \frac{\Omega_1 - \left(\Omega_1 + \frac{\mathrm{d}J/p}{\mathrm{d}t} \right)}{\Omega_1} = \frac{-1}{p\Omega_1} \frac{\mathrm{d}J}{\mathrm{d}t} = \frac{-1}{p\Omega_N} \frac{\mathrm{d}\Delta J}{\mathrm{d}t} \tag{8.61}$$

Then follows for the damping torque component M_D:

$$M_D = \frac{2M_{kippAsyn}}{s_{kipp} p\Omega_1} \frac{\mathrm{d}\Delta J}{\mathrm{d}t} = D \frac{\mathrm{d}\Delta J}{\mathrm{d}t}, \tag{8.62}$$

inserted in the differential equation results in:

$$\frac{J}{p} \frac{\mathrm{d}^2 \Delta J}{\mathrm{d}t^2} + D \frac{\mathrm{d}\Delta J}{\mathrm{d}t} + M_{synN} \Delta J = 0 \tag{8.63}$$

Solution of the differential equations appears as damped oscillation:

$$\Delta J = e^{-t/T_D} \sin \Omega_e t \tag{8.64}$$

with mechanical natural frequency:

$$\Omega_e = \sqrt{\Omega_{eN}^2 - \frac{1}{T_D^2}} \tag{8.65}$$

of damping:

$$D = \frac{2M_{kippAsyn}}{s_{kipp} p\Omega_1} = \frac{2 \frac{3p}{w_1} \frac{U_1^2}{2X_2^*}}{\frac{R_2^*}{X_2^*} w_1} = \frac{3p}{w_1^2} \frac{U_1^2}{R_2^*} \tag{8.66}$$

and time constant:

$$T_D = \frac{2J}{pD} \sim R_2^* \tag{8.67}$$

In order to show significant effect of damper windings and to rapidly reduce activated oscillations by load changes, T_D needs to be chosen as short as possible, whereas D needs to be as high as possible. Thus follows R_2^* needs to be low, resulting in increased copper expense for the damper windings.

Besides oscillation damping caused by load impulses, damper windings show two additional important functions:

1. Negative-sequence rotating fields with a slip value of (2 - *s*) arise from unbalanced load. Computation requires the method of symmetrical components (see chapter 2.6). Occuring harmonics in stator voltage and current cause additional iron- and ohmic losses. With presence of suitable damper windings, the inverse-field is compensated by counteracting magnetomotive force of damper currents.

2. Adequate thermal capacity assumed, synchronous machines are capable to independently start-up using the damper cage similar to induction machines with squirrel cage. Since the stator rotating field would induce high-voltages in (open) exciter windings during start-up, the exciter windings are temorary short-circuited. Exciter voltage will not be applied on the windings until no-load speed is reached – at this point, the machine is jerkily pulled into synchronism. This coarse synchronizing is accompanied by torque pulsations and current pulses and is therefore solely utilized for low-power applications.

8.8 Permanent-field synchronous machines

If electrical excitation for synchronous machines is replaced by permanent-field excitation, exciter voltage source, exciter winding and exciter current supply by collector ring and brushes are unnecessary, but exciting field can not be controlled any longer. These machines are used for low power applications in two different types:

8.8.1 Permanent excited synchronous motor with starting cage

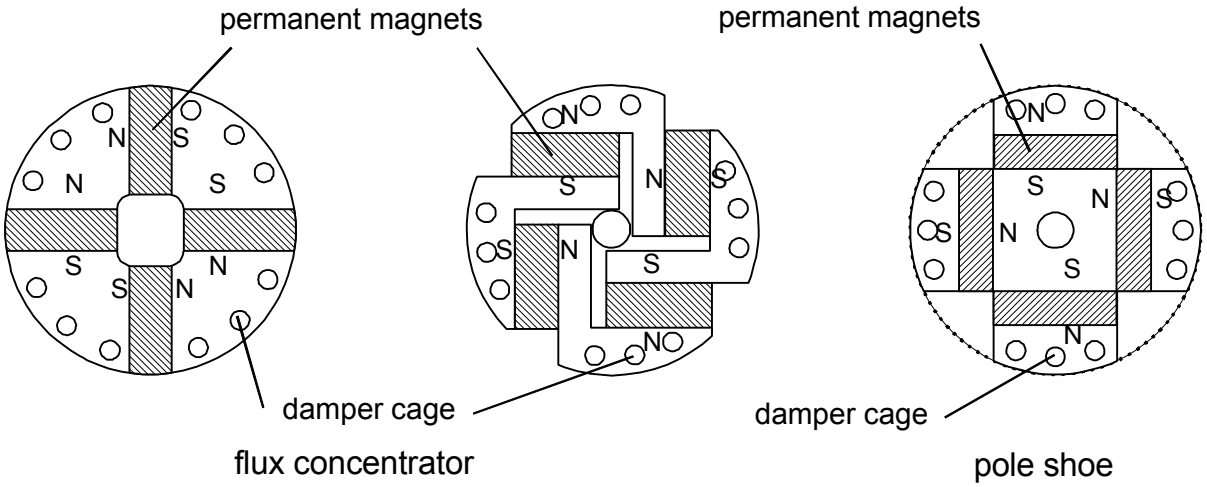

Fig. 233: Permanent excited synchronous motor (PESM), "line start motor"

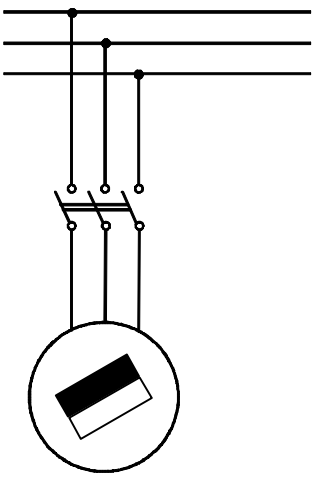

Fig. 234: PESM, ecd

Different types of rotors are shown in the picture. Rotor consists of permanent magnet excitation as well as of a starting cage. Stator has a usual three-phase winding. In principle line start motor is a combination of induction and synchronous machine.

The motor is supplied directly by system voltage. Acceleration corresponds to induction motor. Near synchronous speed motor is pulling into synchronism. After that the motor works as a synchronous machine at power mains.

- advantages: self-starting, improved $\cos(j)$, high efficiency
- disadvantages: better utilization, because of the combination of two types of machines
- applications: drives with long term operation (pumps, ventilators, compressors)

8.8.2 Permanent-field synchronous motor with pole position sensor

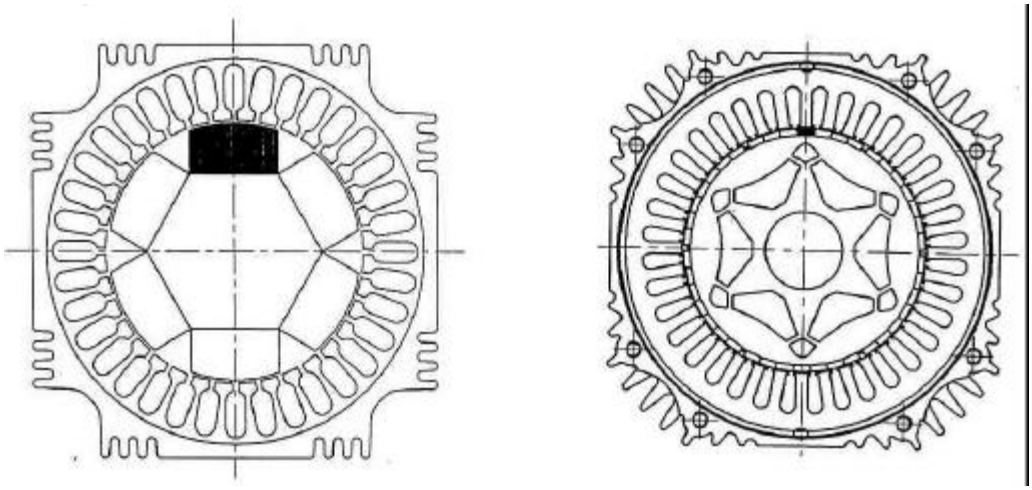

Fig. 235 a, b: perm.-field synchronous motor with pole position sensor, “servo motor”

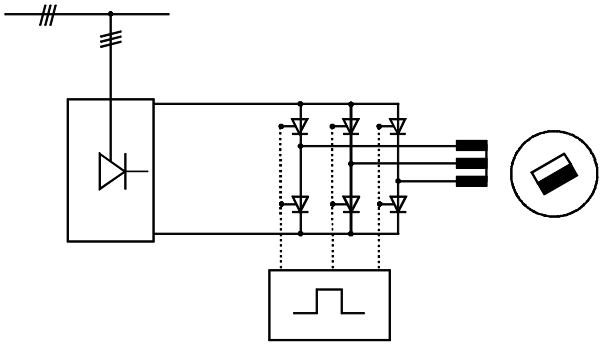

Stator consists of usual three-phase winding. Rotor is permanent-field excited by rare-earth or ferrite magnets. The converter is controlled by a pole position sensor to be placed on the shaft.

Fig. 236: servo motor with converter

method of operation:
Three-phase winding of the stator is supplied by a sinusoidal or block format three-phase system depending on pole position. This results in a rotating magnetomotive force which exactly rotates at rotor speed and creates a time-constant torque together with the permanent magnet excited rotor. Switching of stator three-phase field depends on rotor position in a way that there is a constant electric angle of 90° between stator rotating magnetomotive force and rotor field.

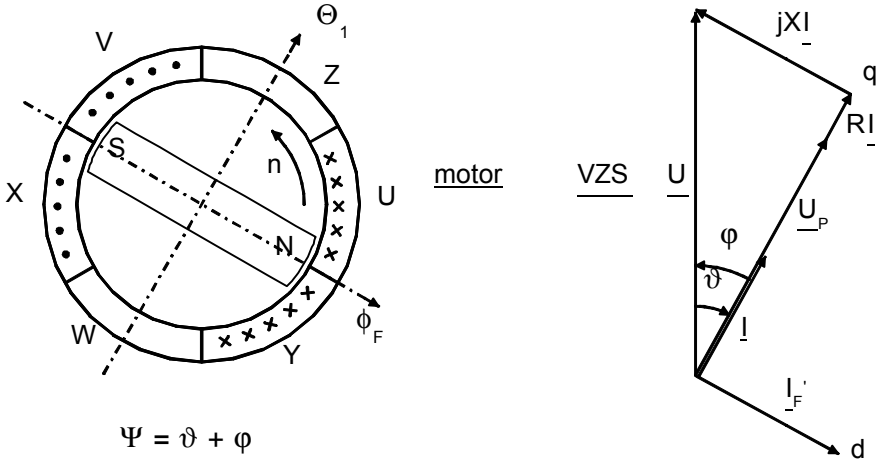

Fig. 237 a, b: servo motor, stator-rotor scheme (a), phasor diagram (b)

Thus results an operating method which does not correspond with usual synchronous machines but exactly with DC machines. Another feature of this machine is armature ampere-turns being shifted about an electric angle of 90° in relation to exciter field. DC machines are adjusted mechanical by commutator. Permanent-field synchronous machines are controlled by power electronics together with a pole position sensor. This machine can not pull out of step any longer and works like a DC machine. From that results the name “electrical commutated DC machine”.

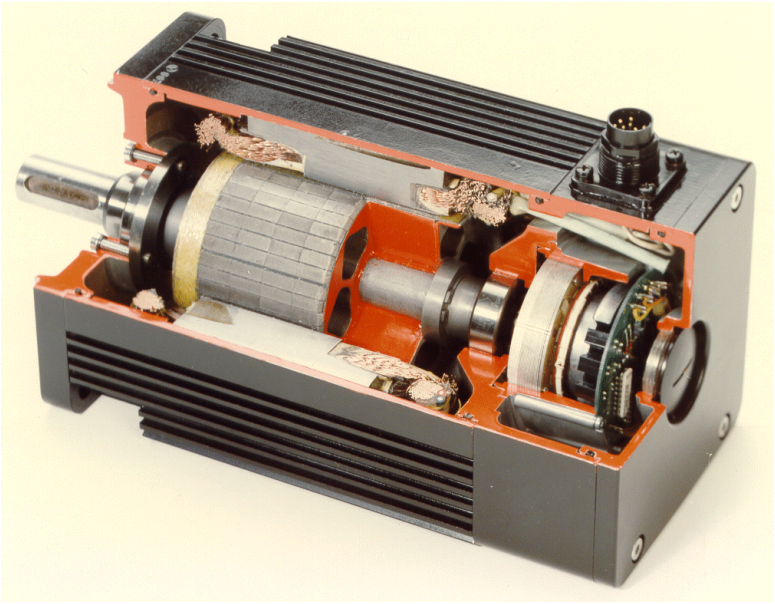

Fig. 238: EC motor (3 kW, manufacturer: Bosch)

EC motors are usually used in robotic drives and machine tools because of their good dynamic performance and easy controllability. The brushless technology is free of wear and maintenance-free.

If the ohmic resistance of stator windings is taken into consideration, the according voltage equitation of the synchronous machine in load reference arrow system (VZS) ensues to:

$$\underline{U} = \underline{U}_p + R \cdot \underline{I} + j \cdot X \cdot \underline{I} \tag{8.68}$$

Torque is:

$$M = \frac{P_D}{\Omega} = \frac{3 \cdot U_p \cdot I}{w / p} \tag{8.69}$$

with the following definitions:

- direct axis *d*: rotor axis $\hat{=} \underline{I}_F'$
- quadrature axis *q*: axis of stator mmf $\hat{=} \underline{I}$

the system is divisible into components:

$$I_q = I \qquad U_q = U_p + R \cdot I \tag{8.70}$$

$$I_d = 0 \qquad U_d = X \cdot I \tag{8.71}$$

Following scaling is useful:

- U_{p0}, synchronous generated voltage at basic speed and nominal excitation,
- X_0, reactance at nominal speed $n_0 = \frac{f_0}{p}$.

Thus torque results in:

$$M = \frac{3 \cdot \frac{n}{n_0} \cdot U_{p0} \cdot I}{\frac{n}{n_0} \cdot \frac{w_0}{p}} = \frac{3 \cdot p}{w_0} \cdot U_{p0} \cdot I \tag{8.72}$$

$\Rightarrow$ Torque controlling by quadrature current component.

Voltage equation of quadrature axis results in:

$$U_q = \frac{n}{n_0} \cdot U_{p0} + R \cdot I \tag{8.73}$$

$$\frac{n}{n_0} = \frac{U_q - R \cdot I}{U_{p0}} \tag{8.74}$$

$$n = 0 \text{ for } I = \frac{U_q}{R} \tag{8.75}$$

$\Rightarrow$ shunt characteristic:

$$n = n_0 \text{ for } U_q = U_{p0} \text{ and } I = 0 \tag{8.76}$$

$\Rightarrow$ speed adjustment by quadrature voltage component: $U_q < U_N$

The direct voltage component computes from:

$$U_d = \frac{n}{n_0} \cdot X_0 \cdot I \tag{8.77}$$

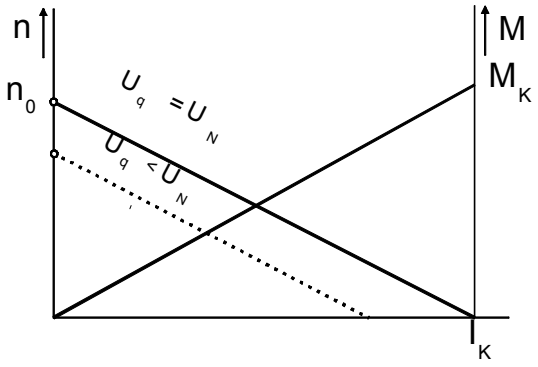

Fig. 239: servo motor, characteristic

Operational bevior similar to separately excited DC machine:

$$U_q \mathrel{\hat{=}} U_A, I \mathrel{\hat{=}} I_A,$$

$$U_{p0} \mathrel{\hat{=}} k \cdot f_n \cdot n_0 \tag{8.78}$$

required in order to match $\underline{I} \perp \underline{I}_F : U_d$.

8.9 Claw pole alternator

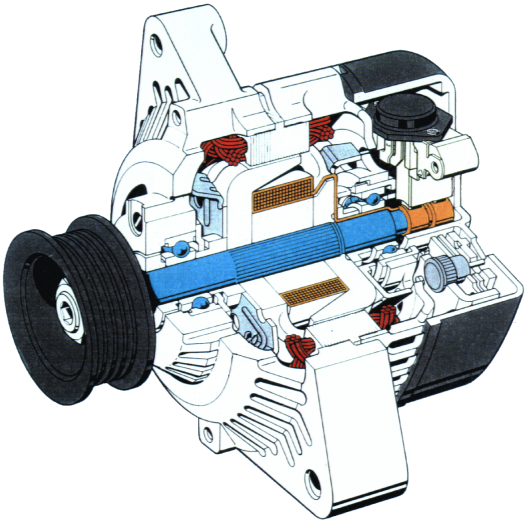

Fig. 240: claw-pole alternator

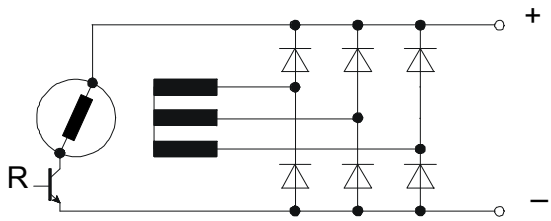

Fig. 241: claw-pole alternator, ecd

Modern claw-pole three-phase alternators consist of a three-phase stator, a claw-pole rotor with ring-form excitation winding, which magnetizes all 6 pole pairs at the same time, as well as a diode bridge and a voltage controller. Flux is really 3-dimensional, in rotor axial and radial, in stator tangential.

Three-phase current that is generated within stator windings is rectified by a diode bridge. Output voltage is kept constant within the whole speed range of 1:10 by controlling of excitation current.

Nominal voltage is 14 V for car applications; 28V is normally used for trucks. Drive is made by V-belt with a mechanical advantage of 1:2 to 1:3. Alternators reach maximum rotational speed up to 18000 min^{-1}. It is mounted directly at the engine and is exposed to high temperatures, to high vibration acceleration and to corrosive mediums.

Within kW range claw-pole alternators are most efficient for cars because of their low excitation copper needs and their economic production process.

Three-phase claw-pole alternators are installed within nearly all cars today. The claw pole alternator principle has totally edged out formerly used DC alternators because it enables much more power at lower weight. It was established when powerful and cheap silicon diodes for rectification could be produced.

Within the last years, power consumption in cars has grown enormously as a result of additional loads for improving comfort and safety and for reducing emissions. Steps to improve power output without needing more space and weight have to be taken.

9 Special machines

In addition to classic electrical machine types, such as DC machine, induction or synchronous machine, new types of electric machines were created in the last few years. Those try to serve the contradictory demands of low weight and high efficiency or are suitable for special drives.

Power electronics and the controlling system enable the machine to have completely new and improved operating characteristics. Because of new geometric arrangements of the torque building components specific loading and flux density combined with specific methods of control higher electric force densities can be achieved.

To this category belong the stepping motor, the switched reluctance motor, the modular permanent –magnet machine and tranverse flux conception.

9.1 Stepping motor

This special type of synchronous machine is mainly used as positioning drives for all kinds of controls or as a switch group for e.g. printers and typewriters in many different ways. The digital control of the stator winding leads to a rotation of the rotor shaft about the step angle a for each current pulse, so that for n control instructions the total angle $n \cdot a$ is covered at the shaft. Stepping motors enable positioning without feedback of the rotor position, which can not be achieved using DC servo drives or three-phase servo drives.

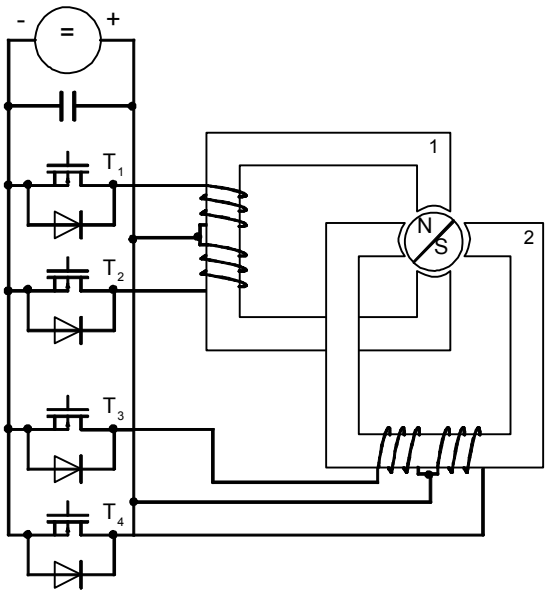

Fig. 242: stepping motor

The basic configuration and the method of operation of stepping motors is shown in Fig. 242. A permanent-magnet rotor (N/S) is arranged between the poles of two independent stator parts (1 and 2). Each of the two stator parts consist of a winding with centre tap that means two halves of the winding. Any half can be supplied with current by the transistors T1 to T4. If, for example, the transistor T1 is switched on, there is a north pole on the top of stator 1 and a south pole at the bottom. If transistor T3 is switched on at the same time north pole is on the right and south pole on the left side of stator 2. That means the rotor turns to the position shown in the Fig. 242.

If now transistor T3 is switched off and shortly after T4 is switched on, the magnetic field in stator 2 reverses. Thus the rotor turns about an angle of 90º in clockwise direction. If then T1 is switched off and T2 on rotor turns round about another 90º. A continuous rotation is achieved by continuation of transistor switching.

With described control each transistor switching leads to a rotor rotation of 90º. So the rotor turns round stepwise. That is why this design is called stepping motor. It is usually used if rotors are supposed to turn about a certain angle of rotation, instead of continuous rotational motion. The angle to be covered at each step is called *step angle*.

Stepping motors as described above, consist of two stator parts which are shifted against each other about 90º each with one winding and therefore two winding phases. Their rotors have two magnetic poles – equal to one pole pair. Therefore a number of phases *m=2* and number of pole pairs *p=1* results.

But it is also possible to equip motor with three, four or five phases. The higher the number of phases is chosen the smaller the stepping angle ensues.

Another opportunity to change the number of pole pairs is designing rotors with four, six, eight or more poles. A reduction of the step angle is achieved, proportional to the increase of the number of phases - therefore an increase of number of pole pairs.

In general full-step mode stepping motors with *m* phases and *p* pole pairs show step angles of:

$$a = \frac{360°}{2 \cdot p \cdot m} \tag{9.1}$$

Stepping motors are produced in different versions. The design being described above is called permanent-field multi-stator motor as claw-pole version.

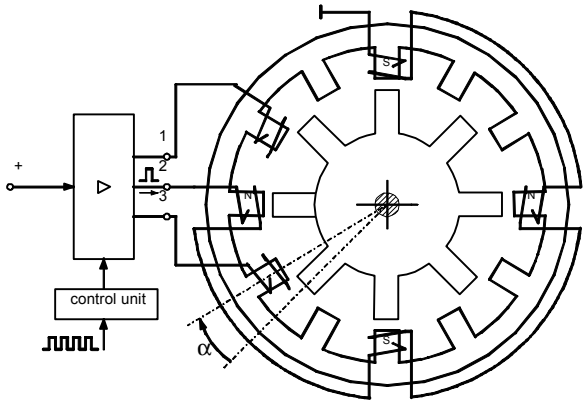

Fig. 243: reluctance stepping motor

Reluctance stepping motors consist of rotors made of magnetic soft material. In principle the rotor looks like a gear wheel. If a magnetic field is generated in stator windings rotor turns into the position in which magnetic flux has minimum magnetic resistance (reluctance). It is typical for such stepping motors that no holding torque is established if there is no magnetic field in stator.

Another type of stepping motor is the permanent-field motor in homopolar design. It is also called hybrid motor. A possible design of such a motor is shown in the Fig. 244. Rotors of this motor type feature permanent-magnets (N/S) with axial magnetization. Toothed (1 and 2) crowns made of magnetically soft material are attached to both sides of the magnet. Teeth of both parts are shifted against each other about half of a pitch and only north poles are established on one side and only south poles on the other side. Stator poles (3) are also toothed, with concentrated windings (4) each. The number of stator poles can be chosen in different ways. E.g. the motor shown in the Fig. 244 consists of six stator poles. The number of phases is usually chosen between two and five.

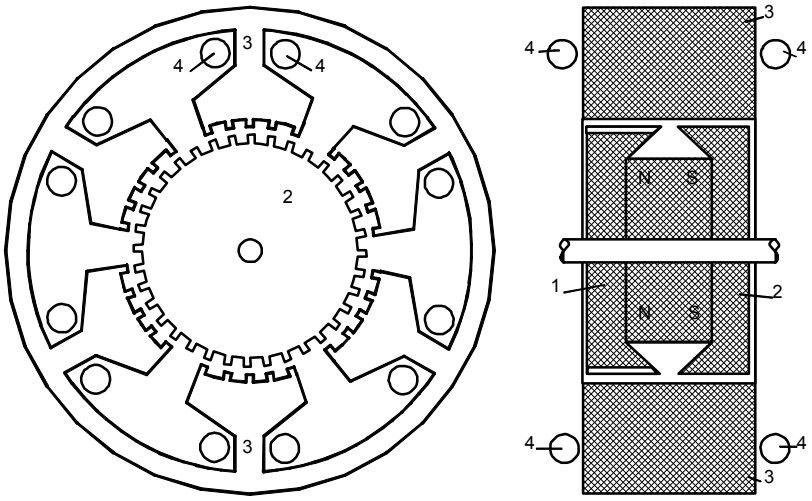

Fig. 244: reluctance stepping motor, homopolar design

In full-step mode, that means current in the phase windings is switched one after another, with z rotor teeth and m stator phase windings step angle is:

$$a = \frac{360°}{2 \cdot p \cdot z} \tag{9.2}$$

Generally it is important to choose control electronics and stepping motor as well adjusted to each other (see Fig. 245). In order to achieve rotational motion of the stepping motor *M* control electronics *St* is supplied from outside with voltage peaks pulses (1, 2, 3). Each pulse leads to a rotor rotation about the step angle as described above. If the rotor of the motor is supposed to rotate about a certain given angle an appropriate number of control pulses is necessary.

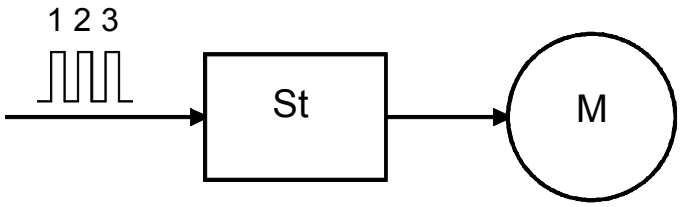

Fig. 245: motor and control electronics system

If stepping motors are operated with a higher step frequency, the frequency needs to be increased from small values to avoid stepping errors at starting operation. Suitable frequency/time acceleration ramps are used. To reach short accelerating time high currents can be fed for a short period of time. Braking is corresponding to that.

9.2 Switched reluctance machine

Switched reluctance machines (SRM) are to be seen as a special type of synchronous machine, which is discussed as an alternative for industry, servo and vehicle drives. Their principle design consists of wound salient poles in the stator and unwound rotors whose number of pole pairs is lower than those of the stator. Stator ampere-turns are switched step-by-step depending on pole position, which requires position encoders. The described method of operation leads to shunt characteristic, similar to those of DC machines.

The simple, robust, cheap and economic concerning manufacturing rotor without exciter windings is to be mentioned as one major advantage, as well as simple, uni-directional inverter design to be used. In cause of the flux vacillation principle of SR machines, power-for-size ratios compared to induction machines can only be reached at high air gap flux density values. This requires small air gap widths and apart from that leads to disadvantageous noise generation.

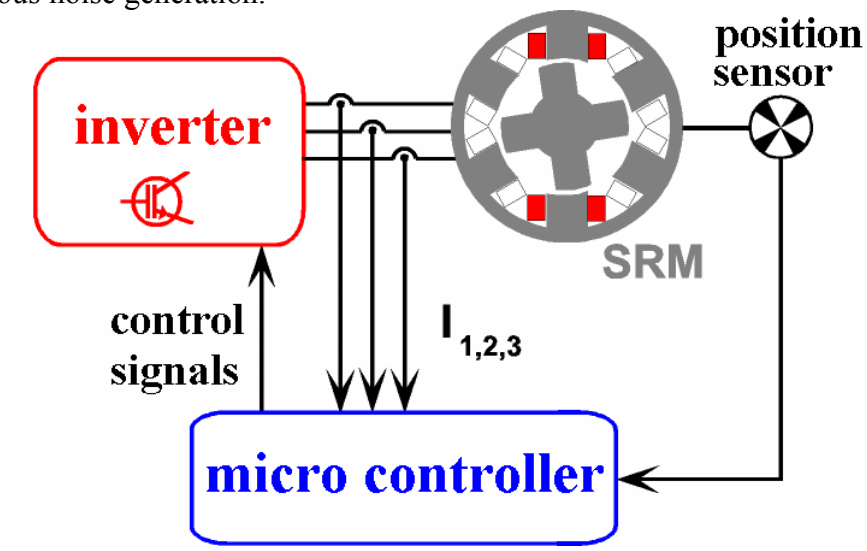

Fig. 246: switched reluctance machine (functional diagram)

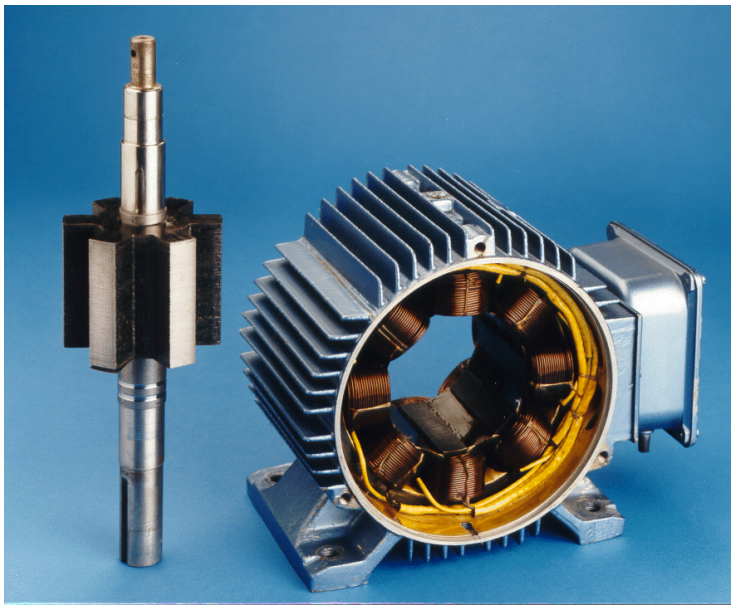

Fig. 247: switched reluctance machine (SRM)

9.3 Modular permanent-magnet motor

The modular permanent-magnet motor concept is a special type of permanent-magnet, converter-fed synchronous machine with pole position sensor. To make use of the advantage of the high inducing diameter for torque exertion the motor is built as revolving-armature machine. Conventional three-phase current machines have stator windings that are embedded in slots and the number of poles is equal to the one of the rotor. In contrast to that the permanent-magnet motor possesses salient stator poles, also called modules, whose number of poles is different from the one of the rotor. Similar to stepping motor or to switched reluctance machine the torque exertion is based on switching convenient stator coils depending on rotor position.

Utilization factor of the permanent-magnet motor is comparable with other types of machines as seen after simple consideration. To reach higher electric force densities current density and specific loading were multiplied compared to conventional machines. This was achieved by very complex intensive cooling processes, like e.g. direct oil cooling of the stator winding and Frigen cooling of the converter.

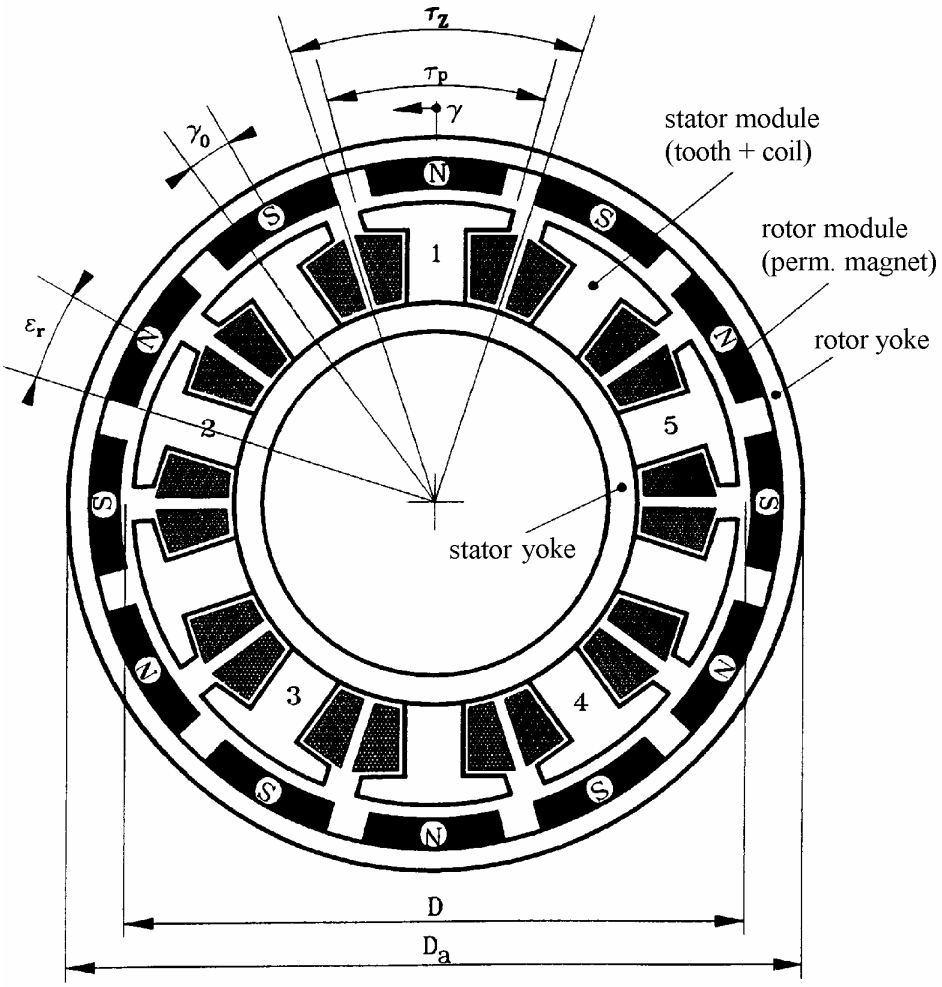

Fig. 248: modular permanent-magnet motor

9.4 Transverse flux machine

Transverse flux machines are basically permanent-synchronous machines with pole position sensor, with stator coils in direction of circumference, which results in uncoupled rotor flux. As a result there are very small pole pitches and a very high rotor specific loading can be achieved. In addition to that flux density of rare-earth magnets can be boosted if the rotor has a collector construction. Compared to other types of machines highest utilization factors are achieved by those steps. Advantage of high electric force density stands in sharp contrast to the disadvantage of a more expensive production technology.

If transverse flux machines are designed as a three-phase machines, conventional three-phase converters can be used.

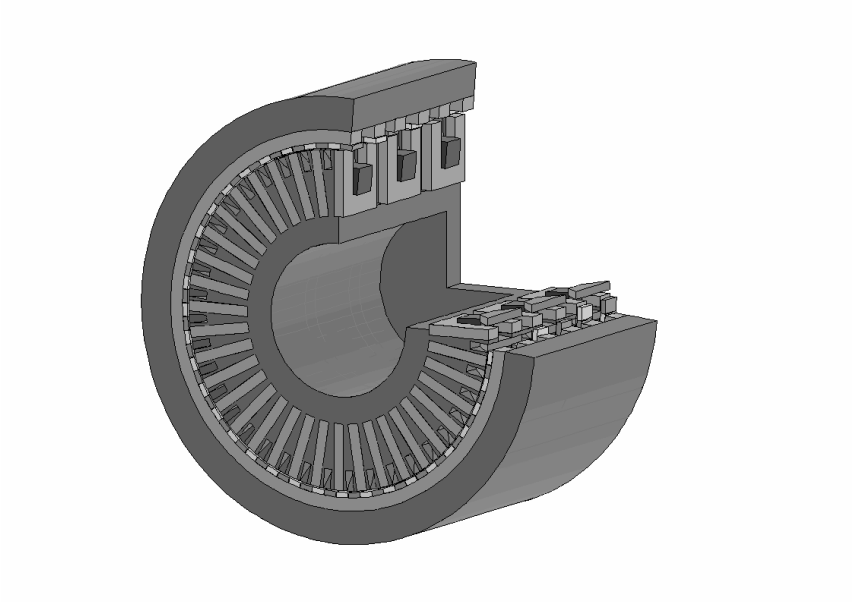

Fig. 249: transvese flux machine, 3-phase design

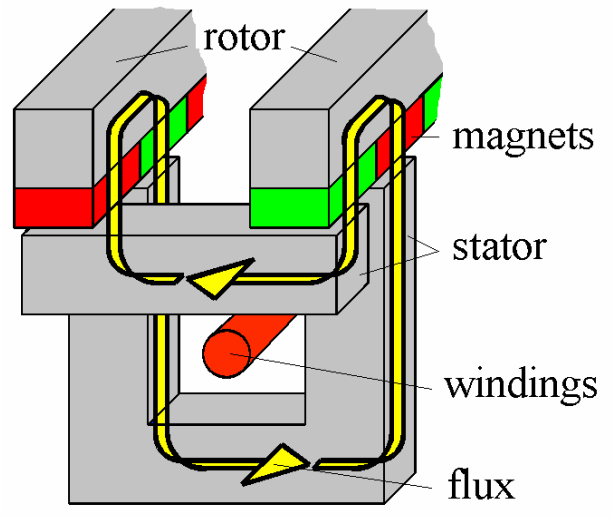

Fig. 250: method of operation, flux

9.5 Linear motors

Since linear motors do not have any gear unit it is more simple converting motion in electrical drives. Combined with magnet floating technology an absolutely contact-less and so a wear-resistant passenger traffic or non-abrasive transport of goods is possible. Using this technology usually should enable high speed. So Transrapid uses a combination of synchronous linear drive and electromagnetic floating. Linear direct drives combined with magnet floating technology are also useful for non-abrasive and exact transport of persons and goods in fields as transportation technology, construction technology and machine tool design. Suitable combinations of driving, carrying and leading open new perspectives for drive technology.

9.5.1 Technology of linear motors

In the following function, design, characteristic features, advantages and disadvantages are demonstrated shortly. In principle solutions based on all electrical types of machines are possible unrolling stator and rotor into the plane.

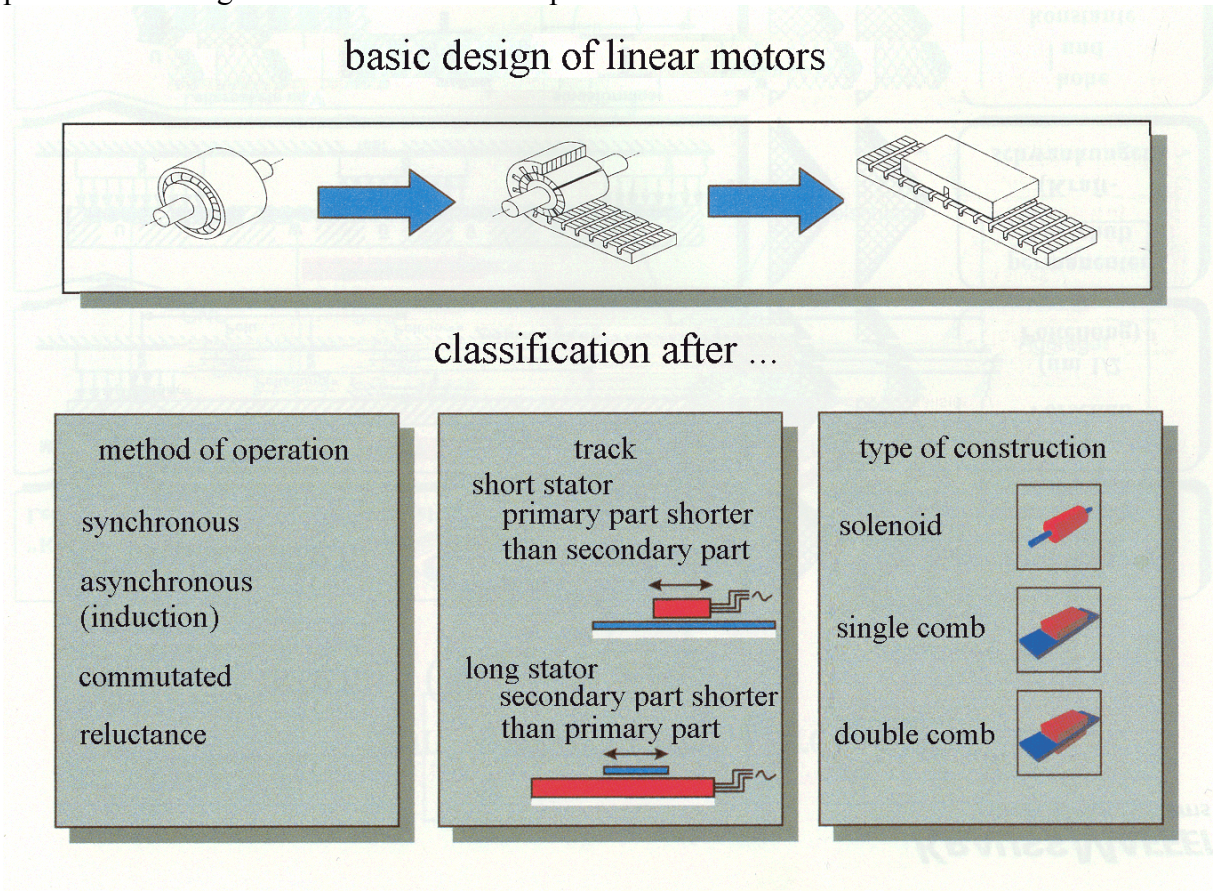

Fig. 251: linear motors, design overview (source: KRAUSSMAFFEI)

Linear motor then corresponds to an unrolled induction motor with short circuit rotor or to permanent-magnet synchronous motor. DC machines with brushes or switched reluctance machines are used more rarely.

Depending on fields of usage linear motors are constructed as solenoid, single-comb or double-comb versions in short stator or long stator implementation.
It is an advantage of long stator implementations that no power has to be transmitted to passive, moved secondary part, while short stator implementations need the drive energy to be transmitted to the moved active part. For that reason an inductive power transmission has to be used to design a contact-less system.

In contrast to rotating machines in single-comb versions the normal force between stator and rotor must be compensated by suitable leading systems or double-comb versions must be used instead. This normal force usually is one order of magnitude above feed force.

In three-phase windings of synchronous or induction machines a moving field is generated instead of three-phase field. This moving field moves at synchronous speed.

$$v_1 = t_p \cdot 2 \cdot f_1 \tag{9.3}$$

As in three-phase machines force is generated by voltage induction in the squirrel-cage rotor of the induction machine or by interaction with permanent-magnet field of the synchronous machine.

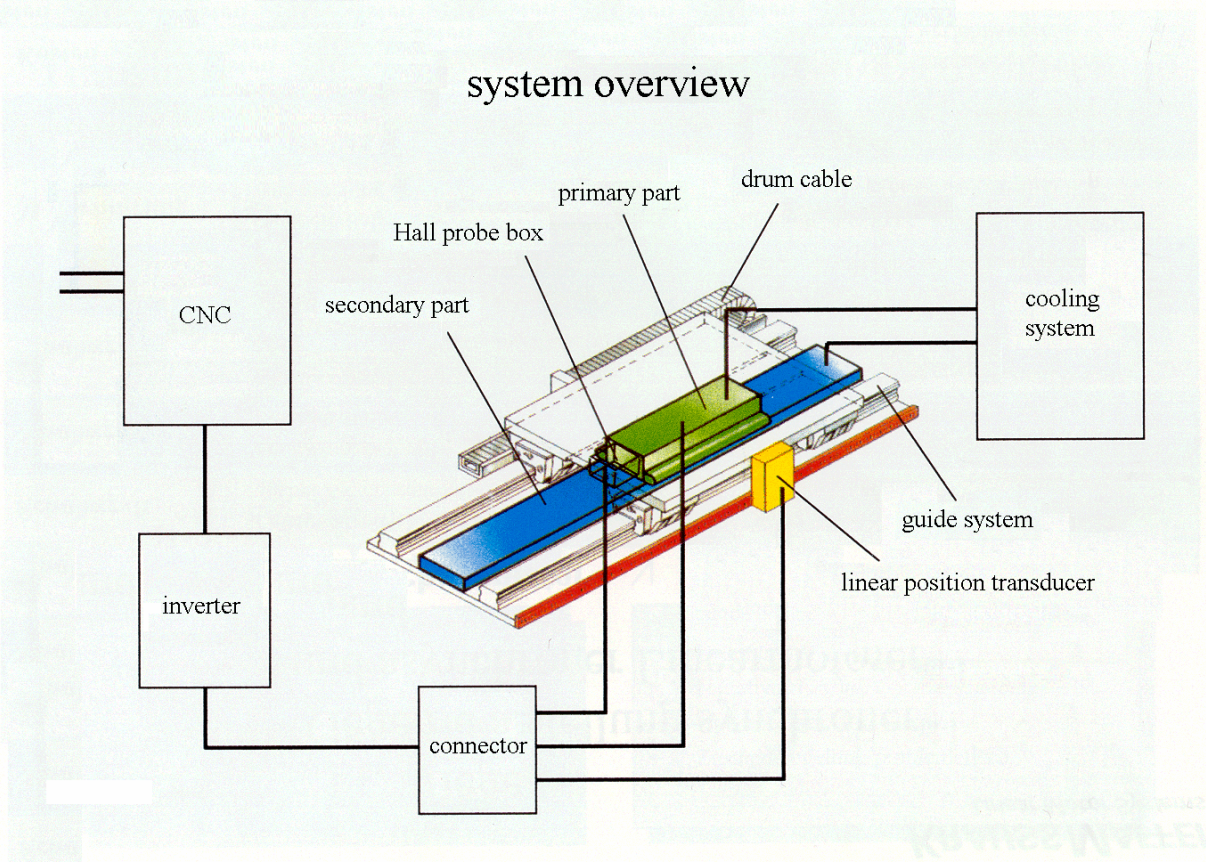

Fig. 252: linear drive, system overview (source: KRAUSSMAFFEI)

Three-phase machine supply is made field-oriented by frequency converters to achieve high dynamic behavior. For that induction machines need flux model and speed sensor, but synchronous machines just need a position sensor. For positioning jobs high dynamic servo drives with cascade control consisting of position control with lower-level speed and current control loop are used. This control structure is usual in rotating machines. Depending on the place the position measurement is installed a distinction is made between direct and indirect position control.

Since many movements in production and transportation systems are translatory, linear drives are useful in these fields. In such motors linear movements are generated directly, so that gear units such as spindle/bolt, gear rack/pinion, belt/chain systems are unnecessary. As a result from that rubbing, elasticity and play are dropped, which is positive for servo drives with high positioning precision and dynamic. In opposition to that there are disadvantages such as lower feed forces, no self-catch and higher costs.

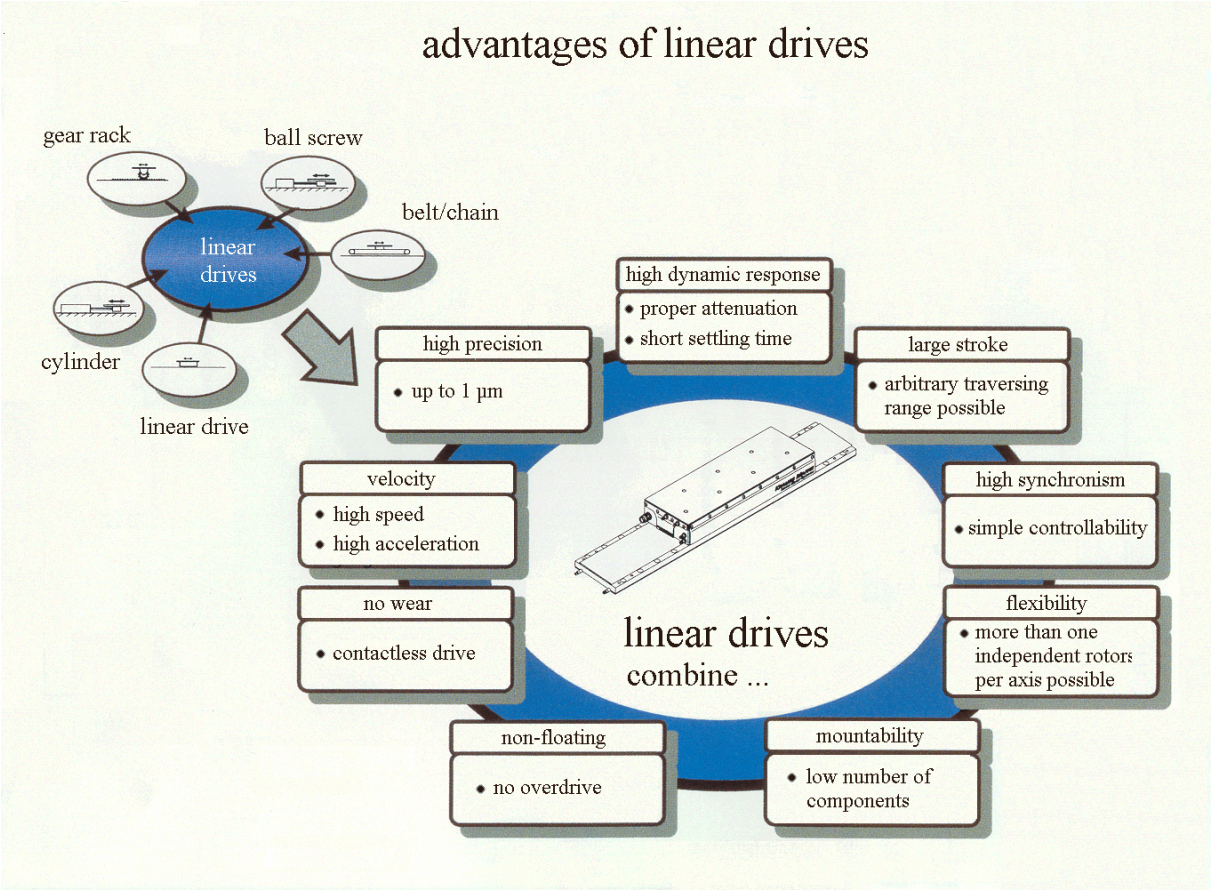

Fig. 253: advantages of linear drives (source: KRAUSSMAFFEI)

9.5.2 Industrial application opportunities

Two different opportunities to implement linear drives are shown at the following pictures.

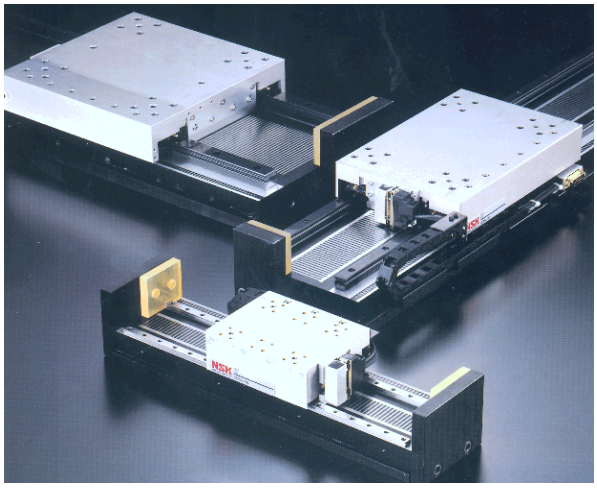

Fig. 254: induction linear motor (NSK-RHP)

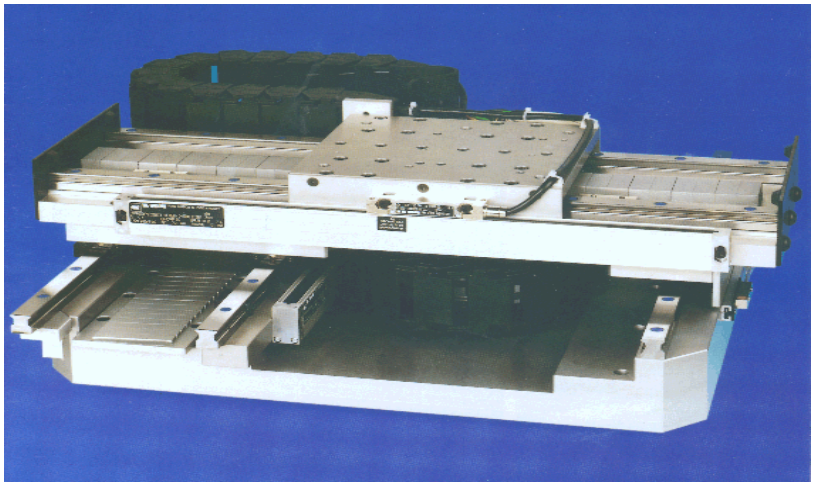

Fig. 255: synchronous linear motor (SKF)

Most promising application fields of linear drives for industrial applications:

- *machine tools*: machining center, skimming, grinding, milling, cutting, blanking and high speed machines.
- *automation:* handling systems, wafer handling, packing machines, pick-and-place machines, packaging machines, automatic tester, printing technology
- *general mechanical engineering:* laser machining, bonder for semiconductor industry, printed board machining, measurement machines, paper, plastic, wood, glass machining.

9.5.3 High speed applications

In the magnet high-speed train *Transrapid* wheels and rail are replaced by a contact-less working electromagnetic float and drive system. The floating system is based on attractive forces of the electromagnet in the vehicle and on the ferro-magnetic reaction rails in the railway. Bearing magnets pull the vehicle from below to the railway, guide magnets keep it on its way. An electronic control system makes sure, that the vehicle always floats in the same distance to the railway. Transrapid motor is a long-stator linear motor. Stators with moving field windings are installed on both sides along the railway. Supplied three-phase current generates an electromagnetic moving field within windings. The bearing magnets, and so also the vehicle are pulled by this field. Long-stator linear motor is divided into several sections. The section, in which the vehicle is located, is switched on. Sections, that make high demands on thrust, motor power is increased as necessary. Drive integrated in the railway and cancelling of mechanical components make magnet high-speed vehicles technical easier and safer. Transrapid consists of two light weight constructed elements. Capacity of the vehicles can be adjusted to certain requirements. Operating speed is between 300 and 500 km/h. A linear alternator supplies floating vehicle with required power. Advantages of magnet high-speed train are effective in all speed areas. After driving only 5 km Transrapid reaches a speed of 300 km/h in contrast to modern trains needing at least a distance of 30 km. Comfort is not interfered with jolts and vibrations. Since vehicle surrounds the railway Transrapid is absolutely safe from derailment. Magnet high-speed train makes less noise than conventional railway systems because there is no rolling noise. Also energy consumption is reduced compared with modern trains. This high-speed system is tested in continues operation at a testing plant in Emsland in Germany and some commercial routes in Germany are planned. A high-speed train route is currently under construction in Shanghai, China, further projects are either in progress or under review.

Fig. 256: high speed vehicle *Transrapid 08*, testing site Emsland, Germany (source: Thyssen)

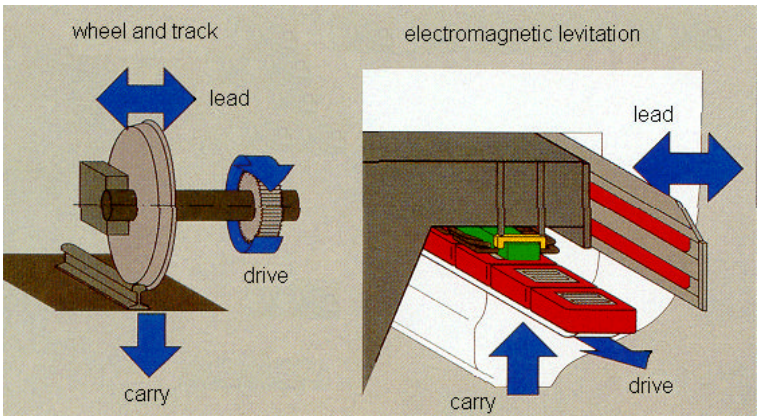

Fig. 257: basics of magnetic levitation (1)

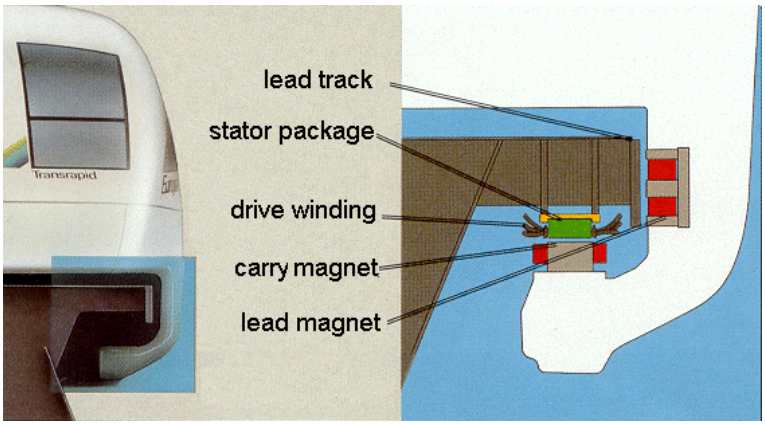

Fig. 258: basics of magnetic levitation (2)

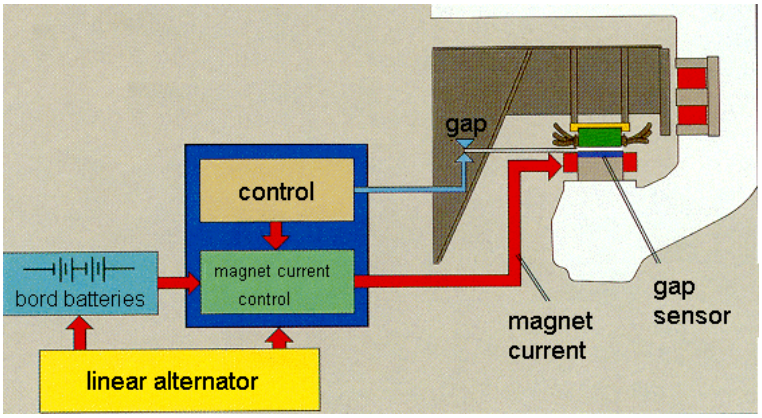

Fig. 259: basics of magnetic levitation (3)

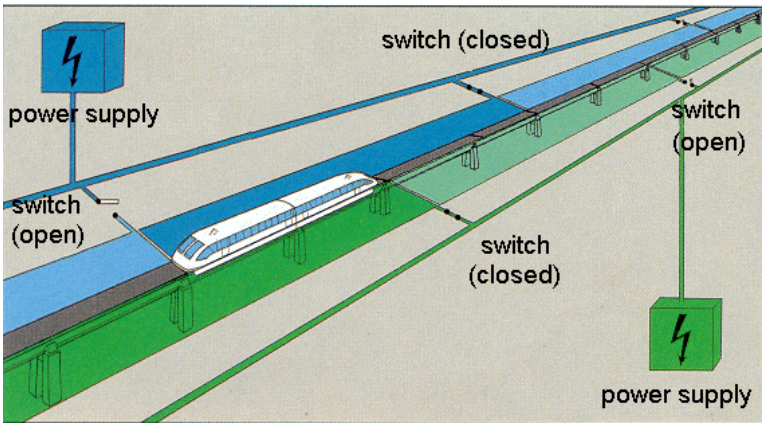

Fig. 260: track system

10 Appendix

10.1 Notations

Physical dependencies appear as quantity equation. A physical quantity results from multiplication of numerical value and unit..

quantity = numerical value × unit

Example: force of a solenoid

$$F = \frac{B^2}{2m_0} A = \frac{(1T)^2 1m^2}{2 \cdot 0{,}4p\,10^{-7}\,H/m} = 4 \cdot 10^6\,N \tag{10.1}$$

Units are to be included into calculations. Fitted quantity equations result from reasonable expansions with suitable units and partial calculation:

for the mentioned example:

$$\frac{F}{N} = 10\left(\frac{B}{0{,}5T}\right)^2 \frac{A}{cm^2} \tag{10.2}$$

Physical quantities are presented by lower case letters. Basically a distinction of upper and lower case letters means an increasing number of possible symbols to be used, whereas important differences between upper and lower case quantity is to be found for current and voltage.

- *u*, *i* → instantaneous values
- *U, I* → steady values (stationary)

1. DC calculations: *DC values*
2. AC calculations: *rms values*

Capital letters are usually used for magnetic quantities. Apart from that *crest values* are also assigned with capital letters in AC considerations. Phasor are assigned to underlined Latin letters (complex calculations).

Examples: $\underline{U}$, $\underline{I}$.

Vectors are indicated by an arrow being placed above Capital Latin letters.

Examples: $\vec{E}, \vec{B}$

Greek letters:
Αα Ββ Γγ Δδ Εε Ζζ Ηη θϑ Ιι Κκ Λλ Μμ Νν Ξξ Οο Ρρ Σσ Ττ Υυ φϕ Χχ Ψψ Ωω

10.2 Formular symbols

A	current coverage; area (in general)
a	number of parallel conductors
B	flux density (colloc. induction)
b	width
C	capacity
c	general constant, specific heat
D	diameter, dielectric flux density
d	diameter; thickness
E	electric field strength
e	Euler's number
F	force; form factor
f	frequency
G	electric conductance, weight
g	fundamental factor, acceleration of gravity
H	magnetic field strength
h	height; depth
I	current; I_w active current; I_B reactive current
i	instantaneous current value
J	mass moment of inertia
j	unit of imaginary numbers
K	cooling medium flow, general constant
k	number of commutator bars; general constant
L	self-inductance; mutual inductance
l	length
M	mutual inductance; torque
m	number of phases, mass
N	general number of slots
n	rotational speed
O	surface, cooling surface
P	active power
p	number of pole pairs; pressure
Q	reactive power; cross section; electric charge
q	number of slots per pole and phase; cross section
R	efficiency
r	radius
S	apparent power
s	slip; coil width; distance
T	time constant; length of period; absolute temperature; starting time
t	moment (temporal); general time variable
U	voltage (steady value); circumference
u	voltage (instantaneous value); coil sides per slot and layer
V	losses (general); volume; magnetic potential
v	speed; specific losses
W	energy
w	number of windings; flow velocity
X	reactance
x	variable
Y	peak value (crest value)
y	variable; winding step

Z	impedance
z	general number of conductors
α	pole pitch factor; heat transfer coefficient
β	brushes coverage factor
γ	constant of equivalent synchronous generated mmf
δ	air gap; layer thickness
ε	dielectric constant
ζ	Pichelmayer-factor
η	efficiency; dynamic viscosity
θ	electric current linkage
ϑ	load angle; temperature; overtemperature
κ	electric conductivity
λ	power factor, thermal conductivity; wave length; ordinal number; reduced magnetic conductivity
Λ	magnetic conductivity
μ	permeability; ordinal number
υ	ordinal number; kinematic viscosity
ξ	winding factor
ρ	specific resistance
σ	leakage factor; tensile stress
τ	general partition; tangential force
Φ	magnetic flux
φ	phase displacement between voltage and current
ψ	flux linkage
ω	angular frequency

10.3 Units

The following table contains most important physical variables and their symbols and units to be used. An overview of possible unit conversions is given in the right column additionally.

physical variable	Symbol	SI-unit	abbrev.	unit conversion
length	L	Meter	m	
mass	M	Kilogramm	kg	1 t (ton) = 10^3 kg
time	T	Second	s	1 min = 60 s 1 h (hour) = 3600 s
current intensity	I	Ampere	A	
thermodynamic temperature	T	Kelvin	K	temperature difference $\Delta\vartheta$ in Kelvin
celsiustemperature	ϑ	Degree Centigrade	°C	$\vartheta = T - T_0$
light intensity	I	Candela	cd	
area	A	-	m^2	
volume	V	-	m^3	1 l (Liter) = $10^{-3}m^{-3}$
force	F	Newton	N	1 kp (Kilopond) = 9.81 N 1 N = 1 kg·m/s^2
pressure	P	Pascal	Pa	1 Pa = 1 N / m^2 1 at (techn. atm.) = 1 kp / cm^2 = 0.981 bar, 1 bar = 10^5 Pa 1 kp / m^2 = 1 mm WS
torque	M	-	Nm	1 kpm = 9,81 Nm = 9,81 kg·m^2 / s^2
mass moment of inertia	J	-	kgm^2	1 kgm^2 = 0.102 $kpms^2$ = 1 Ws^3 impetus moment GD^2 GD^2 = 4 J / kgm^2

physical variable	Symbol	SI-unit	abbrev.	unit conversion
frequency	F	Hertz	Hz	1 Hz = 1 s^{-1}
angular frequency	ω	-	Hz	$\omega = 2\pi f$
rotational speed	N		s^{-1}	1 s^{-1} = 60 min^{-1}
speed (transl.)	V	-	m / s	1 m / s = 3,6 km / h
power	P	Watt	W	1 PS = 75 kpm / s = 736 W
energy	W	Joule	J	1 J = 1 Nm = 1 Ws 1 kcal = 427 kpm = 4186,8 Ws 1 Ws = 0,102 kpm
el. voltage	U	Volt	V	
el. field strength	E	-	V / m	
el. resistance	R	Ohm	Ω	
el. conductance	G	Siemens	S	
el. charge	Q	Coulomb	C	1 C = 1 As
capacity	C	Farad	F	1 F = 1 As / V
elektr. constant	ε_0	-	F / m	$\varepsilon = \varepsilon_0\varepsilon_r$ ε_r = relative diel.-constant
inductance	L	Henry	H	1 H = 1 Vs / A = 1 Ωs
magn. flux	f	Weber	Wb	1 Wb = 1 Vs 1 M (Maxwell) = 10^{-8} Vs = 1 Gcm
magn. flux density	B	Tesla	T	1 T = 1 Vs / m^2 = 1 Wb / m^2 1 T = 10^4 G (Gauß) 1 G = 10^{-8} Vs / m^2

physical variable	Symbol	SI-unit	abbrev.	unit conversion
magn. field strength	H	-	A / m	1 Oe (Oersted) = $10 / 4\pi$ A / cm 1 A / m = 10^{-2} A / cm
magn.-motive force	θ	-	A	
magn. potential	V	-	A	
magn. constant	μ_0	-	-	$\mu_0 = 4\pi 10^{-7}$ H / m μ_0 = 1 G / Oe
permeability	μ	-	-	$\mu = \mu_0 \mu_r$ μ_r = relative permeability
angle	α	Radiant	rad	1 rad = 1 m / 1 m $\alpha = l_{curve} / r$

10.4 Literature reference list

Books and scripts listed as follows may exceed the teaching range significantly. Nevertheless they are recommended best for a detailed and deeper understanding of the content of this lecture.

B. Adkins
The general Theory of electrical Machines, Chapman and Hall, London

Ch.V. Jones
The unified Theory of electrical Machines, Butterworth, London

L.E. Unnewehr, S.A. Nasar
Electromechanics and electrical Machines, John Wiley & Sons

Electro-Craft Corporation
DC Motors, Speed Controls, Servo Systems, Pergamon Press

Ch. Concordia
Synchronous Machines, John Wiley, New York

Bahram Amin
Induction Motors – Analysis and Torque Control

Peter Vas
Vector Control of AC Machines, Oxford Science Publications

T.J.E. Miller
Switched Reluctance Motors and their control, Magna PysicsPublishing